

APPLICATION OF GEOGRAPHICAL INFORMATION
SYSTEMS TO LAHAR HAZARD ASSESSMENT ON AN
ACTIVE VOLCANIC SYSTEM

by

Amii Rebecca Darnell

A thesis submitted for the degree of Doctor of Philosophy
University of East Anglia, Norwich
School of Environmental Sciences

August 2010

© This copy of the thesis has been supplied on condition that anyone who consults it is understood to recognise that its copyright rests with the author and that no quotation from the thesis, nor any information derived therefrom, may be published without the author's prior, written consent.

ABSTRACT

Lahars (highly dynamic mixtures of volcanic debris and water) have been responsible for some of the most serious volcanic disasters and have killed tens of thousands of people in recent decades. Despite considerable lahar model development in the sciences, many research tools have proved wholly unsuitable for practical application on an active volcanic system where it is difficult to obtain field measurements. In addition, geographic information systems are tools that offer a great potential to explore, model and map hazards, but are currently under-utilised for lahar hazard assessment.

This research pioneered a three-tiered approach to lahar hazard assessment on Montserrat, West Indies. Initially, requirements of potential users of lahar information (scientists and decision-makers) were established through interview and evaluated against attainable modelling outputs (given flow type and data availability). Subsequently, a digital elevation model, fit for modelling lahars, was used by a path of steepest descent algorithm and a semi-empirical debris-flow model in the prediction of lahar routes and inundation areas. Limitations of these established geographical information system (GIS) based models, for predicting the behaviour of (relatively under-studied) dilute lahars, were used to inform key parameters for a novel model, also tightly coupled to a GIS, that simulated flow routes based on change in velocity. Importantly, uncertainty in model predictions was assessed through a stochastic simulation of elevation error. Finally, the practical utility of modelling outputs (visualisations) was assessed through mutual feedback with local scientists.

The new model adequately replicated past flow routes and gave preliminary predictions for velocities and travel times, thus providing a short-term lahar hazard assessment. Inundation areas were also mapped using the debris-flow model to assist long-term planning. Ultimately, a GIS can support 'on the ground' planning decisions, but efficacy is limited by an active volcanic system which can restrict feedback to and from end-users.

LIST OF CONTENTS

ABSTRACT.....	II
LIST OF FIGURES	VII
LIST OF TABLES	XIV
LIST OF ACRONYMS	XVI
ACKNOWLEDGEMENTS.....	XVIII
CHAPTER 1: INTRODUCTION	1
1.1 RATIONALE AND MOTIVATION	2
1.2 AIMS AND OBJECTIVES	5
1.3 THESIS STRUCTURE	6
CHAPTER 2: BACKGROUND AND REGIONAL SETTING.....	8
2.1 FRAMING VOLCANIC HAZARDS AND LAHARS.....	9
2.1.1 Placing volcanic disasters in context	9
2.1.2 Introducing the lahar hazard	13
2.1.2 Lahar disasters: lessons learned from history.....	14
2.2 NATURAL HAZARD MANAGEMENT	18
2.2.1 General and evolving approach to natural hazard management.....	18
2.2.2 Evolving techniques in natural hazard assessment.....	21
2.2.2.1 <i>The role and challenges of hazard zonation</i>	21
2.2.2.2 <i>Recognition of uncertainties</i>	22
2.2.3 Volcanic hazard management	24
2.2.3.1 <i>Traditional framework for volcanic hazard management</i>	24
2.2.3.2 <i>Volcanic hazard modelling</i>	26
2.2.4 Implications for lahar hazard management	27
2.3 ASSESSING AND MODELLING THE LAHAR HAZARD	28
2.3.1 Lahar hazard identification.....	28
2.3.2 Lahar definitions and nomenclature	29
2.3.3 Background considerations for lahar modelling	32
2.3.4 History of lahar runout and intensity calculation methods	34
2.3.4.1 <i>Overview</i>	34
2.3.4.2 <i>Empirical relationships</i>	34
2.3.4.3 <i>Two-dimensional non-numerical methods</i>	36
2.3.4.4 <i>Numerical/ physical models</i>	40
2.3.4.5 <i>Summary of current modelling techniques</i>	44
2.3.5 Reflection on the key factors for lahar modelling.....	46
2.3.5.1 <i>Data inputs, e.g. DEM</i>	46
2.3.5.2 <i>Model concept and inherent assumptions</i>	47
2.3.5.3 <i>Parameters and calibration</i>	48
2.3.5.4 <i>A framework for lahar modelling?</i>	48
2.3.6 Lahar hazard zonation	50
2.4 USE OF GEOSPATIAL DATA AND TOOLS FOR HAZARD MANAGEMENT, MODELLING AND COMMUNICATION	51
2.4.1 An introduction to GIS potential for hazard management	51
2.4.2 Geospatial data and tools applied for preparedness, mitigation and decision utility	53
2.4.3 Geospatial data and tools applied for response and recovery.....	55
2.4.4 GI Science and research using GIS.....	58
2.4.4.1 <i>An overview</i>	58
2.4.4.2 <i>Spatial data acquisition and integration (including interoperability)</i>	59
2.4.4.3 <i>Uncertainty in geographic information, spatial ontologies and geographic representation</i>	61
2.4.4.4 <i>Spatial cognition and visualisation</i>	64
2.4.4.5 <i>GIS and Society (including public participation)</i>	65
2.4.5 Potential of geospatial data and tools for lahar hazard assessment	68
2.5 REGIONAL SETTING: MONTSERRAT, WEST INDIES	69
2.5.1 Overview	69
2.5.2 Geography, geology and climate.....	69
2.5.3 Chronology of an andesitic dome-building eruption	72

2.5.4 Impacts of the eruption (1995—present)	73
2.5.4.1 Physical change	73
2.5.4.2 Demographic change.....	73
2.5.4.3 Economic change.....	74
2.5.5 Management of the Volcanic crisis (short-term) 1995—1999	76
2.5.6 Management from emergency towards reconstruction and recovery (long-term and current strategies).....	78
2.5.6.1 Synopsis of current hazard management	78
2.5.6.2 International commitments to disaster risk reduction	80
2.5.7 Belham Valley lahars	81
2.6 EVALUATION OF GAPS IN RESEARCH TO DATE.....	87
2.6.1 Drawing out intellectual themes	87
2.6.2 Synopsis of gaps in the literature	88
CHAPTER 3: AN APPLICATION-DRIVEN APPROACH TO TERRAIN MODEL CONSTRUCTION.....	90
3.1 INTRODUCTION	91
3.2 BACKGROUND: DIGITAL TERRAIN REPRESENTATION.....	92
3.3 STUDY AREA	93
3.4 METHODOLOGY	95
3.4.1 Application overview – lahar modelling.....	95
3.4.2 Data acquisition.....	96
3.4.3 Identifying uncertainty	96
3.4.4 DEM creation.....	98
3.4.5 Modelling error in the DEM	100
3.4.5.1 Method 1: Spatially independent errors.....	101
3.4.5.2 Method 2: Spatial dependence using the Grid-Cell Uncertainty Model (GCUM).....	101
3.4.6 Uncertainty propagation and sensitivity analysis	103
3.5 RESULTS	105
3.5.1 DEM construction with spatially independent error.....	105
3.5.2 Spatially independent vs. dependent error.....	110
3.5.3 Flow model parameters	113
3.6 DISCUSSION	113
3.6.1 Flow model response to the terrain model.....	113
3.6.2 Uncertainty implications for hazard management	114
3.6.2.1 Comparing DEMs and fitness for use.....	114
3.6.2.2 Sensitive areas of the study site.	115
3.6.2.3 Other influences on the flow path	115
3.6.3 Implications for an application-driven approach to DEM construction	116
3.6.3.1 Survey design and DEM construction	116
3.6.3.2 Applying error fields	117
3.7 CONCLUSIONS	118
CHAPTER 4: AN EXAMINATION OF GIS APPROACHES FOR LONG-TERM LAHAR HAZARD MAPPING ON MONTSERRAT, WEST INDIES.....	120
4.1 INTRODUCTION	122
4.2 REGIONAL SETTING.....	123
4.3 MODEL SELECTION FOR FLOW SIMULATION.....	125
4.3.1 Approach to modelling.....	125
4.3.2 Single-direction flow routing.....	127
4.3.3 LAHARZ.....	127
4.4 CHANNEL RESPONSE TO LAHAR PERTURBATION: FIELD-BASED OBSERVATIONS.....	131
4.4.1 Updating elevation models	131
4.4.2 Establishing geomorphological change	136
4.4.3 Volcanic activity and lahar events.....	138
4.4.4 Working with available data: constraining volume estimates for modelling.....	140
4.5 IMPLEMENTING LAHAR MODELS	143
4.5.1 Simple flow routing	143
4.5.1.1 Determining the path of steepest descent from an elevation cost surface	143

4.5.1.2 Uncertainty in elevation and probability of flow	144
4.5.2 Implementing LAHARZ	146
4.6 RESULTS	149
4.6.1 Dominant paths from single-direction flow routing.....	149
4.6.2 Delineating lahar hazard zones with LAHARZ	152
4.6.3 Comparison of model outputs with observed morphological change	156
4.7 DISCUSSION	157
4.7.1 Comparison of inundation areas	157
4.7.2 Model requirements and limitations	159
4.7.2.1 Single-direction flow routing	159
4.7.2.2 LAHARZ.....	160
4.7.3 Implications for lahar hazard management on Montserrat.....	161
4.8 CONCLUSIONS	163
CHAPTER 5: DEVELOPING A SIMPLIFIED GIS APPROACH TO DILUTE LAHAR MODELLING	164
5.1 INTRODUCTION	165
5.2 METHODS.....	166
5.2.1 Model Formulation	166
5.2.1.1 Equation of Motion - Manning's Equation	167
5.2.1.2 Conservation of mass: LAHARZ.....	171
5.2.2 Implementation in a GIS.....	172
5.2.2.1 Generating a velocity-cost surface	172
5.2.2.2 Quantification and propagation of error.....	173
5.2.2.3 Movement of mass.....	174
5.2.3 Application to dilute lahars on Montserrat, West Indies	177
5.2.3.1 Setting and model suitability.....	177
5.2.3.2 Selection of roughness coefficients.....	179
5.3 RESULTS	182
5.3.1 Dominant routes and flow depths	182
5.3.2 Flow velocities and travel times	185
5.4 DISCUSSION	187
5.4.1 Potential utility of the approach	187
5.4.2 Verification and uncertainties	189
5.5 CONCLUSIONS	190
CHAPTER 6: PRACTISING EFFECTIVE RESEARCH OF SECONDARY VOLCANIC HAZARDS DURING A PROLONGED ERUPTION: LAHARS ON MONTSERRAT, WEST INDIES	192
6.1 INTRODUCTION	194
6.1.1 Volcanic hazard preparedness	194
6.1.2 Communication issues and an emerging knowledge transfer gap	195
6.1.2.1 Communication between scientists.....	196
6.1.2.2 Communication between administrators and scientists.....	196
6.1.2.3 Communication methods	197
6.1.3 Mitigation of lahar hazards	198
6.1.4 Aims.....	199
6.2 REGIONAL SETTING	200
6.2.1 The people and the place: Belham Valley, Montserrat.....	200
6.2.2 Existing hazard management	203
6.3 PHASE I: EVALUATION OF MANAGEMENT OPTIONS	205
6.3.1 Methodological overview of Phase I	205
6.3.2 End-user requirements for short- and mid-term mitigation.....	207
6.3.3 End-user requirements for mid- and long-term planning.....	208
6.4 REFLECTION ON USER-REQUIREMENTS VS. ATTAINABLE OUTPUTS OWING TO DATA RESTRICTIONS AND MODELLING OPTIONS.....	209
6.4.1 Evaluation of requirements.....	209
6.4.2 Defining research objectives and researcher role.....	211
6.4.2.1 Fieldwork and data constraints	211
6.4.2.2 Research objectives and model outputs	211

6.4.2.3 Researcher role.....	213
6.5 PHASE II: LAHAR MODELLING AND HAZARD ASSESSMENT.....	214
6.5.1 Phase II overview.....	214
6.5.2 Achieving short- to mid-term management outputs (<i>i</i> and <i>ii</i>).....	215
6.5.3 Achieving mid- to long-term management outputs (<i>iii</i> and <i>iv</i>).....	216
6.5.3.1 Modelling for long-term hazard assessment (output <i>iii</i>).....	216
6.5.3.2 Visualisation for a dual focus hazard map (output <i>iii</i>).....	217
6.5.3.3 Management options and mitigation scenarios (<i>iv</i>).....	218
6.6 PHASE II: RESULTS AND ANALYSIS.....	219
6.6.1 Results relevant to short- to mid-term planning objectives (<i>i</i> and <i>ii</i>).....	219
6.6.2 Results relevant to mid- to long-term planning strategies (<i>iii</i> and <i>iv</i>).....	221
6.6.2.1 Inundation mapping (output <i>iii</i>).....	221
6.6.2.2 Structural mitigation and possible futures (output <i>iv</i>).....	223
6.7 PHASE III: MAINTAINING COOPERATIVE RELATIONSHIPS AND MUTUAL FEEDBACK.....	225
6.7.1 Methodological overview.....	225
6.7.2 Results from mutual feedback.....	226
6.7.2.1 Post-modelling consultations with scientists and non-scientists at MVO.....	226
6.7.2.2 Post-modelling consultations with decision makers.....	227
6.8 DISCUSSION.....	228
6.8.1 Reflecting on model outputs and end-user demands.....	228
6.8.1.1 Short- to mid-term outputs (<i>i</i> and <i>ii</i>).....	228
6.8.1.2 Mid- to long-term outputs (<i>iii</i> and <i>iv</i>).....	229
6.8.2 Reflections on the interface between research and usage.....	230
6.8.3 Wider implications and further work.....	231
6.9 CONCLUSION.....	232
CHAPTER 7: CONCLUSIONS AND FUTURE RESEARCH.....	234
7.1 EVALUATION OF AIMS AND OBJECTIVES.....	235
7.2 EVALUATION OF EFFICACY OF GIS FOR LAHAR HAZARD ASSESSMENT.....	236
7.2.1 Monitoring lahars, data acquisition and handling.....	236
7.2.1.1 Review of lahar monitoring and data availability for lahar modelling.....	236
7.2.1.2 Data handling: DEM construction.....	237
7.2.1.3 Data handling: uncertainties and elevation error.....	238
7.2.2 Improving knowledge of lahars through modelling.....	239
7.2.2.1 Utility and limitations of existing GIS models.....	239
7.2.2.2 Model improvements.....	240
7.2.2.3 Treatment of unknowns and data uncertainties.....	240
7.2.3 Transfer of academic research on lahars.....	241
7.2.4 Summary of the utility of GIS for lahar hazard assessment on Montserrat.....	242
7.3 SUMMARY OF CONTRIBUTIONS TO NEW KNOWLEDGE.....	243
7.4 AVENUES FOR FURTHER INVESTIGATION.....	245
7.4.2.1 Merapi Volcano, Central Java, Indonesia.....	247
7.4.2.2 Mt Ruapehu, New Zealand.....	248
7.4.2.3 Others.....	249
7.5 CLOSING REMARKS.....	253
REFERENCES.....	255
APPENDICES.....	288
APPENDIX 1: FIELD DATA.....	289
APPENDIX 2: ANIMATION.....	289

LIST OF FIGURES

Figure 2.1	Disaster management cycle showing the temporal dimension (clockwise) (after Drabek and Hoetmer, 1991; Cova, 1999)	18
Figure 2.2	The warning process and its subsystems (after Alexander, 2007).	19
Figure 2.3	Volcanic hazards mitigation viewed as an inverted pyramid as basic science filters down to decision-makers and local authorities (modified substantially from Tilling, 1989, and Alexander, 2007)	25
Figure 2.4	Variation of shear stress with shear rate for different models of flow behaviour (after Oertel, 2004).	30
Figure 2.5	Volcaniclastic flow types, sediment-support and depositional mechanisms (After Smith and Lowe, 1991; Pierson, 1995; Lavigne and Thouret, 2000)	31
Figure 2.6	Maximum runout of a gravity-driven flow, L , down a valley from a vertical drop, H , is defined by the slope of the energy-line (travel- or reach-angle, θ) (after Wadge and Isaacs, 1988).	36
Figure 2.7	D8 algorithm for flow direction over a small section of an example DEM	37
Figure 2.8	a) the H/L energy cone is adopted by LAHARZ to define the proximal hazard zone. Processing begins where the H/L bounding cone intersects the valley thalweg; b) the centre of the lahar mass follows the valley thalweg downstream, but at each processing cell three cross-sections define the dispersion.	39
Figure 2.9	Potential applicability of some of the models (and rheological laws) described in the text. Arrows show origination and direction of spread of application (e.g. the energy-line concept was designed for avalanches but has been applied to lahars). Please refer to citations in the main body text.	45
Figure 2.10	Schematic showing the considerations for modelling for the scientist	49
Figure 2.11	Qualitative hazard matrix for debris flows (level of hazard where h is the flow-depth and v is the velocity). After Hurlimann <i>et al.</i> (2008) and Rickenmann (2005b as cited in Hurlimann <i>et al.</i> , 2008).	50

Figure 2.12	Example geospatial activities contributing to phases of the disaster management cycle (After Johnson, 2000; NRC, 2007).	53
Figure 2.13	A conceptual view of uncertainty (after Longley <i>et al.</i> , 2001; 2005).	62
Figure 2.14	The public participation ladder in GIS (After Arnstein 1969; Carver, 2003 and references cited therein)	66
Figure 2.15	a) Position of Montserrat in the Caribbean; part of the subduction zone is also shown (after Susnik, 2009); b) the current access restrictions on Montserrat (Hazard Level 3, MVO, http://www.mvo.ms/).	70
Figure 2.16	Pre-eruption geological map of Montserrat; coordinates in Montserrat National Grid (contour interval = 100 m). Dating in thousands of years (ka) from $^{40}\text{Ar}/^{39}\text{Ar}$ geochronology (after Harford <i>et al.</i> , 2002).	71
Figure 2.17	Summary of some of the key events of the eruption to February 2010 (after http://www.mvo.ms/ ; Herd <i>et al.</i> , 2005; Edmonds <i>et al.</i> , 2006)	72
Figure 2.18	Belham Valley Montserrat and rain-gauge network; names for the currently active gauges are shown in bold text (150 m contours) (After Alexander <i>et al.</i> , in press).	82
Figure 2.19	Multiple flows down the Belham Valley have greatly changed the geomorphology: a) the mouth of the valley in 1996 (looking east), the shoreline is marked by a line of palm trees (courtesy R. Herd, UEA); b) the mouth of the valley in 2006 (looking south-east) has greatly extended into the sea, the palm trees marking the 1996 shoreline have been highlighted.	84
Figure 2.20	Photographs illustrating the effects and damage caused by lahars in the Belham Valley a) large boulders up to 2–3 m diameter have been deposited in the mid-reach (flow right to left); b) boulders also in the upper-reach (looking upstream); c) damaged house in November 2006; d) house in 2007, an extra 1m of deposit; e) rear of house in 2007 shows accumulated debris; f) lahar debris litters the floor of the Belham Valley in 2007, Soufrière Hills can be seen in the background.	85
Figure 2.21	Warning signs are in place at the major crossing points for the Belham Valley. Lahars are often locally referred to as floods or mudflows.	86

Figure 3.1	(a) Photo of the mouth of the Belham Valley taken November 2006 (looking east); (b) the location of the study area on Montserrat (DEM after Wadge 2005).	94
Figure 3.2	Potential sources, and transfer, of uncertainty from DEM creation to model output. Relative timing of uncertainty quantification in this case is indicated by the dotted box.	97
Figure 3.3	Differences in average slope and standard deviation of slope – between original DEM and the mean of 10 realisations at a given ρ . Error bars show minimum and maximum values (primary 10-m DEM, stdv = 0.5 m).	102
Figure 3.4	An overview of the uncertainty and sensitivity testing showing the input parameters (P) and the output (probability surface).	104
Figure 3.5	Lower-reach study area showing the distribution of the 20127 GPS points and 250 × 250 m subsection of the study area that was used to test the interpolation techniques (bottom left corner: 375450, 1850400 Montserrat National Grid)	105
Figure 3.6	Wireframe (viewed on a 10-m grid) showing interpolation of source data through (a) rasterized secondary TIN, (b) spline from ten sample points with spline weight = 5, and (c) TOPOGRID. Elevations have a vertical exaggeration of factor 2.	106
Figure 3.7	Parameter change: (a) and (b) DEM construction method (stdv = 0.1 m); (c) observed channels (incised and outer/border) from aerial photographs.	108
Figure 3.8	Parameter change: DEM resolution (stdv = 0.5 m).	109
Figure 3.9	Parameter change: standard deviation of error (secondary 5-m DEM).	110
Figure 3.10	Proportion of cells experiencing some flow. (DEM details are abbreviated, e.g. primary 5 m, stdv 0.1 m = p5m01).	111
Figure 4.1	Island of Montserrat a) Soufrière Hills Volcano and the Belham River, its drainage basin and tributaries (100 m contours derived from Wadge, 2006); b) Hazard Zones map at current Hazard Level 3 (March 2010, courtesy of MVO). Coordinates are in Montserrat National Grid.	124

Figure 4.2	Relationships between a) H and L , which describe the extent of the proximal hazard zone, and b) A and B , which describe the extent of the distal lahar inundation zone (After Iverson <i>et al.</i> , 1998); Google Sketchup used for 3D visualisation	129
Figure 4.3	Retained GPS survey points for entire study area (33357 points) and lower-reach (20127 points; used in Chapter 3). Coordinates in Montserrat National Grid.	132
Figure 4.4	a) Valley surface cross-section showing coverage by GPS survey; b) fusing the up-to-date GPS-derived DEM with the contour-derived DEM required the creation of artificial voids which were then filled by feathering with a neighbourhood averaging window; c) lateral extension of the GPS-derived DEM.	134
Figure 4.5	a) distribution of GPS points, and planimetric view of the merged section of the study area for b) void, fill and feather, and c) lateral extension method. Profile graphs show the resultant cross-sections looking downstream. Coordinates in Montserrat National Grid. (After Darnell <i>et al.</i> , 2009)	136
Figure 4.6	a) spatial distribution of net deposition November 2006—November 2007; b) channel profiles for 2006 and 2007	137
Figure 4.7	Daily rainfall recorded at Garibaldi Hill rain gauge (GAR) and regional monthly-averaged daily rainfall from the Climate Prediction Center Merged Analysis of Precipitation (CMAP) centred on Latitude 16.25, Longitude 298.75	139
Figure 4.8	Schematic of steepest descent method used to define probable flow routes (implementation was in ArcGIS)	143
Figure 4.9	Considerations for elevation error propagation (necessary user inputs are highlighted)	144
Figure 4.10	a) standard deviations (σ) on an elevation error pdf with a normal distribution and no bias (e.g. mean error, μ , is zero), e.g. for stdv = 0.5 m; b) an elevation error sampling scenario for a Monte Carlo simulation (after Smemoe, 2007)	146

Figure 4.11	Belham stream network (flow accumulation threshold 500) and H/L energy cone (0.24) as generated in the setup of LAHARZ. The volcano apex, or maximum elevation, is also shown. The proximal hazard zone is from the apex to the energy cone boundary. Coordinates are provided in Montserrat National Grid.	147
Figure 4.12	Observed channels, in November 2006, and geometry of past deposits (given by Figure 4.5)	149
Figure 4.13	Inundation probability maps, the first column shows results using end point A, and the second from end point B; rows represent increasing stdv of error. Inundated cell count and total area are also shown for comparison.	150
Figure 4.14	a) Belham thalweg automatically generated in LAHARZ; and b) inundation areas for varying lahar volumes from LAHARZ; additionally the geometry of past deposits has been overlain (from Figure 4.11).	153
Figure 4.15	a) example hazard map showing changes in hazard relative to the key towns and road network; b) existing hazard zones map (at Hazard Level 3) for the same section of the Belham Valley (digitised from MVO hazard map).	154
Figure 4.16	Hazard maps for the lower-reach between the Belham crossing and the shoreline: a) hazard zones inferred from LAHARZ; b) inundation probability field from the elevation cost surface, stdv = 0.5 (close-up of Figure 4.13, mid-right). Coordinates are provided in Montserrat National Grid.	155
Figure 4.17	a) relationship between natural log transformed input volumes (for various LAHARZ model runs) and lahar travel distance downstream (last stream-cell); b) natural log transformed observed net deposition at corresponding sample locations downstream (extracted from data presented in Figure 4.5).	156
Figure 5.1	a) definition sketch for two-dimensional free surface flow; b) an example channel cross-section showing wetted perimeter (both after Brutsaert, 2005).	168
Figure 5.2	Methodological overview for deriving velocity cost surface(s) and likely flow paths	174

Figure 5.3	a) A channel cross-section showing intermediate fill-levels that can be extracted from LAHARZ, the final fill level can also be calculated and used to ascertain flow depths at each of the inundated cell locations (after Schilling, 1998); b) the minimum (rectangular) wetted perimeter can be established by calculating an approximate depth from the number of inundated cells (given by LAHARZ) and their resolution. The cross-sectional area, A , is the same for both diagrams and can be given by the semi-empirical equation in LAHARZ (Equation 5.2).	176
Figure 5.4	Stage (flow height) indicators included damaged vegetation, stranded boulders and high-water marks. These photographs progress in sequence from the lower-reach (i and ii) to mid-reach (iii) to upper-reach (iv, v and vi); arrows represent flow directions. A measuring stick with 0.1 m divisions was used for scale.	178
Figure 5.5	Photographic examples of roughness, arrows represent flow direction. Geographical locations of the photos (A—F) can be seen in Figure 5.6.	180
Figure 5.6	Digitised boundaries for six different land-cover classes (laid over aerial image taken 24 June 2006, DigitalGlobe Incorporated); letters A—F represent the approximate locations of the stage indicators in Figure 5.5.	181
Figure 5.7	Inundation probability maps for velocity cost surface with spatially distributed R (using LAHARZ for flow depths). Inundated cell count and total area also shown.	182
Figure 5.8	Calculated maximum flow depths from LAHARZ at stage indicator locations i—vi for two input volumes.	184
Figure 5.9	Example averaged velocity distribution over simulated probability field, for $\text{stdv} = 0.5$ m and spatially variable R (identifier: pb05h574vrf2); mean, μ , and standard deviation, σ , of velocity in each reach of the Belham are also shown.	186
Figure 6.1	Permanent population on Montserrat by official enumeration district; all other areas are uninhabited. The Belham River drainage basin has been highlighted and towns and villages in close proximity to the catchment have been labelled; those retaining inhabitants have their demographic breakdown shown in tabular form. (Population information from the Physical Planning Unit; statistics correct as of November 2007).	201

Figure 6.2	a) zones of the Hazard Level System with some defining features highlighted; b) current Hazard Level 3 (March 2010, courtesy of MVO).	204
Figure 6.3	Summary schematic of Phase II and contributions from the different chapters	215
Figure 6.4	Alternate ways of conveying the short- to mid-term hazard: a) probable dominant flow routes and b) corresponding spatial distribution of velocity (after Figure 5.7 and Figure 5.9, Chapter 5)	220
Figure 6.5	Planimetric inundation area from LAHARZ compared to the geometry of past deposits (as of November 2006).	222
Figure 6.6	Belham Valley hazard map produced in ESRI's ArcMap (aerial photograph courtesy of the Physical Planning Unit Montserrat, permission by DMCA)	222
Figure 6.7	'Exploded' 3D visualisation of the lahar hazard zones displayed in a GIS (ESRI's ArcScene).	223
Figure 7.1	Geospatial activities that have contributed/ shown potential for contribution to lahar hazard management on Montserrat (amended from Chapter 2, Figure 2.12).	242

LIST OF TABLES

Table 2.1	Ten highest ranking disasters precipitated by natural hazard(s) from 1980—2009, impacts shown as fatalities and economic losses. * EM-DAT has separated the Indian Ocean tsunami (2004) into two separate disasters, dependent on principal country affected; thus the Venezuela flash flood (1999) has also been included in the ranking. (After CRED, 2010, and Munich Re, 2010)	11
Table 2.2	Ten highest ranking volcanic disasters of the 20th Century, ordered by number of fatalities (after Witham, 2005).	12
Table 2.3	20th Century deaths from lahars and debris flows (associated with volcanic activity), where number of deaths > 10. Syn-eruptive lahars are given a ‘primary’ classification and lahars, and very dilute flows, indirectly related to eruptions are classified as ‘secondary’. *Estimates where death-by-lahar is unknown. **Indirectly associated with volcanic activity. Dev refers to level of development. (After Tanguy <i>et al.</i> , 1998, Witham, 2005, and Scott <i>et al.</i> , 2005)	15
Table 3.1	Basic confusion matrix Method 1 (columns : control) against Method 2 (rows : test) for Primary 10m, stdv 0.5 m, End Point 26. ErrorO = Errors of Omission (expressed as proportions), ErrorC = Errors of Commission (expressed as proportions)	112
Table 3.2	Raw disagreement from confusion matrices (as a proportion), Kappa statistic and confidence limits	112
Table 4.1	LAHARZ assumptions (After Iverson <i>et al.</i> , 1998)	130
Table 4.2	n flows of equal volume, V_i , required to satisfy observed mean deposit depth of 2.71 m, assuming a uniform deposit depth of d_s .	141
Table 5.1	Manning’s coefficient values for different land-cover types	181
Table 5.2	Zonal statistics of the regular grid of maximum flow depths shows the variation of flow depths within each reach of the channel	184
Table 5.3	Probability map statistics for different input parameters, end point A	186
Table 5.4	Individual flow path statistics for different input parameters, end point A	187

Table 6.1	Potential users for lahar hazard information and their timescale(s) of interest	209
Table 6.2	Attainable outputs relevant to end-user requirements	212
Table 6.3	Area inundated (for one model run) and output statistics for individual flow paths, averaged from 100 simulations (control_1 data were taken from Chapter 5, Section 5.3.2); where μ = mean value and σ = standard deviation of values.	224
Table 7.1	Overview of evidence for attainment of project objectives	235

LIST OF ACRONYMS

ASTER	Advanced Spaceborne Thermal Emission And Reflection Radiometer
BCS	British Cartographic Society
CRED	Centre for Research on the Epidemiology of Disasters
D8	Deterministic-eight
DEM	Digital Elevation Model
DFID	Department for International Development
DMCA	Disaster Management Coordination Agency
ESRC	Economic and Social Research Council
EM-DAT	Emergency Events Database
FEMA	Federal Emergency Management Agency
GI	Geographical Information
GIS	Geographical Information System
GoM	Government of Montserrat
GPS	Global Positioning System
HLS	Hazard Level System
HMG	Her Majesty's Government
IAVCEI	International Association of Volcanology and Chemistry of the Earth's Interior
IDNDR	International Decade for Natural Disaster Reduction
ISDR	International Strategy for Disaster Reduction
ITCZ	Inter-tropical Convergence Zone
LiDAR	Light Detection and Ranging
MVO	Montserrat Volcano Observatory
NDPRAC	National Disaster Preparedness and Response Advisory Committee
NGO	Non-government Organisation
NRC	National Research Council
NERC	Natural Environment Research Council
PDF	Probability Distribution/Density Function
PPGIS	Public Participation Geographical Information System
PRA	Participatory Rural Appraisal
RMSE	Root Mean Square Error
SAC	Scientific Advisory Committee
SAR	Synthetic-aperture Radar
SDP	Sustainable Development Programme
SDSS	Spatial Decision Support System
SID	Small Island Developing

SRTM	Shuttle Radar Topography Mission
TIN	Triangulated Irregular Network
UCGIS	University Consortium for Geographical Information Science
UEA	University of East Anglia
UN	United Nations
UNDP	United Nations Development Programme
UNDRO	United Nations Disaster Relief Organization
WCDR	World Conference on Disaster Reduction

ACKNOWLEDGEMENTS

This research was supported financially by an ESRC-NERC interdisciplinary studentship which funded three happy years at UEA and also enabled me to travel to the beautiful island of Montserrat, West Indies, for fieldwork. I am indebted to the staff at Montserrat Volcano Observatory, Disaster Management Coordination Agency and Governor's Office for their support, guidance and data. This research would not have been possible without them, nor without the in-field expertise of Ricky Herd.

Source code for LAHARZ was made available for academic use by Steve Schilling at the United States Geological Survey and Gary Hunter (University of Melbourne) provided the Grid-cell Uncertainty Model. Chapter 3 also benefited from the comments of two anonymous reviewers. Particular gratitude also goes to Jerry Phillips at the University of Bristol for steering me through some of the physics required for Chapter 5.

I have also received invaluable personal support from my fellow PhD students at UEA. Particular thanks to Sian, Paul, and Anna, for intellectual discussion, diversion, an ear, and occasionally a shoulder. Heartfelt thanks also to the folks back 'home' in Leicester: Clare and the girls; Mum and Allan; Dad and Paula. The greatest appreciation is reserved for Andrew, for his endless patience and encouragement.

Finally, I have been very fortunate to have the unfailing encouragement from a great supervisory team; to Andrew Lovett, Jenni Barclay and Ricky Herd, I offer my sincere thanks.

CHAPTER 1: INTRODUCTION

This first chapter acts as a guide to orientate the reader through the thesis and to frame the research in its wider context. The overall aim of this research is to evaluate the usefulness of GIS-based modelling of lahars for making ‘on the ground’ planning decisions with regard to an active volcanic system. The thesis presented here is that in order to develop methodologies that have a practical utility for local hazard managers, it is necessary not only to balance user-requirements with modelling options and data restrictions, but also to consider the uncertainties introduced through imitating the behaviour of complex phenomena. Furthermore, GISs are uniquely positioned to contribute to lahar hazard management, far beyond churning out traditional hazard zonation maps.

1.1 RATIONALE AND MOTIVATION

Lahars (flows of volcanic-derived sediment and water) have been responsible for some of the worst volcanic disasters of the 20th Century (Witham, 2005). Their high density combined with their fluidity means that they are capable of travelling great distances, causing death and immense devastation. Relatively recently, lahars from an eruption of Nevado del Ruiz, Columbia, in 1985 killed over 22 000 people (Pierson *et al.*, 1990; Voight, 1990) and in 1998 a lahar at Casita volcano, Nicaragua, took over 2 500 lives (Kerle *et al.*, 2003; Scott *et al.*, 2005). In both of these cases, management of the crises were heavily criticised (Chapter 2).

Lahars are inherently spatial phenomena, highly reliant on topography; radial valleys emanating from a volcano act as conduits to these flows which can be syn- or post-eruptive. Traditionally, lahar hazard assessment heavily relied on mapping deposits and dating previous flows, with the assumption that the same general areas are likely to be inundated by the same kinds of events in the future (e.g. Crandell, 1984; Tilling, 1989). This process was carried out by scientists, or specifically sedimentologists and volcanologists. Hazard managers and decision-makers then enforced appropriate zonation of land according to relative levels of observed hazard severity. Generally separate from this, lahar models seeking to emulate the movement and behaviour of past flows were developed, and left, in academia.

The practice of hazard zonation continues, to an extent reliant on past flows, but increasingly using inundation forecasts from lahar models. Ideally, the insights and improvements in understanding gained from models should be used to inform hazard management decisions. An important question is how to ensure a hazard assessment is communicated effectively to improve the management of volcanic crises, and in particular, how to assure pertinent information and data generated in academia are not under-utilised.

Potential runout, inundation areas and intensities (i.e. flow depth and velocity) are relevant for a lahar hazard assessment. However, lahar behaviour can be difficult to emulate through models (see Chapter 2). The term 'lahar' refers to a rapidly moving mixture of solids and water, of which the unconsolidated sediment is

volcanic in origin (Smith and Lowe, 1991; Vallance, 2000). Therefore, 'lahar' is an enveloping non-descriptive name, encompassing a range of different flow types that vary according to the proportion of volcanic debris and water, which can also alter during an individual event (see Chapter 2, Section 2.3.2). Nonetheless, a suite of models are found in the literature that generally either simplify behaviour by ignoring the sediment-fluid interactions, modelling the solid-phase or fluid-phase, or incorporate the complexities of the mixture by relying on heavy parameterisation (Chapter 2, Section 2.3.4.5). State-of-the-art lahar models are excellent research tools but can be impractical to apply because they are typically data intensive and intellectually complicated. For preliminary hazard assessment, simple semi-empirical lahar models have shown promise (e.g. Schilling, 1998) and, furthermore, it is likely that the most influential parameters (and essential data) for lahar modelling will be discovered and isolated through the testing of uncomplicated models.

Additionally, lahars share characteristics with gravitational flows from different systems, from sediment-rich debris avalanches (e.g. Savage and Hutter, 1989), across a spectrum to water-rich hyperconcentrated flows (e.g. Vignaux and Weir, 1990; Macedonio and Pareschi, 1992), differing only in the origin of their sediment supply. There are significant unanswered questions regarding improving knowledge of lahar behaviour through study of equivalent flow types not derived at volcanoes and what, if anything, can be learned from analogous flow types (e.g. stream-flow, which is too dilute to be classified as lahar).

A major challenge for scientists working on active volcanic systems is the availability and/ or acquisition of data. This can limit modelling options; but, it should be recognised that data quality and data handling are just as important for gaining confident insights. Data uncertainties, and the propagation of error, are emerging issues in natural hazard assessment (mapping), burgeoning issues in GI Science (Chapter 2, Section 2.4.4.3; Chapter 3 and references therein), and relatively unconsidered notions in lahar modelling (exceptions include Toyos *et al.* (2007) and, informally, Stevens *et al.* (2002) and Hubbard *et al.* (2007)). With lives at stake, it is vital that information relating to a lahar hazard assessment appropriately reflects uncertainties.

Hazard managers and decision-makers rely on scientific assessment and advice to ensure that the appropriate mitigation and preparedness measures are in place before a crisis. However, preventable human disasters occur even when forecasts are good (e.g. Nevado del Ruiz, Columbia, 1985 (Voight, 1990)). Differing agenda, combined with the high-stress environment of an active volcanic system, foster communication difficulties (Chapter 2; Chapter 6). Recent guidelines have made themes of the conduct of scientists and the communication issues that arise during a volcanic crisis (IAVCEI Subcommittee for Crisis Protocols, 1999; McGuire *et al.*, 2009) and it has become much more relevant than previously recognised to establish the role of the visiting scientist (or external researcher) (Chapter 6).

In addition to new ways of interacting, scientists and decision-makers are also embracing 'new' tools. Recently, Geographical Information Systems (GISs) have been used by volcanologists to generate lahar hazard (and risk) zonation maps; lahars are included in some of these maps as part of a multi-volcanic hazard assessment (e.g. Pareschi *et al.*, 2000a), and a number of maps focus on the lahar-specific hazard (e.g. Hubbard *et al.*, 2007). Yet, despite the potential plethora of applications of GISs for disaster and emergency management (Coppock, 1995; Cova *et al.*, 1999; Cutter, 2003), employment of a GIS in aspects of lahar hazard management beyond map-making is seldom described in the literature (Chapter 2). There are relatively few examples of GIS-based models for lahar hazard assessment; notable exceptions are the semi-empirical LAHARZ suite of programs developed by Schilling (1998) from the work of Iverson *et al.* (1998) and Titan2D, a more physically-based model (Pitman *et al.*, 2003). There is clearly a need to evaluate the practical role(s) of geospatial methods and GISs in a 'real-world' lahar hazard management situation.

Lahars can be generated by a variety of means (Chapter 2, Section 2.1.2) and on Soufrière Hills Volcano, Montserrat (West Indies) they are associated with intense rainfall (Barclay *et al.*, 2007). Montserrat was chosen primarily because it currently lacks a review of the lahar-specific hazard (Chapter 6). Until 2001 (Matthews *et al.*, 2002), very little research had been undertaken on lahars on Montserrat; and, to date, no research has been published on modelling these lahars. However, it is known that these flows are characteristically dilute (Barclay *et al.*, 2007), a relatively

under-studied flow type (Chapter 2). Thus, insights into controls on the behaviour of Montserrat lahars may be generally applicable to other water-rich lahar systems.

Montserrat represents an active volcanic system that originally presented as a crisis (July 1995) and developed into a protracted eruption, with no opportunity to enter long-term recovery. Lahars are a threat to persons and property on Montserrat that is concurrent with other hazards. The longevity of the eruption, with continued volcanic events (e.g. pyroclastic flows and surges, sector collapse and tephra fall), provides a suite of volcanic hazard management challenges. These difficulties have been historically exacerbated on Montserrat by communication issues between (and amongst) scientists, decision-makers and the local population (Haynes *et al.*, 2008a; Chapter 2, Section 2.5).

The literature pertinent to the production of a lahar hazard assessment can be segregated into three intellectual themes:

- (1) monitoring lahars, acquisition and handling of data;
- (2) improving knowledge of lahars through modelling; and
- (3) transfer of academic research on lahars to agencies of hazard management.

Reflection on the role of GIS and geospatial activities across and within these themes will help to achieve the aims and objectives of the research.

1.2 AIMS AND OBJECTIVES

The general aim of this research is to examine the efficacy of geospatial data and tools as aids for lahar hazard assessment on an active volcanic system.

Specific objectives are:

- To understand the influence of lahars on the local environment using GIS.

- To improve understanding of lahar movement using GIS-based modelling approaches.
- To develop a digital elevation model (DEM) suitable for the objectives above.
- To delineate potential inundation areas and quantify factors relating to lahar intensity; and, to translate this information into a formal hazard assessment.
- To appreciate uncertainties in model predictions.
- To assess effective application of research findings using consultations with local scientists and authorities.

1.3 THESIS STRUCTURE

First, this thesis investigates the types of lahar models and techniques available, and then proceeds to consider the suitability of these methods for the study area. Through fieldwork, potential user requirements are considered and relevant data are acquired. A surface representation for lahar modelling is then produced. From this base, existing GIS-based models are compared and a novel, improved model is developed. Maps and visualisations of hazard zones are produced and the practical utility of the results for hazard managers and local decision-makers is evaluated.

Following this introduction, and the subsequent literature review, the main body of the thesis is comprised of four core chapters that have been written to stand independently as research papers. There is some inevitable overlap of material to allow the context to be set for individual research aims.

In Chapter 2 pertinent background information is introduced to set the research perspective. The broad issue of lahar hazard management is discussed, with reference to historic examples and the potential role of a GIS for lahar hazard management is highlighted. Gravitational-flow models are also evaluated from a range of sub-disciplines (e.g. from landslides to sediment-laden floods). The regional setting is also established. Through reflection on gaps in the existing literature, a research niche is established.

An application-driven approach to terrain model construction is presented in Chapter 3. The importance of uncertainty in elevation is considered, and propagation of error to a single-direction flow routing algorithm allows the robustness of various alternative surfaces to be tested. The utility of the novel methodology as a standard for handling terrain data is discussed. This research has also been published following peer-review (Darnell *et al.*, 2010).

Standard GIS-based models for lahar simulation are examined in Chapter 4. The surface (tested in Chapter 3) is used to update regional elevation data and methods for fusing datasets are investigated. System response to lahars is evaluated over the period of one rainy season. Two models are then used which simulate the behaviour of different end-member types of lahars: sediment-rich and water-rich. The utility of these methodologies for delineating inundation areas for long-term hazard mapping is discussed.

In Chapter 5, a novel GIS-based tool for lahar hazard assessment is developed. Existing approaches for modelling water flows have shown their potential for approximating the behaviour of dilute lahars. These ideas are developed into a GIS-based approach for routing flow according to maximum velocity.

An evaluation of the knowledge gap between science and applied research is presented in Chapter 6. Findings from Chapters 4 and 5 are presented through a range of different visualisations and evaluated in consultation with local authorities and scientists on Montserrat. Moreover, mitigation options consistent with user requests are discussed. Tangible benefits of the research are thus assessed.

Key themes woven between the chapters are made explicit in the final chapter (Chapter 7), leading to a conclusion on the utility of geospatial activities and GIS for lahar hazard assessment on Montserrat. Suggestions for advancements of the current research are also proposed and discussed.

CHAPTER 2: BACKGROUND AND REGIONAL SETTING

In this chapter a context for the study is provided through a review of the relevant research fields. Volcanic hazards and lahars are framed within the wider context of natural hazard disasters. Evolving approaches to natural hazard management and, more specifically, volcanic hazard management are described. The utility of methods and application to lahar hazard management are further discussed. The review then focuses on techniques for lahar hazard assessment, specifically: identification, modelling and zonation.

The potential for using geographic information systems (GISs) for hazard research is then examined. GIS are currently under-utilised for this application. Current endeavours in GI Science can also inform research using GIS; some key issues (including spatial data acquisition, uncertainty analysis and spatial cognition) are considered. Finally, the regional setting for this thesis, Montserrat (West Indies), is introduced. Montserrat is a small island developing state dealing with the prolonged eruption of Soufrière Hills Volcano and provides a valuable case study with wider implications for dilute lahar modelling and hazard management.

Chapters 3—6 follow and have been written as self-contained papers.

2.1 FRAMING VOLCANIC HAZARDS AND LAHARS

2.1.1 Placing volcanic disasters in context

Over the past few decades (1980—2009) more than 9 000 natural disasters were recorded globally, accounting for over two million fatalities and a combined total estimated damage of US\$ 2.6×10^{12} (CRED, 2010). Statistics also show that there was a dramatic increase in economic losses from disasters over this period (Smolka, 2006) and a rising trend in the number of people affected (Basher, 2006). As a response to these rising losses, and a recognised potential to reduce them through proper application of existing knowledge and technology, the United Nations General Assembly designated the 1990s as the International Decade for Natural Disaster Reduction (IDNDR). This body of coordinated action programmes began by putting socio-economic aspects as components of effective disaster prevention into perspective, and continues to do this through its successor, the International Strategy for Disaster Reduction (ISDR) (<http://www.unisdr.org/>). Increased interest in mitigating the effects of extreme events was also exemplified by the Hyogo Declaration adopted by the World Conference on Disaster Reduction in 2005. These initiatives also operate in parallel to concerns regarding climatic variability and its potential to exacerbate the frequency and intensity of natural hazards. All these international enterprises filter down to national strategies in individual ratifying countries.

From the outset, a couple of definitions are necessary. A ‘natural hazard’ is a physical phenomenon which causes undesired consequences for persons, settlements, infrastructure and goods. A ‘disaster’, precipitated by a natural hazard, is ‘a serious disruption of the functioning of a community or a society involving widespread human, material, economic or environmental losses and impacts, which exceeds the ability of the affected community or society to cope using its own resources’ (UN/ISDR, 2009, p9). Two key points can be taken from this definition: (a) not all natural hazards result in disasters, there must be conditions of vulnerability to that hazard and an insufficiency of capacity or coping mechanisms (Basher, 2006);

and (b) disasters are also the product of social, political and economic environments (Wisner *et al.*, 2004). Insight into effective hazard management practices can be gained from a forensic analysis of past disasters; first order statistical analyses (e.g. fatalities and economic losses) can demonstrate relative severity. Records of historical disasters and associated statistics are now available as interactive Internet databases. For example, the Centre for Research on the Epidemiology of Disasters (CRED), with the World Health Organisation, has been compiling an Emergency Events Database (EM-DAT) for disasters requiring international assistance (<http://www.emdat.be/>; see also Peduzzi *et al.*, 2005).

The scale of historic volcanic disasters in terms of areas affected and people killed is considerably less than that of hydro-meteorological events such as floods, storms and droughts (Basher, 2006) and other geological events such as earthquakes (Tomblin, 1977). From 1980–2009 the ten costliest natural disasters, in economic terms, were not precipitated by any volcano-related hazards (Munich Re, 2010), nor were volcanoes responsible for any of the ten most fatal natural disasters (CRED, 2010) (Table 2.1). The total number of people killed by volcanoes during this period was approximately 25 200, or 1.2% of all fatalities due to natural disasters (CRED, 2010). However, the bulk of these volcano-related deaths are attributed to the 1985 eruption of Nevado del Ruiz (Columbia) which killed over 23 000 people and resulted in material losses of US\$1000 million (Tilling, 1989; Voight, 1990; CRED, 2010). Very few natural hazards in the last 30 years have resulted in fatalities of this magnitude; for example, only 34 natural disasters have killed more than 5 000 people in a single event (CRED, 2010).

Databases specific to the socio-economic impacts of volcanic disasters have been compiled (Simkin and Siebert, 1994; Tanguy *et al.*, 1998; Witham, 2005) and an extract for 20th Century volcanic disasters is provided in Table 2.2. Currently, the Smithsonian's Global Volcanism Program seeks better understanding of all volcanoes by extensively documenting their eruptions in an active (regularly updated) Internet database for electronic query (Siebert and Simkin, 2010).

Rank	Killed (CRED, 2004)		Overall economic losses (Munich Re, 2010)	
	Event (principal country affected)	People	Event (principal country affected)	US\$ million
1	Drought, 1983—1984 (Ethiopia)	300 000	Hurricane Katrina, 2005 (USA)	125 000
2	Sumatra-Andaman earthquake/ 'Indian Ocean' tsunami, 2004 (Indonesia)*	165 708	Kobe earthquake, 1995 (Japan)	100 000
3	Drought, 1983—1985 (Sudan)	150 000	Wenchuan earthquake, 2008 (China)	85 000
4	Cyclone Gorky, 1991 (Bangladesh)	138 866	'Northridge' earthquake, 1994 (USA)	44 000
5	Cyclone Nargis, 2008 (Myanmar)	138 366	Hurricane Ike, 2008 (USA)	38 000
6	Drought, 1981—1985 (Mozambique)	100 000	Floods, May—September 1998 (China)	30 700
7	Wenchuan earthquake, 2008 (China)	87 476	Niigata earthquake (Japan)	28 000
8	Kashmir earthquake, 2005 (Pakistan)	73 338	Hurricane Andrew, 1992 (USA)	26 500
9	Manjil-Rudbar earthquake, 1990 (Iran)	40 000	Floods, June—August 1996 (China)	24 000
10	Sumatra-Andaman earthquake/ 'Indian Ocean' tsunami, 2004 (Sri Lanka)*	35 399	Hurricane Ivan, 2004 (USA)	23 000
10*	Flash flood, 1999 (Venezuela)	30 000		

Table 2.1 Ten highest ranking disasters precipitated by natural hazard(s) from 1980—2009, impacts shown as fatalities and economic losses. * EM-DAT has separated the Indian Ocean tsunami (2004) into two separate disasters, dependent on principal country affected; thus the Venezuela flash flood (1999) has also been included in the ranking. (After CRED, 2010, and Munich Re, 2010)

While the scale of volcanic disasters (Table 2.2) may not be as great as other natural hazards (Table 2.1), in contrast to causes of other natural disasters, volcanoes present a relatively unique set of management issues. First, volcanic hazards are capable of early identification. Most active (land) volcanoes have been identified and these number relatively few; around the order of twenty volcanoes are erupting at any given moment and only 1 300 have been active in the past 10 000 years (Simkin, 1993). Furthermore, volcanoes impact specific locations (usually proximal to an identified vent) (Tomblin, 1977) and there is typically precursor

activity to an eruption, often enabling forecasts and early warnings to be issued (UNDRO, 1985). Secondly, volcanic hazards can be as diverse as they are severe. Damage from volcanoes is extremely intensive within the relatively small areas they affect (Tomblin, 1977; UNDRO, 1979). An eruption can present as multiple individual hazards, such as pyroclastic flows (rapidly moving mixtures of rock debris and hot gas), tephra fall (rock debris), lava flows (molten rock) and lahars (rapidly moving mixtures of rock debris and water). The types of hazard depend on the eruption (defined by the properties of the magma, mechanism for energy release etc.) and external factors (such as influx of water for lahars). Thus, all volcanic eruptions can behave differently; some of these differences are shown in Table 2.2.

Rank	Event	Principal hazard(s)	People	Reference
1	Peléé, 1902 (Martinique)	Pyroclastic flows and surges	29 000	Roobol and Smith (1975); Fisher and Heiken (1982)
2	Nevado del Ruiz, 1985 (Columbia)	Lahars	23 080	Voight (1990)
3	Santa Maria, 1902 (Guatemala)	Tephra and epidemic	8 750	Rose (1972) Williams and Self (1983)
4	Kelut, 1919 (Indonesia)	Lahars	5 110	See Thouret <i>et al.</i> (1998) and references therein
5	Santa Maria, 1929 (Guatemala)	Pyroclastic flows and lahars	5 000	See Rose (1973) and references therein
6	Lamington, 1951 (Papua New Guinea)	Pyroclastic flows	2 942	Taylor (1954)
7	El Chichon, 1982 (Mexico)	Seismicity and tephra	2 000	Varekamp <i>et al.</i> (1984); Tilling (2009) and references therein
8	Lake Nyos, 1986 (Cameroon)	Gas	1 746	Kling <i>et al.</i> (1987); Sigurdsson (2007)
9	Soufriere, 1902 (St Vincent)	Pyroclastic flows	1 565	Roobol and Smith (1975)
10	Merapi, 1930 (Indonesia)	Pyroclastic flows	1 369	See Newhall <i>et al.</i> (2000) and references therein

Table 2.2 Ten highest ranking volcanic disasters of the 20th Century, ordered by number of fatalities (after Witham, 2005).

2.1.2 Introducing the lahar hazard

The destructive capability of volcanoes can also linger beyond an eruptive event. Loose volcanic material left proximal to a volcano by primary volcanic activity such as pyroclastic flows, tephra fall and (partial) edifice failure, can be remobilised by water into lahars during, and beyond an eruption. 'Lahar' is a general term for a rapidly flowing mixture of rock debris and water (strictly that is other than stream-flow) from a volcano (Smith and Lowe, 1991). Sudden water release and/ or flank collapses are the triggering mechanisms for lahars. The melting of summit glacier or snow cap (e.g. by fall of hot tephra), outburst from crater lakes and rainfall runoff can all generate lahars through rapid water input. Magma ascent can also lead to upheaval of the water table (Roobol and Smith, 1975). Furthermore, although most flank collapses behave as debris avalanches, lahars can be generated if there is adequate pore and hydrothermal water (Vallance, 2000; Scott *et al.*, 2001; Scott *et al.*, 2005). Initiation requires a mass sufficiently saturated with water, subsequent failure of the mass and sufficient conversion of gravitational potential energy to internal kinetic energy which induces a widespread deformation that can be recognised as a flow (Iverson, 1997). Triggering mechanisms influence the volume, discharge rate and characteristics of the flow (Fagents and Baloga, 2006) and thus play a fundamental role in the down-valley destructive power of a lahar (Macedonio and Pareschi, 1992).

Like water flows (stream-flow), lahars are fluid enough to travel long distances in channels with modest slopes and to inundate vast areas (Iverson, 1997; UNDRO, 1985). Runout distances vary greatly from a few kilometres to more than a hundred kilometres in confined channels (Scott *et al.*, 2001; Newhall and Hoblitt, 2002). A key component of this mobility is the ability of flows to grow in volume in distal areas (Scott *et al.*, 2005). Therefore, lahar hazard can actually increase with distance from the vent, if water or sediment is still being added (Newhall and Hoblitt, 2002).

Lahars that remain in their channel are (typically) of little immediate threat (Newhall and Hoblitt, 2002). However, 'large' flows can inundate floodplains and in contrast to floods, lahars can be much more destructive owing to their sediment load (Kerle and Oppenheimer, 2002). Lahar velocity, discharge and transport

capacity are typically much higher than 'normal' stream flows (Lavigne and Thouret, 2002). Damage to properties or infrastructure can result from the impact of fast moving boulders, inundation by layers of muddy debris, or undermining by bank erosion (Jakob and Weatherly, 2008). Furthermore, after coming to rest, their deposits can be too deep, too soft or too hot to cross (UNDRO, 1985).

2.1.2 Lahar disasters: lessons learned from history

Databases of volcano-related deaths (Tanguy *et al.*, 1998; Witham, 2005) reveal some interesting trends. For example, from AD 1783 to 1998 lahars have been responsible for 17% of all volcano-related fatalities (Tanguy *et al.*, 1998). In the 20th Century, primary and secondary lahars (directly and indirectly associated with volcanic eruptions respectively) were partly responsible for three of the deadliest volcano-related disasters (Table 2.2), accounted for 11% of all injuries directly linked to volcanic activity, 18.5% of all people made homeless, and evacuations of over one million people (Witham 2005). Tanguy *et al.* (1998) argue at least some of these events could have been anticipated and losses reduced through adequate scientific and social response.

Table 2.3 shows 20th Century fatalities associated with lahars and debris flows in volcanic terrains. Most of the information is taken from Witham's (2005) database and corroborated with the Tanguy *et al.* (1998) study. However, it is unclear why debris flows have been given a separate classification. The standard definition of lahars includes any water-sediment-flow from a volcano excluding the very dilute stream-flow, i.e. includes volcanic-induced debris flows (Smith and Lowe, 1991; Vallance, 2000). In Witham's (2005) database, the debris-flow distinction appears to reflect a more sediment-rich (or drier) type of flow than their definition of lahar. Water-sediment flow types will be discussed in greater detail in Section 2.3.2.

Most individual lahar/ debris-flow events, with associated fatalities, in the 20th Century have occurred in South-east Asia and, more generally, in areas of low development (Table 2.3). However, the table is dominated by individual events with extreme loss, or 'disasters'. A few of these are examined in further detail below.

Date	Volcano	Country	Region	Dev	Event	Killed
22/05/1901	Kelut	Indonesia	South-east Asia	L	Primary lahar	100
05/05/1902	Pelee	Martinique	Caribbean	H	Primary lahar	423
29/08/1909	Semeru	Indonesia	South-east Asia	L	Primary lahar	221
12/01/1914	Sakura-jima	Japan	East Asia	H	Debris-flow	58
10/09/1914	White Island	New Zealand	Oceania	H	Debris-flow	11
1914	Aoba	Vanuatu	Oceania	M	Primary lahar	12
19/05/1919	Kelut	Indonesia	South-east Asia	L	Primary lahar	5 110
24/05/1926	Tokachi	Japan	East Asia	H	Primary lahar	144
02/11/1929	Santa Maria	Guatemala	Central America	M	Primary lahar	5 000*
18/10/1948	Villarica	Chile	South America	H	Primary lahar	40
12/1949	Villarica	Chile	South America	H	Primary lahar	36
1952	Binuluan	Philippines	South-east Asia	M	Primary lahar	12
24/12/1953	Ruapehu	New Zealand	Oceania	H	Secondary lahar/ flood	151
17/03/1963	Agung	Indonesia	South-east Asia	L	Primary lahar	163
21/05/1963	Villarica	Chile	South America	H	Primary lahar	15
10/12/1963	Irazu	Costa Rica	Central America	H	Primary lahar	30
03/03/1964	Villarica	Chile	South America	H	Primary lahar	25
24/04/1966	Kelut	Indonesia	South-east Asia	L	Primary lahar	211
29/12/1971	Villarica	Chile	South America	H	Primary lahar	15
25/11/1976	Merapi	Indonesia	South-east Asia	L	Secondary lahar/ flood	29
11/11/1976	Semeru	Indonesia	South-east Asia	L	Primary lahar	40
19/09/1978	Semeru	Indonesia	South-east Asia	L	Secondary lahar/ flood	12
30/04/1979	Merapi	Indonesia	South-east Asia	L	Secondary lahar/ flood	80
14/05/1981	Semaru	Indonesia	South-east Asia	L	Secondary lahar/ flood	372
30/06/1981	Mayon	Philippines	South-east Asia	M	Secondary lahar/ flood	47
14/09/1984	Ontake	Japan	East Asia	H	Debris-flow	29
13/11/1985	Nevado del Ruiz	Columbia	South America	M	Primary lahar	23 080
10/02/1990	Kelut	Indonesia	South-east Asia	L	Primary lahar	35
01/1991	Santa Maria	Guatemala	Central America	M	Debris-flow	25
14/06/1991	Pinatubo	Philippines	South-east Asia	M	Primary lahar	100*
1992	Pinatubo	Philippines	South-east Asia	M	Primary lahar	26
04/10/1993	Pinatubo	Philippines	South-east Asia	M	Primary lahar	14
06/06/1994	Huila	Columbia	South America	M	Debris-flow	650
22/11/1994	Merapi	Indonesia	South-east Asia	L	Primary lahar	64
06/09/1995	Parker	Philippines	South-east Asia	M	Secondary lahar/ flood	60
30/10/1998**	Casita	Nicaragua	Central America	L	Secondary lahar/ flood	2 500

Table 2.3 20th Century deaths from lahars and debris flows (associated with volcanic activity), where number of deaths > 10. Syn-eruptive lahars are given a 'primary' classification and lahars, and very dilute flows, indirectly related to eruptions are classified as 'secondary'. *Estimates where death-by-lahar is unknown. **Indirectly associated with volcanic activity. *Dev* refers to level of development. (After Tanguy *et al.*, 1998, Witham, 2005, and Scott *et al.*, 2005)

On November 13, 1985, a small plinian eruption of Nevado del Ruiz (Colombia) produced the deadliest set of lahars in recorded history (Pierson *et al.*, 1990). Pyroclastic flows and surges melted snow and ice to form debris flows (sediment-rich lahars) which killed 23 080 people (magnitude from Witham, 2005). It transpired that the town of Armero had been built on the pathway of historical flows (Voight, 1990) and potential for the tragedy had been predicted by scientists (Pierson *et al.*, 1990). Yet there was a lapse of four hours between the eruption and the initiation of evacuations and few agreed to leave their homes; by hour-eight a lahar had enveloped Armero (Wisner *et al.*, 2004).

The eruption of Pinatubo (Philippines) in June 1991 demonstrates the longer-term impacts of a volcanic disaster; there were not only immediate casualties (mainly from tephra and lahars) but also population displacement on a massive scale (Vallance, 2000). Witham (2005) put the figure of the total affected (including injuries, homelessness and evacuations) at over one million people. Scientists had foreseen the eruption and were able to reduce losses by evacuating people in successive zones months before the main event (Newhall *et al.*, 1997). However, the extreme sediment yields from pyroclastic flows left an almost unlimited sediment supply for subsequent lahars (Hayes *et al.*, 2002). Lahars generated by rain falling on the unconsolidated 1991 deposits were a very significant immediate and long-term hazard to areas surrounding the volcano as far out as 50–60 km (Pierson *et al.*, 1992).

Lahars can also be indirectly associated with volcanic activity. On May 5, 1998, very intense rains caused upper slopes of the Sarno Mountains (Italy) to fail. Resulting sediment-rich lahars (debris flows) killed 150 people and there was substantial damage to property (Toyos *et al.*, 2007). The collapsed material consisted largely of tephra from numerous eruptions of Vesuvius, 12-15 km upwind of Sarno (Scott *et al.*, 2001). Long-term urbanisation and the progressive degradation of natural vegetation were factors contributing to the 1998 disaster (Pareschi *et al.*, 2000b). Sarno lahars are not included in Witham's (2005) database, due to their initiation away from a volcano; however, they are included here due to their volcanic-derived sediment content. For a full review of flank-collapse debris flows (including lahars) see Scott *et al.* (2001).

The Casita (Nicaragua) event in 1998, also absent from Witham's database, has been included in Table 2.3 as although not directly related to an eruption, the debris-flow was initiated at the volcano (thus by definition a lahar). On October 30, 1998, hurricane precipitation triggered a small flank collapse, which evolved into a watery debris-flood (<60% sediment by volume) and further bulked to become a debris-flow (Scott *et al.*, 2005). Two-thousand five hundred lives were lost and the local responsible agencies were heavily criticised for their 'lethargic response' (Kerle *et al.*, 2003). However, later rainfall generated lahars in 1999 and 2000 took no lives due to an active education programme and lessons learnt from the 1998 event (Devoli *et al.*, 2000 as cited in Scott *et al.*, 2005). Whilst the 1998 event could have been predicted - communities were developed on a prehistoric lahar pathway (Scott *et al.*, 2005) - recent work by Kerle and Oppenheimer (2002) and Kerle *et al.* (2003) revealed that satellite imagery available at the time could not have significantly improved the disaster response.

Notwithstanding the examples above, not all lahars result in disasters. Primary lahars (concurrent with eruptions) have forced many mass evacuations in recent history with no deaths, e.g. Nevado del Ruiz (1986), 15 000 'affected' (injured, homeless and/ or evacuated); Nevado del Ruiz (1989), 5 000 affected; Unzen (Japan, 1991), 1 200 affected; Soufrière Hills (Montserrat, 1995), 7 500 affected (Witham, 2005). In these instances hazard management was effectual for avoiding disasters.

2.2 NATURAL HAZARD MANAGEMENT

2.2.1 General and evolving approach to natural hazard management

There is a conceptual framework for how societies respond to disasters, which often is referred to as the emergency or disaster management cycle (Figure 2.1). The temporal dimension of management is reflected through four (often overlapping) phases: mitigation, preparedness, response and recovery, cycling back to mitigation. Hazard management activities can start anywhere in the cycle, i.e. with a sudden onset event, predicted threat, or identification of a 'new' hazard after many years. For example, after a potential hazard has been recognised, long- and short-term planning objectives are referred to as mitigation and preparedness respectively (Figure 2.1).

Potential impacts can be assessed through improving understanding of behaviour and processes using field observations, modelling or some combination of the two (hazard assessment). Poor management, or extreme events, will lead to disasters.

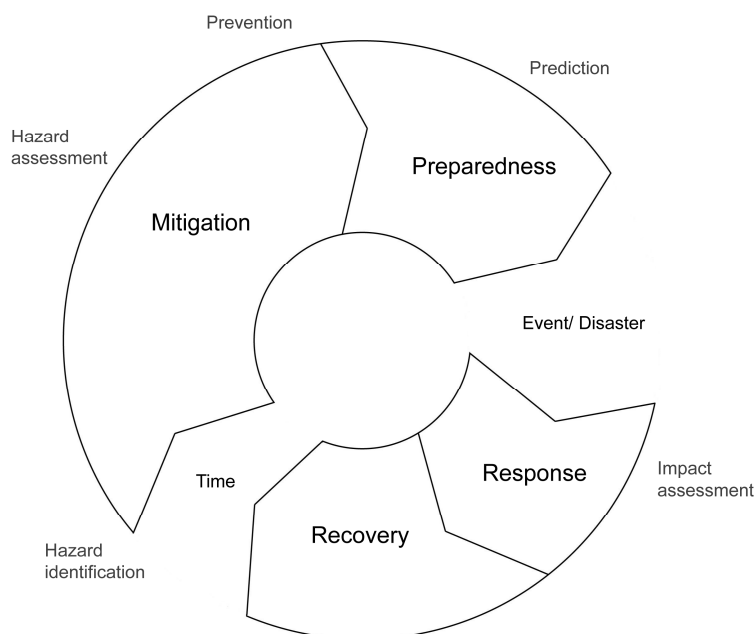


Figure 2.1 Disaster management cycle showing the temporal dimension (clockwise) (after Drabek and Hoetmer, 1991; Cova, 1999)

An appraisal of impacts will guide response and recovery. Planning for the next event may begin immediately or many years may pass before the next event is likely. Thus the position of society in the cycle determines which activities are available, and the timescales in which they are operable.

Another interesting prescribed system governs the warning process, immediately before an event (Figure 2.2). Applicable to all natural hazards, this framework describes the downward filter of precise information, from the sciences, to organisational and social components. However, the linkages between these subsystems tend to be fragile (Alexander, 2007) and the traditional division of primary responsibility, shown in Figure 2.2, is becoming increasingly blurred.

It has now been recognised, in natural hazard studies, that a top-down approach to data sharing in disaster management is not entirely effective (e.g. Radke *et al.*, 2000). There is a lack of (effective) transfer of research findings from science to agencies responsible for hazard management (e.g. Gomez-Fernandez, 2000). It has further been argued that the necessity is not for more information, but rather for wider application of existing technology (Tilling, 1989).

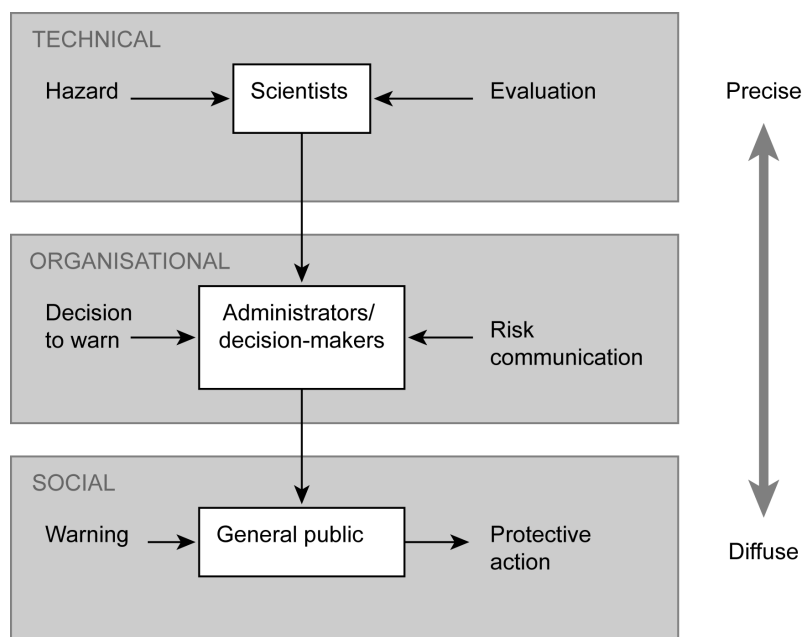


Figure 2.2 The warning process and its subsystems (after Alexander, 2007).

Consequently, there has been a call for a reorientation of research from the traditional approach in which scientists set the agenda to one in which end-users do (Alexander, 2008 (referring to mass-movement studies)). Furthermore, other interested parties can aid hazard assessment processes, e.g. there is scientific basis for incorporating (subjective) judgements on sparse or missing data (e.g. Neri *et al.*, 2008). It has been argued that ultimately a partnership between the scientific/academic community and the emergency management community is required for sustainable hazard management (Ferrier and Haque, 2003). Moreover, if disaster reduction is to be attainable, the social and natural physical sciences need to work together for risk communication (e.g. Barclay *et al.*, 2008; Darnell and Barclay, 2009).

The term 'natural hazard' does not reflect the diversity of disciplines working in disaster studies, including sociology, psychology, policy studies and risk management (Zerger and Smith, 2003). Hazard management typically focuses on technological solutions including engineering solutions, the study of hazard intensity, event, frequency and hazard detection (Zerger and Smith, 2003; Figure 2.2). This is consistent with the 'technological-fix paradigm' that deems the geophysical processes that produce hazardous events to be more important than, for example, socio-economic considerations (Rashed *et al.*, 2007). Since the 1990s, the IDNDR natural hazard research has shifted focus to a more socially sensitive methodology (Chester *et al.*, 2002), including considerations of risk, vulnerability and societal sustainability.

The Office of the United Nations Disaster Relief Coordinator (UNDRO) established a set of terms for use in disaster studies to be widely understood and accepted; they defined risk as the expected number of lives lost, persons injured, damage to property and disruption of economic activity due to a particular natural phenomenon (UNDRO, 1979). There have been attempts to quantify risk based on such socio-economic factors. For example, hazard (H), vulnerability (V) and value of exposed elements (E) can define a standard expression of risk (R):

$$R = E \times V \times H$$

[Equation 2.1, Tilling 1984]

Or, more simply,

risk of a disaster, $R = H \times V$ [Equation 2.2, Wisner *et al.*, 2004]

In natural hazard studies, risk has been assessed through hazard identification, estimation of risk and vulnerability and social consequence evaluation (Ferrier and Haque, 2003). Hazard maps (frequently used tools for communicating spatial variation of threat) have often simply been augmented with vulnerability factors to evaluate (quantitative) risk (e.g. Mejia-Navarro *et al.*, 1994; Lirer and Vitelli, 1998; Gomez-Fernandez, 2000; Pareschi *et al.*, 2000a; Thouret *et al.*, 2000). Ferrier and Haque (2003) developed a general (multi-hazards) framework for quantifying risk in a community through numerical ranking of the frequency of the event, the severity or magnitude of an event and the social consequence (a combination of community perception of risk level and collective will to address the problem). These rankings were then multiplied to give a score to compare community exposure levels from different hazards. However, the notion that risk can be adequately quantified has been largely discredited by the social sciences (e.g. Jasonoff, 1999).

2.2.2 Evolving techniques in natural hazard assessment

There are also techniques for assessment that apply to all natural hazards, and like the frameworks for management above (Figures 2.1 and 2.2) these are evolving.

2.2.2.1 *The role and challenges of hazard zonation*

Zonation maps are a crucial output from the assessment of many natural hazards (Radke *et al.*, 2000). Locations of natural hazards vary spatially, the media through which hazardous effects are propagated possess physical properties that vary spatially and the populations that might be exposed are also spatially distributed (Emmi and Horton, 1995); therefore maps are an obvious receptor for hazard assessment results (Monmonier, 1998). For long-term forecasts (months—years), maps can aid land-use planning (e.g. Lirer and Vitelli, 1998) and, in the shorter term

(days-weeks), can help mobilise planners and an affected population into action during an emergency phase. Maps are traditionally crucial in the risk communication process as the graphical display of information is easier for non-technical users to understand (Crozier *et al.*, 2006). Therefore mapping of lahar hazards is an important mechanism for disaster prevention and disaster management (Huebl and Fiebiger, 2005).

However, drawing lines of equal hazard on a map can be difficult for scientists due to natural variability and model uncertainty. For example, no flood inundation extents can be precisely defined by a single line (Smemoe *et al.*, 2007). Furthermore, even the most rigorous estimation techniques can be undermined by climatic change and land development (Monmonier, 1998). In addition to the difficulties faced by the scientific community, the exact location of each line may be scrutinised carefully by decision-makers because of the possible legal implications and far-reaching land-use decisions (Jakob, 2005). Therefore, a local hazard map is only ever a snapshot in time, scientists and local regulators have to decide if and when to re-draw a hazard map (Jakob, 2005). It follows that for sustainable management a map-making methodology should be capable of straightforward updating. Increasingly the digital map-making capabilities of GIS are being exploited for natural hazard assessment (this will be discussed further in Section 2.4).

Guidelines have been introduced for some natural hazards; for example, Multinational Andean Project (2008) introduced standard terminology, techniques, classification systems and cartographic symbols for landslides. Furthermore, in the USA, the Federal Emergency Management Agency (FEMA) have introduced guidelines and specifications for flood hazard mapping partners (http://www.fema.gov/plan/prevent/fhm/gs_main.shtm, accessed May 2010). Generally, however, there is an absence of standardised methods and techniques for producing hazard zonation maps; especially when individual countries or agencies work independently in a study area.

2.2.2.2 Recognition of uncertainties

Generally, the value of scientific advice to a policy-maker or manager will depend on how well its validity and relative importance can be assessed (Brown *et al.*, 2007).

However, uncertainty in hazard predictions is inevitable. Distinction is made between two kinds of uncertainty: aleatory and epistemic, the former is related to the randomness of natural phenomena and the latter is due to the insufficient knowledge about the validity of alternative mathematical models and the values of their input parameters (Barani *et al.*, 2007). Uncertainties in model predictions originate from inadequate sampling of model inputs, poorly constrained parameter values, and simplified representations of complex environmental processes, among others (Brown *et al.*, 2007).

Uncertainty is also intrinsic to decision-making because of the choices that have to be made (Agumya and Hunter, 1999). Estimation of decision uncertainty requires knowledge of the uncertainty present in all the data employed and how it propagates and is amplified as the data are processed and transformed (Agumya and Hunter, 1999). Uncertainty increases when decision-making is data-starved, the process of extracting support information is flawed or communicating information accurately or effectively is impeded (Radke *et al.*, 2000).

However, more informed decision-making in emergency management can be enabled if data and model assumptions are made explicit to end-users through a consideration of uncertainty (Zerger, 2002). Monte Carlo procedures that rely on repeated random sampling of input variables to compute their results are a common approach to considering uncertainties in hazard assessment, particularly in model predictions (e.g. Emmi and Horton, 1995; Gomez-Fernandez, 2000; Calvo and Savi, 2009). For continuous variables, the procedure begins with the selection of a range and a probability distribution function (*pdf*) for an, or each, input variable (e.g. Tarantola *et al.*, 2002). Values are then sampled from the *pdf*(s) and model response to variation in the inputs is evaluated. The Monte Carlo procedure has also been applied to mass movements for triggering, propagation and stoppage (Calvo and Savi, 2009), combined with simple flow routing (e.g. Gomez-Fernandez, 2000), probabilistic modelling of uncertainties in earthquake-induced landslide hazard assessment (Refice and Capolongo, 2002) and for demonstrating floodplain uncertainty (Smemoe *et al.*, 2007). Emmi and Horton (1995) used a Monte Carlo simulation of error propagation to induce random disturbances in ground shaking

and intensity zone boundaries. They were then to be able to assess the effect of error on the model without actually refining the data.

Additionally, or alternatively, event or logic tree analysis is an inductive logic technique that constructs a network of possible scenarios, starting from an initiating event through intermediate events to a set of ultimate possible adverse consequences (Agumya and Hunter, 1999). Using this structure, Monte Carlo procedures can also be applied to any of the branches.

2.2.3 Volcanic hazard management

2.2.3.1 Traditional framework for volcanic hazard management

Volcanic eruptions are uncontrollable phenomena but effective management can mitigate the impacts of their products, and potentially stop the manifestation into disasters. Long-term planning has often been central to volcanic hazard management, as with many other natural hazards. Traditionally, volcanic hazard mitigation (or certainly the literature) has focused on hazard identification, assessment and zonation (Tilling, 1989), with the principal objective of producing maps showing zones of equal hazard (Crandell, 1984). These maps were typically drawn by volcanologists based on the records of each volcano's history, supplemented and extended back by stratigraphic studies (UNDRO, 1979; Crandell, 1984; UNDRO, 1985; Tilling, 1989). The inference is that all historic hazards were considered separately and amalgamated. Decision-makers and local authorities then would use this spatial information as the first element of a volcano emergency plan (UNDRO, 1985). Volcanic hazard maps remain a crucial store for long-term forecasts and for long-term planning (e.g. Barclay *et al.*, 2008), but they are now increasingly informed by assessment using (computer) modelling. For active volcanic environments, local morphology can change over even shorter time intervals e.g. between the preparation of a given map and the date of the next eruption (Thouret *et al.*, 2000). Thus, it is necessary that maps for volcanic hazard management should be reliable, applicable but also flexible and rapid (Malin and Sheridan, 1982).

Short-term forecasts occur in the preparedness phase of the disaster management cycle (Figure 2.1) and are also carried out by monitoring scientists. Precursors for an eruption are common, and include elevated seismic activity, ground deformation, hydrothermal phenomena and chemical changes of gas discharges (UNDRO, 1985). These signs of instability or unrest are collectively termed a volcanic crisis and require continuous scientific monitoring (IAVCEI Subcommittee for Crisis Protocols, 2000). Ability to forecast is being advanced by new technology and becoming more quantitative, incorporating probabilistic terms that take into account uncertainties (Sparks, 2003). However, there is no perfectly reliable indicator for an eruption. Scientists make predictions and pass these on to decision-makers. Information is then transferred, as necessary, to the general public. One of the most difficult aspects of volcanic hazard management is whether to evacuate (Woo, 2008).

The various activities, and players, in a traditional approach to volcanic hazard mitigation are shown in Figure 2.3. This schematic is adapted from the guidelines for effective mitigation provided by Tilling (1989). Note the similarities with transfer from scientists to decision-makers to the general public from Figure 2.2.

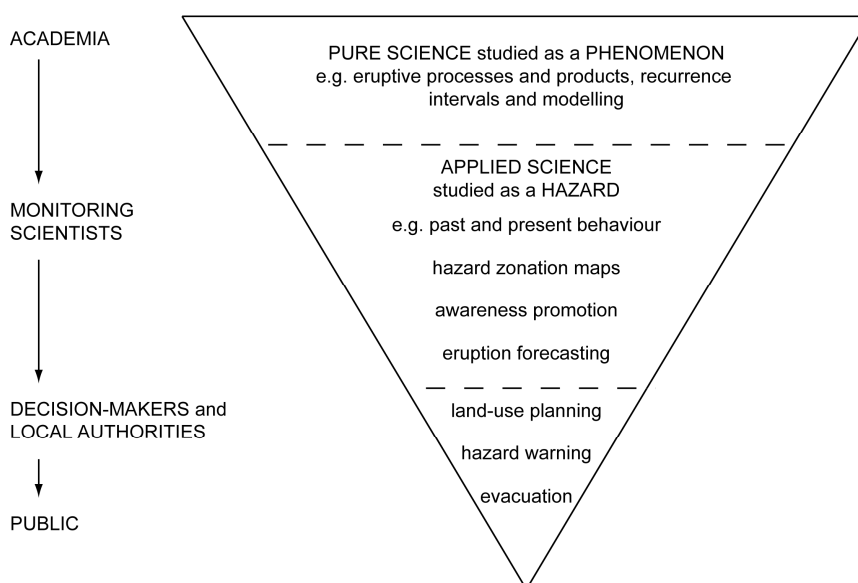


Figure 2.3 Volcanic hazards mitigation and transfer of science viewed as an inverted pyramid (modified substantially from Tilling, 1989, and Alexander, 2007)

2.2.3.2 Volcanic hazard modelling

The use of models as part of the hazard assessment process has increased dramatically with the copious use of computer-based technology. Modelling can glean information on a range of factors associated with volcanic phenomena. Modelling approaches have also evolved.

Deterministic hazard assessment approaches are event- or scenario-based, i.e. they recreate an event through a model of a physical process or a 'what-if' scenario. Degrees of hazard are typically assessed by threshold classes of process intensity for different events with a given recurrence interval (e.g. Staffler *et al.*, 2008). However, recently there has been a paradigm shift in volcanic hazard management to include probabilistic concepts, such as 'treatment of uncertainties' and 'short- and long-term hazard forecasting' (Neri *et al.*, 2008), leading some authors to define hazard as the probability of a point being affected by a hazardous process during a considered time interval (e.g. Felpeto *et al.*, 2007). A probabilistic approach is useful as uncertainties are inevitable when trying to simulate or predict natural phenomena (see above, Section 2.2.2.2).

Newhall and Hoblitt (2002) proposed an event tree scheme to estimate the probability of all the relevant possible outcomes of a volcanic crisis. Event trees have become common for a practical holistic approach to volcanic crises and include both primary and causal (secondary) hazards (e.g. Newhall and Hoblitt, 2002; Neri *et al.*, 2008). Branches are used to summarise all the relative likelihoods relating to the genesis and style of eruption, development and nature of volcanic hazard, and the probability of occurrence of different volcanic risks. Likelihoods are obtained through statistical analysis of data or formal elicitation of expert judgements (Newhall and Hoblitt, 2002; Marti *et al.*, 2008). Further, this approach allows easy updating as and when new information becomes available (Neri *et al.*, 2008). An event tree is useful for both short-term (Newhall and Hoblitt, 2002) or long-term (Marti *et al.*, 2008) probabilistic eruption forecasting. Marzocchi *et al.* (2004) further developed the event tree scheme (Newhall and Hoblitt, 2002) by proposing a Bayesian strategy for estimating the probability at each node (including formal probabilistic treatment of the available data and their aleatoric and epistemic uncertainties). Thus, the Bayesian Event Tree is a probabilistic model that merges all

kinds of volcanological information (representing a synthesis of present knowledge) to obtain a probability of a volcanic event (Marzocchi *et al.*, 2008).

2.2.4 Implications for lahar hazard management

A lahar hazard assessment would traditionally follow the framework for volcanic hazards mitigation (Figure 2.3), but also, as a natural hazard, the disaster management cycle (Figure 2.1) and framework for transfer of hazard information (Figure 2.2) are applicable. Thus, lahar hazard appraisal starts with identification, followed by assessment (including severity, inundation areas analyses through past flows and modelling) and finally zonation. These will be discussed in the next section.

2.3 ASSESSING AND MODELLING THE LAHAR HAZARD

2.3.1 Lahar hazard identification

Conditions that favour lahars (e.g. volcanic eruptions, heavy rainfall) can be recognised and used as warnings that aid mitigation (Carranza and Castro, 2006). However, although lahars occur at identified volcanic complexes, they can be syn-eruptive (e.g. Nevado del Ruiz lahars, Columbia, 1985, Voight, 1990), post-eruptive (e.g. lahars following years after the 1991 eruption of Pinatubo, Philippines, Hayes *et al.*, 2002), or can be unrelated to recent volcanic activity (e.g. Casita debris flow, Nicaragua, in 1998, Scott *et al.*, 2005). Furthermore, the time between recognition of hazardous conditions and lahar occurrence can be insufficient to develop mitigation plans (Carranza and Castro, 2006).

With the basic assumption that events of the same type are likely to strike the same area in the same way and with the same frequency as those in the past (e.g. Pareschi *et al.*, 2000a), a deposit-based and geomorphological analysis of past flows can reveal likely future flow routes. In the field, possible signs of debris-flow activity (in the transport zone) include: (1) well-defined boulder trains and levees; (2) scour marks, stage (flow height) indicators and impact scars; (3) isolated boulders, much larger than could be moved by flood flow (Jakob, 2005). Yet, while some landforms show evidence of frequent and damaging events, less frequent events often require more detailed study to detect (e.g. Jakob and Weatherly, 2008). Precise delineation of the areas affected by past lahars is often difficult to reconstruct in detail from the stratigraphic record alone (Aguilera *et al.*, 2004). Perhaps more unusually, dendochronology has also been used to calculate the magnitude of historical flows, e.g. Jakob and Weatherly (2008) used tree-ring dating and scarring in Washington State (USA) to verify and complement other forms of analysis identifying the extent of hyperconcentrated flows.

In addition to ground surveys, aerial photographs can be used for recognising and analysing deposits (Jakob, 2005). For example, Joyce *et al.* (2009) achieved some success in detecting recent (2007) lahar paths at Mt Ruapehu (New Zealand) – the

best results were found from integrating LiDAR (Light Detection and Ranging) and satellite data. Kerle *et al.* (2003) used satellite optical and radar imagery to investigate the morphology and flow deposition area following the devastating lahar at Casita volcano (Nicaragua) in 1998. Other sources of information for hazard identification include: published materials, historical records, newspaper articles and consultations with long-term residents (Ferrier and Haque, 2003). Eyewitness accounts (anecdotal evidence) and newspaper reports can be an invaluable information sources, e.g. documenting occurrence of flow events (e.g. Jakob and Weatherly, 2008), arrival times and even descriptions of debris-flow composition (Scott *et al.*, 2005). Aguilera *et al.* (2004) interviewed elderly inhabitants to reconstruct lahar paths and to determine local flow depth and/ or the arrival time of historic lahars from Cotopaxi (Mexico).

2.3.2 Lahar definitions and nomenclature

Before a discussion of lahar modelling, it is necessary to detail some of the nuances of lahar types and behaviour. The term 'lahar' is generic rather than descriptive, encompassing a wide spectrum of sediment : water ratios and flow rheologies (Manville *et al.*, 2009). Rheology relates to the deformation and flow of matter under a mechanical forcing (Owens and Phillips, 2002). For a fluid flowing between two parallel plates, the force per unit area required to produce the motion is known as the 'shear stress', and the rate at which a shear is applied is the 'shear rate'; for simple shear, the shear rate can be considered a gradient of velocity that is established in the fluid. Different types of fluids behave differently under stress. A Newtonian fluid, such as water, has a viscosity (colloquially referred to as 'resistance to flow') proportionately constant between the shear stress and the shear rate (Figure 2.4); it continues to flow regardless of the force acting on it. *Normal stream flows* are typically multiphase (sediment and water) and behave as Newtonian fluids, provided sediment concentrations are low enough so that the dispersed particles do not interact (Pierson, 1995).

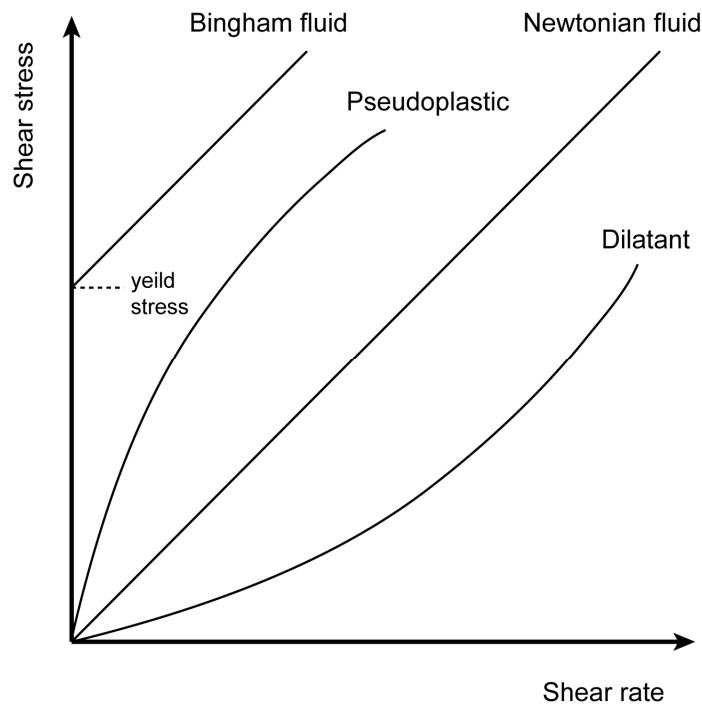


Figure 2.4 Variation of shear stress with shear rate for different models of flow behaviour (after Oertel, 2004).

Strictly lahars are non-Newtonian fluids; their flow (rheological behaviour) is dependent upon lahar composition, scale, time and shear-rate (Pierson, 1995). For a non-Newtonian fluid, viscosity (known as apparent viscosity) changes with applied shear rate, and rheological behaviour defines the relationship between deformations and stresses. Sediment is deposited on a grain-by-grain basis. Lahars encompass a continuum between hyperconcentrated-flow and debris-flow processes, although the definition permits inclusion of (volcaniclastic) debris avalanches (Smith and Lowe, 1991; Figure 2.5).

For *hyperconcentrated flows*, water and solids behave as separate phases; the fluid starts to acquire yield strength and becomes non-Newtonian (Pierson, 1995). Flow is intermediate between dilute, fully turbulent, normal stream-flow and viscous generally non-turbulent debris-flow (Smith and Lowe, 1991). Fluid is the transporting medium, with clasts supported by turbulence, buoyancy and, to a lesser extent, particle-particle interactions (Pierson, 1995).

	Sediment concentration (by volume)	Flow type and dominant sediment support mechanism	Fluid flow behaviour	Depositional mechanism and deposits
sediment : water ↓	Below 3—10 to 20%	Stream-flow <i>Turbulence</i>	Newtonian	Grain-by-grain deposition <i>Deposits are stratified</i>
	20 to 50—60%	Hyperconcentrated-flow <i>Intermediate between fully turbulent stream-flow and viscous, generally non-turbulent, debris-flow</i>	Non-Newtonian	Deposit grain-by-grain or in pulses
	Above 50—60%	Debris-flow <i>Grain dispersive forces, cohesive matrix strength and a small amount of fluid buoyancy</i>		En-masse freezing <i>Deposits are massive, matrix-supported and similar in thickness to moving flow</i>
	Debris avalanche <i>Grain dispersive forces and cohesive matrix strength</i>			

↓
loss of stratification and grading of deposits

Figure 2.5 Volcaniclastic flow types, sediment-support and depositional mechanisms (After Smith and Lowe, 1991; Pierson, 1995; Lavigne and Thouret, 2000)

Debris flows are denser than hyperconcentrated flows, and flow starts to behave as a coherent, plastic single-phase mass driven by inertial forces (Fagents and Baloga, 2006). Sediment cannot be selectively deposited (Pierson, 1995). Both solid and fluid phases vitally influence the motion and distinguish them physically from related phenomena such as avalanches and stream flows (Iverson, 1997). The hydraulics of debris flows are controlled partly by channel characteristics and partly by the rheologic properties of the sediment : water composition of the flows (Pierson, 1995). The physics of debris flows are comprehensively discussed by Iverson (1997).

The transition between ‘normal’ stream-flow and hyperconcentrated-flow occurs at the boundary between Newtonian and non-Newtonian fluid (Hessel, 2006). Thus

the sediment : water ratio for different flow types depends on the ability to acquire yield strength. Stream flows have been calculated at a sediment concentration below 3–10% (Pierson, 2005) or 20% by volume (Lavigne and Thouret, 2002); hyperconcentrated flows between 20 and 50–60% by volume, and debris flows above 50–60% (Lavigne and Thouret, 2002).

Any lahar flow type may progressively change character along its flow path (Smith and Lowe, 1991; Vallance 2000). Flow transformations are common in lahar events (Smith and Lowe, 1991). For example, debris flows triggered by rainfall at Merapi Volcano (Indonesia) are sometimes preceded, and always followed, by longer hyperconcentrated-flow phases (Lavigne and Thouret, 2002). Furthermore, landslides originating on volcanic flanks have been known to transform into debris avalanches and ultimately debris flows (Scott *et al.*, 2001), e.g. 1998 Casita (Nicaragua) debris flows (Scott *et al.*, 2005). Hyperconcentrated flows are typically more erosive than sediment-rich debris-flow phases (Vallance, 2000).

Changes in flow composition, and volume, can occur as a result of bulking (increase of mass or solids concentration) and debulking (decrease of mass or solids concentration). Total flow volumes can increase by as much as four times in relatively steep channels as eroded sediment is incorporated (Pierson, 1995). Some have argued lahar magnitude is determined more by the volume of material entrained along the channel than by the volume of the initiating event (Bovis and Jakob, 1995). Lahars can also increase in volume by dilution in an active stream channel (Vallance 2000).

2.3.3 Background considerations for lahar modelling

Data acquisition from an active volcanic system can be challenging. At ungauged sites accurate volume estimates can be prevented by an incomplete sediment record, erosion of deposits and the scarcity of eye-witness accounts (Bovis and Jakob, 1999). Logistical issues such as time and accessibility can hinder direct measurements (Carrivick and Rushmer, 2006). However, computer-based models can simulate beyond observations, improving knowledge of phenomena and

reconstructing parameters. A plethora of models have been developed to map inundation areas (e.g. Schilling, 1998; Pitman *et al.*, 2003), incorporate transitory flow behaviour through bulking and debulking (Fagents and Baloga, 2006), consider the solid-fluid interaction typical of the denser flow types (e.g. Denlinger and Iverson, 2001) etc.; all occupy a place along a spectrum from dilute to more (sediment) concentrated debris flows (Figure 2.5). However, in general, as models become more complicated, more data are required.

Limitations on the extent to which any natural phenomena can be fully understood or adequately represented by a finite group of parameters need to be recognised. Many models are designed for a specific region and thus are non-transferable or require extensive calibration. Furthermore, predictions that appear accurate over short timeframes associated with most research may become increasingly inaccurate at longer timescales (Wilcock *et al.*, 2003). In hydrology, with an abundance of established models, there is increasing evidence of non-uniqueness in model structures and parameter sets whereby there are multiple possible combinations of variables that can reasonably fit the available data or observations: a problem known as 'equifinality' (Beven, 2000; Hall *et al.*, 2005; Pappenberger *et al.*, 2005). Furthermore, often the complexity of models largely exceeds the requirements for which they are used (Saltelli *et al.*, 2000) and, principally, complex models will have similar uncertainties to simpler ones, but on a larger scale because more parameter values are required (Pappenberger *et al.*, 2005). These points place limitations on the role highly sophisticated models can play as predictive tools. It is necessary to avoid over-reliance and inappropriate use.

Ultimately, the best model will be the simplest one that provides the information required by the user whilst remaining a valid representation of reality (Bates and De Roo, 2000). The 'art' of this lies in the capability of the modeller to differentiate between the different processes operating within a system, isolating the relevant processes and ignoring others (Codilean *et al.*, 2006). For decision-makers in particular there is a need for low resolution, robust models that provide just enough certainty to warrant management action under a range of conditions (Wilcock *et al.*, 2003). Developers of models that are aimed at decision-makers have a responsibility

to anticipate all potential uses of their models, avoiding vague descriptions or complex expectations (Renschler, 2005).

2.3.4 History of lahar runout and intensity calculation methods

2.3.4.1 Overview

Modelling approaches for lahars cover a spectrum of gravity-driven flow types (see Figure 2.5). Thus, some methods are more suitable than others to replicate the behaviour of a given lahar, and come from a variety of sub-disciplines. The methods available for runout analysis can be divided into different classes (empirical, analytical, simple flow routing and numerical) and operate in different spatial dimensions (one-dimensional and two-dimensional) (e.g. Hurlimann *et al.*, 2008). Rickenmann (2005) divides debris-flow runout predictive models into empirical-statistical and dynamic models, where dynamic models are physically based and consider the momentum energy conservation of the flow. Dynamic models are also referred to as numerical models by authors within different disciplines, and depending on assumptions made about the solid-fluid mixture, can be further divided into single-phase and two-phase flows. Thus, summarising modelling approaches, and understanding the applicability of a technique, is complex and involves considerable overlap.

A few of the main approaches from the literature will now be discussed.

2.3.4.2 Empirical relationships

Empirical relationships for gravity-driven flows present correlations that are established using large datasets from field observations and analogue experiments. The most familiar of these defines maximum runout distance, L , using the travel- or reach-angle of the 'energy line' (Figure 2.6). Originally developed for landslides, the concept of the energy-line is used to measure the rate of dissipation of potential energy due to gravity from a vertical drop, H , (Heim, 1882, as cited in Malin and Sheridan, 1982). The angle the energy-line makes with the horizontal is dependent on the volume, V , of the fallen mass. Modellers typically stop flow when it reaches a

specified average slope value. For practical reasons, H and L are commonly estimated from the distal limits of the observed source area and deposit (Iverson, 1997). The concept was later adapted to explain the behaviour of pyroclastic flows and surges (e.g. Sheridan, 1979; Malin and Sheridan, 1982; Wadge and Isaacs, 1988; Macias *et al.*, 2008) and debris flows (e.g. Iverson, 1997; Rickenmann, 1999; Toyos *et al.*, 2007). Although commonly a one-dimensional approach for runout down a valley, Malin and Sheridan (1982) expanded the concept by sweeping the energy-line through a 360° arc, known as the ‘energy cone’ (thus, simultaneously considering flow down all conduits).

For a given volume, debris flows usually show greater mobility than landslides and rockfalls (Iverson, 1997; Rickenmann, 1999); and thus reach-angle will be shallower for debris flows. Rickenmann (1999) derived the following relationship from regression analysis of 160 debris-flow events:

$$L = 1.9V^{0.16}H^{0.83} \quad \text{[Equation 2.3]}$$

However, other relationships have been established from different datasets (see Rickenmann, 2005). Standards for the ratio H/L for debris flows are 0.1–0.3 dependent on the size of event (Iverson *et al.*, 1998; Carranza and Castro, 2006). However, for lahars in general the energy-line concept may not be suitable; depending on sediment concentrations, lahars can be highly mobile and show more attenuation than the abrupt en-masse deposition of granular debris flows (Schneider *et al.*, 2008). Empirical models are strictly valid only for conditions which were the basis for their development (e.g. Hurlimann *et al.*, 2008). If applying the energy-line concept to lahars, a shallower reach-angle or lower H/L must typically be used, e.g. as low as 0.04 for hyperconcentrated flows (Schneider *et al.*, 2008).

Alternatively, areas proximal to a volcano’s vent, subject to eruptive phenomena (e.g. pyroclastic flows etc.), can be thought of as source areas for lahars and thus some authors have started lahar modelling in the distal zone, i.e. after the energy-line/ energy-cone (Iverson *et al.*, 1998; Carranza and Castro, 2006).

Further empirical relationships for debris flows are discussed in Rickenmann (1999).

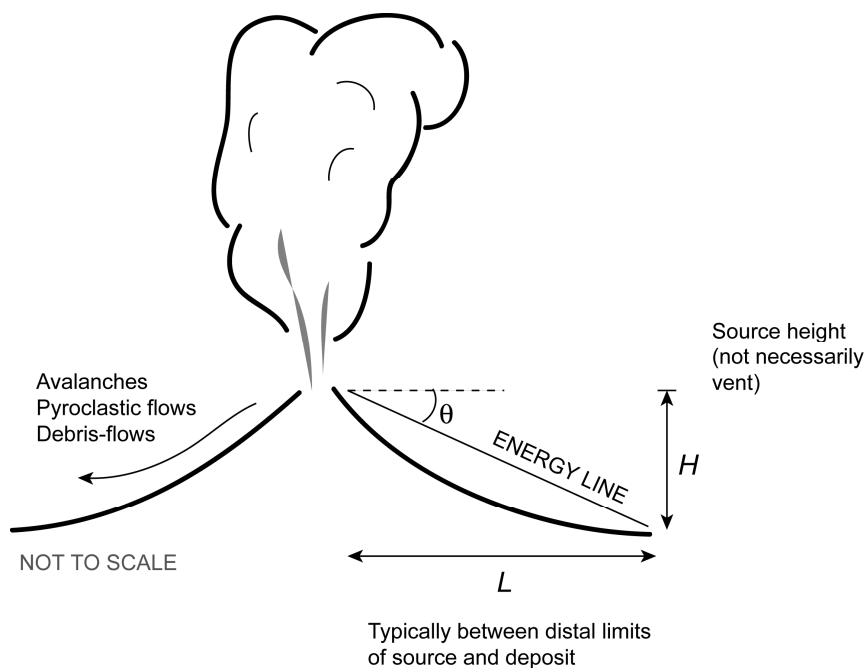


Figure 2.6 Maximum runout of a gravity-driven flow, L , down a valley from a vertical drop, H , is defined by the slope of the energy-line (travel- or reach-angle, θ) (after Wadge and Isaacs, 1988).

2.3.4.3 Two-dimensional non-numerical methods

Two-dimensional methods typically simulate runout and/ or inundation area over a digital elevation model (DEM). A DEM is a regular grid that describes the continuum of land surface using a matrix of elevation values (Maune, 2007). Therefore, two-dimensional models are particularly suited to implementation in a Geographical Information System (GIS) (see further discussion in Section 2.4).

Simple flow routing

Flow directions based on DEMs are needed in hydrology to determine the paths of water, sediment, and contaminant movement (Tarboton, 1997). Simple flow routing algorithms typically do not incorporate any frictional laws and assume that topography plays the main role in path direction. In theory, these algorithms can be adopted for first-order runout routing for any gravity-driven flows.

Typical single-direction flow models route flow from a starting cell to one of its eight (adjacent or diagonal) neighbours based on slope gradient. The most common of these is the D8 algorithm which directs flow in the direction of the steepest slope, or greatest change in gravitational potential energy (O'Callaghan and Mark, 1984) (Figure 2.7). The resultant flow route is commonly known as 'the path of steepest descent'. While the algorithm is extensively used in hydrology for determining overland flow, in steep terrain D8 can be used to predict the central flow line of a debris-flow (Huggel *et al.*, 2003).

Huggel *et al.* (2003) also modified the single-direction flow algorithm (D8) to allow flow to divert up to 45° on both sides of the steepest path. The central flow line of a debris-flow is assumed to follow the path of steepest descent but lateral spreading is permitted. The modelled debris-flow stops when the average slope of 11° ($H/L = 0.19$) is reached (see energy-line discussion in the previous section, Figure 2.6). This approach was later used by Schneider *et al.* (2008) for assessing lahars from ice-capped volcanoes and Noetzli *et al.* (2006) for rock-ice avalanches (using a greater reach-angle).

For lava flow, Felpeto (2001; 2007) suggested assigning a flow direction to one of the downslope neighbouring cells, with the probability proportional to the height difference between a cell and its neighbour. The selection of the cell where the flow will propagate was made by mean of a Monte Carlo algorithm. This approach was also adopted by Gomez-Fernandez (2000) for lava movement.

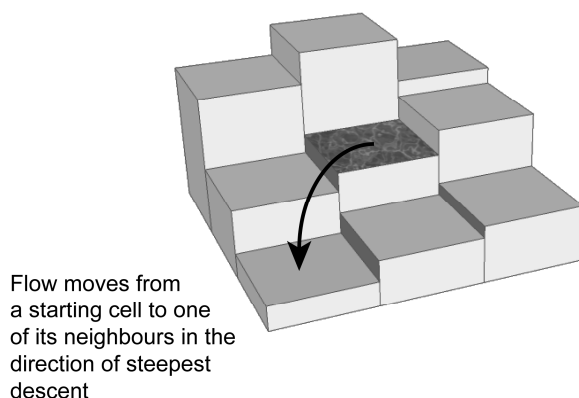


Figure 2.7 D8 algorithm for flow direction over a small section of an example DEM

In contrast to single-direction routing there are alternative simple flow routing algorithms that account for dispersion. Multiple-direction flow routing algorithms include flow diversion from the steepest flow direction (e.g. Wolock and McCabe, 1995). These algorithms can partition flow fractionally from a cell to each lower neighbour by weighting flow in proportion to slope (e.g. Quinn *et al.*, 1991).

For water flows, Tarboton (1997) suggested using triangular facets to remove the limitation of only eight possible flow directions, naming the algorithm D-Infinity (or D^∞). This reduces grid bias and the coarse 'stepped' nature of D8 results. Theoretical advantages and disadvantages of different flow-routing algorithms have been discussed in Tarboton (1997) and Seibert and McGlynn (2007). For lahar simulation, a major limitation is that volume can only be incorporated indirectly and intensity cannot be calculated explicitly (Hurlimann *et al.*, 2008).

LAHARZ

LAHARZ (Schilling, 1998) is a flow-routing model that takes into account flow volume. The central flow line of a lahar follows the path of steepest descent (D8, as above) but dispersion is permitted through semi-empirical equations that govern inundated planimetric and cross-sectional areas. LAHARZ also makes use of the H/L energy cone concept for defining the limits of volcanoclastic deposit, and thus furthest point upstream for lahar initiation (Figure 2.8a). The area encompassed by the energy-cone is referred to as the proximal hazard zone (affected by primary volcanic hazards e.g. flank collapse and pyroclastic flows). Once processing has begun, flow moves downstream along the path of steepest descent (which is typically the line defining the lowest points along the valley, and is referred to as the valley thalweg). Lahar volume is spread laterally in three cross-sections (Figure 2.8b). The area of each of these is defined by A as follows,

$$A = 0.05V^{2/3} \quad \text{[Equation 2.4]}$$

where V is the input volume. Flow is considered a continuum and volume is constant (no material is deposited or entrained). For each cross-section, A can be derived in a GIS using the DEM heights. Processing then moves to the next downstream cell on

the thalweg. For full details see Schilling (1998). When the number of cells inundated (multiplied by cell resolution) reaches the area given by the planimetric area, B , flow stops.

$$B = 200V^{2/3}$$

[Equation 2.5]

The semi-empirical equations that define inundation areas were first proposed by Iverson *et al.* (1998) and later automated in a GIS to create the LAHARZ suite of programs (Schilling, 1998). The equations were developed using known deposit areas from 27 lahar (debris-flow) paths from nine different volcanoes (see Iverson *et al.*, 1998).

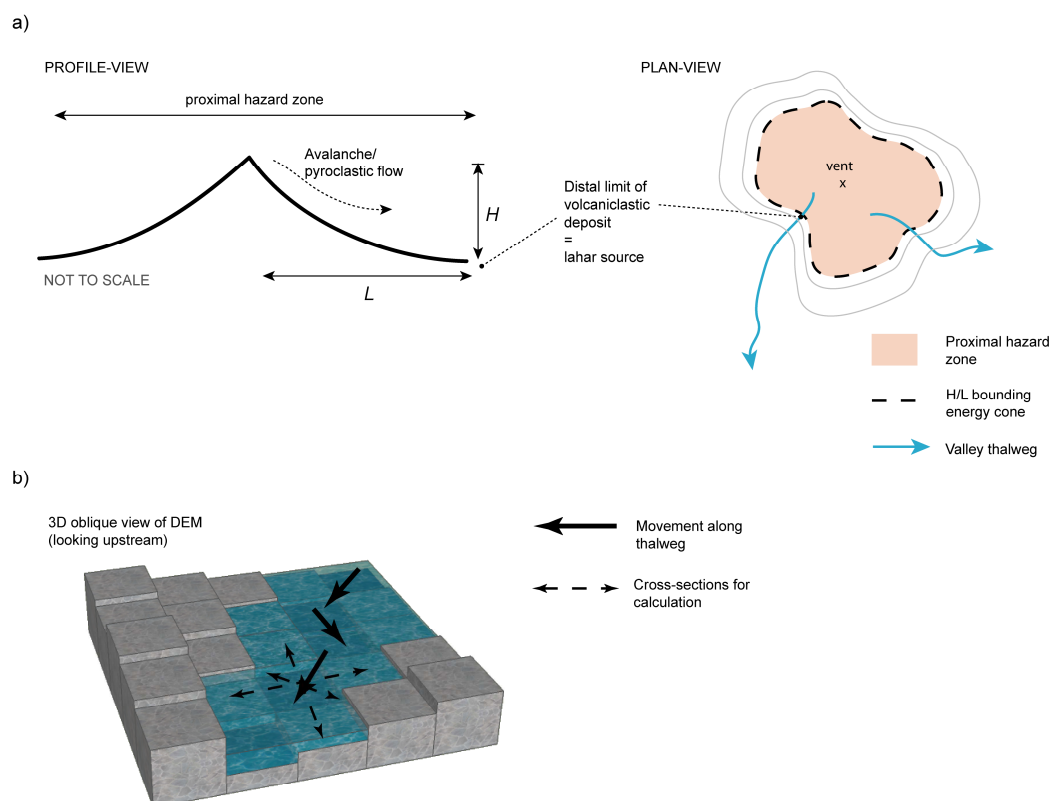


Figure 2.8 a) The H/L energy cone is adopted by LAHARZ to define the proximal hazard zone. Processing begins where the H/L bounding cone intersects the valley thalweg; b) the centre of the lahar mass follows the valley thalweg downstream, but at each processing cell three cross-sections define the dispersion.

LAHARZ has been widely used for the construction of lahar hazard maps in South America (Canuti *et al.*, 2002), Central America (Davila *et al.*, 2007; Hubbard *et al.*, 2007; Capra *et al.*, 2008; Macias *et al.*, 2008) and New Zealand (Stevens *et al.*, 2002). Applied flow types range from hyperconcentrated-flow, through to debris-flow and debris-avalanche. However, some authors have heavily criticised LAHARZ e.g. because of its inability to trace the evolution of other parameters downslope (Fagents and Baloga, 2006), and for potential lack of transferability because it was calibrated from nine volcanoes (Carranza and Castro, 2006). However, claims that LAHARZ incorporates no physics (e.g. Carranza and Castro, 2006; Sheridan, 2004) are misinformed as, although not detailed considerations of flow behaviour, some physical basis is included in the expression coefficients. Further, while applying LAHARZ to lahars from Popocatepetl (Mexico) Munoz-Salinas (2009) heavily criticised the model as the use of a high resolution and detailed DEM did not guarantee a realistic lahar simulation. Yet the jagged edges at distal limits, for example, have been remarked on by Iverson *et al.* (1998) in model development and LAHARZ should only be applied, as intended, for a preliminary hazard assessment.

Some authors have used LAHARZ as a basic model but made minor modifications. DFLOWZ, a modified version of LAHARZ for debris flows, takes uncertainty into account and can model both confined and unconfined flow (Berti and Simoni, 2007). Coefficients were recalibrated with data from 27 historical debris flows (typically more sediment-rich) in the Italian Alps. Carranza and Castro (2006) developed a model similar to LAHARZ but a DEM was used to derive the spatial data used as inputs (proximity to lahar source zone, proximity to drainage lines, elevation and slope), modelling was carried out by weights-of-evidence, by logistic regression and evidential belief functions, and outputs were probabilities.

2.3.4.4 Numerical/ physical models

Numerical models describe flow dynamics and distinguish between one-phase and two-phase flows depending on the mixture composition and mechanical processes contributing to momentum conservation (Sosio *et al.*, 2007). In most models, the water-sediment mixture of a debris-flow is assumed to be a single component fluid with particular rheologic characteristics (defined by constitutive equations or

rheologic ‘laws’). Three common flow resistance laws have been defined: Bingham laminar flow, Newtonian turbulent flow, or dilatant grain shearing in the inertial regime (Rickenmann, 1999; refer also to Figure 2.4). The Bingham model essentially simulates different kinds of liquid with thinning or thickening, akin to a viscoplastic fluid (Rickenmann, 2005); Newtonian behaviour is analogous to normal water flow (and uses turbulent friction coefficients such as Manning or Chezy); and dilatant shearing refers to dry granular flows (see also Figure 2.4). Some models also have a stop term (using frictional-turbulent Voellmy fluid flow rheology) for anticipating the total runout distance (Rickenmann, 2005).

Thus, there are models for single-phase ‘dry’ (e.g. Savage and Hutter, 1989), single-phase ‘wet’ (e.g. Macedonio and Pareschi, 1992), and saturated binary mixtures (e.g. Iverson, 1997; Denlinger and Iverson, 2001). As a crude simplification, for ‘wet’ single-phase debris flows, flow is governed by the interstitial fluid (e.g. Pierson, 1995), and for two-phase, granular flow pore pressure and frictional effects from grain interactions are important (e.g. Iverson *et al.*, 1997). Single-phase ‘dry’ models consider the avalanching flow of granular materials in a cohesionless granular continuum of particles (Savage and Hutter, 1989; Pitman *et al.*, 2003; Pudasaini *et al.*, 2005).

Numerical models require topographic profile cross-section shape (or typically a DEM if modelling in two-dimensions), initial volume or input hydrograph and rheological or friction parameters (Hurlimann *et al.*, 2008). Typically appropriate values for rheological parameters are estimated from field observations (Hurlimann *et al.*, 2008). Numerical models can be used to derive runout distances and intensity (flow depth and velocity) (Sosio *et al.*, 2007). Some examples are elaborated below.

One-dimensional flow of a ‘wet’ single-phase fluid

One-dimensional numerical models provide calculations along a previously selected topographic profile (Hurlimann *et al.*, 2008). The most common examples borrow methods from hydrology and solve mass and momentum conservation equations (known as the shallow water or St Venant equations) for unsteady-state stream-flow flow (e.g. Chow, 1959) and adapted to lahars (Macedonio and Pareschi, 1992; and Caruso and Pareschi, 1993). There are also methods using Kinematic wave

approximation (see Vignaux and Weir, 1990). Aguilera *et al.* (2004) used a model based on the mass and momentum balance equations for a bulk mixture, where the equations of the model were analogous to those for clear-water flow, but differed in the energy-dissipation coefficient which accounted for lahar rheology.

One-dimensional unsteady-state stream-flow models typically assume all energy dissipation can be parameterised by a single roughness coefficient (e.g. Laenen and Hansen, 1988), and this is not well known for lahars (Fagents and Baloga, 2006). However, such models have successfully been applied to channelled lahars, but topography plays a key role with regard to deposition pattern and thus to create inundation areas results must be extrapolated into two-dimensions (Rickenmann, 2005).

HEC-RAS is a one-dimensional 'off-the-shelf' flood inundation model that may be applicable to approximate the (unsteady) behaviour of dilute lahars (Hydrologic Engineering Center, 2008). Popular in the field of hydrology, the model has also been applied to glacial outburst floods with entrained sediment (e.g. Alho *et al.*, 2007; Alho and Aaltonen, 2008; Yochum *et al.*, 2008).

One-dimensional flow of a 'dry' single-phase fluid

Notable single-phase dry models include snow avalanche modelling by Voellmy (1955). This model has a turbulent and a sliding friction component (Rickenmann, 2005) and has been found robust in terms of the numerical stability of simulations (Rickenmann, 2005). However, the Voellmy fluid approach is more correctly referred to as a mass point analytical model as only the centroid of the moving mass is simulated (Hurlimann *et al.*, 2008).

The single-phase grain flow model of Savage and Hutter (1989) is one of the most frequently cited models for debris flows and avalanches. Originating from equations of mass and momentum balance (and similar to the shallow water equations), basal sliding properties are described by Coulomb-type friction behaviour. Variations of the mechanical behaviour within the flow are ignored as mixture density is taken as a constant. This model was generalised by Iverson (1997) and later adapted by Iverson and Denlinger (2001), Pitman *et al.* (2003) and Pudasaini *et al.* (2005) etc.

Two-dimensional flow of a 'wet' single-phase fluid

For two-dimensional flow of a single-phase fluid, the hydraulic model FLO-2D (O'Brien *et al.*, 1993) is a well-known tool (Hurlimann *et al.*, 2008). FLO-2D is a volume conservation model, which assumes Bingham plastic rheological behaviour and adds a friction term accounting for channel roughness and turbulence (Sosio *et al.*, 2007). It has been used, for example, for the propagation of rainfall-triggered debris flows in the Italian Alps (Calvo and Savi, 2009); to determine maximum flow depths and velocities which contributed to the development of a hyperconcentrated-flow intensity map for Washington State (USA) (Jakob and Weatherly, 2008); and compared with LAHARZ for predicting runout of (debris-flow) lahars from the Pichincha volcano complex (Ecuador) (Canuti *et al.*, 2002). FLO-2D can be extensively adapted to diverse modelling conditions including urban areas (Canuti *et al.*, 2002); however, it should only be used for the middle and long-term management of areas prone to inundation due to fieldwork and data requirements (e.g. sediment concentration), and the lengthy preliminary phase (Canuti *et al.*, 2002). Further, as commercial software, the model itself is expensive to obtain (approximately \$3500 US, January 2010).

Two-dimensional flow of a 'dry' single-phase fluid

Titan2D (Pitman *et al.*, 2003) is a program originally developed for the dry granular flow of debris avalanches and is based on the earlier work of Savage and Hutter (1989), Iverson (1997), Iverson and Denlinger (2001) and Denlinger and Iverson (2001) (Sheridan *et al.*, 2005). Similar to the shallow water equations, the conservation equations for mass and momentum are solved, but with a Coulomb-type (dry, sliding) friction term for the interactions between grains and between the granular material and the basal surface. Titan2D can simulate the change in flow thickness because it considers the initial volume of the collapsing mass driven downslope by gravity where the resistance forces are given by basal and internal friction angles of the collapsing material (Capra *et al.*, 2008). From flow depth and momentum the flow limit, run-out path, flow velocity, deposit thickness, and travel time can be calculated. Titan2D has also been applied to pyroclastic flows (e.g.

Macias *et al.*, 2008). Titan2D is advantageous because it is freely available software that uses a DEM and runs in a GIS.

McDougall and Hungr (2004) presented a numerical method for the analysis of debris flows and avalanches using smoothed particle hydrodynamics. The model has a number of unique capabilities, including the ability to account for material entrainment, and rheology variation (by selecting different rheological laws).

One-dimensional flow of a two-phase fluid

A one-dimensional granular avalanche approach has been adapted for debris flows by including the effects of pore fluid (Iverson, 1997). Motion is governed by inertial forces, internal shear and normal forces in response to boundary forces (i.e. local topography) (description from Fagents and Baloga, 2006). Total runout distance is simulated and velocity and depth are functions of time (Rickenmann, 2005).

However, the selection of the rheological law (e.g. Bingham viscoplastic, or Voellmy fluid), and suitable parameter values, are of crucial importance (Hurlimann *et al.*, 2008).

Two-dimensional flow of a two-phase fluid

Recently 2D non-homogenous debris-flow models have been growing in popularity (e.g. Iverson and Denlinger, 2001; Pudasaini *et al.*, 2005). Motion of a sliding mass is described by a mixture of a solid and a fluid phase under conditions of saturation.

A two-phase version of Titan2D has been developed that allows fluid flow with granular flow (Williams *et al.*, 2008; Procter *et al.*, 2009). Williams *et al.* (2008) coupled Titan2D (Pitman, 2003) and the Pitman-Le two-phase debris-flow model (Pitman and Le, 2005) to enable the simulation of more types of gravitational mass flows. The new model was applied to Tungurahua (Ecuador) lahars (Williams *et al.*, 2008) and Ruapehu (New Zealand) lahars (Procter *et al.*, 2009).

2.3.4.5 Summary of current modelling techniques

Figure 2.9 summarises the potential applicability of some of the runout prediction models and laws discussed above to different gravitational flow types. Depending on lahar classification, and sediment content (a major driver for rheology), different

models are more suitable. Key references are Rickenmann (1999; 2005) and Hurlimann *et al.* (2008).

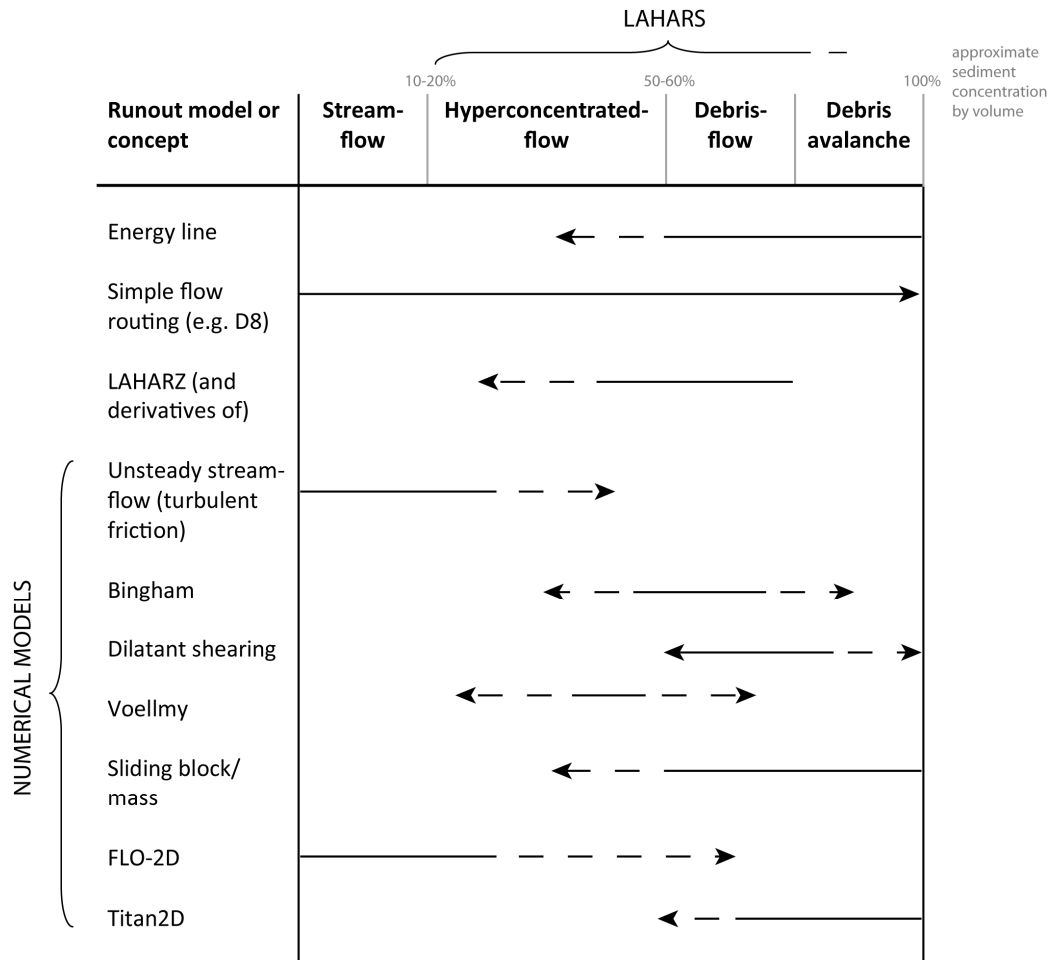


Figure 2.9 Potential applicability of some of the models (and rheological laws) described in the text. Arrows show origination and direction of spread of application (e.g. the energy-line concept was designed for avalanches but has been applied to lahars). Please refer to citations in the main body text.

More recently researchers have applied established commercial hydraulic models to lahars, e.g. Delft FLS (Brown *et al.*, 2007); Delft3D (Carrivick *et al.*, 2009). Whilst these models are more realistic they also make much greater demands on data, time and processing. Alternatively, models have been developed specifically for debris flows (as above), but because of the complex interactions of solid and liquid phases, these models either require a great amount of input data or simplify behaviour and use empirical data. For example, LAHARZ is a semi-empirical model whose coefficients capture the gross underlying physics with minimal demands on user input (Iverson *et al.*, 1998; Schilling, 1998). In contrast, Titan2D is a physically based model for flows with high sediment content (Pitman *et al.*, 2003), but the physical background is complex and this software is very computationally intensive. Ultimately, physical models are advantageous if knowledge of typical lahar behaviour and composition are available from detailed fieldwork. Statistical based models avoid the necessity of detailed flow mechanics but they typically provide no temporal or derivative information.

2.3.5 Reflection on the key factors for lahar modelling

Previous studies have formally, and informally, established the relative importance of various factors (e.g. inputs) for lahar modelling.

2.3.5.1 Data inputs, e.g. DEM

Quality of surface representation is one of the most influential elements for runout assessment (e.g. Huggel *et al.*, 2008; Schneider *et al.*, 2008). Lahars, flash floods, glacial lake outburst floods, and debris flows are all gravity-driven flows; to a first order flow movement is dependent on local elevation variations of the surface over which they pass, thus topography is a significant control on the movement of gravitational flows. For example, transit-time predictions decrease with increasing topographic resolution (Fagents and Baloga, 2005) and inundation areas from runout models are sensitive to the quality of the input DEM (e.g. Stevens *et al.*, 2002). DEMs are an increasingly popular way of incorporating topographic

information into lahar and debris-flow models. DEMs of volcanic terrain can be obtained by (1) digital photogrammetry based on stereoscopic pairs of aircraft or satellite images; (2) digitisation and interpolation of topographic maps; (3) radar interferometry; (4) laser scanning (LiDAR); or (5) field survey (see Kervyn *et al.*, 2007; Maune, 2007). However, the approximations needed to represent a continuous variable such as terrain over a finite number of gridded cells result in errors in any DEM. These errors can propagate to model predictions (e.g. Darnell *et al.*, 2008). Different DEM products have different accuracies (e.g. Stephens *et al.*, 2002) and perform better for different operations.

2.3.5.2 Model concept and inherent assumptions

Models can only approximate lahar behaviour and require simplifying assumptions (see Section 2.3.3). Therefore, model selection will be a potentially great source of uncertainty (or lack of confidence in decisions). The main choices are between one- or two-phase and, for the former, wet or dry, and consideration should depend on bulk composition and flow type. Additional considerations include assumptions of constant volume and/ or rheology. However, selection of unsuitable concepts can impact hazard assessment. For example, total volume and bulk composition are the main factors which contribute to debris-flow hazard, establishing both flow mobility and impact energy (Sosio *et al.*, 2007). For a given volume, debris flows usually show greater mobility than landslides and rockfalls and have greater runout (Iverson, 1997; Rickenmann, 1999). Composition can also influence velocity. Debris flows can travel twice as fast as water floods of comparable depth and channel slope (Pierson, 1995), but this does not apply to all flows. Rickenmann (1999) found that mean flow velocity does not depend on the composition of flow. Furthermore, the incorporation and loss of material (bulking and debulking) can significantly increase lahar transit time, mobility, rheology and inundation limits (Scott *et al.*, 2001; Fagents and Baloga, 2006); however, few models have attempted to model this and Iverson (2003) further argued that the evolving behaviour of debris flows is too complex to be represented by any rheological law. Thus, it is unsurprising that behavioural approximations are made using simplifying assumptions.

2.3.5.3 Parameters and calibration

Calibration is the process by which model parameters are fitted to improve the correspondence between model predictions and observation (Hall *et al.*, 2005). Thus, the model becomes tailored to a particular set of circumstances. Calibration issues have become a focus in hydrological modelling due to the problem of equifinality (where multiple unique model calibrations can produce equally acceptable outputs) (see Beven, 2000).

Hall *et al.* (2005) and Pappenberger *et al.* (2005) have examined sets of Manning's roughness coefficients and the effect of parameter variance on flood inundation. Further, the use of a single parameter at all as adequate for accounting for friction has been criticised (see references and discussion in Pappenberger *et al.*, 2005). In lahar modelling, LAHARZ was calibrated for 27 flows from nine volcanoes and thus may not be (as) applicable for other flows from different volcanoes (Carranza and Castro, 2006). Some authors have recalibrated the model (see Section 2.2.2.3).

Good modelling practice requires the modeller to provide an evaluation of modelling predictions (Ratto *et al.*, 2001). Uncertainty analysis has been touched on briefly in Sections 2.2.2.2 and 2.2.3.2; however, there is a further element that determines how uncertainty in model predictions is determined by uncertainty in model inputs and parameter values, termed sensitivity analysis (Lilburne and Tarantola, 2008). This is an extremely interesting area of study, perhaps even the future of modelling, but requires a more in-depth coverage and discussion than can be performed by this review. The interested reader is referred to Saltelli *et al.* (2000).

2.3.5.4 A framework for lahar modelling?

Given the literature presented above, Figure 2.10 is an initial reflection on the considerations for lahar modelling in this research. For volcanic hazards, including lahars, hazard zonation was historically based on an examination of deposits of inundated areas (Section 2.2.3.1); now this usually involves some form of numerical modelling or simulation. Once the lahar hazard has been identified (Section 2.3.1), appraisal of the spatial distribution of the hazard (runout and inundation areas) and

intensity (flow depth and velocity) can be achieved through modelling (Section 2.3.4). Modelling requires an acceptance of certain concepts with their inherent assumptions (Section 2.3.5.2) and a need for a finite group of parameters to adequately describe the phenomenon (lahar) (Section 2.3.5.3). These are in turn governed by data restrictions and quality (Sections 2.3.3.1 and 2.3.5.1). Additionally, it has been recognised that a top-down approach to information dissemination from the sciences is not always effective (Section 2.2.1), thus the modeller should be aware that end-user (decision-maker) involvement in some aspect(s) of the hazard assessment process may make outputs more transferable, and ultimately have greater utility. Finally, an evaluation of confidence in the findings should be provided.

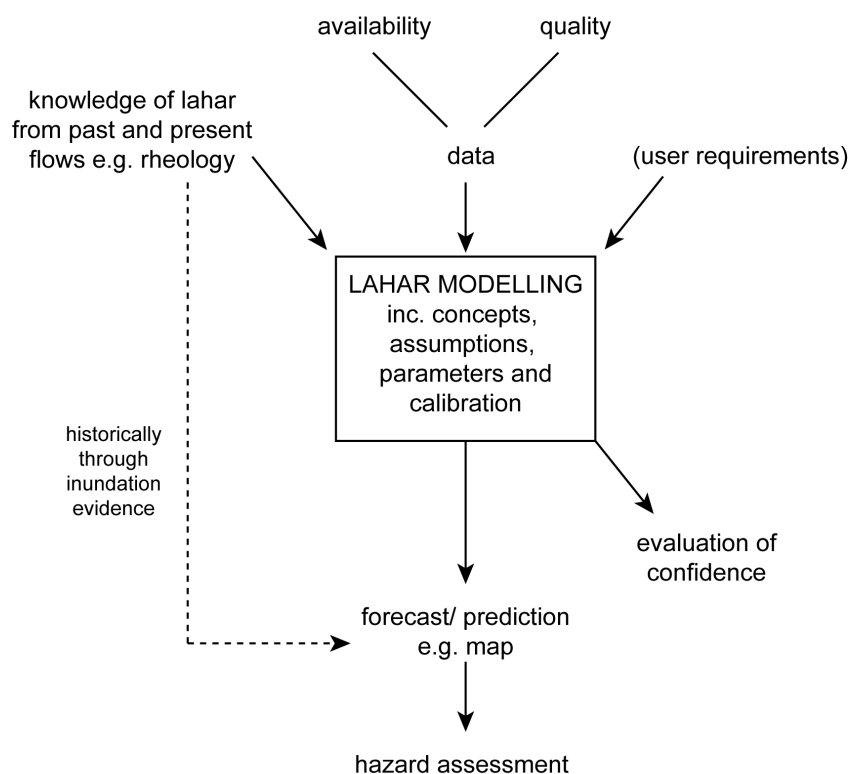


Figure 2.10 Schematic showing the considerations for modelling for the scientist

2.3.6 Lahar hazard zonation

Previous sub-sections have focussed on modelling techniques, but the step from model output (e.g. inundation area) to hazard zonation has not been presented. There are many techniques for this. One scheme uses intensity and probability to determine the hazard level for debris-flows and landslides, e.g. the qualitative Hazard Matrix by Hurlimann *et al.* (2008) (Figure 2.11). Zones of equal hazard can then be presented on a map. However, there is an absence of standardised techniques or guidelines. Tradition dictates that lahar hazard zones are delineated from inundation extents of historic or prehistoric flows and for forecasting, should be extended for all valleys draining from a volcano (Crandell, 1984). Boundaries distinguishing zones of relative hazard can be subjective or physical.

Nevertheless, practical lahar hazard zone mapping is frequently left to the discretion of local responsible agencies and scientists. This is not an issue unique to lahars; hazard zonation has been discussed more generally in Section 2.2.2.1.

			Probability of occurrence		
			<i>High</i>	<i>Medium</i>	<i>Low</i>
Intensity	$h > 1.0$ m or $v > 1.5$ ms ⁻¹	<i>High</i>	High	High	Moderate
	$h < 1.0$ m and 0.4 ms ⁻¹ < $v < 1.5$ ms ⁻¹	<i>Medium</i>	Moderate	Moderate	Low
	$h < 0.4$ m and $v < 0.4$ ms ⁻¹	<i>Low</i>	Low	Low	Very low
	Unaffected areas			Very low	Very low

Figure 2.11 Qualitative hazard matrix for debris flows (level of hazard where h is the flow-depth and v is the velocity). After Hurlimann *et al.* (2008) and Rickenmann (2005b as cited in Hurlimann *et al.*, 2008).

2.4 USE OF GEOSPATIAL DATA AND TOOLS FOR HAZARD MANAGEMENT, MODELLING AND COMMUNICATION

2.4.1 An introduction to GIS potential for hazard management

There has been a recent shift in hazard assessment from inventory-style maps to those that offer interpretation of multiple attributes (e.g. hazard zone, number of occupants, vulnerability) in a GIS environment (Rosenbaum and Culshaw, 2003). A GIS allows efficient management of large volumes of (spatially and temporally variable) data. In particular, for natural hazards, GIS data are easily updated and expanded and thus can be available immediately after an event (Kerle and Oppenheimer, 2002). A map from a GIS is a transient by-product of the database (Schuurman, 2002); the real benefits of a GIS stem from its ability to combine digital visualisation with data querying, interrogation and modelling.

GIS can contribute to the whole sequence of disaster reduction – from identifying areas at risk, monitoring and forecasting hazards, through warnings of their onset and measures to minimise loss of life, injury and damage to property, to coping with disaster once it has occurred (Gatrell and Vincent, 1991; Coppock, 1995). Other early discussions of GIS technology for disasters and emergency management are provided by Carrara and Guzzetti (1996), Cova (1999), Goodchild (2003a; 2003b) and in an ESRI White Paper (Johnson, 2000). Figure 2.12 provides some example GIS activities at various stages of the disaster management cycle. Arguably, geographic information and the technologies that acquire, interpret and disseminate such information (GIS, remote sensing etc.) have now become essential in all aspects of this cycle (Goodchild, 2006).

Relatively simplistic applications of GIS utilise only their cartographic strengths (Zerger and Smith 2003). However, it has been argued that predictive and operational models should be embedded in a GIS for successful hazard management (Radke *et al.*, 2000); for example, a model setup in a GIS can be long-term, data can be updated regularly, and maps can be output as required. Tools are now being developed that automate phases of hazard assessment in a GIS (Felpeto *et al.*,

2007). GIS and modelling can be tightly integrated (or coupled) where all modelling occurs within the GIS, or more loosely coupled, either for pre-processing (data preparation) or post-processing data, commonly through mapping (Fedra, 1993; Zenger and Wealands, 2004). Intermediately, GIS can be used as a modelling framework that combines modules or scripts replicating different aspects of a model (e.g. Pullar, 2003). The merit of GIS integration with modelling has been explicitly discussed with respect to hydrological models due to the well established practices and standards for hydrologists and hydraulic engineers (Sui and Maggio, 1999). For hydrological modelling the data models supporting most conventional GISs are not efficient for solving the complex equations inherent in space and time variant models (Sui and Maggio, 1999; Zenger and Wealands, 2004). However, some hydrological functions are now embedded in GIS software packages (e.g. a hydrology extension for ArcGIS Spatial Analyst), and hydrological models are embedding GIS-like functionalities (e.g. HEC-RAS, Hydrologic Engineering Center, 2008) (Sui and Maggio, 1999). Thus, there is potential for coupling of models for hazard forecasting with GIS. Conventionally, a GIS does not include the capability for dynamic analysis (Burrough, 1998). Nonetheless, simple models (such as the energy cone for debris flows) can be effectively, albeit sometimes inefficiently, implemented in a GIS as they can exploit many of the spatial functions of the GIS (Felpeto *et al.*, 2007). The powerful capabilities of GIS to process DEMs are also often used (Sui and Maggio, 1999). Lahar and debris-flow runout models that make use of a DEM can be tightly coupled to a GIS (e.g. LAHARZ (Schilling, 1998), Titan2D (Pitman *et al.*, 2003)).

Therefore, the potential for GIS in hazard management outstretches its current uses. A brief synopsis of the application of geospatial data and tools in the disaster management cycle will be described. As an additional note, there has been significant evaluation of the potential of GIS in the response phase of the cycle, especially following the 9/11 terrorist attacks in New York (USA), 2001 (Cutter *et al.*, 2003; NRC, 2007). Although not a natural disaster, these acts of terrorism had a profound effect on getting geographers, scientists from other disciplines and decision-makers, talking about geospatial data and tools (Longley *et al.*, 2005); thus, some pertinent references are made here.

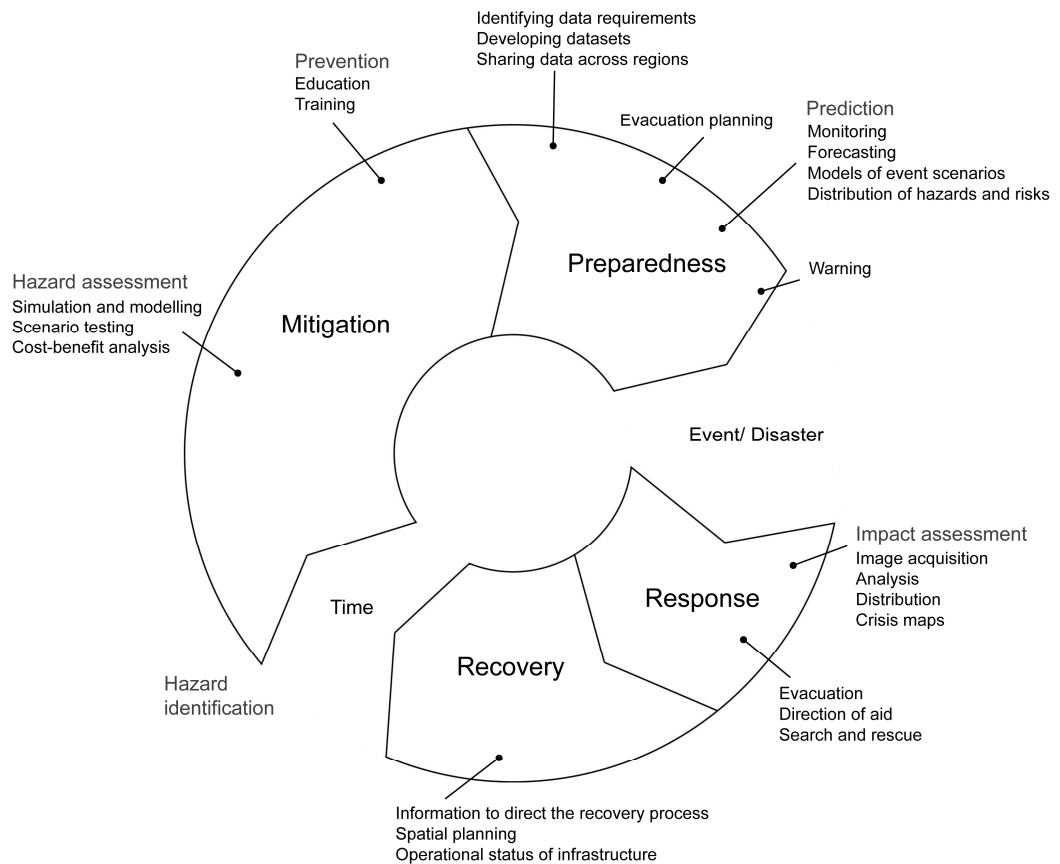


Figure 2.12 Example geospatial activities contributing to phases of the disaster management cycle (After Johnson, 2000; NRC, 2007).

2.4.2 Geospatial data and tools applied for preparedness, mitigation and decision utility

Geospatial preparedness actions include ascertaining data requirements, assimilating and developing datasets and sharing data (Figure 2.12). These data can include framework data (e.g. elevation, political, cadastral information) and foundation data (e.g. soil types, land-use, water pipes etc.) that are used for a variety of planning activities, such as evacuation routes (NRC, 2007). For example, a well-structured database of demography and resources is needed for land-use

planning and evacuation programmes (Lirer and Vitelli, 1998). A GIS can also be used to identify neighbourhoods that may face transportation difficulties (vulnerability) during an evacuation (Cova and Church, 1997; Cova 1999).

GIS can be used to visualise and compare multiple alternative mitigation plans relatively quickly (NRC, 2007). Cost-benefit analysis can be performed to provide a formal, quantitative evaluation of the ability to reduce losses through mitigation options (Bernknopf *et al.*, 2006; Gamper *et al.*, 2006). Spatial decision support is one of the central functions ascribed to GIS (Jankowski *et al.*, 2001). A decision support system can be considered as an integration of computer hardware and software specifically designed to complement the human thought process in problem-solving, decision-making and information processing, allowing the user to undertake 'what-if' questions (Gatrell and Vincent, 1991). A spatial decision support system (SDSS) can be a contingency planning tool to evaluate a range of management strategies prior to an event (Zerger and Smith, 2003). It is anticipated that the next generation of SDSS tools will integrate GIS, dynamic models and custom graphical user interfaces to provide comprehensive disaster management decision support tools (Zerger and Smith, 2003).

For volcanic hazard management, GIS can also be used as a data repository to monitor an impending or ongoing eruption (e.g. Lirer and Vitelli, 1998; Pareschi *et al.*, 2000a). More recently, the data management capabilities of GIS have been exploited for the long-term monitoring and forecast of potentially active volcanoes (Gogu *et al.*, 2006). The GEOWARN project is a geo-spatial warning system which stores, analyses and visualises vast amounts of multi-disciplinary data, e.g. infrared thermal images, real-time surface movements heat and gas fluxes; integrated modelling techniques are able to detect eruption precursors and issue warnings (<http://www.geowarn.ethz.ch/>). Due to the broad requirements of different users, i.e. different volcano observatories, the main GIS package (ESRI's ArcGIS embedded with MS Access) was complemented with other software for data exchange (Gogu *et al.*, 2006). However, this demonstrates that the functionality of GIS is now being tested in volcanology, well beyond a technology to simply generate maps.

2.4.3 Geospatial data and tools applied for response and recovery

Geospatial information can be invaluable immediately following an event for incident management and tactical decision making (NRC, 2007). One of the most important application areas of GIS after a crisis is in emergency services dispatch (Zerger and Smith, 2003). For example, the shortest path algorithm, standard to many GIS packages, can use the road network to find optimal routes between user-defined start and end nodes (Gatrell and Vincent, 1991). This is useful for directing emergency services in addition to designing evacuation routes. Furthermore, GIS can provide one of the primary components for computer-aided dispatch systems (Johnson, 2000). However, there is a time window within which information must be delivered to have value (Radke *et al.*, 2000). Critical for effective response is a pre-existing database provided quality control is assured and data are updated (Goodchild, 2003b). Continuous updating of databases is required for near real-time management of volcanic crises (e.g. Gomez-Fernandez, 2000; Felpeto *et al.*, 2007).

However, Zerger and Smith (2003) found that there is a general inertia among users to utilise computer-based GIS for real-time decision-making where paper maps have been used for decades. Paper maps were also a preference on the ground during response to the 9/11 terrorist attacks in New York (USA), 2001, signifying the capabilities of GIS and spatial technologies beyond map-making were not fully exploited (Kevany, 2003).

To complicate the response effort, access to geospatial data and tools can resemble a donut – abundant far away from an impacted area, but almost non-existent at the geographic centre of a crisis where computers and infrastructure are damaged (NRC, 2007). For example, GIS had to be re-established in the hours following the 9/11 terrorist attacks as GIS facilities had to be evacuated (Kevany, 2003; Goodchild, 2006). GIS and related spatial technologies were widely used to support response and recovery efforts, but there were also lessons learned; for example, the importance of metadata and a use of standards to aid the exchange and integration of information (ESRI, 2002; Kevany, 2003; NRC, 2007). Use of geographical datasets in emergencies has traditionally been hindered by licensing and access restrictions and a lack of interoperability of formats (Goodchild, 2003a;

Kevany, 2003). Data sharing and pooling of information (nationally and internationally) between administrative departments and government bodies can be difficult (NRC, 2007). However, advancements are being made in GIS interoperability through wider Internet use and the use of standards (see later discussion in Section 2.4.4.2).

With infrastructure affected and access frequently impeded, disaster management can benefit from the synoptic coverage provided by satellite imagery (Kerle and Oppenheimer, 2002). Remote sensing has traditionally been used by scientists for detection and mapping of hazard and effects, and rarely for more complex investigations (Showalter, 2001). However, remote sensing is now playing a key role in management and mitigation of natural disasters, e.g. pre-disaster geomorphic mapping and DEMs, rapid search and rescue in an event crisis, regional extent and relative severities and assist in disaster recovery by highlighting locations with resources (see Gillespie *et al.*, 2007; Teeuw, 2007). Ultimately, the utility of remote-sensing data (for real-time management) strongly depend on the disaster type and its onset time (Kerle and Oppenheimer, 2002).

Data availability in crises has recently been transformed by the Internet, Google Earth and geobrowser mashups (the combination of content from more than one data source into a single dynamic map service) (Butler, 2006a; 2006b; Nourbakhsh, 2006; Goodchild, 2009). Google Earth uses Keyhole Markup Language (KML) format, which facilitates transfer of geospatial data in real-time (Nourbakhsh, 2006). Other satellite data can be acquired on an emergency basis (e.g. through International Charter Activation, Bessis *et al.*, 2004). For example, following the 12th January 2010 earthquake in Haiti (West Indies), high resolution satellite images were available worldwide on the Internet within a day to show the extent of the damage and for interactive viewing on Google Earth (e.g. <http://news.bbc.co.uk/1/hi/world/americas/8458690.stm>, accessed January 2010). MapAction (and other non-government organisations, NGOs) deployed to Haiti to support ground relief coordination the day after the earthquake (attempting to plug the hole of the donut). MapAction are a NGO of specially trained professionals that work 'on-the-ground' in disaster zones providing frequently updated situation maps showing where relief help is most urgently needed. Maps (produced using ArcGIS) were

crucial during search and rescue operations (<http://www.mapaction.org/deployments/depldetail/192.html>, accessed January 2010). Also in Haiti, volunteer map-makers helped update local transportation networks using Global Positioning Systems (GPS) data uploaded and distributed (worldwide) freely via OpenStreetMap (<http://news.bbc.co.uk/1/hi/8517057.stm>, accessed May 2010). Furthermore, the benefits of opening up disaster operations can go beyond the immediate logistics of disaster response; individuals, moved by pictures, may make donations and encourage their governments to do the same (Nourbakhsh, 2006).

For lahar path detection, it has been suggested that a combination of remote sensing data products are needed for the best results; however, manual interpretation of aerial photographs has been found to be the most accurate method (Joyce *et al.*, 2009). Morphology and drainage structure of the flow deposition area following the 1998 lahar at Casita volcano (Nicaragua) was examined using various optical and radar sensors by Kerle *et al.* (2003) (see also Section 2.1.2). They concluded that the greatest synergistic potential came not from combining optical data with radar, or high with low spatial resolution, but in adding auxiliary information such as GIS elevation or map data. Furthermore, an earlier study by Kerle and Oppenheimer (2002) concluded that available imagery at the time of the disaster could not have significantly improved disaster response.

Further technological advances may increase ability to respond to future events. For example, the potential of real-time intelligent 3D GIS has been explored subsequent to 9/11, highlighting the issue of emergency response in urban areas, integrating the ground transportation system with the internal conduits of multi-level structures (Kwan and Lee, 2005). The technology to capture the internal three-dimensional structure of buildings is valuable for building evacuation, and is an area where substantial progress will be made over the next few years (Goodchild, 2009). The value of knowing the real-time locations of disaster victims and rescue teams is palpable, and this is fast becoming feasible with the latest developments in positioning technologies (Goodchild, 2009). In the wake of a disaster, GIS is becoming integral in supporting damage assessment, rebuilding and public education (Cova, 1999).

2.4.4 GI Science and research using GIS

2.4.4.1 An overview

The potential, and constraints, on the utilisation of GIS for disaster management have been introduced above, and also discussed by Carrara and Guzzetti (1996), Cova (1999), Radke *et al.* (2000) and Cutter (2003). Cutter (2003) summarises the main constraints as: understandable user interfaces; data quantity, quality, and integration; real-time data and information. These are wider issues that can be informed by progress in Geographic Information Science (hereafter, GI Science).

GI Science as a term came from the seminal work of Goodchild (1992). He recognised that geographical data are unique and associated problems could not be adequately subsumed under some larger field (Goodchild, 1992). First, the fundamental difference between geography and other scientific disciplines is that definitions of geographic objects of study are rarely unambiguous (Longley *et al.*, 2005). Furthermore, concepts of space are complicated by the continuous, spatial dependence and curved surface of the Earth (Goodchild, 1992). GI Science is concerned with ontology, representation, and computational issues, whereas geography attempts to explain and predict geographic phenomena (Mark, 2003).

The practice of GI Science is diverse, covering issues of technology, society, human cognition and the understanding of the nature of the Earth's surface (Goodchild, 2008). Crucially, GI Science is not simply a new name for GIS training and applications (Mark, 2003), nor is GIS limited to a mechanical pushing of buttons (Goodchild, 2009). Thus, Mark (2000) identified two important and distinct research streams: research in basic GI Science, and research using GIS (Mark, 2000). Research may use GIS to implement the storehouse of knowledge known as GI Science (Longley *et al.*, 2005). Research using GIS may also reveal important research topics for GI Science to address, and contribute to the GI Science research agenda (Mark 2003).

GI Science is perhaps best described through its research priorities. Reviews of the GI Science research field are provided by Mark (2003) and Goodchild (2008). A useful summary is the overarching 'Grand Challenges for GI Science'; the result of a National Science Foundation (NSF) Workshop in 1999 (see Mark, 2000). The four

themes were: (1) the representation challenge; (2) the uncertainty challenge; (3) the user interface or cognition challenge; and (4) the simulation or modelling challenge. The geographic information basic research committee, the University Consortium for Geographical Information Science (UCGIS) has identified the long-term research challenges (<http://www.ucgis.org/priorities/research/2002researchagenda.htm>, accessed May 2010):

- Spatial ontologies
- Geographic representation
- Spatial data acquisition and integration
- Scale
- Spatial cognition
- Space and space/ time analysis and modelling
- Uncertainty in Geographic Information
- Visualisation
- GIS and society
- Geographic information engineering

This list has been revised and expanded; for further information the reader is referred to McMaster and Userly (2005) and <http://www.ucgis.org/priorities/research/2006ResearchNextSteps.htm> (accessed May 2010).

Some of the GI Science issues are pertinent to disaster management and have been introduced in Sections 2.4.2 and 2.4.3; these will be discussed more widely, with reference to the UCGIS research challenges. There are also cross-cutting issues.

2.4.4.2 Spatial data acquisition and integration (including interoperability)

For natural hazards ground survey is costly, time-consuming and often difficult to perform (Coppock, 1995). Data limitations can lead to ignorance of data quality and use of unfit data because no other alternative (Agumya and Hunter, 1999). Thus, data acquisition and integration may be the single largest contribution area needed for emergency preparedness and response (Radke *et al.*, 2000).

UCGIS objectives for GI Science pertaining to spatial data acquisition and integration include (but are not limited to) improving the logic and technology for data capture and improving data capture standards (Jensen *et al.*, 2005). A major obstacle in the context of disaster management is the interoperability of systems to exchange information based on shared understanding of meaning and mutually agreed formats (Goodchild, 2003a). However, the Internet has played a key role in connecting systems over a common network protocol (Abdalla *et al.*, 2007). The Open GIS Consortium (OGC) has also emerged as a mechanism for achieving greater interoperability, leading the development of standards, or specifications, for geospatial and location based services (Abdalla *et al.*, 2007; Goodchild, 2009).

Remote sensing is a key source of data for disaster management. Although remote sensing is frequently recognised as a discipline in its own right, UCGIS objectives for research include evaluation of new sensors and sensor data systems, encouraging the increased use of remote sensing and utilisation with real-time GIS (Merry *et al.*, 2000). Over the past few years there has been a noticeable change in spatial resolution of remote sensing products and in spectral sensitivity. Technological advances are making satellite data products generally cheaper and ubiquitous. However, traditionally, coverage can be costly to obtain, have low spatial or temporal resolution, and be incomplete or uncertain in terms of repetition (Coppock, 1995; Kerle and Oppenheimer, 2002). Furthermore, optical data has limited utility in cloudy conditions (e.g. Kerle and Oppenheimer, 2002); and although Synthetic-aperture radar (SAR) can operate in any weather conditions it is poor in densely vegetated areas and areas covered in snow (e.g. Joyce *et al.*, 2009). Landsat and Advanced Spaceborne Thermal Emission and Reflection Radiometer (ASTER) multispectral archive data are good for exploratory studies at a relatively low cost but high cost for near real-time acquisition limits the use of these data for rapid hazard assessment (Kervyn *et al.*, 2007). ASTER thermal imagery has also been used in warning systems (e.g. Gogu *et al.*, 2006).

Knowledge of topography is required for an assessment of many natural hazards, including gravitational flows such as floods and lahars (Section 2.3.5.1). Airborne- and satellite-derived elevation data have been reviewed recently in Maune (2007); of additional note for hazard response, there are publicly available datasets. Shuttle

Radar Topography Mission (SRTM) elevation data is (freely) available on a near-global scale at resolutions of 30 m (1 arc second) for USA and 90 m for the rest of the world. However, there have been problems associated with voids in the dataset (Luedeling *et al.*, 2007; Reuter *et al.*, 2007; Kuuskivi *et al.*, 2005; Grohman *et al.*, 2006; Nikolakopoulos *et al.*, 2006), but these have largely been rectified. SRTM data may be acceptable for initial modelling in the short-term, dependent on event magnitude (spatial distribution). However, due to the significance of DEM quality on modelling results (Section 2.3.5.1), a higher resolution dataset is usually needed to improve reliability of mid- to long-term predictions. From June 2009, a new 30 m resolution global DEM was made available (free of charge) by the United States' National Aeronautics and Space Administration (NASA) and Japan's Ministry of Economy, Trade and Industry (<http://www.gdem.aster.ersdac.or.jp/>). However, there have been some accuracy issues and problems with cloud in certain areas. Other products for DEM generation, for mapping volcanic terrain, have been discussed in detail by Kervyn *et al.* (2007).

Furthermore, on-the-ground GPS data have revolutionised the capture of vector data and greatly improved positional accuracy (Longley *et al.*, 2005), but there remain insurmountable obstacles e.g. tree canopy and urban canyons interfering with GPS (Goodchild, 2009). Additionally, there are even recent developments in low-cost sensors that can be distributed over an impacted area and used to detect the presence of chemicals or fire (Goodchild, 2006).

2.4.4.3 Uncertainty in geographic information, spatial ontologies and geographic representation

Uncertainties in geographic information are inherent due to generalisations of real-world phenomena. Spatial data uncertainty exists in continuous variables (e.g. elevation and slope), categorical variables (e.g. land-cover classification) and in objects (e.g. position of roads) (see Zhang and Goodchild, 2002). All spatial information contains uncertainty; the correct conceptualisation of uncertainty is fundamental to the correct use of that information (Fisher, 1999). The way in which a geographic phenomenon is conceived prescribes the way it is measured, which in turn prescribes analysis (Longley *et al.*, 2001, 2005; Figure 2.13).

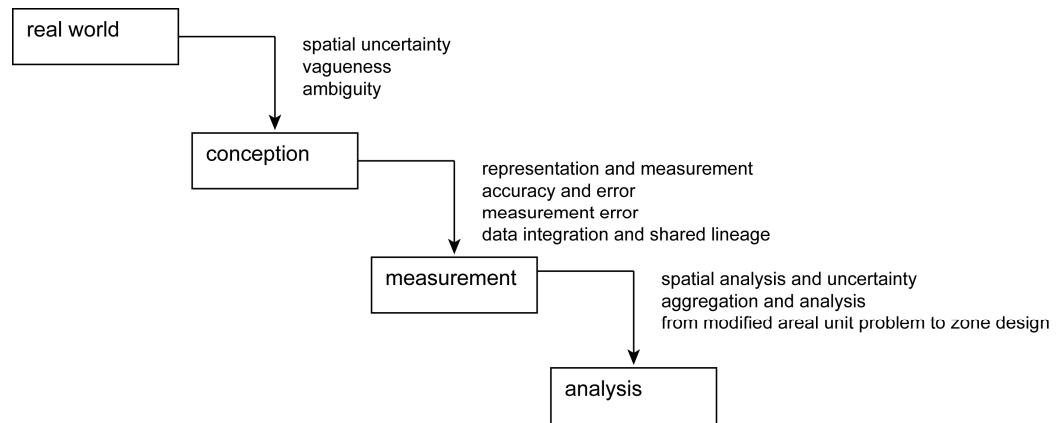


Figure 2.13 A conceptual view of uncertainty (after Longley *et al.*, 2001; 2005).

Consistent with this framework for conceptualisation, there are three elements of uncertainty pertaining to the conception, measurement and analysis of geographic phenomena (Longley *et al.*, 2005):

a) Uncertainty in the conception of geographic phenomenon: spatial uncertainty, vagueness and ambiguity.

Only rarely are there natural units of analysis, for example the field view of geographical phenomena is inherently continuous in space, so how can an environmental impact study delimit spillage from an oil tanker?, the investigator must make subjective decisions (Longley *et al.*, 2005). Vague concepts are poorly defined and give rise to an inability to apply labels to geographical phenomena. The Sorites Paradox is summarised as ‘what is a heap?’ and it little by little presents a logical argument that if one grain of sand is not a heap, and two are not a heap, then a million grains of sand are not a heap; it is one way to describe to test for a vague concept (Fisher, 1999; 2000). Land cover classes are vague geographic phenomena, for example, what is the absolute or relative incidence of oak trees in a zone that qualifies it for the label oak woodland (Longley *et al.*, 2005; Fisher, 2010)? Arbitrary

decisions are often taken to create a working definition (Longley *et al.*, 2005).

Vagueness can be address by fuzzy set theory, where, simply, membership to the label is defined within the range 0—1 indicating the relative strength of the degree of membership (Fisher, 1999; Fisher 2010). In contrast, ambiguity arises when there is doubt on how to apply a classification to geographical phenomena due to different perceptions of it (Fisher, 1999). This is particularly true across languages and cultural groups (Longley *et al.*, 2005).

b) Uncertainty in the representation and measurement of geographic phenomena

The handling of data and views of reality through different data models require different measurements of geographical phenomena. For example, reality may be viewed as fields or discrete objects and represented through raster or vector data models, each characterised by different uncertainties. For a full discussion the reader is referred to Longley *et al.* (2005). It is highly unlikely that geographical complexity can be reduced to models with perfect accuracy (Zhang and Goodchild, 2002). There will always be discrepancies between recorded measurements and the truth due to the assumptions we have to make, even if geographic phenomena are well defined or labelled (Longley *et al.*, 2005). Errors refer to inaccuracy and precision and are used with the assumption that true values are obtainable (Zhang and Goodchild, 2002). Measurement error is generated by the procedures of digital data capture (Longley *et al.*, 2005). Uncertainty can also come from integration of multiple data sources into a single geographic dataset; this can reveal errors when they are overlaid from one or more original datasets (see Longley *et al.*, 2005).

c) Uncertainty in the analysis of geographic phenomena

Uncertainty is an inherent property of knowledge and knowledge production (Coculelis, 2003). Turning raw spatial data into spatial information requires scientific analysis, yet the conception and measurement of many geographic phenomena are uncertain; thus, the precise nature of spatial variation may never be known (Longley *et al.*, 2001). Inappropriate inferences from aggregate data about the characteristics of individuals are also made (Longley *et al.*, 2005). Scale also has great impacts for

analysis. Taken together, the effects of scale and aggregation are generally known as the modifiable areal unit problem (Openshaw, 1984; Longley *et al.*, 2005).

GI Science research priorities include (but are not limited to): developing strategies for identifying, quantifying, tracking, reducing, and reporting (including visually representing) uncertainty in geographic data and GIS-based analyses (UCGIS, 1998; McMaster and Uery, 2005). Uncertainty considerations have great relevancy for natural hazard management (Section 2.2.2.2). Uncertainty can undermine trust which might have been put into the work or operator (Fisher, 1999; Haynes *et al.*, 2008b). Confidence in results is critical to their acceptance and to public recognition of risks (Zerger, 2002).

2.4.4.4 Spatial cognition and visualisation

Maps are important decision support tools (Longley *et al.*, 2005), yet they are never totally objective (Stefanovic, 2003). It has been argued that the traditional plan-view map presents a 'gods eye view' (Goss, 1995), perhaps giving false legitimacy to scientific results. Map visualisation relies on creating an impression of data properties within the mind of the observer (Gahegan, 1999). All maps present alternative views, embodying their authors' prejudices, biases and partialities (Wood, 1992) and present a specific argument or form of propaganda (Dorling and Fairbairn, 1997; Wood and Fels, 2008). Thus, maps can be used by disaster managers to persuade and control (Monmonier, 1998).

Paper maps are only one form of visualisation. A GIS is a flexible medium for the production of maps, allowing variable scale, querying of attributes and reclassification of data (Longley *et al.*, 2005). Furthermore, it is this flexibility that allows user interactivity to feedback from a visualisation and perform 'what if' scenario testing (Longley *et al.*, 2005). Yet, however subjective mapping products may be, they are still useful for the communication of hazard information, and are often the preferred output for decision-makers (e.g. Zerger and Smith, 2003). Thus, outputs from a GIS can, and should, be tailored to different information needs of different interested parties (Radke *et al.*, 2000). Intelligent visualisation techniques are needed to reduce the information load and to ensure quick and accurate

information transfer (Andrienko and Andrienko, 2007). General map design can be informed by the British Cartographic Society's introductory text (BCS, 2008) and Brewer (2005) among others. Furthermore, Hallisey (2005) provides an assessment and epistemological review of map visualization from a more social perspective.

Issues relating to the representation of geographic phenomena (introduced in Section 2.4.4.3) are also relevant to spatial cognition. UCGIS objectives for GI science pertaining to spatial cognition include questions such as: are current data models being limited by human cognitive models of space, place and environment? How can GIS be used to represent and communicate important information in different ways? (Montello *et al.*, 1998; McMaster and Usery, 2005) Goodchild summarised the relationship between GIS and spatial cognition as follows, while recognising that there has been significant improvement recently in this area of GI Science,

"GIS is in many ways the interface between the informal, loose world of human cognition and discourse and the rigorous, formal, and precise world of digital computers" (Goodchild, 2009, p. 6).

2.4.4.5 GIS and Society (including public participation)

Controversy surrounding the social implications of GIS applications arose in the 1990s (Pickles, 1995; Wright *et al.*, 1997; Pickles, 1997; see also Schuurman, 2000). Some of the key criticisms have been summarised (for a GIS audience in Longley *et al.*, 2001, p25) and include: the way human society is reflected, favouring certain perspectives (see also Section 2.4.4.4); the idea that GIS as a tool can be inherently neutral and immune from ethical debates; GIS is technology led and not demand-driven (see also Hassan, 2005); and GIS remains a tool in the hands of the (already) powerful. There has been a subsequent growth of a more socially aware type of GIS that is context- and issue-driven rather than technology-led, and seeks to emphasise community involvement in the production and/ or use of geographic information (Dunn, 2007).

Public participatory approaches enhance public involvement in environmental planning and decision-making. There is a strong need for public participation, both in developing GIS for emergency preparedness and for gaining access to it during a

disaster (Radke *et al.*, 2000). The public possess a repository of diverse experiences and local knowledge that can contribute to academic and scientific knowledge. In return the public will receive participation in the policy processes affecting their lives. Figure 2.14 shows the increasing levels of public participation in the decision-making process (Carver, 2003). Public Participation GIS (PPGIS), through the interaction of community interests and GIS technology, develops a richer database. Critical issues pertaining to PPGIS are discussed comprehensively by Elwood (2006), Sieber (2007) and Dunn (2007) among others. Public interaction with digital spatial data is becoming more ubiquitous through products such as Google Earth and Google Maps (Butler, 2006b); this is liable to have implications for PPGIS, for example by allowing non-experts to upload data to and increasing the democratisation of GIS (Dunn, 2007; MapAction, 2008). The role of the public as an important and rapidly growing source of geographic data has been discussed in several recent publications (see, e.g. Elwood, 2008; Goodchild, 2009).

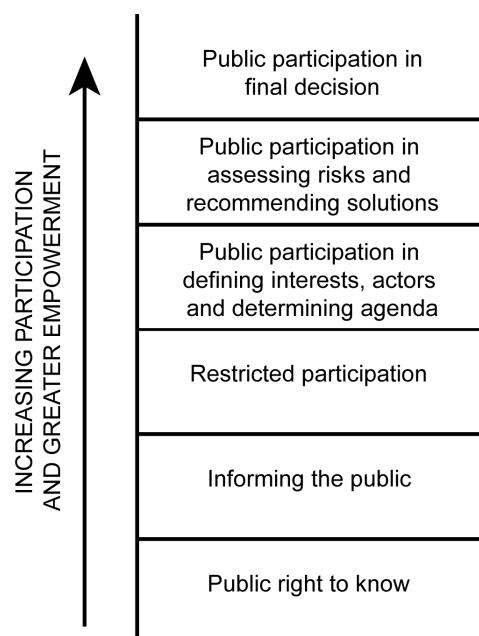


Figure 2.14 The public participation ladder in GIS (After Arnstein 1969; Carver, 2003 and references cited therein)

However, participatory approaches raise important questions about interpretation of accuracy (e.g. Goodchild, 2009); public participatory maps are not spatially accurate in a geometric sense (although relative locations are preserved) (Williams and Dunn, 2003). Furthermore, participatory approaches will inevitably involve multiple workers from different disciplines or researchers crossing disciplines; thus there may be problems with researchers who have little history of working together (e.g. development studies and GIS practitioners) (Williams and Dunn, 2003).

Public participation is, of course, not limited to GIS. There has also been a general call for (natural) scientists to show more cultural respect, in relation to risk analysis; this involves integrating vulnerability analyses and also public knowledge. As a response to rising global interest in public participation, the International Association for Public Participation (IAP2, <http://www.iap2.org/>) was founded in 1990. Public participation is also becoming increasingly prevalent in hazard management. For example, Participatory Rural Appraisal (PRA) methods for incorporating scientific with traditional knowledge have been tested for volcanic hazard management on Ambre Island, Vanuatu (Cronin *et al.*, 2004a) and Savo, Solomon Islands (Cronin *et al.*, 2004b). The former used a participatory mental mapping technique with the public and found that the derived volcanic hazard management guidelines (supported by an alert system and map) were more readily accepted than the earlier 'top-down' plans imposed by outside governmental and scientific agencies. The latter described how PRA can initiate dialogue within diverse stake-holder groups. Thus, PRA techniques can be used to involve many members of the community and outside interested parties. However, it is noted that there are problems getting the involvement of the less powerful community members (e.g. women, youth and non-landowners) (Cronin *et al.*, 2004b).

The public participation ladder in GIS (Figure 2.14) also has parallels with trends in approaches to risk communication by scientists: from original command and cajole to a move towards more public involvement (Fischhoff, 1995).

2.4.5 Potential of geospatial data and tools for lahar hazard assessment

This thesis focuses on lahar hazard assessment, one aspect of the disaster management cycle which is directly connected to mitigation and preparedness activities. Given the discussion above, geospatial data and tools can potentially contribute to such an appraisal by:

- Providing a data repository (e.g. spatial distribution of field data)
- Delineating inundation areas from past deposits
- Acquiring data, e.g. GPS, satellite imagery
- Developing a surface representation (i.e. DEM) for lahar modelling
- Integrating GIS and simple lahar modelling; however, from experience with coupling GIS with hydrological models, it would be likely that only simple models could be developed and preliminary findings gained.
- Exploring cost-benefit or 'what-if' scenarios for mitigation
- Undertaking evacuation planning
- Producing and/ or updating hazard zonation maps.

This list is not exhaustive. Core themes from GI Science also have potentially relevancy for lahar hazard assessment. These have been identified in the section above as: data acquisition and handling; uncertainty analysis; spatial cognition and visualisation and; GIS within society. Following an introduction to the study area, the final part of this chapter will discuss the wider gaps in the literature.

2.5 REGIONAL SETTING: MONTSERRAT, WEST INDIES

2.5.1 Overview

Montserrat is a British Overseas Territory in the West Indies that has been ravaged for nearly 15 years by a prolonged volcanic eruption. There was no historical precedent for volcanic activity on Montserrat; in July 1995 an eruption of the Soufrière Hills volcano began, with steam venting explosions after 400 years quiescence (Young *et al.*, 1998). The Montserrat crisis is unusual as a natural hazard due to its protracted nature. Long-term management is required, but of a type that responds to sudden impact events from individual and multiple hazards after periods of repose lasting months to years. From one perspective the initial crisis can be thought to have past, but the population is perpetually prevented from entering a recovery phase; hazard management is always mitigating and preparing for the next hazard.

2.5.2 Geography, geology and climate

Soufrière Hills Volcano lies in the south-central part of the island of Montserrat, West Indies (16.7° N, 62.2° W; Figure 2.15). Montserrat is part of the Lesser Antilles volcanic island arc, formed by the subduction of the Atlantic oceanic lithosphere (North Atlantic Plate) beneath the Caribbean Plate (Kokelaar, 2002). Montserrat consists of three volcanic massifs (Silver Hills, Centre Hills, Soufrière Hills-South Soufrière Hills) which range in age from late Pliocene (2.6 million years) to Recent (Wadge and Isaacs, 1988; Harford *et al.*, 2002; Hincks *et al.*, 2005). In addition, Garibaldi Hill and St George's Hill are topographic highs (Figure 2.16). Soufrière Hills is the youngest and only active volcanic complex. It has a crater (English's crater) approximately 1 km in diameter breached on the east-northeast side, attributed to a large sector collapse (Hooper and Mattioli, 2001).

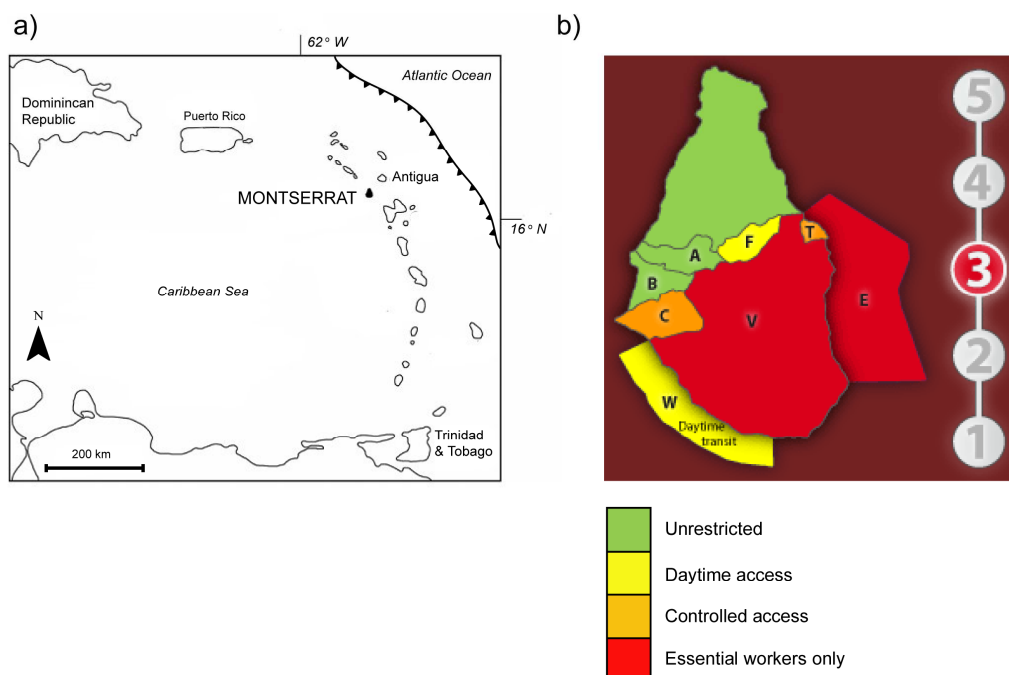


Figure 2.15 a) Position of Montserrat in the Caribbean; part of the subduction zone is also shown (after Susnik, 2009); b) the current access restrictions on Montserrat (Hazard Level 3, MVO, <http://www.mvo.ms/>).

The island had a pre-eruption land area of 98 km², but with frequent pyroclastic flows, e.g. down Tar River Valley and towards Plymouth, the island is growing. The majority of Montserrat is mountainous with small amount of coastal lowland and consists almost exclusively of volcanic rock. The rugged land surface is punctuated with deep valleys, known locally as ‘ghauts’.

Montserrat’s climate is maritime subtropical, with little daily or seasonal temperature fluctuations. Montserrat lies at the northern edge of the Inter-tropical Convergence Zone (ITCZ) and receives an annual mean rainfall 890 mm/yr (Barclay *et al.*, 2006). Due to the ITCZ seasonal cycle a wet season occurs from April to November, with two peaks in May and September (Barclay *et al.*, 2006). The tropical climate supports dense rainforest on the Centre Hills; lower montane and montane rain forest, palm break and elfin woodland represent the climax vegetation (Procter and Fleming, 1999).

In addition to the ongoing volcanic hazard, Montserrat is also vulnerable to hurricanes, tsunamis, earthquakes and the mountainous topography causes frequent landslides. For example, Hurricane Hugo in 1989 damaged 90% of buildings on the island (Kokelaar, 2002).

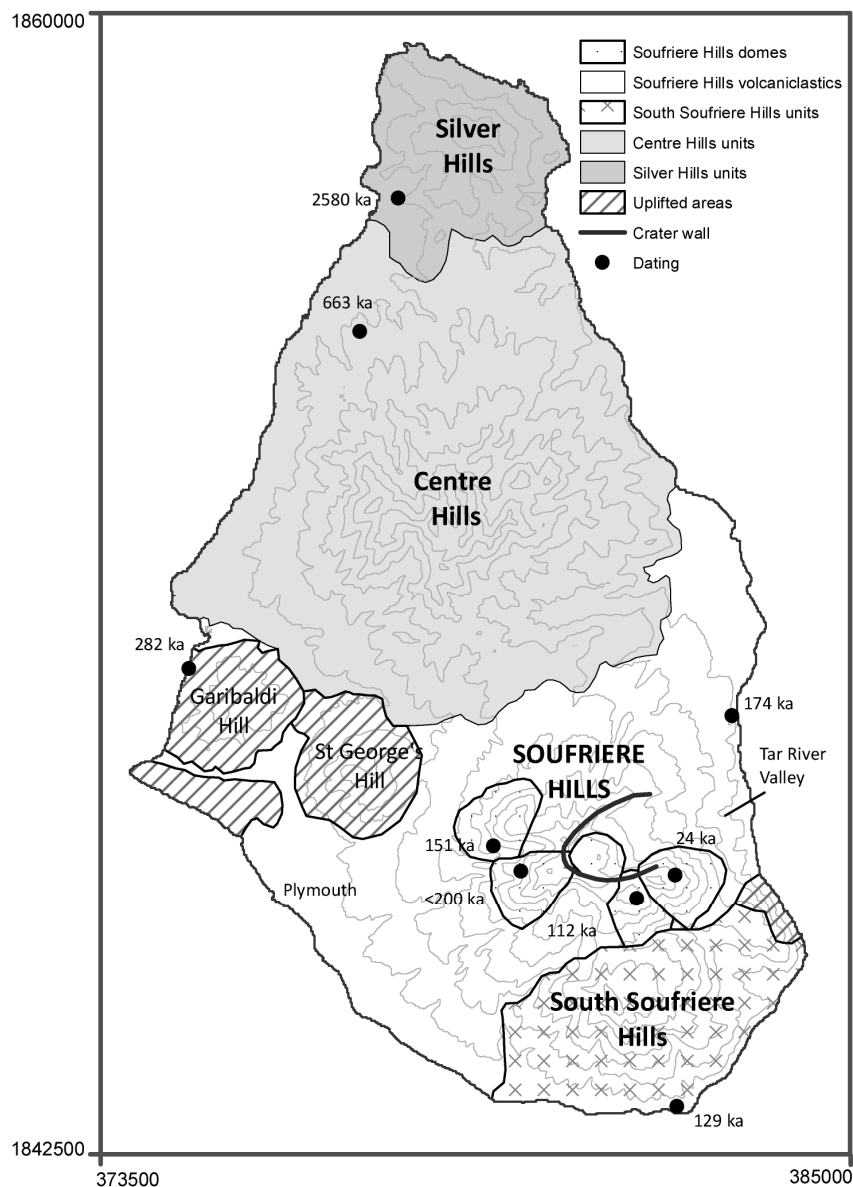


Figure 2.16 Pre-eruption geological map of Montserrat; coordinates in Montserrat National Grid (contour interval = 100 m). Dating in thousands of years (ka) from $^{40}\text{Ar}/^{39}\text{Ar}$ geochronology (after Harford *et al.*, 2002).

2.5.3 Chronology of an andesitic dome-building eruption

Radiocarbon dating suggests that the last period of major activity at Soufrière Hills took place around 400 years ago (Shepherd *et al.*, 1971; Young *et al.*, 1998). Following a few years of pre-eruptive seismic activity, the 1995 eruption commenced with phreatic explosions associated with heating of shallow water and the opening of a 1–2 m diameter steam vent (Young *et al.*, 1998); lava dome growth was later confirmed in November 1995 (Sparks, 1998). Since then the volcano has continued on a cycle of viscous (andesitic) magma extrusion, lava dome growth and subsequent flank or sector collapse, followed by a period of residual activity (Druitt and Kokelaar, 2002). The chronology of the eruption is summarised in Figure 2.17.

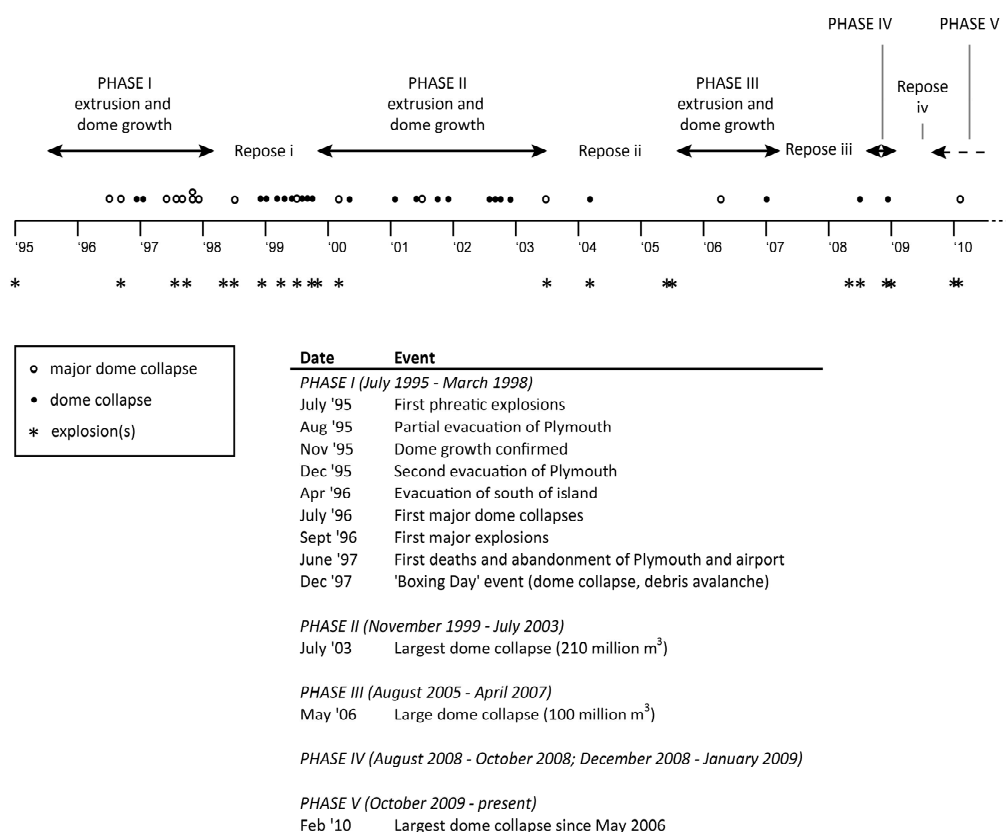


Figure 2.17 Summary of some of the key events of the eruption to February 2010 (after <http://www.mvo.ms/>; Herd *et al.*, 2005; Edmonds *et al.*, 2006)

The primary hazards are dome and flank collapse events, explosions, pyroclastic flows and surges, block and ash falls, and debris avalanches (Hooper and Mattioli, 2001; Herd *et al.*, 2005; Edmonds *et al.*, 2006). Secondary volcanic hazards refer to those phenomena indirectly associated with the eruption e.g. lahars (locally known as mudflows) and landslides.

2.5.4 Impacts of the eruption (1995—present)

2.5.4.1 Physical change

Montserrat has effectively lost two-thirds of its land area to the volcano, with over 60% of the island permanently designated as unsafe for human habitation or activity. The most suitable areas for settlement have been lost, including over 70% of the buildings (Clay *et al.*, 1999). Most of the higher potential agricultural and pasture land has been buried or made inaccessible (Dittmer, 2004).

Volcanic flows (e.g. pyroclastic flows) have filled many of the major drainage channels (ghauts) with volcanic debris, and deposition at the mouths of river systems has extended the coastline (Hincks *et al.*, 2005). Furthermore, the remobilisation via rainfall of loose material deposited has resulted in profound changes to the geomorphology of many of the river systems surrounding the volcano.

Vegetation on the flanks of the Soufrière Hills, and adjacent South Soufrière Hills, has largely been destroyed by pyroclastic flows, ash fall and acidic gas (Hincks *et al.*, 2005). The period for vegetative regeneration is estimated at 10—20 years, once ash deposition and lahars have ended (Clay *et al.*, 1999).

2.5.4.2 Demographic change

Prior to the start of the eruption, there was a high standard of health, education and living on Montserrat (Clay *et al.*, 1999; Dittmer, 2004). Most of the population, infrastructure, public and private sectors were concentrated on the southwest coast in the capital city of Plymouth (Figure 2.16). This was destroyed two years after the eruption began.

Of the *circa* 11 000 people that were resident on Montserrat before the eruption began, 92% suffered at least one evacuation when nearly two-thirds of the island was designated unsafe for human habitation (Kokelaar, 2002). Evacuations proceeded in stages; the first evacuation of Plymouth was ordered in August 1995 but after two weeks the population returned, reflecting lower activity levels. This led to a feeling of transience by local people and sustained in them hope that they could return to their homes in the longer-term (Dittmer, 2004). Plymouth was evacuated three times before being permanently abandoned in June 1997 (Bowen, 1997).

Initially, those residents who were able to leave the island were asked to do so voluntarily to ease pressure on shelters. Financial incentives were offered by the British Government, reducing the island's population to about 2 500. Residents that remained were predominantly single persons or small family units at the poorest end of the economic spectrum (Fox, 2002). However, the move to the north was not 'an even trade' as the land was comparably barren and infertile (Dittmer, 2004) and temporary accommodation for evacuees was substandard (Pattullo, 2000; Fox, 2002). Despite initial enthusiasm toward the UK's Assisted Return Package scheme (Clay *et al.*, 1999), by the end of 2007 government figures indicated that the population had only rebounded to *circa* 4 500. The influx has mainly been due to guest workers involved in construction projects (Stone, 2003; Dittmer, 2004).

The immediate social consequences of the volcanic eruption were shrinkage of the island, relocation of evacuees, social fragmentation, a decline in the quality of services (Pattullo, 2000). Now the population is living with the continual hazards from the volcano, access restrictions and, for those that choose to stay further south, periodic evacuations (e.g. when dome growth is directed towards the west, parts of the west coast are evacuated). Fine airborne ash penetrates into homes and is an inconvenience and possible health hazard (Horwell *et al.*, 2003; Hincks *et al.*, 2006).

2.5.4.3 Economic change

In the first four years of the eruption the total capital loss was estimated at £1 billion (Clay *et al.*, 1999). The economy is now virtually non-existent except for the public sector and linked public construction (Clay *et al.*, 1999; Dittmer, 2004). The GoM is

attempting to revive the tourism industry. Tourism was one of the main contributors to the economy before the volcanic crisis, contributing to 25% of GDP (DFID, 2005). The pre-eruptive form of tourism was fairly unique to Montserrat consisting mainly of low-density retirement homes for foreigners (Dittmer, 2004). However, the tourism industry virtually collapsed as Montserrat's identity became synonymous with danger (Dittmer, 2004). Since the onset of the crisis Montserrat has been reliant on DFID assistance.

DFID is the UK government department responsible for promoting sustainable development and reducing poverty. Its central focus in the Caribbean is to assist the region to achieve sustainable reductions in poverty in line with the Millennium Development Goals. For Overseas Territories, Country Policy Plans set out how the UK will contribute to achieving policy objectives and promote development. However, DFID is seeking to reduce Montserrat's dependence on external support, with the aim of achieving self-sufficiency within ten years (DFID, 2005). A newly constructed Sustainable Development Plan should help achieve this goal. Montserrat needs rapid private sector development and re-positioning in the tourist market (DFID, 2005). The tourist sector should have improved since the opening of the new Gerald's airport in 2005 and subsequent reconnection with transport networks.

Contrary to the DFID plan, others argue that it is better to embrace the uniqueness of the island, for example by developing a postgraduate school of disaster studies (Economist, 2003). A return to agriculture is almost impossible as the fertile land of the south is largely inaccessible or destroyed (Dittmer, 2004). However, volcanic activity has also resulted in the deposition of a new resource of volcanic materials such as sand and gravel that may be used in construction (Norton, 2005). A major challenge for rejuvenation of the economy will be to attract back or retain skilled people.

2.5.5 Management of the Volcanic crisis (short-term) 1995—1999

Initial extrusion and the first phase of dome growth commenced November 1995 and were punctuated by periods of explosive activity and dome collapse until March 1998. There was then a period of repose until renewed extrusion and dome growth in November 1999. This marks the first cycle of the eruption and also reflects the period covered in a Geological Society of London publication (Druitt and Kokelaar, 2002). MVO was setup in response to the escalating activity in 1995, before then the Seismic Research Unit of the University of the West Indies, had been actively monitoring Montserrat for several decades, with permanently installed seismographs and occasional field visits (Aspinall *et al.*, 2002).

Montserrat was unprepared for the volcanic eruption despite a relatively recent report outlining the potential of an eruption and the susceptibility of Plymouth to volcanic hazards (Wadge and Isaacs, 1987). The revised report was also published and internationally distributed as a journal article (Wadge and Isaacs 1988). Although copies were delivered to the Governor's Office and to the Commissioner of Police on Montserrat, local authorities denied all knowledge of the report until volcanic activity began in 1995 (Bowen, 1997); later the loss of documents was attributed to Hurricane Hugo in 1989 (Pattullo, 2000). This lack of preparedness also resulted in the ill-advised rebuilding of key facilities in Plymouth after the hurricane, wiping out £16.8 million of redevelopment aid (provided by HMG) almost immediately after completion (Bowen, 1997). Crucially, both the GoM and the UK Government proved themselves to be unprepared for the communication and public information roles that managing the emergency required (Clay *et al.*, 1999; McGuire *et al.*, 2009).

There was an initial shaky start to the management of the crisis (e.g. Aspinall *et al.*, 2002; Kokelaar, 2002). No contingency plans had been made and *ad hoc* arrangements were made reactively as the eruption progressed (Clay *et al.*, 1999). The Wadge and Isaacs (1987; 1988) report was initially adopted and then adjusted to meet new developments at the volcano (Aspinall and Cooke, 1998). Short-term management decisions were made. Eleven different hazard maps were produced in just over a year, reflecting both changing alert levels issued by MVO (Aspinall *et al.*,

2002) and the desire by the local authorities to allow as much access as possible (Kokelaar, 2002); however, the number of maps and their multiple zones (microzonation) complicated communication to the general public (Pattullo, 2000; Kokelaar, 2002).

The complexity of HMG management and the administrative system for Montserrat as self-governing, contributed to management failures in the early stages of the volcanic crisis (Clay *et al.*, 1999). GoM adopted a 'wait and see' attitude, assuming less serious impacts, whereas HMG had to prepare for the worst case (Clay *et al.*, 1999); it has been argued that this dual focus protected the wider interests of the citizens of the island (Davis *et al.*, 1998). Differing agenda also existed between the administrative authorities and scientists at MVO. For example, the (single runway) airport was kept open until its evacuation during the advance of a pyroclastic flow (Kokelaar, 2002). Initially there were divergences in opinions between scientists at MVO and authorities became frustrated with the perceived indecision (Aspinall and Cooke, 1998); misunderstandings of the uncertainties in volcanic monitoring were initially mistaken for incompetence of the scientists by local authorities and in some cases the public (Haynes *et al.*, 2008a; 2008b). However, generally the close link between scientists and emergency managers raised public confidence and improved the response of the population (McGuire *et al.*, 2009). Trusted and influential locals (including radio presenters and church leaders) were also exploited by scientists and authorities as 'translators' (Haynes *et al.*, 2008a).

Aspects of the organisation and delivery of aid by DFID have been criticised (see details in Bowen, 1997). The growing perception from Montserrat was that DFID was acting ungenerously and adopting cost minimising solutions to the detriment of longer term development (Clay *et al.*, 1999). Post-disaster accommodation was one of the most controversial aspects of the entire emergency response (Fox, 2002). For example, tents procured were second-hand from the American army and in poor condition (Bowen, 1997; Clay *et al.*, 1999; Fox, 2002). Five different types of short-medium term temporary shelters were provided before permanent structures were erected – two years after the onset of the eruption (Fox, 2002). Inadequate conditions in the early stages of the eruption may have contributed to people

entering the exclusion zone to tend to their property (Pattullo, 2000). However, HMG regards management of Montserrat as an overall success; ‘...everyone has had a roof over their head, no one has gone hungry’ Clay *et al.*, 1999, p1).

Nineteen people died in pyroclastic flows on 25 June 1997 after entering the exclusion zone. Eighty members of the public were in the ‘evacuated’ area that day, despite warnings from local authorities and scientists (Loughlin *et al.*, 2002). There were a combination of factors contributing to the fatalities e.g. people had become de-sensitised to risks (Aspinall and Cooke, 1998; Loughlin *et al.*, 2002) and conditions in the temporary shelters prompted people to return to their homes (Pattullo, 2000). Furthermore, access was restricted but barriers were not firmly enforced (Voight, 1998). Later a news article published in *Nature* was highly critical of science communication preceding the June 1997 disaster; it claimed a survey of islanders had shown Montserratians had ‘lost faith’ in scientists warnings and this had directly contributed to the deaths (Masood, 1998). An earlier *Nature* editorial (*Nature*, 388, 1; 1997) had also attributed the deaths to poor communication, using the disaster as a call for cooperation across disciplinary boundaries. Scientists responded in earnest, highlighting the many lives that had been saved and reiterating the uncertainties (and often unpredictability) of volcanic phenomena (Aspinall *et al.*, 1998; Voight, 1998).

2.5.6 Management from emergency towards reconstruction and recovery (long-term and current strategies)

2.5.6.1 Synopsis of current hazard management

Soufrière Hills is continuously monitored by scientists at Montserrat Volcano Observatory (MVO). This includes visual observations and instrument monitoring of seismicity, ground deformation and gas. Principal sources of uncertainty pertain to eruptive scenarios, e.g. direction of dome growth and potential for collapse (through explosion or edifice failure).

Primary hazards are monitored individually by MVO. Hazard and risk assessments are reviewed every six months by a panel comprised of MVO personnel and

scientific advisors. Known as the Scientific Advisory Committee (SAC), this panel release preliminary statements followed by a main report and a technical report; all are publicly available from the MVO website (<http://www.mvo.ms/>).

For each hazardous process, the probability that they will occur and affect a given area (fixed zone) of Montserrat is estimated. Uncertainties from complex potential eruptive scenarios are considered through probability trees and Monte Carlo procedures; probability density functions for different hazards are determined by numerical models where available (Hincks *et al.*, 2005). Expert judgement is used where results are unavailable (e.g. Newhall and Hoblitt, 2002).

Given an estimate of the probable hazards affecting a particular zone, the risk to which a given number of people in that area will be exposed is calculated. Risk levels are mainly expressed as potential loss-of-life estimates and as annualised individual risk exposures (qualitative description based on UK Chief Medical Officer's scale). Risk in all zones is then considered against the island-wide Hazard Level System (a relatively new system set-up in August 2008). Ultimately the responsibility for determining the Hazard Level and response falls to the National Disaster Preparedness and Response Advisory Committee (NDPRAC). The committee is comprised of a panel including the Governor, representatives of the Government of Montserrat, Disaster Management Coordination Agency (DMCA) and MVO. The DMCA implement decisions, act on scientific advice and have the primary responsibility for liaising and communicating with the public.

Maps created on advice from MVO, and in consultation with the SAC, are used to communicate hazard zones to local government officials and general public. Each incarnation of the hazard zones map reflects the dangers from all primary volcanic hazards and restricts movement and access according to the Hazard Level System (new system set up in August 2008). Montserrat is currently at Hazard Level 3 (Figure 2.15b) (May, 2010). The public are also informed of changes in volcanic activity through daily reports by MVO personnel on a local radio station and through the MVO website. Furthermore, MVO outreach has, as far as is practicable in a crisis, an open-door policy for interaction with the public (Aspinall *et al.*, 2002).

In addition to community-level evacuation plans (that are reviewed and updated annually) there is a plan for the evacuation of the entire island – Operation Exodus (GoM, 2005).

2.5.6.2 International commitments to disaster risk reduction

Following the abandonment of Plymouth and relocation to the northern part of the island in 1997 a Sustainable Development Plan (SDP) was established with DFID funding; by 2001 £75 million of assistance had been received to develop the north of Montserrat (GoM, 2006). The volcano dome collapse of July 2003 resulted in ash that enveloped the entire island triggering national, regional and international response (GoM, 2005). The United Nations Development Programme (UNDP) country office in Barbados has further supported disaster mitigation, capacity building and institutional strengthening in support of Montserrat's Post-Emergency Resettlement Programme through United Nations Volunteer placements in the areas of physical and social infrastructure. This assistance, co-funded by DFID and GoM, amounted to US\$750,000 (UNDP, 2003).

Prior to the World Conference on Disaster Reduction, WCDR, (Kobe, Hyogo, Japan 18-22 January 2005) ISDR encouraged national authorities to provide information to identify needs and elaborate policy recommendations for the preparatory process of the WCDR. Two of the main outputs of the WCDR were the Hyogo Declaration and the Hyogo Framework for Action. The GoM prepared their national report and highlighted their commitment to achieving a sustainable form of disaster risk reduction (GoM, 2005). This national report placed disaster risk reduction central to national policy and strategy, and stressed disaster risk reduction and environmental impact assessments must be carried out before any development projects are approved (GoM, 2005).

Montserrat is classified by the UN as a non-UN member 'small island developing state' (SID). Most SIDs are remote, small in land area and population (less than 1.5 million), with a very narrow resource base and fragile land and marine ecosystems that are highly vulnerable to natural disasters and Montserrat fits comfortably in this definition (http://www.un.org/esa/dsd/dsd_aofw_sids/sids_members.shtml, accessed May 2010). While Montserrat has not submitted a National Adaptation

Plan for Action and has not ratified the Kyoto Protocol (May 2010), Montserrat's national report states climate change and national adaptation plans are led by the Minister of Agriculture (GoM, 2005). Furthermore, the new SDP (2003-2007) aimed to accelerate Montserrat's dependency on foreign aid and ultimately lead to self sufficiency (GoM, 2006). It is unclear how much progress has been made.

"The Montserrat experience can be used as a useful case of a small island developing state where collaboration of political establishment, civil service, scientific communities and disaster reduction sectors are making positive changes to reduce risk to disasters by committing to the integration of risk reduction into all planned development." (GoM, 2005).

2.5.7 Belham Valley lahars

Lahars are not formally monitored on Montserrat. MVO are committed to monitoring primary volcanic hazards only and thus lahars are not a priority. However, this means that the Hazard Level System is not reflective of lahars, nor are the island-wide hazard maps (e.g. Figure 2.15b).

Lahars are recorded in daily and weekly MVO reports on activity at the volcano. However, these reports rely on visual observations and thus probably represent an under-reporting of lahars (Barclay *et al.*, 2004). Short-period seismic records can show lahars but the seismic network was designed to monitor primary activity and thus during periods of high volcanic activity it can be impossible to distinguish lahars (Barclay *et al.*, 2004). There was a purpose-designed lahar monitoring network installed in the Belham Valley, but this data was never retrieved and the equipment has not been maintained (Barclay *et al.*, 2004).

Lahars occur frequently in all major drainages, but only one could channel lahars towards populated areas, the Belham River Valley (Figure 2.18). Most Belham Valley lahars are rainfall-induced and not limited by sediment availability. Thus, they can occur without concurrent volcanic activity. The likelihood of lahar occurrence reflects the seasonality of the Montserratian rainfall (Barclay *et al.*, 2004). Lahars in

the Belham valley correlate with days when > 10 mm rain fall in 24 h, with more lahars triggered in the late rainy season (Barclay *et al.*, 2007). However, there is less of a correlation of rain and lahar events in the dry season, thus rainfall alone is not responsible for triggering all lahars (Barclay *et al.*, 2007). Other sources of water come from the stream-flow of tributaries that do not contain loose volcanic sediment (Barclay *et al.*, 2004), i.e. those draining the Centre Hills.

There is significant spatial variability of rainfall intensity across the island due to topographic enhancement (Barclay *et al.*, 2004; Barclay *et al.*, 2006). Preinstalled rain-gauges (when operating) have been recording rainfall at a one-minute resolution from 2001 onwards (Matthews *et al.*, 2009). However, the rain-gauge network coverage (Figure 2.18) is not comprehensive and the gauges become clogged by ash (fine tephra). Furthermore, due to rainfall variability with topography over the island, single gauges are not representative of rainfall intensity over a large area (Barclay *et al.*, 2006).

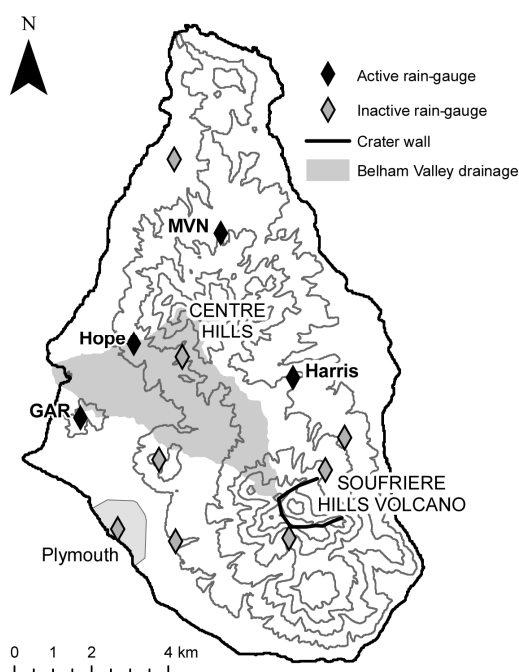


Figure 2.18 Belham Valley Montserrat and rain-gauge network; names for the currently active gauges are shown in bold text (150 m contours) (After Alexander *et al.*, in press).

Sediment load is introduced by new eruptive material and also through erosion of and entrainment of pre-existing deposits. Vegetation damage makes more sediment available and also increases runoff (Barclay *et al.*, 2004; Alexander *et al.*, in press).

Prior to the onset of the modern eruption (pre-1995), the ephemeral Belham River produced only low sediment-concentration flows (stream-flow). From the same rainfall patterns post-1995, changes in the catchment have produced discharge events with a much more variable sediment load (Barclay *et al.*, 2007). In general Belham Valley lahars have very low sediment concentrations, producing deposits more akin to concentrated stream-flow than hyperconcentrated-flow or debris-flow (Barclay *et al.*, 2007). Thus, most flows display Newtonian characteristics and are strictly not lahars; some authors prefer the term 'sediment-charged flash floods' (e.g. Alexander *et al.*, in press). These dilute flows have been compared with flows in analogous systems such as flash floods in ephemeral streams, flash floods following forest fires and floods in steep mountain streams (Susnik, 2009). Although rare, non-Newtonian hyperconcentrated-flow and debris-flow have been observed and display competence to transport boulders up to 2 m diameter (Barclay *et al.*, 2007). These more extreme events have been caused by changed runoff resulting from synchronous tephra fall and widespread vegetation damage (Alexander *et al.*, in press). While the considerable temporal and spatial variation in the nature of the flows is acknowledged, the collective term 'lahar' is used here.

Lahars have caused great geomorphological change to the Belham Valley. Figure 2.19a shows the floodplain as it used to be just after the modern eruption began, a golf course, and Figure 2.19b shows the same area after ten years of lahars. Damage from lahars can also be seen on houses that bordered the Belham River (Figure 2.20). While Belham lahars are not formally monitored, there are warning signs in place at major crossing points (Figure 2.21).

Lahars on Montserrat differ from examples documented at other volcanoes in that (a) the eruption has been continually supplying sediment, (b) rainfall is the only significant trigger, and (c) the system is small, with a relatively low catchment top and short travel distance to the sea (Barclay *et al.*, 2007). As documented above, there has been some previous research on lahars in the study area; however, this does not preclude further original work.



Figure 2.19 Multiple flows down the Belham Valley have greatly changed the geomorphology: a) the mouth of the valley in 1996 (looking east), the shoreline is marked by a line of palm trees (courtesy R. Herd, UEA); b) the mouth of the valley in 2006 (looking south-east) has greatly extended into the sea, the palm trees marking the 1996 shoreline have been highlighted.



Figure 2.20 Photographs illustrating the effects and damage caused by lahars in the Belham Valley a) large boulders up to 2—3 m diameter have been deposited in the mid-reach (flow right to left); b) boulders also in the upper-reach (looking upstream); c) damaged house in November 2006; d) house in 2007, an extra 1m of deposit; e) rear of house in 2007 shows accumulated debris; f) lahar debris litters the floor of the Belham Valley in 2007, Soufrière Hills can be seen in the background.



Figure 2.21 Warning signs are in place at the major crossing points for the Belham Valley. Lahars are often locally referred to as floods or mudflows.

Moreover, these framing studies (e.g. Barclay et al., 2007; Susnik, 2009; Alexander et al., in press) have demonstrated the need for an improved understanding of Belham lahars and have established relationships with local scientists. Furthermore, the small size of the catchment provides a manageable case study, ideal for model testing and development. Any ideas developed can potentially be applied to other lahar and non-lahar systems worldwide, especially small catchments with water-rich gravitational flows.

2.6 EVALUATION OF GAPS IN RESEARCH TO DATE

2.6.1 Drawing out intellectual themes

Three intellectual themes can be mined from the different literary sources and these will run through the thesis:

- (1) monitoring lahars, acquisition and handling of data;
- (2) improving knowledge of lahars through modelling; and
- (3) transfer of academic research on lahars to agencies of hazard management.

These themes have emerged in the discussions of the state-of-the-art of natural hazard management, lahar hazard assessment, application of GIS, and implications from (and for) GI Science. The evidence is synthesised below.

Monitoring lahars, acquisition and handling of data

The difficulties in data acquisition from an active volcanic system were first highlighted in Section 2.3.3. Models can predict lahar movement when field observations are few, but in turn models can have great data demands (Section 2.3.4.5).

Lahars are not formally monitored on Montserrat as they are secondary volcanic hazards (Section 2.5.7); thus, this research needed to acquire the raw data for modelling. One of the key requirements for most modelling approaches has been identified as a digital elevation model (DEM) (Section 2.3.5.1).

The issue of data handling was discussed briefly in a reflection on the key factors for lahar modelling (Section 2.3.5); however, the procedures for turning data into information and for dealing with uncertainties in spatial data were discussed in further detail with reference to research using GIS and GI Science (Section 2.4.1). Uncertainties when dealing with natural phenomena are also being regarded with increasing importance in the field of natural hazard studies, and hazard assessment

techniques are starting to move beyond simple uncertainty recognition towards attempts to quantify (Section 2.2.2).

Improving knowledge of lahars through modelling

Modelling is now central to assessment of natural hazards (Section 2.2.2.1) and, in particular lahars (Section 2.3).

To the author's knowledge, no modelling studies have been performed for Belham Valley lahars, despite their obvious value (Section 2.5.7).

Transfer of academic research

A core mechanisms for transfer of hazard information has typically been the hazard zonation map, integral to natural hazard management (Section 2.2.2.1), now produced through runout and inundation studies (Section 2.3.4), and informed by the GI Science research agenda (Section 2.4.4.4).

However, the short-comings of a top-down approach to information transfer were introduced in the context of disaster risk reduction for natural hazards in general (Section 2.2.1), and also have been raised as a critique of GIS-based research and GI Science (Section 2.4.4).

Montserrat has a history of problems with transfer of hazard information (Section 2.5.5).

New research in these themes will thus have relevancy across several disciplines and sub-disciplines. Additionally there are some gaps in the literature.

2.6.2 Synopsis of gaps in the literature

The need for a comprehensive lahar hazard assessment on Montserrat is demonstrated by current gaps in knowledge about the lahar hazard. However, such research on Montserrat would also inform other gaps in the literature. For example:

- *Dilute lahars*. The majority of lahar models are not universally applicable to all flow types and indeed there is a prevalence of debris-flow models. There

is an absence of general dilute lahar models. Some immediate questions emerge, e.g. are debris-flow models applicable to dilute flows (e.g. Montserratian lahars)? To what extent can stream-flow models be applied to dilute lahars?

- *DEM fit for lahar modelling.* The importance of surface representation for lahar modelling was introduced in Section 2.3.5.1. However, the techniques for generating DEMs and incorporation of elevation uncertainties have not figured prominently in evaluations of model performance. New research in generating DEMs that are applicable (fit for) lahar modelling would potentially be of great interest to volcanologists. Furthermore, although there is a general trend towards probabilistic assessment of natural hazards, there is an absence of lahar models that incorporate such uncertainties. A DEM might be the ideal vessel to consider uncertainty and demonstrate its propagation to model results.
- *Effective information transfer.* There is a recognised void between research generated in the sciences, and applied research that has on-the-ground practical utility. A mechanism for generating effective transfer of lahar hazard assessment results would have benefits beyond this case study.
- *A GIS focus to lahar hazard assessment.* There are some examples of research using GIS for volcanic risk management (e.g. Pareschi *et al.*, 2000a) and lahar modelling (e.g. Schilling, 1998; Pitman *et al.*, 2003). However, in many cases GISs have not been used to their full potential and implications from, and for, GI Science have not been thoroughly contemplated.

Over the next four chapters these themes and gaps in the literature will be examined. There will be cross-cutting issues. An evaluation of these findings in the context of wider research will be given in the final chapter (Chapter 7).

CHAPTER 3: AN APPLICATION-DRIVEN APPROACH TO TERRAIN MODEL

CONSTRUCTION

Terrain is a surface phenomenon that is measured, modelled, and mapped. However, it is continuously variable and must be simulated by points or mathematical equations that are inherently approximations. The error induced by digitally represented terrain can propagate to surface derivatives and geographical information science applications where topography is considered. This can lead to uncertainty in model predictions and the use of data that are unfit for the application to which they are intended. This article outlines the problem of uncertainty in terrain representation and demonstrates the consequences for volcanic mudflow modelling. The response of a simple least-cost single flow algorithm to input parameters was investigated in order to assess output variation from the different sources of input variation. Elevation error was modelled with a probability density function and propagated through stochastic simulation (Monte Carlo). Such combined uncertainty and sensitivity analyses enabled a qualitative judgement of the relative significance of elevation error on the flow model prediction. Different methods for terrain model construction were considered and show that supplementing global positioning system measurements with information from field notes and reconnaissance photographs greatly improved the model performance and reduced the uncertainty. It is concluded that in terms of validity of model results, there is no substitute for constructing an elevation model that is informed by the terrain.

3.1 INTRODUCTION

Geographical Information Science (GI Science) is concerned with the position, spatial relationships and attributes of geographic phenomena. This information is stored digitally for querying, processing and display. Spatial data analyses range from relatively simple enquiry tasks to more complex modelling, but the veracity of results is always dependent on the quality of the input data.

Adequate terrain representation is fundamental for many GI Science applications such as hydrological flow routing (Raaflaub and Collins, 2006), soil erosion prediction models (Warren *et al.* 2004) and viewshed analyses (Fisher, 1998). The quality of digitally modelled topographic information can be greatly influenced by the method of construction. In GI Science there is a general tendency for data-driven modelling, where data availability guides the generation of the digital terrain representation (Schneider, 2001). This is largely due to a tradition of restrictions imparted by scarce data and high prices. However, such an approach does not prioritise surface reconstruction fit for intended applications, nor is it sympathetic to the characteristics of the terrain that may impede its adequate representation. Therefore, detrimental consequences when using first and second order derivatives from a data-driven surface construction are potentially greater than those from an application-driven approach. With a general increase in data supply and availability it is now imperative that more consideration is given to data quality and fitness. Furthermore, an acknowledgement of uncertainty is important for greater confidence in decisions that are informed by data, enabling scientists to defend their predictions (Beven, 2000).

For modelling volcanic debris flows the adverse consequences of using unfit data can be particularly extreme. Debris flows are not only hazardous in themselves, but they also cause morphological change, potentially altering the route of the next flow. Understanding flow movement can help predict potential inundation and landscape change. Inadequate data will greatly distort these results, particularly on a local scale. In this chapter, the influence of digital terrain representation quality on the output of a flow model is investigated. A single flow direction algorithm was

used to identify the path of steepest descent for a type of volcanic mudflow. The effect of varying data quality on flow routing was investigated through uncertainty identification and propagation. Sensitivity analysis augmented the uncertainty analysis and together they were used to assess the merits of an application-driven methodology for digital terrain representation.

3.2 BACKGROUND: DIGITAL TERRAIN REPRESENTATION

For a successful geographical information system, it is essential to have an accurate view of the world (Goodchild, 1992). Vector models represent discrete objects (points, lines and polygons) and can be stored using positional geometry. Continuous data, including surfaces, are poorly represented as such. Instead, fields preserve the continuity of surfaces through a finite number of variables defined at every location. For example, a terrain surface can be mathematically defined by its elevation, z , varying as a function of x and y : $z = f(x, y)$. One of the most familiar ways to represent topographic reality in a geographical information system (GIS) is the regular gridded digital elevation model (DEM). For this, finite data are collected and values assigned to data points through interpolation. Elevations are stored as a simple matrix and estimator values for a specific location can be obtained by querying a cell in the grid. Algorithms can be used to calculate terrain derivatives such as slope and aspect.

However, topographic reality can only be represented digitally to a certain level of accuracy. Errors at finite positions are inherent due to the approximations needed. Our lack of knowledge about the reliability of a DEM's representation of the true value is referred to as uncertainty (Hunter and Goodchild, 1997). Error is contained within all DEMs and can be considered the disparity in the elevation value projected by a DEM and its true value. In a DEM the main sources of error pertain to (1) variation in the accuracy, density and distribution of measured source data, (2) processing and interpolation, and (3) characteristics of the terrain surface being modelled (Fisher, 1998; Fisher and Tate, 2006). Error can propagate through to

surface derivatives (e.g. Holmes *et al.* 2000; Aerts *et al.* 2003) and thus to GIS applications utilising DEMs and terrain analysis. This will ultimately affect confidence in the results of GIS operations. Therefore, the real relevance of DEM error becomes apparent when the link is made between DEM quality and application quality (Fisher and Tate, 2006).

Thus, it is important to establish whether the chance of an incorrect output is significant for the application concerned (Fisher 1998; Li *et al.* 2000). Alternative data sets can be compared in terms of their suitability for an application (de Bruin *et al.* 2001; Hunter and de Bruin, 2006), and to examine the consequences that using them may have for subsequent decisions (Agumya and Hunter, 1999). However, determining the minimum data quality requirement for a specific application is often difficult. A threshold of acceptance or level of tolerable risk in decisions must be identified and met (Agumya and Hunter, 1999). In this chapter an approach to a fitness for use evaluation through uncertainty and sensitivity analyses is presented. Uncertainty analysis was performed to understand the propagation of error through the application. In addition, by sequentially changing inputs pertinent to the flow algorithm and also terrain model, local sensitivity analysis was able to (qualitatively) apportion output variation to different sources of input variation (Crosetto and Tarantola, 2001).

3.3 STUDY AREA

The study area is a section of the Belham River valley on the volcanic island of Montserrat (West Indies). Soufrière Hills Volcano is currently active (August 2009) and when volcanic debris is mobilised by rainfall the valley acts as a conduit for lahars (akin to dilute debris flows or mudflows). These lahars are gravitational flows and therefore primarily dependent on topography. However, due to the typically low sediment concentration of Belham lahars, simulation of flows falls somewhere between traditional debris-flow modelling (sediment-rich flows) and hydrological

routing (water-rich flows). As a first step towards a spatial hazard assessment, topographic data were used to direct a relatively simple flow routing model.

The lower section of the valley (including the river mouth) was considered as it incorporated the greatest spatial variability in topography (Figure 3.1). Recorded elevations in this locality range from sea level (zero metres) to circa 25 m, over a distance of 1500 m. Terrain undulates on a local scale with micro-topographic changes including sediment banks (0.5 to 2 m for this section of the study area) and dense blocks of persistent vegetation on raised terraces (0.75 to 2.5 m). Channels carved out by the lahars, and the ephemeral river, are also features of this landscape.

Due to the intimate relationship between terrain characteristics and error, certain types of terrain are more suited to the creation of accurate DEMs (Carlisle, 2005). The valley floor of the study area can be considered gently sloping, with dense pockets of vegetation, associated with rapid changes in elevation (raised terraces).

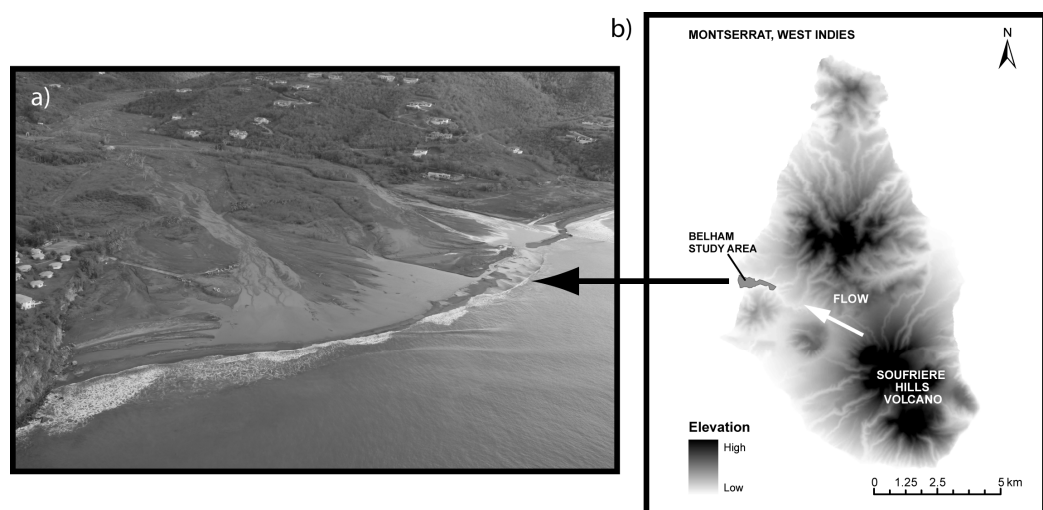


Figure 3.1 (a) Photo of the mouth of the Belham Valley taken November 2006 (looking east); (b) the location of the study area on Montserrat (DEM after Wadge 2005).

There are also areas of high surface roughness where gravel carried by the lahars has been deposited en masse (see also Figures 2.19 and 2.20, Chapter 2). Previous studies have shown the positive correlation of error and terrain slope e.g. Hunter and Goodchild (1997), Veregin (1997) and Fisher (1998), or surface roughness (Kyriakidis *et al.* 1999). Thus, due to the heterogeneous nature of the terrain, it was anticipated that errors in the DEMs would be spatially variable.

3.4 METHODOLOGY

3.4.1 Application overview – lahar modelling

Understanding the factors governing lahar inundation zones is crucial for hazard assessment on Montserrat. Due to the downslope propagation of these flows, and their topographic constraints, an adequate terrain model is essential for modelling flow paths. The simplest method for specifying flow directions is to assign flow from one cell in a DEM to one of its eight direct neighbours with the lowest elevation. This single flow direction algorithm, designated D8 (Deterministic-8), has been widely used (e.g. Jenson and Domingue, 1988; Veregin, 1997; Tarboton, 1997) and is provided within mainstream GIS software packages (such as ESRI ArcGIS). The Belham Valley acts as a conduit, naturally channelling lahars into convergent flow, thus a single flow algorithm should be viable for a first approximation of system preferential flow (i.e. a least-cost flow path). Least-cost routing has successfully been used for route planning in landslide prone areas (Saha *et al.* 2005) and optimization in spatial decision support systems (Aerts *et al.* 2003). This approach was adopted as it was easy to implement, used global functions to consider the entire DEM, and also included terrain derivatives that were important for flow modelling and for assessment in terms of the propagation of error.

3.4.2 Data acquisition

Data capture in an active volcanic environment is challenging. In late 2006 available satellite data of the study area were of poor quality, showing abundant cloud cover. Elevation data were gathered in the field (when the authorities permitted work in the valley) through a roving Global Positioning System (GPS). The GPS equipment, from the Montserrat Volcano Observatory (MVO), was an Ashtech base kit and a Leica rover kit. Surveys were carried out over several days and fixed to the MVO's continuous GPS network using RINEX files from their sites. Position and height measurements were taken every second. Leica GeoOffice was used to post-process the data and transform from WGS84 to the local Montserrat grid system (a Transverse Mercator projection made onto the Clarke 1880 ellipsoid). Only points resolved to an accuracy of 0.1 m (minimum) in the vertical and horizontal planes were retained for analysis. The overall accuracy of a roving survey such as this introduces error due to the motion of walking. However this was estimated to be in the order of only a few centimetres.

GPS positions were gathered along the path of motion and this was constrained by obstacles; therefore resulting in an irregularly distributed dataset. However, this flexibility allowed areas of importance (as identified in the field) to be recorded i.e. potentially relevant micro topographic changes. Detailed field notes were supplemented by ground photography and oblique aerial photographs taken from a helicopter reconnaissance mission.

3.4.3 Identifying uncertainty

The accuracy of a lahar simulation depends on two factors: the veracity of the model, and the accuracy of the DEM (Stevens *et al.* 2002). Uncertainties are inevitable in hazard prediction, yet the adoption of simple techniques to assess data quality can provide responsible agencies with greater confidence in their decisions. The types of uncertainty associated with the creation of a DEM and its subsequent use for flow modelling are illustrated in Figure 3.2.

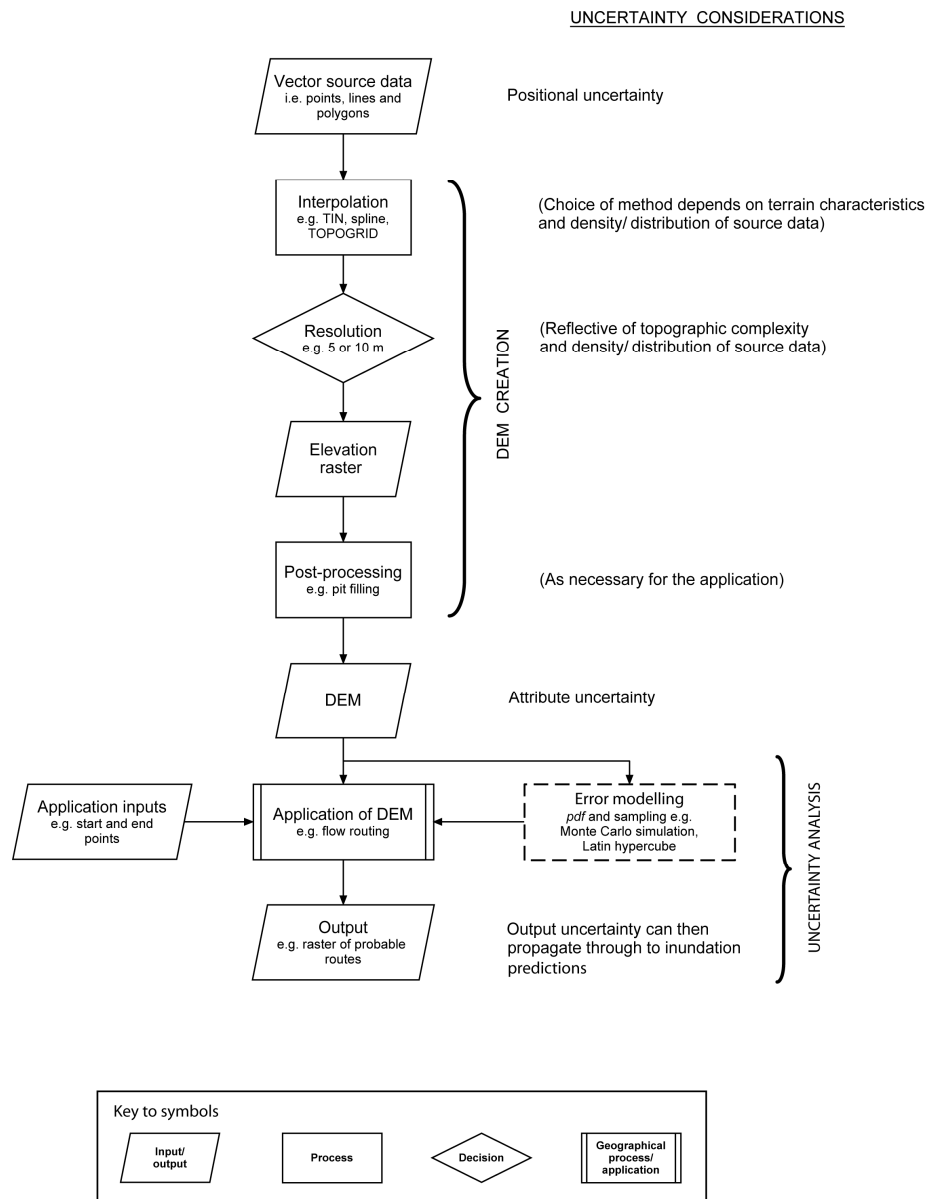


Figure 3.2 Potential sources, and transfer, of uncertainty from DEM creation to model output. Relative timing of uncertainty quantification in this case is indicated by the dotted box.

In this particular case, the source data had positional uncertainty associated with the accuracy of GPS point data (in the x , y , and z domains) and interpolation and processing techniques induced (further) error as the DEM was constructed. This produced a regular grid with attribute value (elevation) uncertainty at each cell location (Heuvelink *et al.* 2007). The DEM was then used as an input to the flow

model and, along with variability associated with the application such as start and end points, error in the DEM propagated to uncertainty in the output. Formally recognising these sources of uncertainty suggests that by simulating the potential range of errors, a DEM user can examine the consequences for their results and adjust the DEM construction accordingly, to suit better their application needs. Elevation is a continuous numerical variable and uncertainty in its estimation can be acknowledged at the source data positions and/ or DEM attribute locations. In this case, error in elevation was considered following DEM construction, as the combined response to uncertainty in source data, interpolation, and processing (Figure 3.2). Uncertainty was most relevant here due to high confidence in the positional accuracy of the GPS source data (i.e. uncertainty was believed greater after DEM creation). Simulating uncertainty from all potential sources was impractical - a recognised challenge when working towards a goal of statistical realism (Heuvelink *et al.* 2007).

3.4.4 DEM creation

ArcGIS was used for processing the point data into an elevation model. For irregularly distributed data the Triangulated Irregular Network (TIN) is a common interpolation method (Hugentobler and Schneider, 2005). The digital surface model produced consists of a set of triangular linear surface patches or facets that are created by drawing edges between data points (nodes) that satisfy the Delaunay criterion (the circumscribing circle of any triangle does not contain any point of the dataset inside it). These triangular facets can represent topographical features (e.g. pits, peaks and passes, and surface changes in slope and aspect) by having the triangle edges fall along the approximations of ridges and river channels etc, and having corners at important turning points (Laurini and Thompson, 1992: p248). However, the raster grid structure of a DEM lends itself well to neighbourhood calculations that are frequently used to derive hydrologic parameters (Wechsler, 2007). Thus a TIN was first created from the GPS data to preserve lines of interest (e.g. channels) and the TIN was then converted to a raster in ArcGIS. This created a

Primary DEM. Such derived results will be more accurate and reliable when more information is provided (Schneider, 2001). In order to obtain a topographically plausible surface representation, knowledge about the shape and the properties of terrain was also incorporated. This required the aerial photographs to be digitised and georeferenced (using field notes, ground photography and 20127 precise GPS points). They were then rectified using cubic convolution (Hughes *et al.* 2006). The supplementary information added in this manner included channels and vegetation terraces. The elevations for these were incorporated with the GPS data to form a new, Secondary DEM. Therefore, information about the terrain surface was not solely limited to the GPS data, but expert knowledge was incorporated to reconstruct the surface more reliably (Schneider, 2001).

However, it is well known that slope direction and hence flow are tightly controlled by facet orientation from a TIN. Alternative methods of DEM interpolation (splines with tension and TOPOGRID) were tested against the rasterised TIN (Secondary) for a 250 × 250 m section of the study area. This subsection was selected for its homogeneity (at 5 m resolution) and incorporated minimal topographic changes. As far as possible, the source data were the same. TOPOGRID (ArcGIS's implementation of ANUDEM v4.6.3 (Hutchinson, 1989)) imposed a drainage enforcement condition using digitised channels in addition to the point elevation data. For the tension spline (Mitasova and Mitas, 1993) channels were converted into point data and merged into the elevation dataset. A range of different sample points and spline weights were tested in ArcGIS.

The ability to represent topographic complexity is controlled by the DEM's grid cell spacing (resolution). Very coarse grid spacing may lead to under-sampling of micro terrain features (information will be lost for those features smaller than the sampling interval). Furthermore, slope varies with DEM resolution (Warren *et al.* 2004). Thus, the choice of resolution will depend on the spatial characteristics of terrain, but this should also be justifiable in terms of the potential accuracy offered by the source data. DEM resolution is discussed in Wechsler (2007) and references therein. From the observations documented in Section 3.3, two resolutions were chosen to preserve features of the terrain: 5 and 10 m. A finer resolution was not supportable due to the irregularly distributed GPS data.

3.4.5 Modelling error in the DEM

For a quantitative spatial attribute $A(\cdot)$, such as elevation, at some location x its 'true' value is $A(x)$ as defined by the model (Heuvelink, 1998): $A(x) = b(x) + V(x)$, where $b(x)$ is the deterministic variable, i.e. the realisation of $A(\cdot)$, and $V(x)$ is the error. For a DEM, if the error is known and quantified, uncertainty is reduced; if accuracy is unknown but error can be simulated, uncertainty can be represented and the consequences for analyses assessed. The latter is considered here, i.e. in the absence of a reference surface (surrogate for the 'true' elevation) it is not possible to model the actual distribution of error in the DEM. This is a common problem for DEM users. DEMs are typically provided by vendors with a summary measure of vertical accuracy in the form of the root mean squared error statistic (RMSE), but rarely do data users have access to more detailed uncertainty information (Darnell *et al.* 2008). In recent studies modelling error, higher accuracy data is often used as a surrogate for the 'true' elevation surface from which error values can be calculated at discrete points (Kyriakidis *et al.* 1999; de Bruin *et al.* 2001; Aerts *et al.* 2003). Conditional stochastic simulation is then used to generate multiple equally probable error surfaces to which the DEM is added. Each resultant surface has the essential properties of both the original DEM and its error (Fisher, 1998). Studying the range of different outputs improves understanding of DEM uncertainty. Furthermore, the quantification of error and its spatial distribution is an improvement on the single global RMSE.

In the absence of a higher accuracy reference surface, DEM error was simulated using unconditioned fields. This required knowledge of the distribution of error, represented by a probability density function (*pdf*) (Heuvelink *et al.* 2007). It was assumed that over a DEM the errors were normally distributed around a mean of zero metres (there was no known bias in the data). The standard deviation of error (*stdv*) was inferred from field knowledge, resulting in the selection of three possible values: 0.1, 0.5 and 1 m. The stochastic input variable (elevation error) was sampled within the bounds set by the *pdf* using Monte Carlo simulation.

Furthermore, within a DEM the magnitude of error for an individual grid cell is related to errors from neighbouring cells (Hunter and Goodchild, 1997; Fisher 1998;

Kyriakidis *et al.* 1999). This complex pattern of spatial variability of error and spatial dependency (termed 'spatial autocorrelation') was considered when undertaking the analyses. Two different methods for simulating the elevation errors were tested. The first assumed no spatial autocorrelation; the second considered a form of spatial dependence. Model outputs from each method were examined to assess the relative severity of error propagation.

3.4.5.1 Method 1: Spatially independent errors.

The error field was generated using Monte Carlo simulation from the *pdf* and added as 'noise' to the DEM (e.g. Hunter and Goodchild, 1995; Fisher, 1998). Using a different random number seed, 100 equally probable realisations of the error surface were generated. An input DEM was then perturbed using each of these error surfaces in turn. Each DEM was subsequently used as an impedance surface (with no additional thematic cost) for the flow algorithm. This was implemented in ArcGIS ModelBuilder.

3.4.5.2 Method 2: Spatial dependence using the Grid-Cell Uncertainty Model (GCUM).

Method 1 used random unfiltered error fields that assumed no spatial autocorrelation, i.e. the error values of neighbouring cells were independent. Neglecting spatial autocorrelation could result in cells having immediate neighbours with extreme peaks and troughs, which rarely occurs in nature (Zerger *et al.* 2002). The autoregressive analytical model developed by Hunter and Goodchild (e.g. 1995) was used to find an appropriate value for the spatial dependency of error (ρ). Like Method 1, it assumed no knowledge of the input data errors, required the input of an error estimate (usually an RMSE for DEMs) and was stochastic. GCUM was a more complex technique but has been widely used (e.g. Murillo and Hunter, 1996; Hunter *et al.* 1995; Hunter and Goodchild, 1997; and Zerger *et al.* 2002). The Grid-Cell Uncertainty Model Tutorial and software code was available from http://www.sli.unimelb.edu.au/people/gjh_notes/grid.htm (accessed March 2008). Full details of the methodology are found in the aforementioned studies.

In this study 10 trial realisations were made for each value of ρ . Differences in the average slope and standard deviation of slope were taken for (each) original DEM and for each realisation at different ρ values (consistent with Hunter and Goodchild, 1995). When a suitable value for the spatial dependency was identified (see Hunter and Goodchild, 1997), 100 realisations were generated and used as input cost surfaces as before. As an illustrative example, Figure 3.3 compares the average slope for the original Primary 10 m DEM with the average slope from the DEM perturbed by a value of ρ . The plot results from a mean difference of 10 realisations of the perturbed DEM and error bars show the range of those 10. The same process was repeated for differences in the standard deviation of slope. There is a gradual increase in the mean differences for average slope and standard deviation of slope as ρ varies from 0 to 0.18, followed by a sudden decrease as ρ approaches 0.25. With a RMSE value of 0.5 m the average slope for the DEM increased by more than about 1 degree. For the Primary 10m DEM, below $\rho = 0.18$ there was negligible change between the mean slope given by the realisations and the mean slope given by the DEM. This value was taken as the transition point for ρ and accordingly used in further analyses.

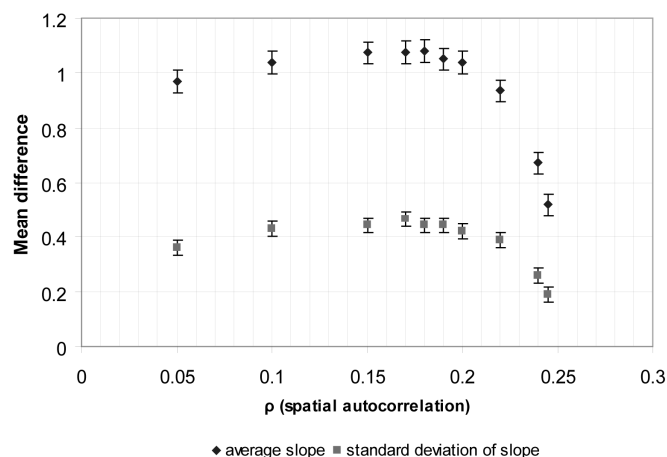


Figure 3.3 Differences in average slope and standard deviation of slope – between original DEM and the mean of 10 realisations at a given ρ . Error bars show minimum and maximum values (primary 10-m DEM, stdv = 0.5 m).

3.4.6 Uncertainty propagation and sensitivity analysis

Sources of uncertainty were identified and error was modelled at the most appropriate juncture - after DEM creation, as identified in Section 3.4.3 (Figure 3.2). Assigning a probability distribution to DEM error allowed the effect of variance in that input on the application output to be considered. However, the DEM error incorporated uncertainty influences from multiple parameters associated with the flow model and DEM. The relative influence of different input variations on the output could be isolated by sequentially varying these parameters (P). In this way uncertainty analysis was complemented by simple sensitivity analysis.

For each DEM, the ArcGIS module COST WEIGHTED DISTANCE was used to generate a cumulative cost surface (topographic consideration only) and associated cost direction grid. For flow routing the neighbourhood search was limited to a 3×3 pixel matrix, resulting in eight possible single flow directions. The SHORTEST PATH module was used to identify the preferential flow path from a selected start point to an end point.

An error field perturbed each terrain realisation and this process was repeated 100 times, generating 100 equally probable surfaces. The flow routing algorithm was applied to each and thus 100 least cost pathways were generated. A cumulative total of a cell's classification as being in the least-cost flow path indicated a likelihood of selection, i.e. a probability surface. This process was repeated for each change in the different input parameters (whilst all others remained constant) (Figure 3.4). The parameters for analysis were: DEM construction method (Primary or Secondary TIN, TOPOGRID or spline), DEM resolution (5 or 10 m), *stdv* (0.1, 0.5 or 1 m), spatial dependency of error (Method 1 or 2), and also flow model start and end point (various) (Figure 3.4). Understanding how responsive the model output was to DEM generation and accuracy enabled fitness for use to be assessed. This local, one-at-a-time, form of sensitivity analysis is commonly employed for a simple, preliminary exploration of model quality (Crosetto and Tarantola, 2001; Frey and Patil, 2002). It is recognised using such a local sensitivity analysis only allows a small portion of the possible input values to be addressed (Frey and Patil, 2002). In contrast simultaneously varying multiple inputs across a range of plausible values

can include interactions among inputs. This form of global sensitivity analysis has been applied to hydraulic models of river flooding for model validation and calibration (Crosetto and Tarantola, 2001; Hall *et al.* 2005). However, here local sensitivity analysis was sufficient to allow an indication of the level of parameter accuracy required to make a model sufficiently useful and valid, enabling prioritisation of data collection needs. After these priorities have been identified, probability distributions of multiple variables could be considered to further the research presented in this chapter.

In addition, the methodology is consistent with Hunter *et al.*'s (1995) suggestions for combating uncertainty in spatial databases: (1) highlighting locations within the study area that are susceptible to changes in parameter values, (2) assessing the likelihood of a cell's membership of a particular class, (3) displaying several realisations of a map to understand the degree of variation associated with the process, and (4) studying the effect on map products where competing datasets, error estimates, algorithms and process models are available.

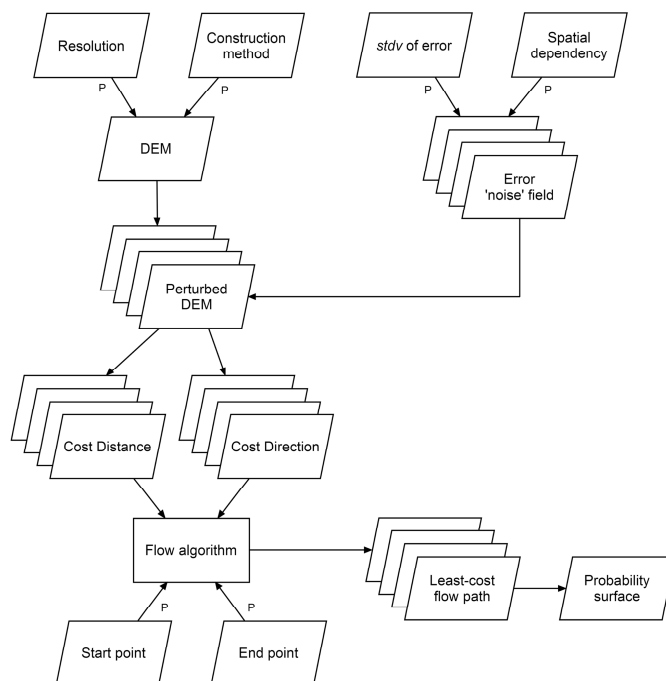


Figure 3.4 An overview of the uncertainty and sensitivity testing showing the input parameters (P) and the output (probability surface).

3.5 RESULTS

3.5.1 DEM construction with spatially independent error

Figure 3.5 shows the spatial distribution of GPS points for the lower-reach of the Belham Valley. A total of 20127 points were retained for analysis. A subsection of this study area was also taken (250×250 m) to trial interpolation techniques for DEM generation.

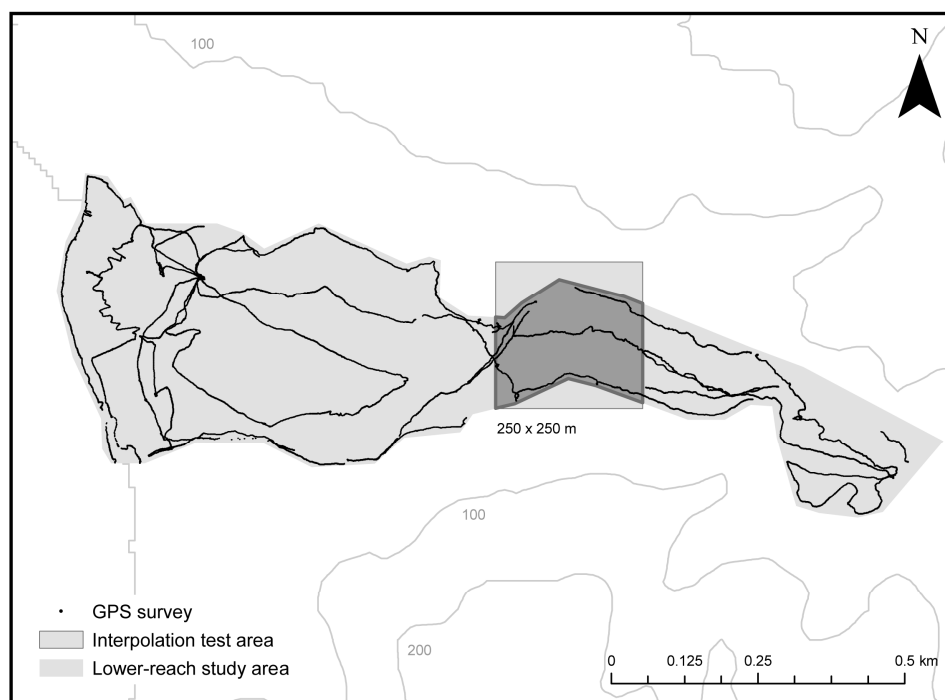


Figure 3.5 Lower-reach study area showing the distribution of the 20127 GPS points and 250×250 m subsection of the study area that was used to test the interpolation techniques (bottom left corner: 375450, 1850400 Montserrat National Grid)

Different interpolation techniques were used to process source data into a 5 m resolution DEM (50×50 cells), with differing degrees of success. Tension spline interpolation persistently suffered from 'overshoots', overestimating local maxima and underestimating minima, producing artificial peaks and troughs in the simulated landscape. This occurred despite adjustment of the tension and sample points to suit best the terrain. However, flow direction simulation using the D8 algorithm with the spline-derived DEM and rasterised TIN did not produce markedly differing results (for 100 realisations of the 'true' surface) (compare Figure 3.6a and 3.6b).

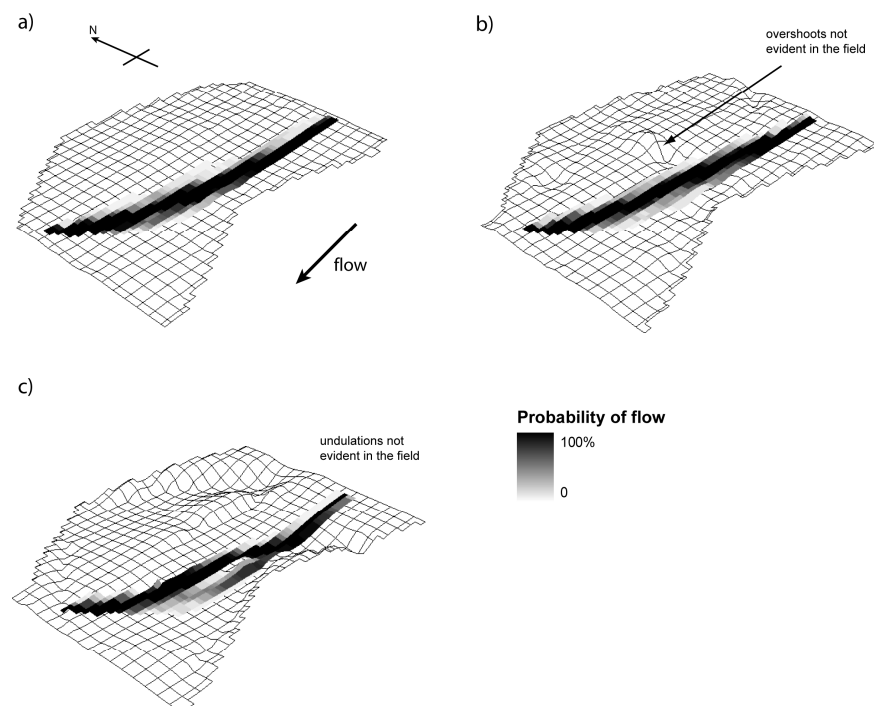


Figure 3.6 Wireframe (viewed on a 10-m grid) showing interpolation of source data through (a) rasterized secondary TIN, (b) spline from ten sample points with spline weight = 5, and (c) TOPOGRID. Elevations have a vertical exaggeration of factor 2.

In this case flow did not encounter any of the overshoots generated by the spline. In contrast, the global drainage condition imposed by TOPOGRID distorted the whole landscape (also shown by Callow *et al.*, 2007) and produced the greatest flow path variability (Figure 3.6c). These preliminary tests suggested that a TIN was preferable for this fluvially-eroded landscape and thus further analyses were conducted with TIN surfaces only.

From a TIN, construction of the Secondary DEM differed from the Primary product in that the former included supplementary information from field knowledge and aerial photographs. Incorporation of supplementary information changed the flow path for all error-perturbed DEM surfaces. Flow paths over the Secondary DEM cost surface took more direct routes than over the Primary DEM, avoiding the major blocks of vegetation (Figure 3.7, flows are from right to left). The probability fields from DEMs with supplementary information agreed better with the observed channels (Figure 3.7(c)).

The Primary DEM was more susceptible to changes in resolution when *stdv* was greater or equal to 0.5 m (compare Figure 3.7(a) and 3.8(a)). Figures 3.8(a) and 3.8(b) show variation in probability surfaces for the 5 m and 10 m DEMs (300 × 200 cells, or 150 × 100 cells respectively); the flows branched into two dominant routes in the lower reaches of the valley at a *stdv* of 0.5 m. At 10 m resolution, paths were distributed over a wider area and took more diverse routes. The proportion of cells in the study area predicted to experience some flow (those cells classified as part of the least cost flow path in at least one simulation) increased from 27% to 45% as resolution changed from 5 to 10 m for the Primary DEM. In comparison, for a similar resolution change, flows with the Secondary DEM only increased from 12% coverage to 16%, indicating that the Secondary DEM was more robust to resolution change and produced less variable results. For the Secondary DEM, resolution had little effect on the general trends (Figures 3.8(c) and 3.8(d)).

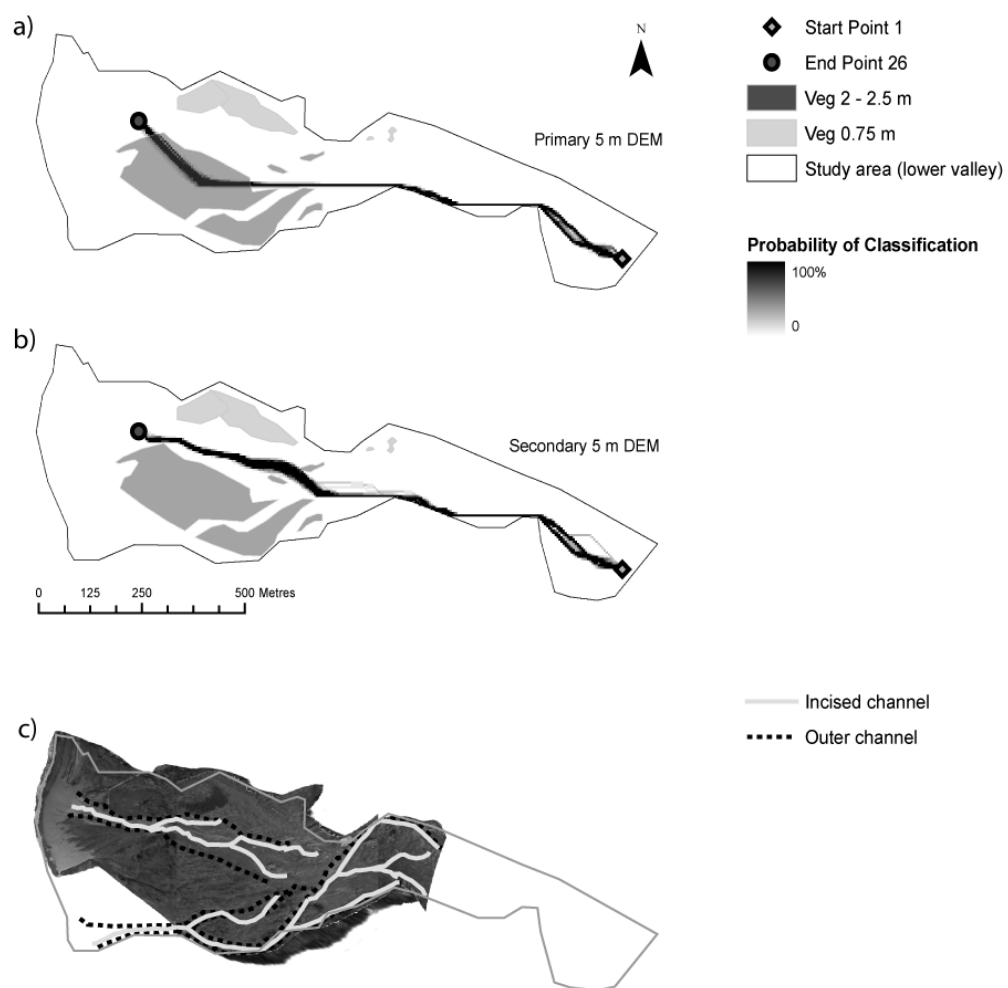


Figure 3.7 Parameter change: (a) and (b) DEM construction method ($stdv = 0.1$ m); (c) observed channels (incised and outer/border) from aerial photographs.

As $stdv$ increased the probability fields became less constrained, incorporating more cells, and thus flow path routes were more uncertain (e.g. Figure 3.8). Figures 3.7(a) and 3.8(a) show the flow algorithm response on the Primary 5 m DEM to respective 0.1 and 0.5 m $stdvs$. The proportion of cells inundated increased from 6% to 27%, corresponding to a 7.8×10^4 m² increase in area. For the Secondary DEM, flow path coverage of the study area (as a measure of variability) increased from 9% to 21%, to 31%, as $stdv$ rose from 0.1 to 0.5 to 1 m respectively. This corresponds to a difference in impacted area of 8.4×10^4 m² between 0.1 m $stdv$ and 1 m $stdv$; the

magnitude is similar to the change exhibited by the Primary DEM when *stdv* is increased from 0.1 to 0.5 m.

Observation of the probability fields from the Secondary DEM reveals the flow channel split into three dominant routes as the standard deviation of error increased from 0.1 to 0.5 m. As the standard deviation of error increased further to 1 m the least cost paths became very erratic in the lower reaches. Key areas sensitive to error were the middle of the study area and in the lower reaches near the shoreline. Overall, the flow model was very sensitive to changes in the *stdv* parameter, especially for the Primary DEM.

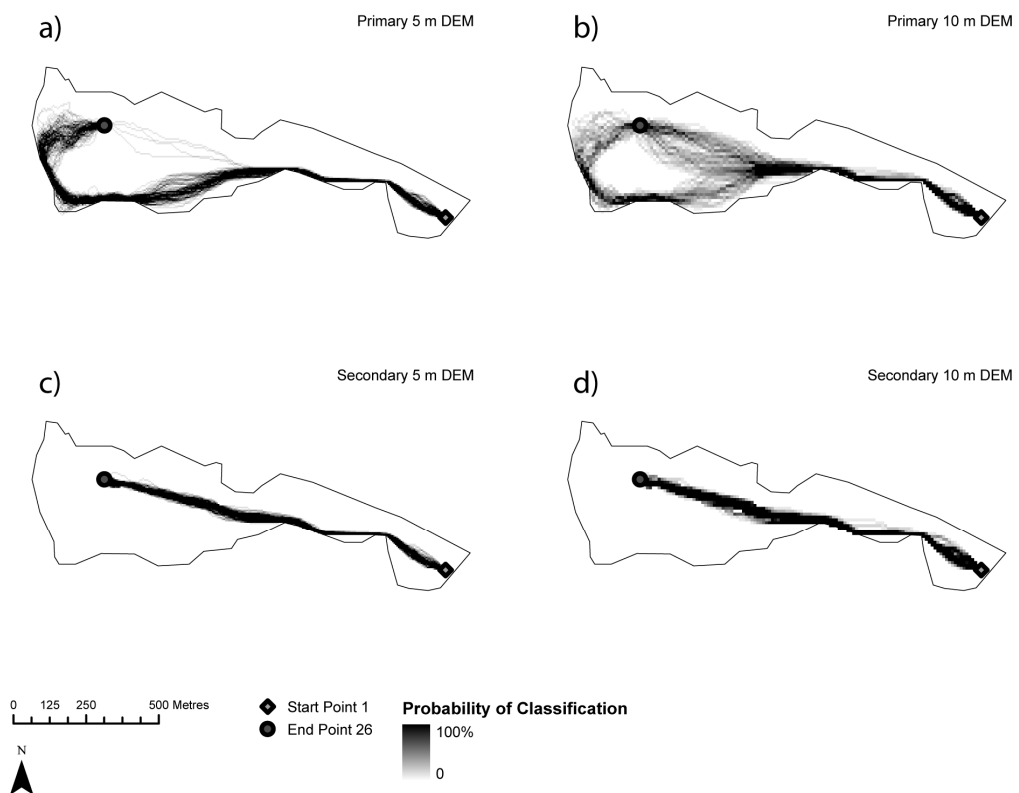


Figure 3.8 Parameter change: DEM resolution (*stdv* = 0.5 m).

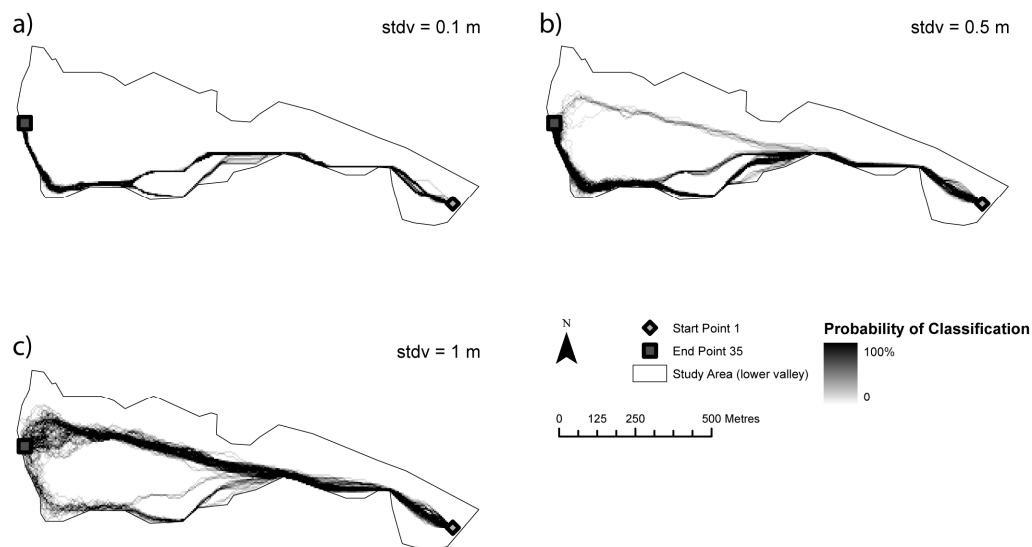


Figure 3.9 Parameter change: standard deviation of error (secondary 5-m DEM).

3.5.2 Spatially independent vs. dependent error

The above results were derived from spatially independent stochastic error simulation (Method 1). This next section summarises the flow model sensitivity to an increased spatial dependency between the individual errors perturbing the DEMs. A visual comparison of all probability surfaces revealed some response of the flow algorithm to changing spatial dependency of error, particularly when *stdv* was low (0.1 m) and the resolution was fine for the valley (5 m). The probability surfaces arising from the Secondary DEMs showed negligible difference with changes in the spatial dependency of the applied error fields.

The proportion of cells experiencing some flow was used as an indicator of variability (i.e. the greater proportion of the study area to experience flow to a cell at least once, the greater the variability and hence uncertainty in flow path classification). Figure 3.10 displays examples of these summary statistics for the different DEM construction methods and resolutions, and *stdvs* of 0.1 and 0.5 m (not all probability fields are represented).

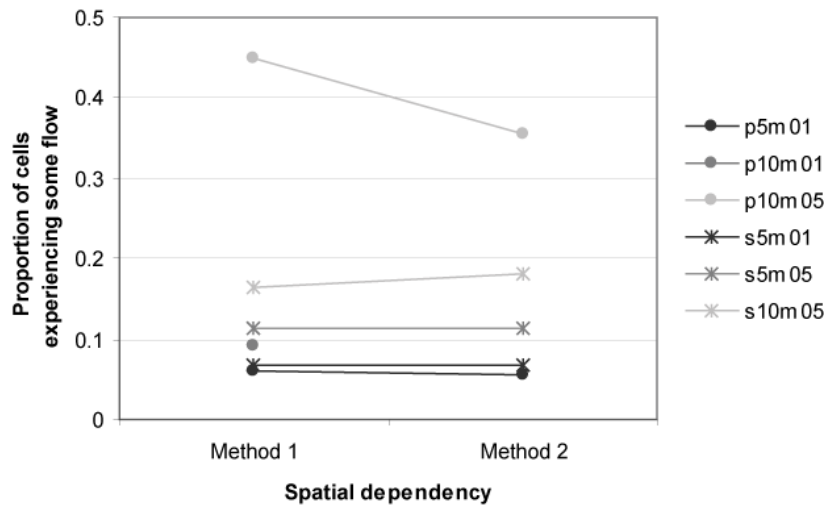


Figure 3.10 Proportion of cells experiencing some flow. (DEM details are abbreviated, e.g. primary 5 m, stdv 0.1 m = p5m01).

The Primary 10 m DEM at *stdv* 0.5 m (p10m05) was the most variable in flow classification for both methods of error perturbation. At low *stdv* (0.1 m) all DEMs performed to constrain flow to approximately 10% of the study area. The Secondary DEMs constrained flow to less than 30% of the study area. In terms of the different methods of error perturbation, Method 2 induced the lowest variability in the Primary 10 m DEM. Generally though, the results from Methods 1 and 2 were similar.

Confusion matrices were derived to compare the spatial distributions of results from different flow model runs. Due to the skewed distributions of probabilities only binary comparisons were implemented. Firstly cells were classified into those experiencing some flow and those with no flow. Secondly cells were grouped into those with a probability of flow greater than 10% and those 0–10%. Both of these classification schemes would be useful to cautious hazard managers in the Belham valley. The confusion matrix for a Method 1: Method 2 comparison is shown as an example in Table 3.1. Cells along the diagonal represent agreement and off-diagonal ones disagreement or confusion. The overall error (or disagreement) in this case was 16%. Table 3.2 summarises confusion matrices, reporting the overall error or raw

disagreement for pairs of maps. With the flow/no flow classification flow paths over the Primary DEM were most different (16% disagreement). When the cells were classified by probability greater than 10%, the levels of disagreement only ranged from 2% to 7%. Generally the Secondary DEMs produced the more similar results, suggesting flow maps from these DEMs are less responsive to changes in the spatial dependency of error. Furthermore, Kappa statistics (Cohen, 1960) were calculated to assess whether the proportions of agreement were greater than expected by chance. All of these statistics indicated that the levels of agreement were much higher than would be expected by chance (Table 3.2). According to the descriptive standards proposed by Landis and Koch (1977) agreements for the Primary DEM results ranged from 'moderate' to 'substantial', and were 'almost perfect' for those using the Secondary DEM.

	No Flow	Flow	Total	ErrorC
No Flow	1942	468	2410	0.1942
Flow	112	1209	1321	0.0848
Total	2054	1677	3731	
ErrorO	0.0545	0.2791		0.1555

Table 3.1 Basic confusion matrix Method 1 (columns : control) against Method 2 (rows : test) for Primary 10m, stdv 0.5 m, End Point 26. ErrorO = Errors of Omission (expressed as proportions), ErrorC = Errors of Commission (expressed as proportions)

Probability surface	Flow/ no flow				Greater than 10%			
	Confusion (raw)	Kappa	Standard	95% confidence	Confusion (raw)	Kappa	Standard	95% confidence
Primary 10 m stdv = 0.5 m	0.1555	0.6796	substantial	± 0.0204	0.0670	0.5551	moderate	± 0.0533
Secondary 10 m stdv = 0.5 m	0.0362	0.8733	almost perfect	± 0.0210	0.0247	0.8600	almost perfect	± 0.0282

Table 3.2 Raw disagreement from confusion matrices (as a proportion), Kappa statistic and confidence limits

3.5.3 Flow model parameters

The start point location was constrained by the shape of the valley; in initial testing, changing its location within the hundred or so metres allowable had little or no effect on the flow downstream. In contrast, the end point location had great consequences for the flow path, e.g. compare Figures 3.8(c) and 3.9(b). The standard deviation of error was the same but in Figure 3.9(b) the paths show three dominant branches and thus greater variability in the flow paths.

3.6 DISCUSSION

3.6.1 Flow model response to the terrain model

Changing the input DEM altered the path of steepest descent and ultimately the cells of likely flow inundation. The flow algorithm was sensitive to changes in DEM construction method, resolution, and the magnitude and spatial dependency of error in elevation. Furthermore, the locations of the flow model start and end points placed obvious constraints on the flow paths. Key observations were:

- *DEM construction.* Of the three interpolation techniques tested, the TIN was the most suitable for the study area. From the rasterised TIN, the Secondary DEMs produced flow paths that correlated well with field observations; the Primary DEMs did not.
- *DEM resolution.* The flow model was sensitive to resolution change but only for the Primary DEM at high standard deviations of error. The Secondary DEM was more robust to resolution change.
- *Error magnitude.* Uncertainty in the DEM has been shown to propagate to the terrain application; the probability surfaces were very sensitive to the standard deviation of error (*stdv*). For larger errors (≥ 0.5 m) the flow paths were more

variable and separated into different dominant flow routes. This was more obvious downstream as the valley widened.

- *Spatial dependency of error.* Spatial dependency in errors induced small change in model outputs.

Assuming no significant interactions, the relative influence of the different DEM computation and quality factors on the flow model can be qualitatively addressed. For example, DEM resolution had an impact on the results, but only for the Primary DEM at high error values. Thus, *stdv* is considered relatively more important (i.e. it impacts at all resolutions). For this application, DEM construction method and magnitude of elevation error have the most significant impacts on model output. To augment the research presented in this chapter, statistical methods for a global sensitivity analysis should address these factors first. Further, the results suggest that the influence of spatially dependent error on the flow model does not warrant further investigation.

3.6.2 Uncertainty implications for hazard management

3.6.2.1 Comparing DEMs and fitness for use

Output uncertainty from a flow algorithm can be used to inform a decision as to whether a DEM is fit for lahar modelling. Cell inundation differed from varying parameters of the DEM and of the flow model. For example, Figure 3.8 showed that 45% ($1.7 \times 10^5 \text{ m}^2$) of the study area was inundated by some flow from a Primary 10 m DEM with a *stdv* of 0.5 m, yet only 16% ($6.1 \times 10^4 \text{ m}^2$) from the Secondary 10 m DEM. For a hazard assessment this is a considerable disparity in area. Probability fields from the Secondary DEM corresponded better with field knowledge. It can be concluded that the Primary DEMs are not fit for flow routing in this study area; the extra information provided by aerial photographs and field knowledge is essential to produce sensible flow paths and also reduce model sensitivity to error. However, the terrain and application are such that DEM resolution can be either 5 or 10 m and produce plausible flow routing results. Thus a Secondary 5 or 10 m DEM would give

viable results and reduce model output uncertainty. A formal test of fitness for purpose was not possible in this instance due to the absence of independent information on flow paths to verify model outputs. Such a situation is common in this type of research where direct measurements are scarce due to the sudden onset of lahars and impassability of certain volcanic zones. Nevertheless, the Secondary DEMs produced robust results suitable for hazard assessment, as determined by expert knowledge.

3.6.2.2 Sensitive areas of the study site.

Analysing the different flow paths shows key areas that are subject to branching (splitting of dominant routes) and erratic behaviour; these areas are in the middle of the study area and further downstream, reaching a maximum at the shoreline. This is probably due to a widening of the valley in mid-reaches and flattening of the valley floor. Uncertainty in elevation data here will induce a greater response in the model output, especially when the DEM resolution is coarse. Thus data accuracy and/ or applying a suitable approximation for the error is particularly critical in these areas.

3.6.2.3 Other influences on the flow path

The D8 algorithm assumed that flow occurred only in the steepest down-slope direction from any given cell. However, this single flow direction approach has been criticised for resolving grid directions too coarsely and introducing bias to the orientation of the numerical grid (Tarboton, 1997). Furthermore, using D8 for flow accumulation, a small elevation difference between two neighbouring cells can have a large effect as one of the cells receives all the flow (Seibert and McGlynn, 2007). Multiple flow direction algorithms have been developed that are less sensitive to DEM induced erroneous flow directions (e.g. Wolock and McCabe, 1995; Tarboton, 1997; Huggel *et al.* 2003; Seibert and McGlynn, 2007). However, flow is dispersed to all neighbours and thus these algorithms can introduce substantial dispersion (Tarboton, 1997), a problem that is most prevalent for concave hillslopes (Seibert and McGlynn, 2007). Despite the limitations for modelling debris flow behaviour the single flow direction algorithm can broadly represent the flow characteristics

(Huggel *et al.* 2003) and is a good first prediction for hazard assessment. Simple models are often applied to obtain a first order approximation of the flow's distal limits (Toyos *et al.* 2007).

Another extension to the research would be to incorporate additional aspects of impedance into the least cost analysis. For example, the heterogeneity of surface friction could be incorporated, e.g. in areas of debulking where boulder deposits were dense. For route planning in landslide-prone areas Saha *et al.* (2005) considered distance, gradient cost and thematic cost for movement from a pixel to its immediate neighbours.

3.6.3 Implications for an application-driven approach to DEM construction

3.6.3.1 Survey design and DEM construction

Pooling all possible information sources from the study area can greatly reduce uncertainty in model outputs. There is no substitute for knowledge of the terrain and its implications for DEM construction. For this study, an irregular distribution of sample points was preferable to record micro-topographic changes and TINs were necessary to preserve lines of interest (e.g. breaklines). This was determined through field experience. Written notes, sketches and reconnaissance photographs were all important to improve the quality of the DEM. Furthermore, assessment of model and DEM performance was achieved using indicators from non-published documents (photographs and personal experience) (e.g. Stevens *et al.* 2002; Huggel *et al.* 2003) where no higher quality reference data were available.

The choice of interpolation technique is highly area specific. Rasterised TINs have been found unsuitable for areas of low relief and stream junctions (Kenny and Matthews, 2005). In this research the terrain justified the use of TINs and generated similar flow paths to those found using more sophisticated interpolation techniques, such as splines with tension (Section 3.5.1). Whilst the TIN honoured all data the tension spline suffered from overshoots and extrapolated beyond the range of data points. Furthermore, TOPOGRID produced an unrecognisable landscape.

3.6.3.2 Applying error fields

Uncertainty in model outputs has been addressed by identifying parts of the study area most susceptible to elevation error, assessing a cell's membership of a particular class and comparing DEMs and their fitness for use. Uncertainty in elevation data quality was also investigated by perturbing the DEMs with error field or adding 'noise'. The magnitude of error (regulated by the *stdv*) affected the model outcome; larger errors produced more variable pathways, thus uncertainty in elevation error propagated to the terrain application. This supports similar findings of error propagation from other studies (e.g. Hunter and Goodchild, 1997; Veregin, 1997) and was true for all methods of error generation.

Incorporating the spatial autocorrelation of error is scientifically supported (e.g. Fisher, 1998; Kyriakidis *et al.* 1999), yet extra time and computer processing power is consumed by the complexity of such analysis. Due to the consequences of making a poorly informed decision it is prudent to take a conservative, cautious approach when undertaking hazard analysis; however sacrificing an overestimate of a 'hazardous' area is also undesirable (Zerger *et al.* 2002). An informed compromise must be made. Unfortunately, as there is no information on the actual magnitude and distribution of error there is no way to verify the plausibility of the results. GCUM (Method 2) was the more scientifically rigorous approach employed. It incorporated a spatial dependence factor that was chosen as suitable for the data, yet this did not alter the results significantly. The kappa test for agreement demonstrated the results were not significantly dissimilar. Furthermore, the differences between kappa values for the methods of error dependency were very small when compared with those induced by changing the DEM construction method (Table 3.2).

Fisher (1998), Heo (2003) and Wechsler and Kroll (2006) have used alternative methods of generating spatially autocorrelated random error fields. Spatial dependency can be adapted for the DEM data but is usually a global value for the DEM. If error is closely related to the terrain, then topographic change should induce a change in the error. Therefore the degree of correlation would probably be terrain dependent and spatially variable. Kyriakidis *et al.* (1999) provides the only example

in the literature of a heteroscedastic spatially autocorrelated error surface (Carlisle, 2005). Here error values vary in relation to another variable, e.g. terrain ruggedness. However, even spatially autocorrelated error adds noise; this creates undulations in the terrain that may not be sensible. Another alternative would be to apply a point-spread function to individual elevation values before the DEM is created. Such an option invokes the question: would it be better to apply the error field, and then smooth? This is similar to the 'to interpolate and thence to model, or vice versa?' issue presented by Jarvis *et al.* (1999).

3.7 CONCLUSIONS

The digital rendering of terrain will always provide an imperfect representation of topographic reality and even small discrepancies can have significant influence on the outputs of terrain applications. The consequences of making a decision based on uncertain predictions can be severe, especially in hazard modelling. Uncertainty from the application of a terrain model can be considered by simulating elevation error and its propagation to output variation. Furthermore, by changing input parameters and evaluating the application response the implication of using derivatives from different DEMs can be assessed relative to each other. Figure 3.2 can provide users with a useful framework for identifying DEM uncertainty and determining an appropriate stage in an application for uncertainty analysis. Creating a DEM that is informed by uncertainty and that is suitable for the terrain application can help limit adverse effects in the following ways: (a) highlighting areas (of the study region) that are most susceptible to changes, (b) assessing a cell's membership of a particular class, and (c) comparing different DEMs. Pre-made DEMs are normally provided with some measurement of accuracy (usually the RMSE) or, alternatively the DEM user may have intimate field knowledge and be able to estimate reasonable bounds of accuracy from that experience. Following justifiable assumptions on the spatial distribution of vertical error, DEM uncertainty can be simulated.

There are numerous methods for applying error to elevation data and investigating the consequences. This research has applied two to different variants of DEM creation. Despite demonstrated propagation of elevation error, it can be inferred from the variation of input parameters that there is no greater influence on flow model outputs than the DEM construction method. Furthermore, the merit of including a measure of spatial dependency of error did not appear justified in this particular application. The flow path sensitivity to correlation between errors did not impact on the relative significance of other parameters and had little effect on flow model output; spatially independent errors were therefore fit for purpose. This study has shown that basic DEM construction can lead to misleading model outcomes, and simply adding noise to the DEM does not compensate for inadequate DEM creation. When DEM construction was supplemented with additional fieldwork information (such as reconnaissance aerial photographs and field notes) confidence in the model output was greatly improved. The overall wisdom of the application-driven approach rather than data-driven approach may be considered positive in light of this practical experience. It is recognised that environmental or financial constraints can restrict data choices despite a general improvement in data availability. However, for validity of model results, there is no substitute for constructing a DEM that is informed by the terrain and evaluated as fit for the application to which it is put.

CHAPTER 4: AN EXAMINATION OF GIS APPROACHES FOR LONG-TERM LAHAR HAZARD MAPPING ON MONTSERRAT, WEST INDIES

An approach to terrain model construction prioritising Digital Elevation Model (DEM) utility for an intended application was presented in Chapter 3. As a product of this, DEMs of a small area of Montserrat (West Indies) were tested for their suitability, or fitness-for-use, for lahar modelling. In this chapter the focus shifts to lahars as hazards, considering runout and inundation areas for a hazard assessment. The main aim of this chapter is to compare and contrast two simple GIS-based lahar runout models using available field data. While simple models can give preliminary information, confidence in their predictions is generally low; a secondary aim was to establish whether the models could be used for long-term predictions of runout and inundation areas on Montserrat.

Field data were collected over two field seasons and provide (1) an overview of gross morphological change after one rainy season, (2) details of dominant channels at the time of measurement, and (3) order of magnitude estimates of individual flow volumes. Comparison of rainfall data and recorded lahars show that individual flows are not well observed but give further estimates of frequency of flows.

Single-direction flow routing, commonly used for simulating normal stream-flow, was tested for runout inundation area prediction against LAHARZ, a semi-empirical model implemented in a GIS and calibrated for debris flows. In this manner, flow type end-member models (applicable to dilute and sediment-rich lahars) were analysed for suitability using flows that contain an intermediate sediment concentration. Both of these models have the advantage that they require minimal input data, i.e. terrain characteristics and a set of test scenarios (e.g. a range of reasonable lahar volumes for LAHARZ). Comparing the areas and ways in which

these models do not adequately capture the observed changes can also provide an indication of where the intermediate sediment concentration flows do not follow behaviour of the end-member systems.

In the hydrological approach, single-direction flow routing guided lahar centroid mass using an elevation cost surface according to the path of steepest descent. Further, Monte Carlo sampling of elevation error enabled inundation probability-of-flow maps to be produced. In the sediment-rich approach, LAHARZ predicted inundation using a sequential range of user-defined input volumes. Inundation areas were then converted into zones of equal hazard. Thus, both GIS-based models used concepts of probabilities and likelihoods to construct hazard maps.

Results suggested both models had associated benefits. Dominant flow routes observed in the field were generally well-replicated using single-direction flow routing. However, LAHARZ was comparatively more successful at mapping lahar dispersion and was more suited to long-term hazard assessment. Ultimately showing the results side-by-side increased their usefulness for conveying the lahar hazard, for short- and long-term predictions respectively. This research suggests these two GIS approaches are complementary for preliminary hazard assessment on Montserrat. However, neither model was able to adequately replicate observed flow routes in the semi-confined lower-reach of the study area. To improve performance of the single-direction flow routing it is suggested the influence of other terrain variables (e.g. spatial variation of channel roughness) should be investigated.

4.1 INTRODUCTION

Lahars, rapidly flowing mixtures of volcanic debris and water, are among the most far-reaching volcanic flows, with the potential to interact with populated areas distant from area(s) of initiation (e.g. Scott *et al.*, 2001; Newhall and Hoblitt, 2002). Thus, consideration of lahar runout and degree of inundation is crucial for hazard assessment, with hazard maps the obvious repository for this information. In the long-term, maps can aid land-use planning and educate local populations about the spatial distribution of hazards (Crandell, 1984; Chapter 2, Section 2.2.2.1).

Lahar hazard assessment has traditionally involved geological mapping of past events from lahar deposits (Crandell, 1984; Oramas Dorta *et al.*, 2007). However, hazard assessment is becoming increasingly reliant on empirical models (e.g. Iverson *et al.*, 1998) or numerical models of runout (e.g. Savage and Hutter, 1989; Iverson *et al.*, 1997; O'Brien *et al.*, 1993). These models do not (necessarily) require lengthy and detailed geological fieldwork and move beyond the assumption that future behaviour will exactly mirror that of past activity. Nonetheless, lahars are complex mixtures of sediment and water, exhibiting a range of characteristics and behaviours on their descent from a volcano (Chapter 2, Section 2.3.2). Modelling their movement is not an easy task; existing models can be difficult, if not impossible, to implement due to high demands on processing and time, and application can be hindered by the lack of available data to inform model starting conditions.

Due to the spatial nature of the phenomenon, geographical information systems (GISs) have great potential as tools for lahar hazard assessment. A GIS can organise pertinent hazard-related data and can be tightly coupled with lahar modelling. For example, a GIS has been used by Schilling (1998), to automate the semi-empirical relationships detailed in Iverson *et al.* (1998), and by Pitman *et al.* (2003) in the implementation of Titan2D. Additionally, a GIS is particularly suitable for dealing with topography that may be dynamic. As well as a platform for modelling lahar behaviour, a GIS can provide visualisations to user-requirements on request and in a range of formats, from traditional-style maps to 3D interactive displays.

Two established GIS approaches for routing gravitational flows were applied to a study area on Montserrat, West Indies: single-direction flow routing, previously tested in a sub-section of the study area (Chapter 3; Darnell *et al.*, 2010), and the widely used LAHARZ suite of programs developed by Iverson *et al.* (1998). The ease of implementation is an attraction of these methods. However, they do not simulate the internal interactions and processes of lahars, nor complex changes in behaviour downslope (see Chapter 2). The aim of this chapter is to gain a better understanding of the benefits and limitations of these simple GIS approaches for runout and inundation analysis; in particular this chapter seeks to explore how model predictions deviate from actual deposition and possible explanations for this. A further objective is to see if they provide insight for determining inundation areas for long-term hazard mapping.

4.2 REGIONAL SETTING

Soufrière Hills Volcano dominates the island of Montserrat, West Indies (Figure 4.1a). Current ongoing activity began in July 1995 and has involved long periods of effusive dome growth accompanied by collapse, pyroclastic flows and occasional vulcanian explosive activity (Kokelaar, 2002; Sparks and Young, 2002; Herd *et al.*, 2005). The protracted eruption can be divided into periods of dome growth and eruptive phases punctuated by pauses in activity lasting a few days to several months (Chapter 2, Section 2.5.3). Heavy rainfall has indiscriminately initiated lahars, even during periods of inactivity at the lava dome. Due to the abundance of volcanic ejecta that has accumulated on the volcano, lahars on Montserrat are typically not sediment-supply limited; they are limited by the frequency of the triggering (rainfall) events (Barclay *et al.*, 2007).

Activity at the volcano has rendered more than half of the island uninhabitable and over two-thirds of the population have emigrated following forced displacements and evacuations (Kokelaar, 2002). The Government of Montserrat, Disaster Management Coordination Agency (DMCA) and Montserrat Volcano

Observatory (MVO) have adopted a Hazard Level System which has been in operation since August 1, 2008. This system divides the southern two-thirds of Montserrat into six zones, with two Maritime Exclusion Zones (Figure 4.1b). Access permission for each of these zones is dependent on the Hazard Level. This level, which ranges from 1 to 5, is set by NDPRAC (National Disaster Preparedness and Response Advisory Committee) on the advice of MVO. Residents are advised of hazard zones using maps distributed by the Disaster Management Coordination Agency (DMCA) and local police. Full details on the hazard management structure are available on MVO website (<http://www.mvo.ms/>) and also provided in Chapter 2. However, the Hazard Level system is entirely attributed to the primary volcanic activity (i.e. pyroclastic flows and surges, ballistics and tephra fall). Lahars are classified as secondary volcanic events, although typically occurring synchronously with, or after, an eruption.

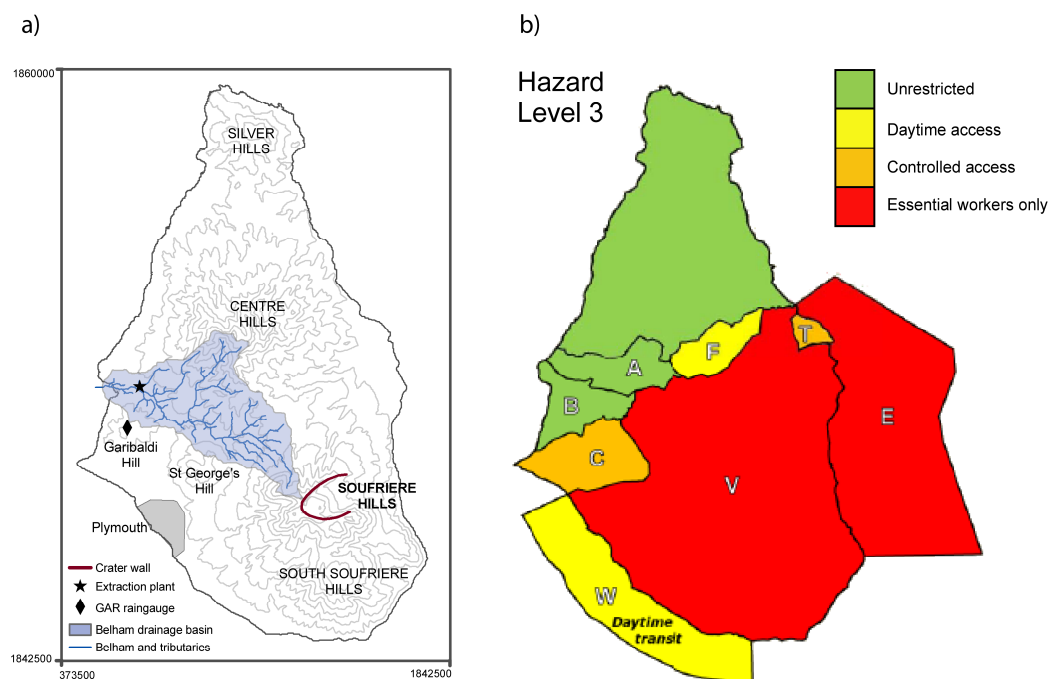


Figure 4.1 Island of Montserrat a) Soufrière Hills Volcano and the Belham River, its drainage basin and tributaries (100 m contours derived from Wadge, 2006); b) Hazard Zones map at current Hazard Level 3 (March 2010, courtesy of MVO). Coordinates are in Montserrat National Grid.

Due to local topography and population relocation the only major drainage that can channel lahars from Soufrière Hills to inhabited distal areas is the Belham River Valley (Figure 4.1a). At Hazard Levels 1—3 this valley is in daytime use by industrial extraction workers and people in transit; at greater Hazard Levels (4 and 5) only ‘controlled’ and ‘essential’ access is permitted. However, lahars are significant hazards in the Belham, throughout all tiers of the Hazard Level System; and due to the reserves of volcanic debris, are likely to remain hazards for many years to come (even if the current activity ceases). Thus, any lahar-specific hazard assessment should be informative on a long-term basis.

Montserrat currently lacks a fine resolution hazard map for the Belham catchment. Two simple GIS-based techniques are examined for their potential utility in predicting lahar runout, both in terms of capturing likely behaviour of individual flows and long-term time-integrated inundation. This analysis was independent from the existing Hazard Level System, but could be used to inform MVO when making recommendations pertinent to lahar hazard management.

4.3 MODEL SELECTION FOR FLOW SIMULATION

4.3.1 Approach to modelling

A lahar modelling approach should be chosen with respect to (a) observed behaviour; (b) data availability; and (c) time and resources (equipment) available.

Belham Valley lahars have been observed by University of East Anglia (UEA) researchers, MVO staff and ‘non-expert’ eyewitnesses, but are not formally monitored. There are relatively few publications stemming from research on these specific lahars (e.g. Barclay *et al.*, 2004; 2006; 2007; Susnik, 2009; Alexander *et al.*, in press); and to date there are no field-data for individual events. However, UEA have preinstalled rain-gauges that (when operating) have been recording rainfall at a one-minute resolution from 2001 onwards (Matthews *et al.*, 2009), topographic change has been observed and measured in the Belham Valley since 2005 (Susnik, 2009),

and a good knowledge of flow rheology, direction and main channels has been developed (see also Chapter 3).

Whilst competent enough to carry large boulders (up to 2 m diameter) lahars on Montserrat are characteristically dilute. Newtonian flow behaviour is dominant and lahars are principally hyperconcentrated-, concentrated- or 'normal' stream-flow (Barclay *et al.*, 2004). Although rare, non-Newtonian flow behaviour has been observed and can be explained by greater sediment availability (Barclay *et al.*, 2007).

Flow simulation and inundation prediction on Montserrat should be able to emulate behaviour somewhere between hydrological routing (water-rich) and traditional debris-flow modelling (sediment-rich). Current lahar modelling approaches in general have been reviewed in Chapter 2. As a spatial phenomenon, lahars are suited to two-dimensional modelling and utilisation of a digital elevation model (DEM) in a GIS environment. Simplification to a single-phase homogeneous fluid is common and reasonable in this case. With a lack of relevant field-data, a model should not include volume changes or rheological (behavioural) changes on descent as these cannot be verified.

The simplest method for specifying the direction of travel for any gravitational flow in a GIS is to assign flow from one cell in a DEM to one of its eight direct neighbours with the lowest elevation (O'Callaghan and Mark, 1984). This can be accomplished with a single flow direction algorithm, termed D8 (Deterministic-8), provided within mainstream GIS software packages (such as ESRI's ArcGIS).

Both models reviewed here are strongly topography-driven and make use of this algorithm in a GIS environment over a DEM. Simple models usually have lighter data and processing requirements, and produce results more rapidly than their more complex counterparts. Fundamentally, because they involve fewer parameters, the results can be more easily understood and full assumptions and limitations can be identified and discussed. Thus, it is also easier to measure cause and effect, and isolate the important parameters.

4.3.2 Single-direction flow routing

Direct use of the D8 algorithm as a lahar simulation model defines flow from a cell in one direction based on the path of steepest descent. Lahar volume is reduced to one point, therefore flow simulations consider only the displacement of the centroid of the entire moving mass (Hurlimann *et al.*, 2008). This simplification accomplishes a very important goal: creating a one-dimensional flow network (or path) over the landscape (Maidment *et al.*, 1996). Consequently, this model would fail to simulate diffusive hillslope processes (Tarboton, 1997; Codilean *et al.*, 2006); but the D8 method can be superior in zones of convergent flow and along well-defined valleys (e.g. Quinn *et al.*, 1991). Such a technique reflects the underlying influence of slope and can be used to quickly pick out the main flow routes arising from topographic control. This methodology has previously been applied with positive results for a small subsection of the Belham Valley (Chapter 3; Darnell *et al.*, 2010).

4.3.3 LAHARZ

Iverson *et al.* (1998) developed semi-empirical equations for the United States Geological Survey (USGS) that were used to predict the valley cross-sectional area, A (Equation 4.1) and planimetric area, B (Equation 4.2), inundated by lahars with various volumes (V). The method was developed to provide a rapid, objective and reproducible hazard assessment to be applicable to many volcanic systems (Iverson *et al.*, 1998). Calibrated with 27 historic and prehistoric debris-flow paths, the predictive equations provide the information necessary to calculate and plot inundation limits on topographic maps. The mapping process is automated in ArcInfo GIS using a suite of programs collectively called LAHARZ (Schilling, 1998). The intrinsic link to flow volume is where LAHARZ and single-direction flow algorithms principally differ (Huggel *et al.*, 2008).

$$A = 0.05V^{2/3}$$

[Equation 4.1]

$$B = 200V^{2/3}$$

[Equation 4.2]

A study area is first divided into two theoretical zones: (1) proximal hazard zone and (2) distal inundation zone. The proximal hazard zone is defined by the geometric relationship between the horizontal runout (L) and vertical descent (H) (Figure 4.2) and this represents the runout area for pyroclastic flows and debris avalanches (see energy cone concept, Chapter 2). Thus, source areas for lahars are somewhere within this area. To clarify, LAHARZ begins its simulation in the distal area, as the lahar exits the proximal hazard zone. The model predicts the three-dimensional inundation areas in the distal zone, moving downslope and spreading away from the valley thalweg. A natural river channel will follow this line defining the lowest points along the length of a river bed or valley – it is determined by LAHARZ using surface hydrology grids generated using the D8 principle.

LAHARZ holds advantages over more complex modelling solutions (e.g. Titan2D; Flo-2D; see references in Chapter 2, Section 2.3.4) because it requires a limited amount of data and relatively little fieldwork (Canuti *et al.*, 2002); it was designed to be used where data, time, funding, or personnel are inadequate for application of traditional methods (Iverson *et al.*, 1998). However, a fundamental theoretical restriction is that lahar volume is assumed constant from source, through the proximal hazard zone, to deposition in the distal region. Thus, entrainment and deposition (bulking and debulking) of material and its effect on lahar behaviour (rheology) are not considered. Volume change is a commonly observed phenomenon (Fagents and Baloga, 2006), but such a simplifying assumption is adopted by most lahar and debris-flow modellers (e.g. Hooper and Mattioli, 2001; Aguilera *et al.*, 2004). A full list of LAHARZ's assumptions is provided in Table 4.1.

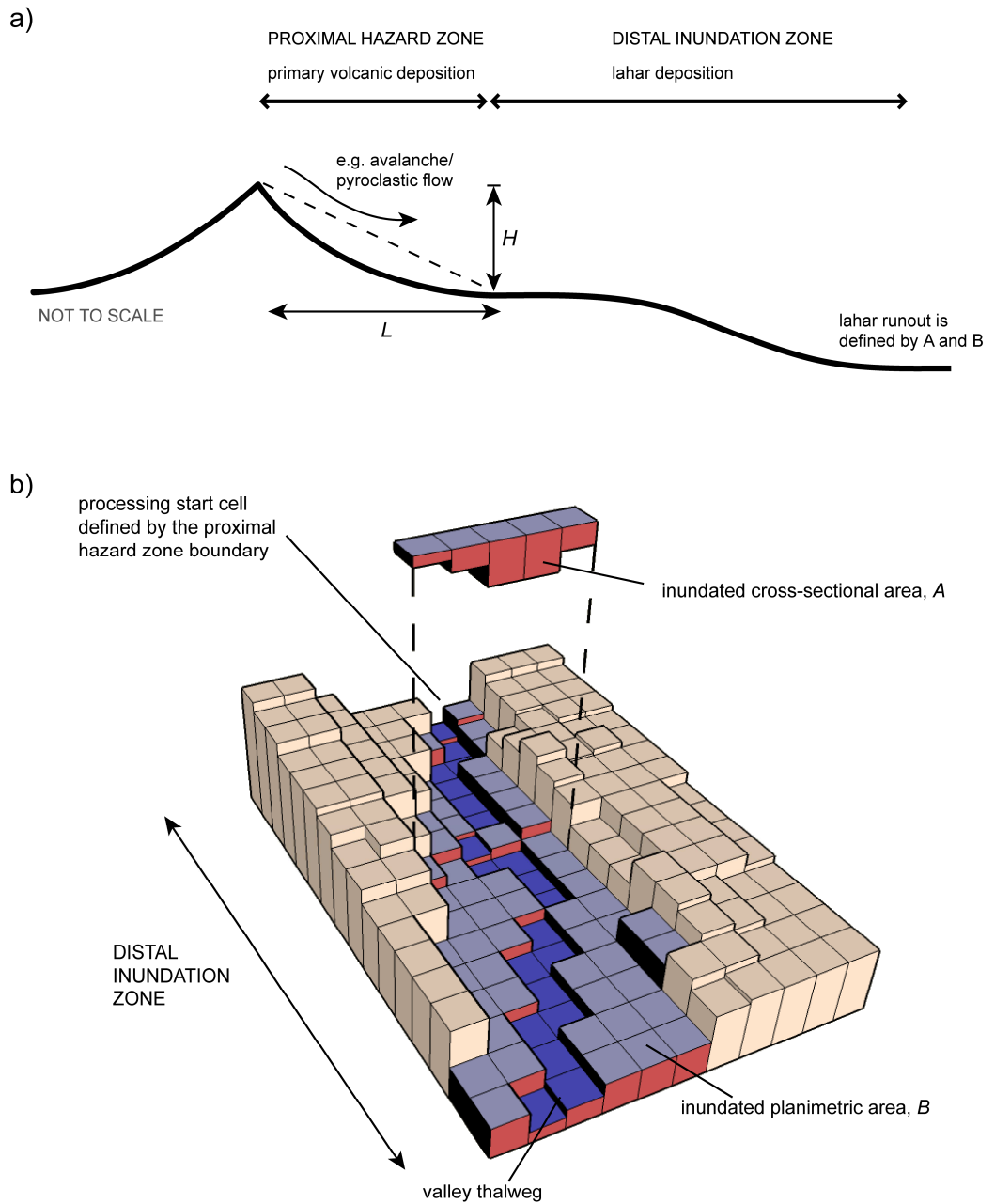


Figure 4.2 Relationships between a) H and L , which describe the extent of the proximal hazard zone, and b) A and B , which describe the extent of the distal lahar inundation zone (After Iverson *et al.*, 1998); Google Sketchup used for 3D visualisation

Assumptions	
General:	<p>Lahars are sudden onset</p> <p>No background channel flow</p> <p>Lahar moves downstream as a waveform</p>
Cross-sectional area:	<p>Maximum lahar discharge produces the maximum inundation of valley cross sectional area</p> <p>Conservation of mass therefore conservation of volume (no erosion, deposition, infiltration or precipitation)</p> <p>Cross-section averaged velocity is directly proportional to \sqrt{gR}, where g is the magnitude of gravitational acceleration and R is the hydraulic radius of the inundation cross-section</p> <p>Constant flow, constant discharge per model run</p>
Planimetric area:	<p>Deposition starts upon leaving the proximal hazard zone; the boundary of which is determined by the H/L energy line/cone.</p> <p>Volume leaving the proximal hazard area matches the volume deposited downstream</p> <p>Deposit mean thickness normal to the surface is constant.</p>

Table 4.1 LAHARZ assumptions (After Iverson *et al.*, 1998)

The semi-empirical equations behind LAHARZ were calibrated using recorded debris flows with their maximum volumes between $8 \times 10^4 \text{ m}^3$ and $4 \times 10^7 \text{ m}^3$. These calibrations may not apply accurately to other volcanoes (Carranza and Castro, 2006); for example Oramas Dorta *et al.* (2007) recalibrated planimetric area for small debris flows in Sarno, Italy, upon finding LAHARZ overestimating inundation areas. Berti and Simoni (2007) also recalibrated the proportionality coefficients using historic data from 27 debris-flow events in the Italian Alps, renaming the model DFLOWZ. More recent efforts have recalibrated LAHARZ for debris flows and debris avalanches (i.e. more sediment-rich flows) (Griswold and Iverson, 2008; Magril *et al.*, 2010). However, there are insufficient data on individual flow events to recalibrate LAHARZ for Belham Valley lahars; the pertinent question is: can LAHARZ be useful for Montserrat considering the (extra) assumptions needed?

4.4 CHANNEL RESPONSE TO LAHAR PERTURBATION: FIELD-BASED OBSERVATIONS

4.4.1 Updating elevation models

The accuracy of any flow model will depend on the nature and veracity of the model, and the accuracy of the topographic dataset over which it is run (Stevens *et al.*, 2002). Lahar movement is primarily controlled by topography and therefore adequate terrain representation is fundamental for the identification, management and mitigation of lahar impact(s). Field-data were first gathered in 2006.

Regional elevation data were acquired in the form of a 10 m resolution island-wide DEM, originally derived from contour lines (1:25 000 tourist map dated 1983) (see Wadge *et al.*, 2006). A study area was extracted that included the volcano summit and the Belham drainage basin (6.2 × 5.4 km). However, the dynamic nature of the volcanic system induces geomorphologic changes to the valley. These adjustments are discernible on an annual/ semi-annual scale, rapidly outdated digital representations of the valley bottom. Thus, elevation data were also gathered in the field through a roving Global Positioning System (GPS) survey in November 2006. The need for a DEM update was reaffirmed by the recorded maximum elevation difference (GPS point vs. contour-derived DEM) exceeding the maximum (vertical) measurement error (5 m for contour-derived DEM and 0.1 m for GPS data) at several ground control points. This elevation difference was also greater than anticipated through resolution effects (generalising micro-topographic variation in 5 × 5 m grid squares will induce deviations from the 'true surface').

GPS equipment, supplied by MVO, was an Ashtech base kit and a Leica rover kit. Surveys were carried out over several days and fixed to MVO's continuous GPS network using RINEX files from their sites. The base antenna was tripod mounted above a temporary benchmark established at MVO and on one occasion above a mark in the survey area on the Belham Beach. The rover antenna was mounted on a 1.5 m aluminium pole. This was generally carried in a rucksack and a height, once mounted, was measured. When positions were surveyed, the pole and antenna

were removed and the pole placed on the survey point; times when the antenna height was changed in this manner were recorded in the field notes.

Recent and re-worked deposits covered the valley floor. The survey followed an irregular path to ensure that local terrain features that could influence lahar flows were captured. At a minimum, three types of sampling were performed: (1) channel long profile (thalweg); (2) cross profiles; and (3) raised terraces and banks (where access was possible). Position and height measurements were taken every second. Only points resolved to an accuracy of 0.1 m (minimum) in the vertical and horizontal planes were later retained for analysis (33357 points retained). This roving survey introduced error due to the motion of walking; however, this was estimated to be in the order of only a few centimetres.

Figure 4.3 shows the extent of the 2006 GPS survey. A study area considering only the lower-reach of the Belham Valley was used in Chapter 3 to test the application of flow routing.

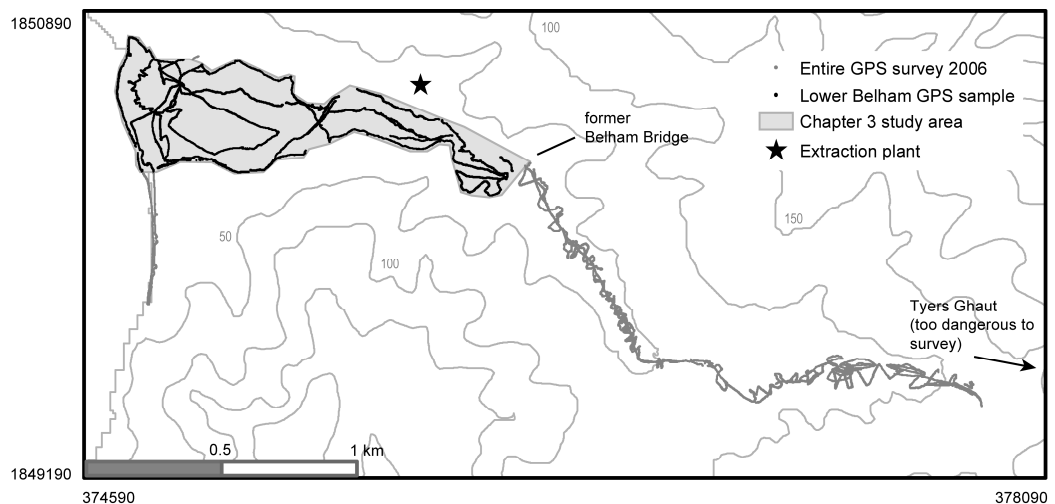


Figure 4.3 Retained GPS survey points for entire study area (33357 points total) and lower-reach (20127 points; used in Chapter 3). Coordinates in Montserrat National Grid.

In-field GPS measurements were also taken a year later in November 2007. Survey design was similar to the preceding year, but University of East Anglia equipment real-time kinematic (RTK) GPS system was used (Topcon). Data were processed automatically in the field, permitting a (marginally) more even coverage as a trace could be seen on-screen. GPS points were sampled every 0.5 m (laterally) traversed resulting in fewer replicated (redundant) data points (15708 retained).

Treating each GPS survey individually, GPS points were interpolated as mass points to create a Triangular Irregular Network (TIN), and the Belham thalweg (main channel) was imbedded in the TIN fabric as a hard breakline. The TIN was then converted to raster format for the ease of neighbourhood calculations common in the derivation of hydrologic parameters. The fitness of the resultant DEM for flow routing was assessed through local, one-at-a-time type sensitivity testing. This analysis led to the augmentation of the GPS data with raised terraces digitised from aerial photographs and field notes (consistent with the method shown in Chapter 3 for the lower-reach).

Two overlapping regular gridded matrices of elevation values were thus produced (contour-derived DEM and GPS-derived DEM) for both GPS survey years (Figure 4.4). Due to the temporal difference of the datasets (on a decadal scale between contour-derived DEM and GPS-derived DEMs) it was not plausible to amalgamate all points, and an exploratory analysis of a simple 'find and replace' algorithm for overlapping cells created sinks at the valley sides. Two further techniques dealing with dataset integration (or fusion) were tested:

1) Void, fill and feather. The 'fill and feather' technique, an interpolation method common for correcting voids in Shuttle Radar Topography Mission (SRTM) data (e.g. Reuter *et al*, 2007), was adapted to smooth the transition boundary of the two datasets. Grid cells in the DEMs were first compared, and where cells overlapped the elevation values of the contour-derived DEM were replaced (filled) with those from the GPS-derived DEM. An artificial void was then created by extruding a buffer zone external to the GPS-derived DEM (Figure 4.4b). The buffer width was determined by distance between the break in slope (contour-derived DEM) and the closest GPS point. These were important features needed to maintain integrity. Finally, a low

pass 5×5 filter (moving average window) was applied to diffuse, or feather, any abrupt change.

2) Lateral extension of recent elevation data. The second approach also prioritised conformity to the GPS-derived topography. For this method, the GPS-derived DEM was extended laterally by a neighbourhood average elevation (Figure 4.4c).

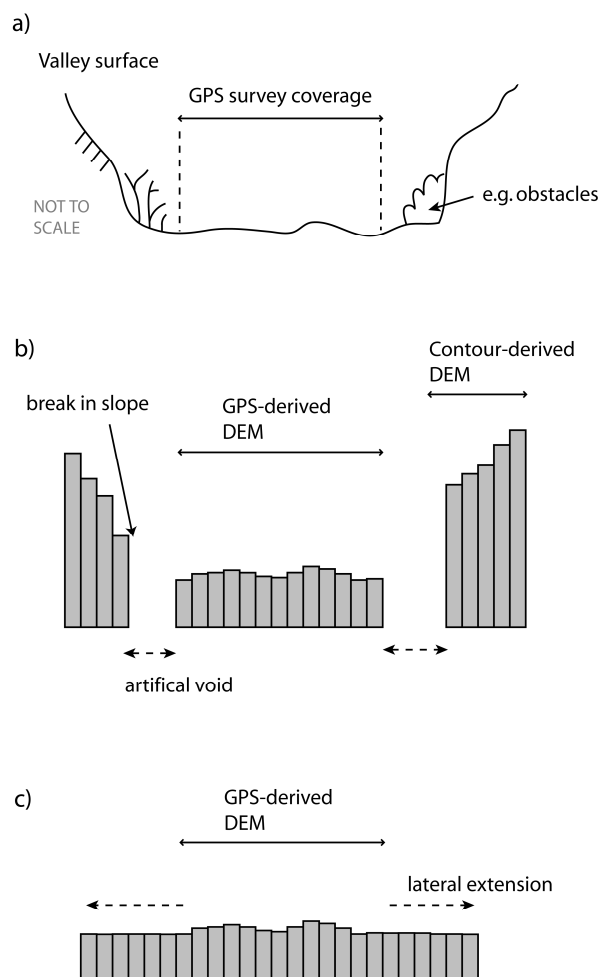


Figure 4.4 a) Valley surface cross-section showing coverage by GPS survey; b) fusing the up-to-date GPS-derived DEM with the contour-derived DEM required the creation of artificial voids which were then filled by feathering with a neighbourhood averaging window; c) lateral extension of the GPS-derived DEM.

A moving window computed elevation values in the NoData pixels based on the local average of the neighbouring elevation values (5×5 pixel window). A series of iterations were performed until the dimensions of the valley floor were exceeded (as determined from a mask digitised using aerial photos). A differential surface was then created by subtracting the contour-derived DEM. Negative values were subsequently reclassified to zero and the result added to the contour-derived DEM, generating a DEM showing only positive elevation change (inferring deposition). To allow negative elevation change within the channel, only negative values from the differential surface were extracted using the valley floor mask. Finally, this erosive surface was added to the deposition-only DEM.

Fused surfaces created from the two methods above are shown in Figure 4.5, the 2007 survey is used for this example. The fill and feather process corrupted the contour-derived DEM, creating artificial slopes in the data that neither conformed to the original surface nor represented the true ground (a common problem with this technique (Grohman *et al*, 2006)). Furthermore, the topographic variance of the two surfaces was too high to match the surfaces over such a distance (Figure 4.5b).

Various buffers and filter neighbourhoods were trialled, resulting in minimal or no improvement. The fused surface from the lateral extension method conformed to field knowledge (Figure 4.5c). Profile graphs show the same channel cross-section as viewed by the different methods (2007 surface). The difference in slope is clearly visible and this would influence flow direction. Considering the above, a final DEM was produced, for both survey years, to 10 m resolution by extending the GPS-derived DEM laterally by a neighbourhood average elevation (method 2); for each year, the grid size covered an area of 6.2×5.4 km (620 by 540 cells). These regular grids of elevation could then be compared and further used as in input for modelling.

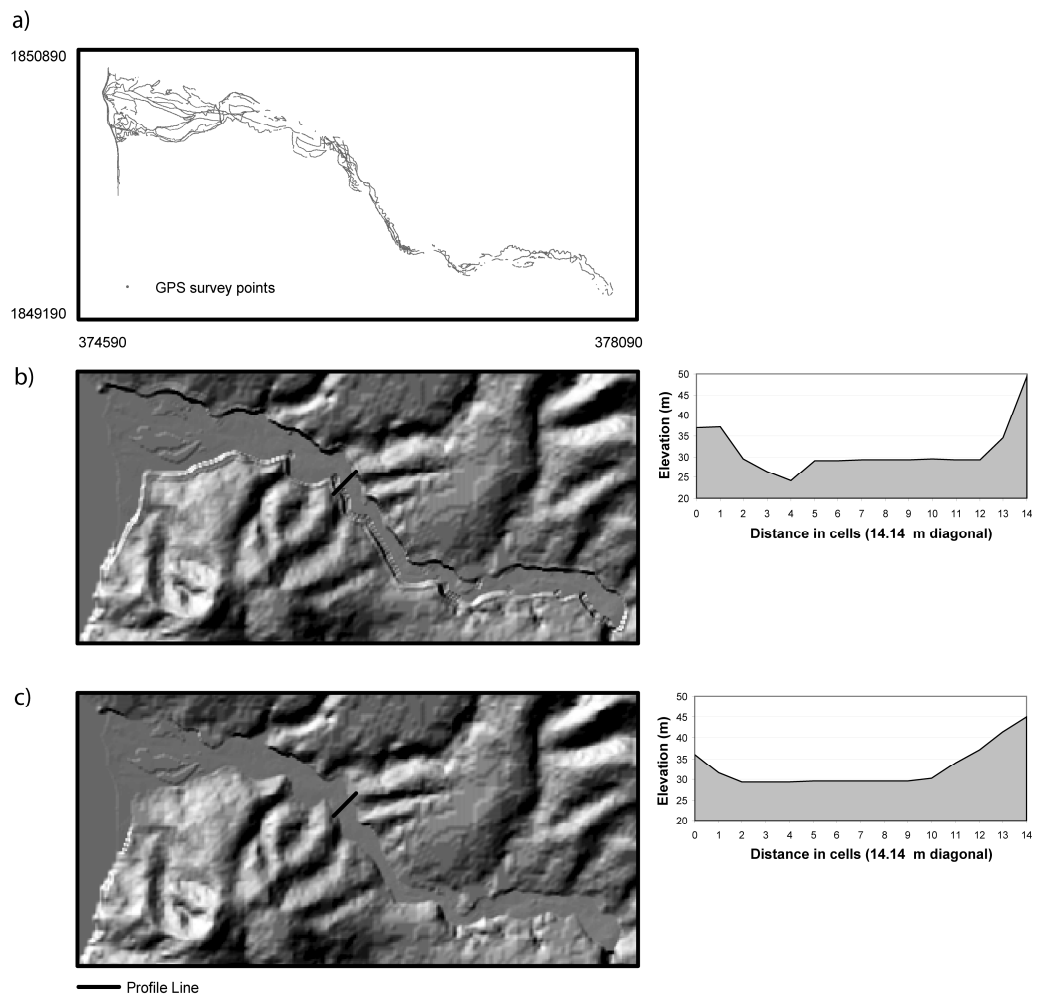


Figure 4.5 a) distribution of 2007 GPS points, and planimetric view of the merged section of the study area for b) void, fill and feather, and c) lateral extension method. Example profile graphs show the resultant cross-sections looking downstream. Coordinates in Montserrat National Grid. (After Darnell *et al.*, 2009)

4.4.2 Establishing geomorphological change

For the period 2006—2007 positive morphological change is shown through a differential surface (Figure 4.6a) and main channel profile (Figure 4.6b).

Over the year lahar deposits covered the valley floor and net erosion was negligible. Observed planimetric inundation area (B_0) was found by summing all cells that experienced morphological change and multiplying by cell dimension, giving

$7.47 \times 10^5 \text{ m}^2$. Over this area, the mean deposit depth was 2.71 m. On a cell-by-cell basis, net deposition generally decreased downstream. In the upper valley there was great variability in net deposition, as indicated by high standard deviation around the mean (8.35 m). Variability in deposit depth decreased downstream, as did mean deposit depth per cell (mean 2.80 m in the mid-reach). In the lower reach the mean net deposit depth was 0.65 m. From deposit depths (cell-by-cell), and considering resolution, the minimum input volume of sediment must have been approximately $2 \times 10^6 \text{ m}^3$. Assuming 20% sediment content by volume for hyperconcentrated lahars (Vallance, 2000), and no sediment removal from the system, total input lahar volume would be $1.0 \times 10^7 \text{ m}^3$ over the year. However, this figure does not consider sediment input from other sources; for example, a pyroclastic flow entered the Belham in January 2007 (De Angelis *et al.*, 2007).

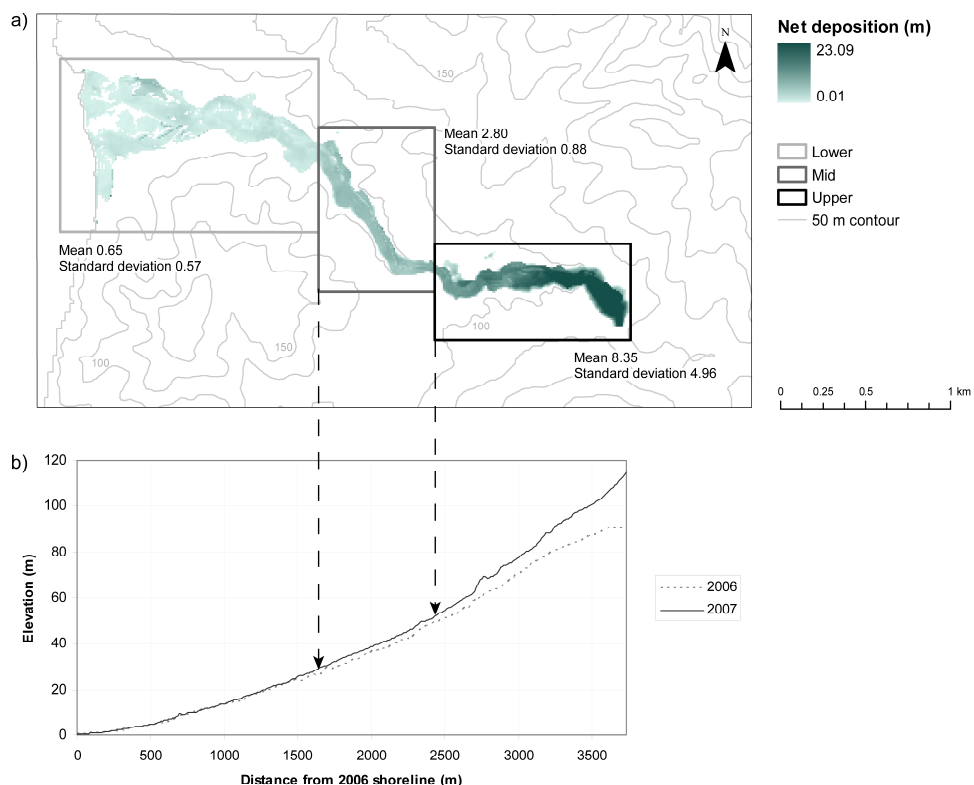


Figure 4.6 a) spatial distribution of net deposition November 2006—November 2007; b) channel profiles for 2006 and 2007

4.4.3 Volcanic activity and lahar events

On 20 May 2006, i.e. before the November 2006 field visit, there was a large dome collapse event (with an approximate volume of $1.0 \times 10^8 \text{ m}^3$), marking the start of a period of slower dome growth which ultimately ceased in April 2007 (SAC9, 2007). Coinciding with the 2006 field season, dome growth switched to the west side (in the direction of the Belham). A partial dome collapse with concurrent pyroclastic flow activity occurred at Soufrière Hills Volcano on 8 January 2007 (De Angelis *et al.*, 2007). The pyroclastic flow descended into the Belham Valley, terminating just upstream of the Sappit confluence (see Figure 4.1) – around a 5km run out (De Angelis *et al.*, 2007). The volume of the distal pyroclastic flow deposits in the Belham Valley and the more proximal surge deposits around Tyers Ghaut was about $3\text{--}4 \times 10^6 \text{ m}^3$ (SAC8, 2007). By the field visit in November 2007 the January pyroclastic deposit had been partially reworked and carved by lahars. For a full chronology of the current eruption the reader is referred to Chapter 2 (Section 2.5.3).

Recorded occurrence of lahars was synthesised from MVO daily and weekly reports (freely available at <http://www.mvo.ms/>). There were 13 reported lahars in the Belham during November 2006—November 2007 and these events have been plotted with daily and monthly-averaged rainfall data (Figure 4.7). However, as lahars are not formally monitored there were no associated intensity or volume data. Rainfall recorded at Garibaldi Hill rain-gauge (GAR) was the only available continuous data as the other tipping-bucket style gauges had been clogged with ash for all or part of the year. GAR is located on the west of the island, away from lahar source areas (proximal hazard zone); therefore regional averaged-monthly data are also presented in Figure 4.7.

On Montserrat the rainfall season runs from April—November and has subsidiary peaks in May and a larger, more prolonged peak centred on September (Barclay *et al.*, 2006). Barclay *et al.* (2007) found that lahars in the Belham Valley correlate with days when $>10 \text{ mm}$ rain fell in 24 h (based on a study of three rainy seasons). A 10 mm threshold is illustrated in Figure 4.7. However, during November 2006—November 2007, there were no direct correlations between *recorded* lahar frequency and daily rainfall, or averaged-monthly rainfall. For example, four lahars

were recorded in July with relatively dry preceding months. Further, the absence of reported lahars during November 2006—March 2007 is prominent; from field observations lahars typically occur year-round on Montserrat. Although that particular time period (highlighted on Figure 4.7) was in the ‘dry’ season on Montserrat, the GAR rain-gauge was recording high daily rainfall figures. It is highly probable that lahars were simply not recorded in the daily and weekly MVO reports due to focus on the increased activity at the lava dome.

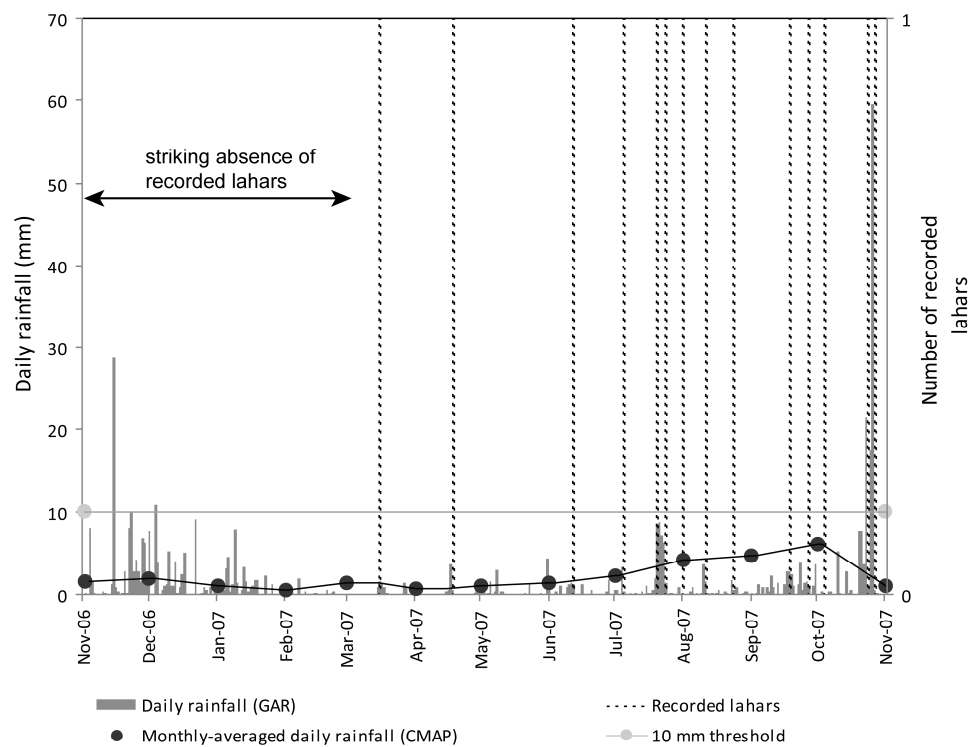


Figure 4.7 Daily rainfall recorded at Garibaldi Hill rain gauge (GAR) and regional monthly-averaged daily rainfall from the Climate Prediction Center Merged Analysis of Precipitation (CMAP) centred on Latitude 16.25, Longitude 298.75 (http://www.cpc.noaa.gov/products/global_precip/html/wpage.cmap.shtml).

4.4.4 Working with available data: constraining volume estimates for modelling

It was not possible to estimate the relative size of flow events from these rainfall data alone (Figure 4.7), nor from the cumulative deposit map (Figure 4.6). If the minimum observed system input volume (V_o), $1.0 \times 10^7 \text{ m}^3$, was to be satisfied by 13 recorded flows (of equal magnitude), each having a volume (V_i) of $7.7 \times 10^5 \text{ m}^3$.

Simple calculations in an attempt to reconstruct the 2007 topography highlighted the problems for estimating the magnitude of individual flows. The simplest approach for inferring deposit thickness was to average input volume over the planimetric area, B (Equation 4.2). This assumed (or approximated) deposition was uniform across all inundated cells, i.e. for a given volume, V_i , the lahar deposit height for every cell, d_i , = V_i / B . Sediment deposit depth, d_s = $(s \cdot V_i^{1/3}) / 200$, where s is the proportion of sediment by volume. Assuming 20% sediment by volume, each flow would theoretically have a uniform deposit depth of 0.092 m; hence, the maximum deposit depth after 13 flows would therefore be 1.196 m, far short of the overall observed mean of 2.71 m (but within the 0–23.09 m observed range).

An estimate for the planimetric area of the Belham Valley floor was found from all cells that had experienced morphological change, $B_o = 746\,800 \text{ m}^2$ (Section 4.4.2). This implied that if the planimetric area calculated by LAHARZ for a given volume was greater than the observed planimetric area ($B > B_o$), lahars would leave the system (run out to sea) and not all volume would be conserved. Another simple scenario considered n flows of equal volume, which in total satisfied the mean observed deposition of 2.71 m. A range of volumes, spaced by arithmetic and geometric progression, were tested mathematically before modelling (Table 4.2).

Only flows that satisfied this condition *and* $B \geq B_o$ resulted in a cumulative volume equal to the observed volume, V_o . Using this approach, minimum requirements (without sediment loss) were 44 flows of $228\,172 \text{ m}^3$ (Table 4.2): planimetric area, $B = B_o$, where $V_i = (\text{sqrt}(B_o / 200))^3 = 228\,172 \text{ m}^3$. Thus, where $V_i > 228\,172 \text{ m}^3$ sediment was lost to sea. Forty-four flows were in far excess of those (13) observed. There were obvious limitations with this method (e.g. implying homogeneous deposition), but these simple calculations did provide order of magnitude estimates.

V_i (m ³)	B (m ³)	d_s (m)	n (rounded)	Cumulative potential sed. volume (m ³)	$B_o - B$ (m ²)	Loss to sea (m ³)	Sed. lost (%)
1000	20000	0.010	271	54211	-726800	0	0
2500	36840	0.014	200	99857	-709960	0	0
5000	58480	0.017	159	158513	-688320	0	0
7500	76631	0.020	138	207711	-670169	0	0
10000	92832	0.022	126	251624	-653968	0	0
25000	170998	0.029	93	463496	-575802	0	0
50000	271442	0.037	74	735754	-475358	0	0
75000	355689	0.042	64	964110	-391111	0	0
100000	430887	0.046	58	1167936	-315913	0	0
125000	500000	0.050	54	1355270	-246800	0	0
150000	564622	0.053	51	1530429	-182178	0	0
175000	625732	0.056	48	1696073	-121068	0	0
200000	683990	0.059	46	1853983	-62810	0	0
225000	739864	0.061	45	2005430	-6936	0	0
228172	746800	0.061	44	2024231	0	0	0
250000	793701	0.063	43	2151357	46901	127126	5.9
500000	1259921	0.079	34	3415066	513121	1390835	40.7
750000	1650964	0.091	30	4475002	904164	2450771	54.8
1000000	2000000	0.100	27	5421079	1253200	3396848	62.7
9064362	8694704	0.209	13	23567340	7947904	21543110	91.4

Table 4.2 n flows of equal volume, V_i , required to satisfy observed mean deposit depth of 2.71 m, assuming a uniform deposit depth of d_s .

General approximations for input volume were also made from field knowledge and published findings. Discharge for previous flows have been estimated at 15–45 m³s⁻¹ (for braided channels) and 60–90 m³s⁻¹ (for a single channel) (Barclay *et al.*, 2007). The largest lahars travel to the shoreline and have an observed duration (from eyewitness accounts) of two hours. Assuming an average discharge of 60–90 m³s⁻¹ within a confined channel, a volume estimate for ‘large’ flows can be constrained to 4.32–6.48 × 10⁵ m³ (water and sediment). These size flows occur

two or three times a year (subjective field observation). Smaller volume flows occur more frequently but do not travel as far. During the rainy season, the smallest lahars occur bi-weekly. Extreme events occur every two or three years and have a magnitude much greater than those regularly observed (e.g. 25/26th May 2006 event(s) as discussed in Alexander *et al.*, in press).

A combination of the above calculations and subjective observations, which came from years of combined field experience, enabled the following assertions: (1) thirteen flows of equal volume would have to be unrealistically large to satisfy the observed volume of remaining sediment; therefore, there were more flows than were officially recorded; (2) it is unlikely that actual flows from Nov 2006—Nov 2007 were equal in magnitude; (3) a differing variety of flow sizes would be required to match the cumulative volume observed; there is no simple method to determine what a suitable combination should be; (4) a typical (annual) frequency distribution of Belham Valley lahars would be approximately inversely proportional to volume.

Numerous uncertainties were highlighted through these preliminary investigations. Thus, the most appropriate way forward was to investigate a range of volume scenarios that were informed by the simple calculations above, but also by (subjective) field knowledge. Thus, from the field-based data and trial calculations, small flows ($1-5.0 \times 10^3 \text{ m}^3$) occur frequently, intermediate volumes ($1-5.0 \times 10^4 \text{ m}^3$) are less likely, and large flows ($1-5.0 \times 10^5 \text{ m}^3$) are relatively unlikely on any individual day. Extreme events ($1-5.0 \times 10^6 \text{ m}^3$) are very unlikely. A range of volumes were considered to encompass small to extreme flows representative of this range of Belham lahars. With uncertainty in the actual volumes of Belham lahars, six flows were modelled: one small ($5.0 \times 10^3 \text{ m}^3$), two intermediate ($2.5 \times 10^4 \text{ m}^3$, $5.0 \times 10^4 \text{ m}^3$), two large ($1.0 \times 10^5 \text{ m}^3$, $1.25 \times 10^5 \text{ m}^3$) and one extreme ($1.0 \times 10^6 \text{ m}^3$). This represented different sizes of lahars over one year, but one in which an extreme lahar may occur.

4.5 IMPLEMENTING LAHAR MODELS

4.5.1 Simple flow routing

4.5.1.1 Determining the path of steepest descent from an elevation cost surface

To assign flow based on the path of steepest descent, the (newly fused) 2006 DEM was used as an elevation cost surface. Within ArcGIS, the cost functions (CostWeightedDistance and ShortestPath) determined the shortest weighted distance (or accumulated travel cost) from a user-defined start cell to each cell (Figure 4.8). The cost assigned to each cell represented the cost per-unit distance for moving through the cell, i.e. the least change in elevation had the highest cost. Flow direction was based on impedance associated with the cost surface and from the direction of movement. The least-cost flow route was calculated by using a back-link raster from an end point at the mouth of the Belham (maximum travel distance). Two end points were used. The first (point A) corresponded to the pre-eruption coastline, and the second (point B) corresponded to the 2006 coastline.

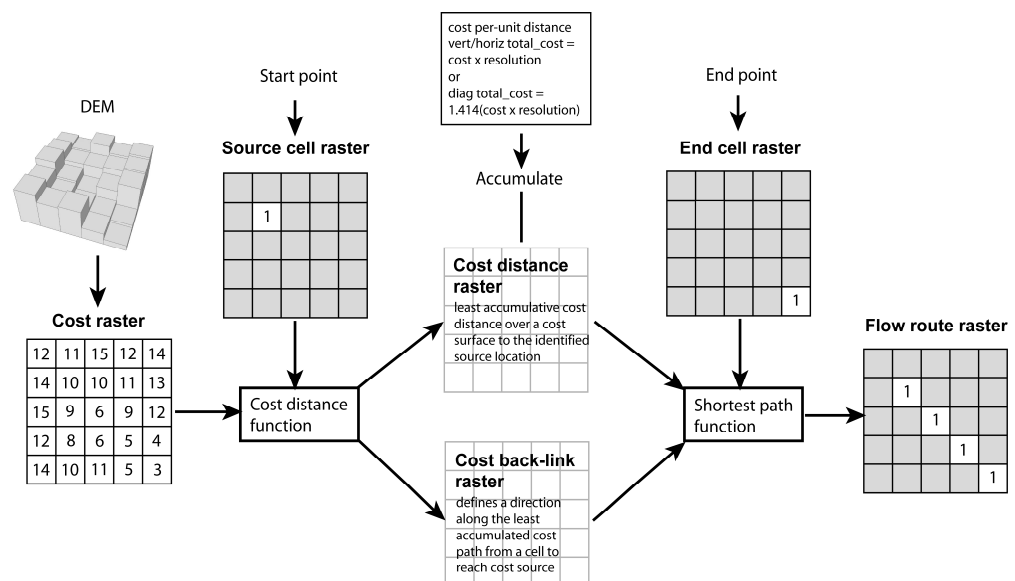


Figure 4.8 Schematic of steepest descent method used to define probable flow routes (implementation was in ArcGIS)

Lahar initiation, or start point was placed at the upstream extent of the GPS survey (where confidence in surface representation was high). In order to examine the fitness of the DEM, this methodology had been previously tested for a sub-section of the study area, documented in Chapter 3 (Darnell *et al.*, 2010).

4.5.1.2 Uncertainty in elevation and probability of flow

Confidence in flow route prediction was then considered by examining elevation error propagation. The importance of DEM accuracy for lahar modelling has been discussed by Stevens *et al.* (2002). Errors in elevation models are inherent due to the approximations needed to represent a continuous surface over a regular grid. These disparities between reality and the values projected by the DEM are caused by (1) variation in the accuracy, density and distribution of measured source data; (2) processing and interpolation; and (3) characteristics of the terrain surface being modelled (see Fisher and Tate, 2006, for a full discussion of these issues). As confidence was high in the positional accuracy of the GPS source data, uncertainty was most relevant following DEM construction; elevation error was then considered as the combined response to uncertainty in source data, interpolation, and processing (Figure 4.9).

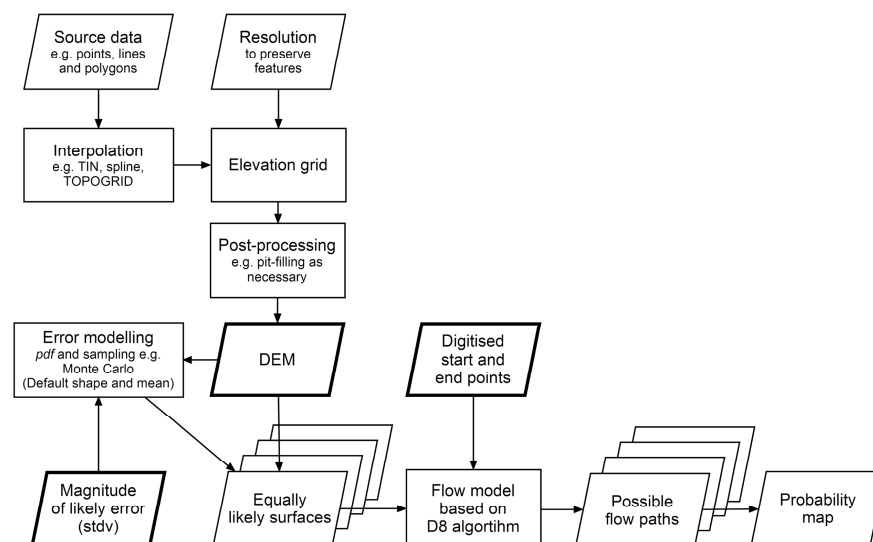


Figure 4.9 Considerations for elevation error propagation (necessary user inputs are highlighted)

In the absence of a higher accuracy reference surface, DEM error was simulated using unconditioned fields. This required estimation of the distribution of error, represented by a probability density function (*pdf*) (Heuvelink *et al.*, 2007). It was assumed that over a DEM the errors were normally distributed around a mean of zero metres (there was no known bias in the data) (Figure 4.10a).

The standard deviation of error (*stdv*) was inferred from field knowledge, resulting in the selection of three possible values: 0.1 m, 0.5 m or 1 m. In reality, a 1 m *stdv* of elevation error was too high – but this would provide extreme testing of the robustness of the flow model to error. The stochastic input variable (elevation error) was sampled within the bounds set by the *pdf* using Monte Carlo simulation; however, this did not guarantee that the entire range of values would be equally sampled (e.g. Smemoe, 2007; Figure 4.10b). Using a random number seed, 100 equally probable realisations of the error surface were generated. The fused 2006 DEM was then perturbed using each of these error surfaces in turn. Each DEM was subsequently used as an input for the slope function. This was implemented using the iteration capability of ArcGIS ModelBuilder. Although ModelBuilder is inefficient for multiple iterations using complex processes, the simple linking of functions coped well here and avoided the necessity of developing programming scripts. The model was also designed to be transferable and user inputs were minimised (Figure 4.9).

For each model run, 100 equally probable flow routes were generated and summed together to generate a map showing the probability of flow. It was anticipated that this would show the dominant flow routes, or movement of the centre of mass for large flows. Flow spread was also indirectly inferred using the error perturbations as slight deviations in the topographic surface. Only uncertainty in elevation was modelled, but the propagation of error to the confidence in main flow routes was indirectly considered. The phenomenon of error propagation has been well-documented (e.g. Veregin, 1995; Heuvelink, 1998; Fisher and Tate, 2006; Darnell *et al.*, 2008). The intention was to reproduce the main observed flow routes and also investigate response to elevation error. For hazard assessment, only the main body of the lahar (or central mass) was modelled for its directional changes and incorporation of uncertainty considered probability of this hazard.

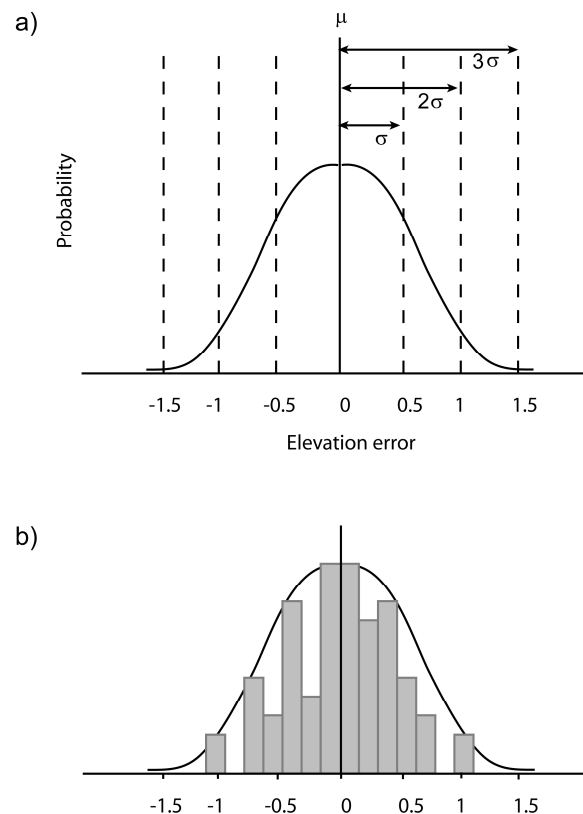


Figure 4.10 a) standard deviations (σ) on an elevation error *pdf* with normal distribution and no bias (e.g. mean error, μ , is zero), e.g. for stdv = 0.5 m; b) an elevation error sampling scenario for Monte Carlo simulation (after Smemoe, 2007)

4.5.2 Implementing LAHARZ

LAHARZ runs in ArcInfo and is essentially a set of scripts, written in Arc Macro Language (AML), connected through menus. Source code is available freely from USGS on request but an ArcInfo Workstation licence is required to run the program in its current form (licence purchasable through ESRI). Software input consisted of a DEM, specified lahar volumes and a specified H/L value (a ratio for the slope of the energy cone). A threshold of flow accumulation was also user-defined as 500 draining cells - this value defined a connected processing 'stream', a thalweg, and the major tributaries (Figure 4.11). The H/L ratio can be thought of as (internally) defining the runout of primary volcanic hazards (such as pyroclastic flows and dome collapse avalanches) and source area for lahars (Chapter 2, Section 2.3.4.2).

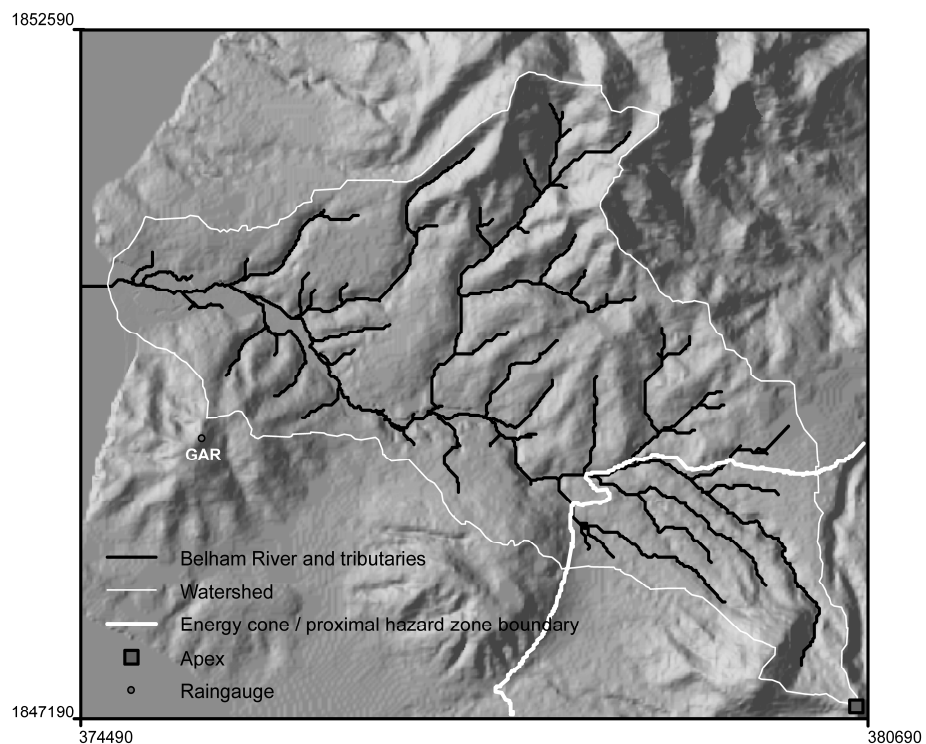


Figure 4.11 Belham stream network (flow accumulation threshold 500) and H/L energy cone (0.24) as generated in the setup of LAHARZ. The volcano apex, or maximum elevation, is also shown. The proximal hazard zone is from the apex to the energy cone boundary. Coordinates are provided in Montserrat National Grid.

This ratio can also be viewed as a boundary, marking the start of lahar deposition downstream. From previous research, a suitable range is 0.1–0.3 depending on the size and type of event (constraining mobility and runout) (Hayashi and Self, 1992). For the Belham catchment the H/L ratio was calculated using the apex (volcano) at the upstream limit of the Belham catchment and the furthest observed upstream lahar deposit (considered as the start of lahar deposition). The vertical and horizontal difference in positions specified the H/L ratio as 0.24. This process was repeated several times as manual selection was achieved through interpretation of a digital display of topography in combination with field experience; little deviation in the ratio to two decimal places was recorded in this pilot test.

A preliminary script established the position of the proximal hazard zone boundary by computing where the H/L energy cone intersected surface topography. Then, using the D8 algorithm, supplementary surface hydrology grids were derived - indicating slope directions and the presence of 'streams'. LAHARZ next located a starting cell where the stream valley intersected the proximal hazard-zone boundary. Calculations progressed downstream cell by cell. At each stream cell LAHARZ constructed a minimum of three valley cross-sections at azimuth intervals of 45° (Schilling, 1998). The channel or valley cross-section area, A , was filled to a level that satisfied the empirical relationship (Equation 4.1). By retaining a cumulative tally of those cells encountered and volume deposited, flow continued until the planimetric area (Equation 4.2) was also satisfied.

In addition to the inbuilt assumptions (Table 4.1), it was assumed that, although LAHARZ was calibrated for debris flows, the proportionality coefficients applied to flows with lower sediment content observed on Montserrat.

A set of inundation zones were produced for different lahar volumes (Section 4.4.4); these then corresponded to hazard zones. However, there was a juxtaposition between the greatest threat from an individual lahar and the probability of that event, defining the hazard; the intensity from a greater volume flow is more dangerous at a given location than a smaller volume flow, however, the smaller volume flow is defined as more hazardous (e.g. Iverson *et al.*, 1998). Thus, it is necessary to consider the cumulative potential hazard, for example, if an intermediate size flow inundates an area x , within that area smaller volume flows are more likely. The inundated area x will thus extend beyond areas covered by smaller flows; overlapping areas will thus represent the greatest cumulative hazard for a given time period (here, one rainy season).

LAHARZ allowed calculation of four flows per processing session; however, inundation areas were output as individual rasters (binary inundated or non-inundated cells) and so results from different processing runs were manipulated in a GIS to produce a hazard map (i.e. with raster math or AND/OR operations). The hazard map divided the Belham Valley region into areas, or zones, of equal hazard. Only six hazard zones were visualised to avoid over-categorising, and hence overcomplicating, the display. Town names and roads were used to orientate the

map-user. Hazard zonation cognition issues are discussed elsewhere (Chapter 2, Section 2.2.2.1 and later in Chapter 6).

4.6 RESULTS

4.6.1 Dominant paths from single-direction flow routing

Figure 4.12 shows the observed main flow routes in the lower-reach; the dominant channel represents the in-field interpretation of the Belham thalweg and other discernable flow routes are designated 'sub-channels' (see also Chapter 3, Figure 3.7).

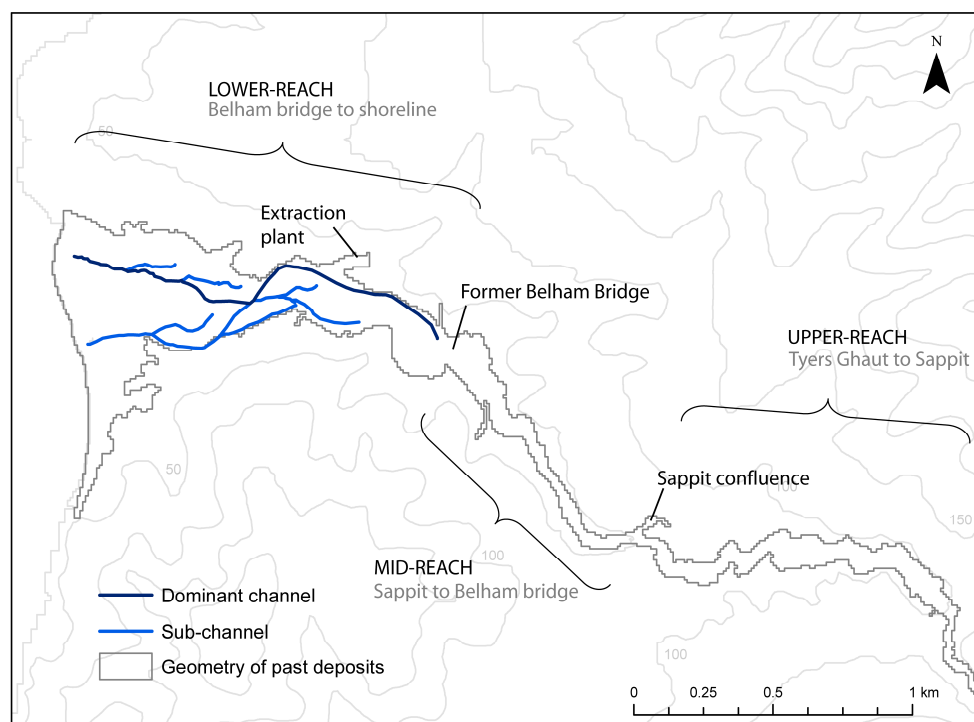


Figure 4.12 Observed channels, in November 2006, and geometry of past deposits (given by Figure 4.6)

Further upstream the valley was more confined and thus, for the most part, the valley floor was one main channel. Implementation of single-direction flow routing using an elevation cost surface aimed to reproduce these main flow routes. Incorporation of elevation error enabled the production of probability-of-flow maps for different magnitudes of error (defined by the *stdv*) and end points (Figure 4.13); thereby estimating 'reasonable' (expected) spatial deviation around prediction of the main routes.

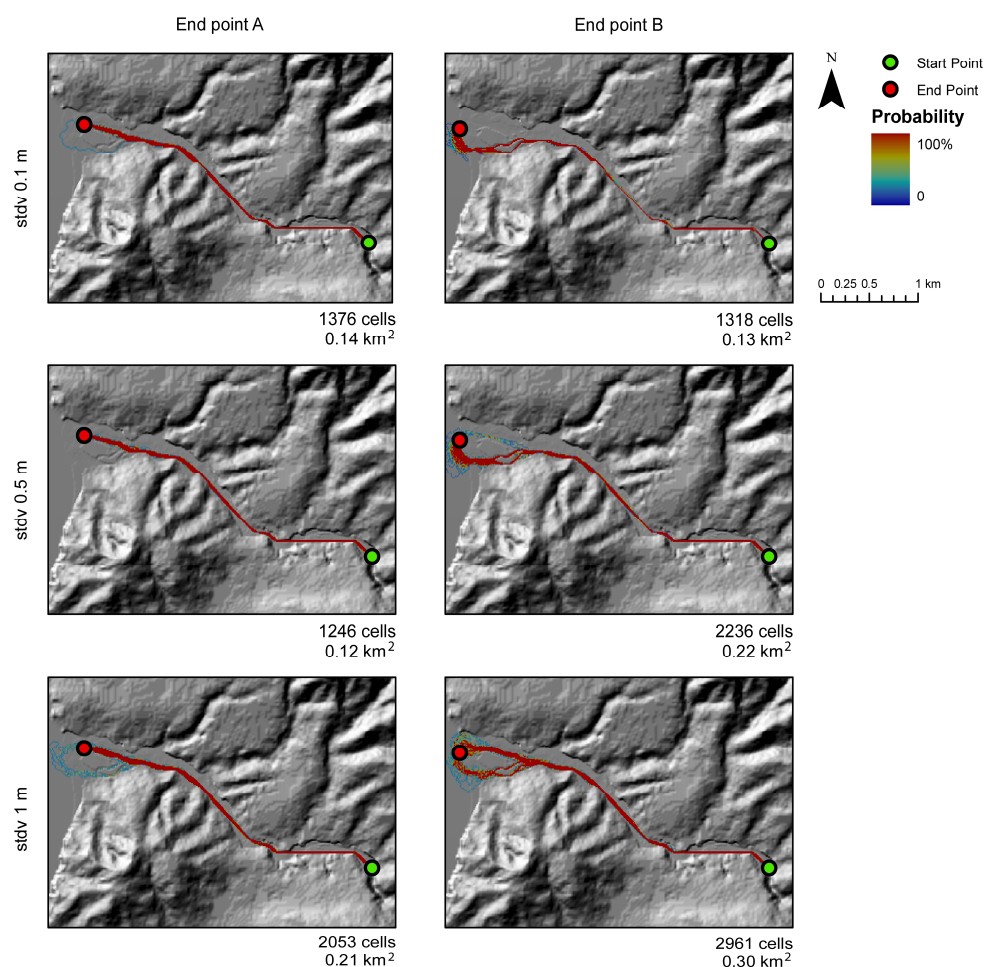


Figure 4.13 Inundation probability maps, the first column shows results using end point A, and the second from end point B; rows represent increasing *stdv* of error. Inundated cell count and total area are also shown for comparison.

Increasing *stdv* generally increased flow path variability and thus total area inundated. In the upper- and mid-reaches there was little lateral deviation from a main flow route for all the different end points and *stdvs* used (Figure 4.13). However, as the valley widened in the lower-reach, both end point and *stdv* influenced the dominant flow routes. Moreover, none of the simulations matched observations for the lower-reach, between the former Belham Bridge and extraction plant. Specifically the observed dominant channel hugged the northern side of the valley bottom, whereas all simulations hugged the southern side, closest to Garibaldi Hill; however, there was an observed sub-channel that took the southern route (Figure 4.12). Near the shoreline simulated flow routes were able to match observed channels.

However, simulations with end point A were more robust to elevation error, e.g. there was little difference between 0.1 m *stdv* and 0.5 m *stdv* (130 cells or 9.6% decrease of inundated area when *stdv* was increased from 0.1 m to 0.5 m; the unexpected decrease is a result of the anomalous flow path in the 0.1 m simulation). In contrast, for end point B, there was a 69.7% increase of inundated area (0.092 km²) when *stdv* was increased from 0.1 m to 0.5 m. A 1 m *stdv* was extreme but simulations with both end points coped well – generally there was little deviation from established routes, especially in the mid- and upper-reaches. Further, the variability in flow paths only served to highlight the sub-channels in the last 0.5 km (approximate) near the shoreline (see Figure 4.12). Hence, this approach is fairly robust to elevation error and its propagation, although there are some issues with the ability of the model to pick out the valley thalweg (main channel) in the lower-reach between the former Belham Bridge and the extraction plant.

In the lower-reach cross-sections generally become wider (Figure 4.12) and the valley floor flattens (Figure 4.6b); thus the topographic differences between cells become less here. Due to the great reliance on topographic control, these differences in valley morphology may influence output inundation areas and increase sensitivity to DEM error.

4.6.2 Delineating lahar hazard zones with LAHARZ

LAHARZ calculated inundation areas for user-specified lahar volumes, spreading away from the valley thalweg. The thalweg was generated automatically from the DEM by LAHARZ (Figure 4.14a; also shown with tributaries in Figure 4.11) and was supported by field observations made in the lower-reach (Figure 4.12). As the lahar input volume increased, flows spread further laterally and were able to reach further downstream (until the processing stream cell encountered the sea) (Figure 4.14b). LAHARZ output was generally wider down the channel (had more lateral spread from the thalweg) in the upper- and mid-reaches than recorded through past deposition (Figure 4.14b). This may be caused by a (a) problem with the DEM representation of the terrain; (b) an inadequate technique for discerning the absolute extent of net deposition; or (c) a problem with the cross-sectional spreading mechanism in LAHARZ. Most likely all of these are contributory factors, but the exclusion of net erosion in the geometry of inundated area would probably cause an underestimation of past lahar extent and explain the greater spreading shown by LAHARZ. However, there was also an area near the shoreline that had observed deposition, yet was not inundated by any of the LAHARZ model runs, including the very large $1 \times 10^6 \text{ m}^3$ volume event. This reflects the inability of LAHARZ to show multiple channels in an unconfined channel (as observed in the field, Figure 4.12). Nonetheless, it is not reasonable physical behaviour for sediment-rich lahars (debris flows) to flow down more than one channel at once; thus, the observed deposition in the lower-reach can be explained by flows with lower sediment content, or a reworking of lahars after initial deposition.

With likelihood of occurrence decreasing with volume, inundation areas were combined to produce a cumulative hazard map (Figure 4.15a) (see Section 4.5.2). This can be compared to the existing long-term hazard map (Figure 4.15b).

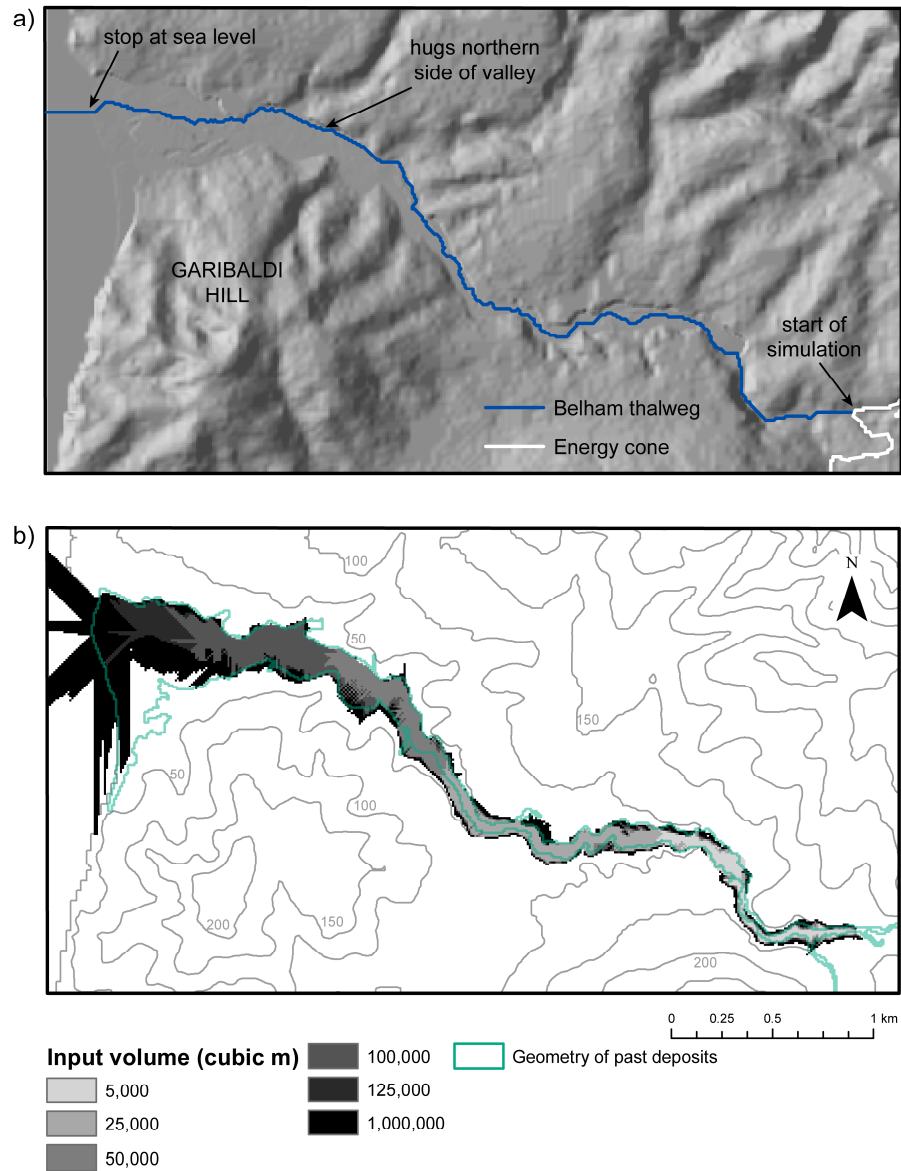


Figure 4.14 a) Belham thalweg automatically generated in LAHARZ; and b) inundation areas for varying lahar volumes from LAHARZ; additionally the geometry of past deposits has been overlain (from Figure 4.12).

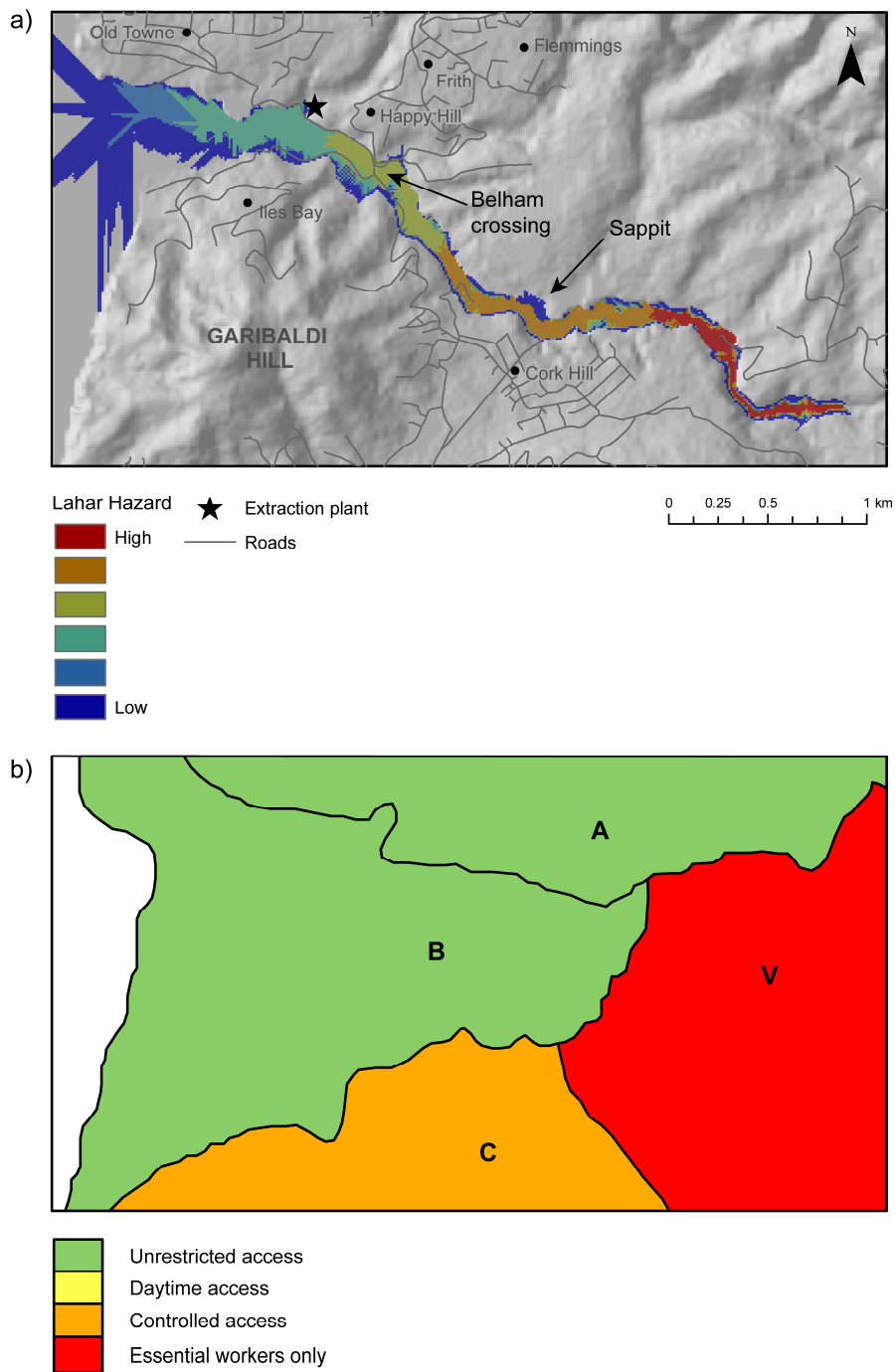


Figure 4.15 a) example hazard map showing changes in hazard relative to the key towns and road network; b) existing hazard zones map (at Hazard Level 3) for the same section of the Belham Valley (digitised from MVO hazard map).

The lower-reach of the Belham is highlighted in Figure 4.16 to show the differences in hazard mapping from the flow routing and LAHARZ. With $stdv = 0.5$ m the simple flow routing was able to show the braided channel near the shoreline (as shown in Figure 4.12). In contrast, LAHARZ was able to show lahar spread but not multiple channels. Furthermore, while single-flow routing represented hazard as gradational probability, LAHARZ depicted hazard by a series of homogenous zones with discrete boundaries.

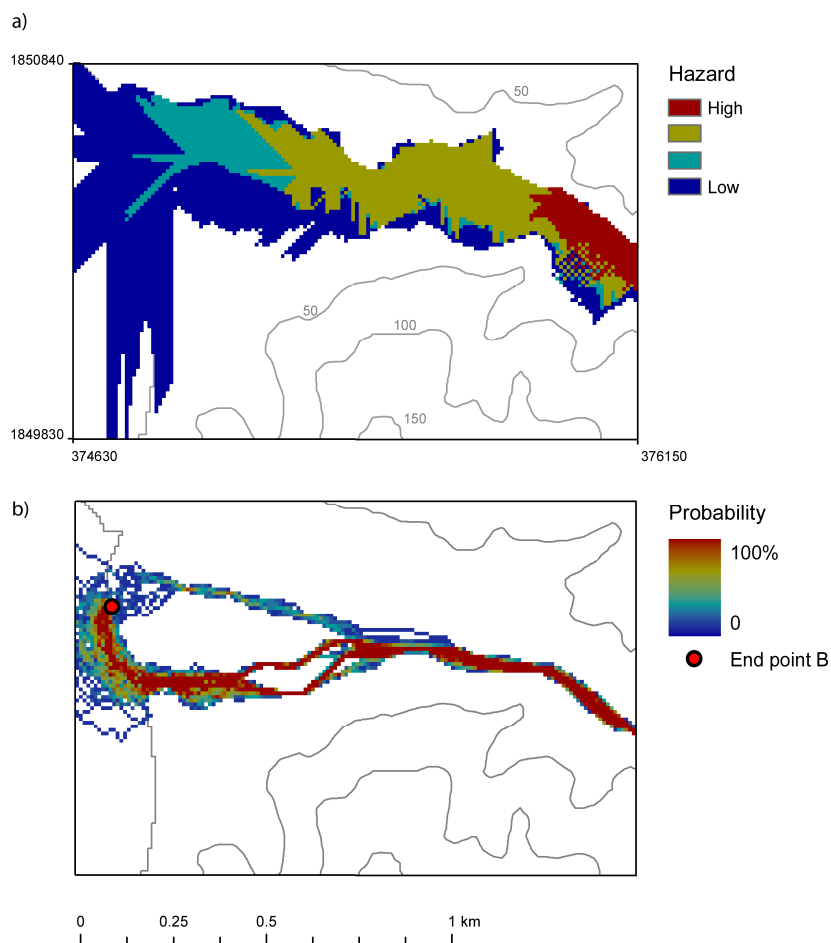


Figure 4.16 Hazard maps for the lower-reach between the Belham crossing and the shoreline: a) hazard zones inferred from LAHARZ; b) inundation probability field from the elevation cost surface, $stdv = 0.5$ (close-up of Figure 4.13, mid-right). Coordinates are provided in Montserrat National Grid.

4.6.3 Comparison of model outputs with observed morphological change

For each volume used as an input for LAHARZ, coordinates were taken from the last stream-cell processed. Volumes where resulting $B > B_o$ were not considered further as they did not achieve their full potential runout (sediment was lost to sea). Figure 4.17a illustrates a significant positive relationship between natural log transformed input volume and lahar travel distance ($R^2 = 0.96$), a result suggested in the graphical outputs of the model (Figure 4.14b).

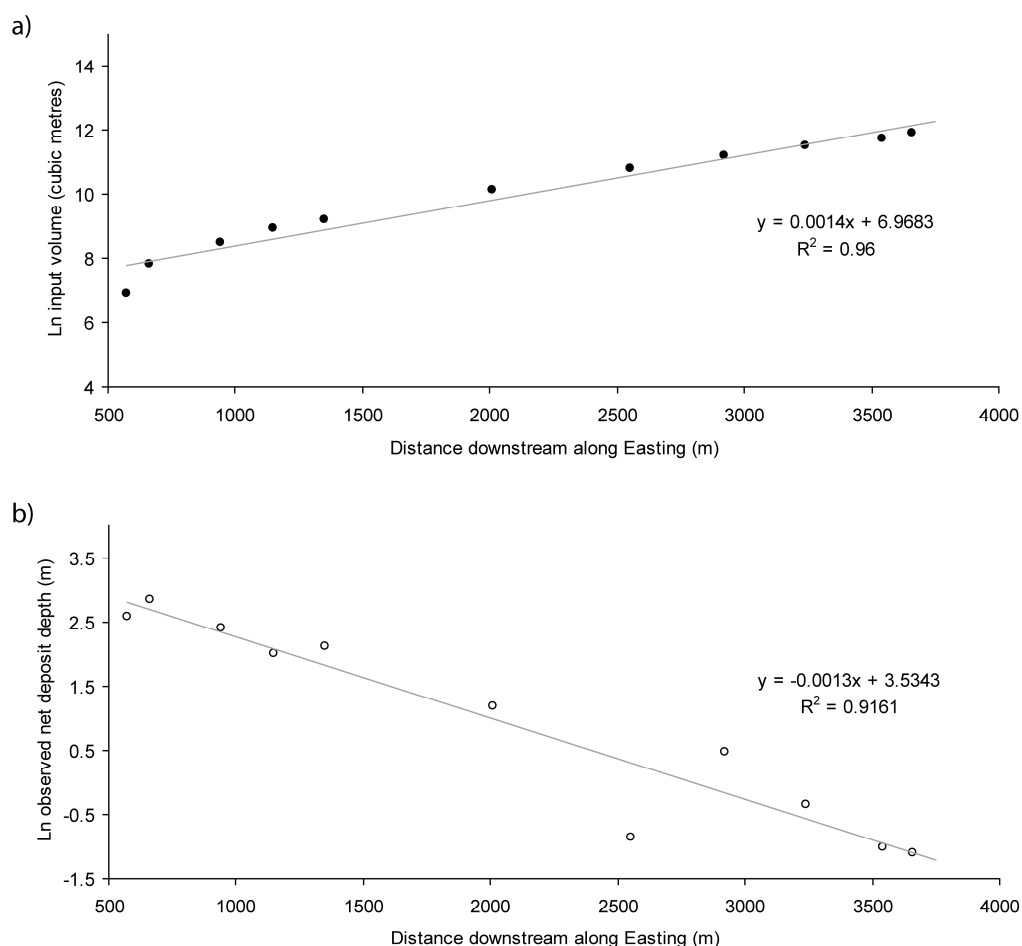


Figure 4.17 a) relationship between natural log transformed input volumes (for various LAHARZ model runs) and lahar travel distance downstream (last stream-cell); b) natural log transformed observed net deposition at corresponding sample locations downstream (extracted from data presented in Figure 4.6).

Preliminary analysis of these data suggested a positive exponential relationship and input volume was natural log transformed prior to linear regression. Such a relationship is likely to result from the changing (generally widening) cross-sectional area downstream. At corresponding locations, the observed net deposition was extracted using information derived from Figure 4.6 and related to distance downstream. Preliminary analysis of these data suggested a negative exponential relationship and net deposition was correspondingly natural log transformed prior to linear regression. Linear regression applied to the transformed data yielded a significant ($R^2=0.92$) negative correlation with distance downstream (Figure 4.17b). Whilst travel distance from modelled individual events (Figure 4.17a) can not be directly related to observed net deposit depth (cumulative system response over a year) (Figure 4.17b), high cumulative hazard areas (small distances downstream) corresponded to areas with greatest net deposition and by inference, most lahar activity.

4.7 DISCUSSION

4.7.1 Comparison of inundation areas

Inundation maps generated by the two models differed in the elements of lahar runout that they illustrated. LAHARZ produced a map of inundated areas (total planimetric) for given volumes, whilst the single-direction flow routing mapped the spatial distribution of dominant flow paths, independent of volume.

Single-direction flow routing maps identified multiple channels near the shoreline, in broad agreement with field observations. Variation in predicted flow routes was markedly less in mid- and upper-reaches. However, this method did not allow general planimetric spreading of lahar volume. Whilst LAHARZ allowed for dispersion (in both total planimetric area and cross-sectional areas downstream), in an unconfined channel the mechanism for spread along three cross-sections resulted in jagged hazard zone predictions. Furthermore, as cross-sections in

LAHARZ were processed from the channel thalweg only, this method was unable to reflect any channel braiding.

In the lower-reach (excluding the near-shoreline region), a tendency for simulations from single-direction flow routing to hang close to the southern side of the valley (Figure 4.13) represented only a relatively minor channel in the field (Figure 4.12). The D8 algorithm was also used by LAHARZ to determine the Belham River (thalweg) and tributaries (Figure 4.11); LAHARZ isolated a different main channel in the mid- and lower-reaches to that identified by single-direction flow routing. The thalweg generated by LAHARZ hung close to the northern side of the valley, agreeing more closely with field observations (Figure 4.14a). Differing outputs from the same algorithm were possibly a result of LAHARZ's use of a flow accumulation grid. This grid, for model setup only, essentially considered movement of a gravitational flow from every cell in the DEM to their immediate neighbours. Flow was accumulated and a cell was assigned to the main flow route if the number of cells draining into it exceeded a threshold (in this case 500 cells). In contrast, the single-direction flow routing algorithm expelled flow (backwards) from one cell to the next from a single end point, finding the easiest (least-cost) route to the start point. In terms of flow behaviour, this approach models movement of mass from one source only and investigates the route taken to arrive at an observed end-point. The two GIS-based approaches thus implement the D8 algorithm in slightly different ways. For individual flows the single-direction flow routing approach (cost surface implementation of D8) seems physically better.

Both models had their own limitations in their predictions of inundation in the lower valley; specifically, the mechanisms used to spread volume (along three cross-sections) were insufficient for LAHARZ in this unconfined section of the channel and single-direction flow routing took a minor observed route between the mid-reach and the extraction plant in the lower-reach. Therefore, consideration of topographic variation alone may not be sufficient to fully explain observed lahar movements. This points to the significance of variables that are not currently included in these formulations, which have a strong influence on flow direction. While terrain slope is likely to have the greatest influence on the direction of lahar movement, other surface factors, such as surface roughness (including vegetation) or degree of

channel confinement, might be influential. Channel roughness and cross-section shape have been shown to influence properties of stream-flow and hyperconcentrated-flow (Macedonio and Pareschi, 1992). Physical lahar-specific variables (e.g. turbulence, rheological regime) were also notably absent from both simple models. An extension to this research could consider improving model performance of simple flow routing in a non-confined channel, perhaps through the addition of parameters considering channel roughness or rheological changes. For hyperconcentrated flows, water and solids behave as different phases with fluid acting as the transporting medium exhibiting some turbulent behaviour, similar to stream flows (Chapter 2; Section 2.3.2). However, these non-Newtonian flows also acquire yield strength, potentially reducing their mobility. Thus, lahar composition is important to flow behaviour. However, with current data limitations in the field context of Montserrat an approach could first trial further factors external to the solid-fluid mixture, and see how successful those results are at matching observations (this is considered in the subsequent chapter); thereby assessing the relative importance of rheology indirectly. Furthermore, a more formal approach to sensitivity testing could quantify the relative importance of input variables for their influence on model output (e.g. global sensitivity analysis as detailed in Saltelli *et al.*, 2000b).

4.7.2 Model requirements and limitations

4.7.2.1 Single-direction flow routing

Simple flow routing required user-input in the form of a regular grid of elevation values – a DEM. The major assumption for single-direction flow routing was that a lahar would preferentially travel over this DEM from a given cell to one of its eight direct neighbours in the direction of steepest descent. Uncertainties in these predictions were considered through likely magnitudes of elevation error (*stdv*). An end point, or points, was also needed to run the model (Figure 4.9). Lahar intensity (depth and velocity; Chapter 2, Section 2.3.3.2), or volumes, was not considered, nor were any internal factors of the solid-fluid mixture.

Alternatives to the D8 algorithm for flow routing have been discussed in Chapter 3 (Section 3.6.2.3), but these may complicate the relationship between topography, cost and flow-direction.

4.7.2.2 LAHARZ

LAHARZ required acceptance of the assumptions in Table 4.1, input volumes, a DEM and specification of H/L . Hydrological flow equations form the theoretical basis for LAHARZ (Iverson *et al.*, 1998) but these were originally calibrated for debris flows (more sediment-rich). Therefore, the magnitude of A and B may not be accurate for Belham (typically dilute) lahars. Notwithstanding the above, when a range of magnitudes are considered there should be reasonable confidence in hazard zoning; with the creation of a relative hazard map (and no absolute values), a specific input lahar volume does not claim to correlate directly with an inundation area. Thus, even though input volumes can be arbitrary without recorded volumes from actual events, relative hazard severity can be assessed by considering order of magnitude increments in volume, as given here.

Uncertainty in the DEM was not considered for its influence on LAHARZ outputs. It was unfeasible to perform stochastic simulation of elevation error to generate multiple realisations of a DEM for use as inputs to LAHARZ; this would have been a very time-consuming process as user input would be required for each DEM to select the start and end cells etc. Error in the DEM would have had an influence on a) thalweg definition (this can be inferred by changing dominance of the main channel from single-direction flow routing) and b) inundated cells across a cross-section. Stephens *et al.* (2002) have discussed the notable response of LAHARZ to different DEM data sources with inferred differing accuracies. However, here Figure 4.13 gave supporting evidence for high confidence in the DEM.

From those that have used LAHARZ (e.g. Stevens *et al.*, 2002; Berti and Simoni, 2007; Oramas Dorta *et al.*, 2007) there has been little discussion about the relative significance of the H/L ratio on model outputs. The H/L energy cone (along with derived channel thalweg) determined the initiation cell, but in preliminary testing its value had little effect on the output inundation area (shifting the start of simulation upstream or downstream along the thalweg by one or two cells only). However,

recent pyroclastic flows have travelled down Tyers Ghaut (see Chapter 2, Section 2.5.3) and into the Belham Valley with runout close to the Sappit confluence; this suggests a shallower H/L ratio could be used to better inform the limits of the energy cone (see Chapter 2, Section 2.3.4.2) for a discussion of pyroclastic flow runout).

4.7.3 Implications for lahar hazard management on Montserrat

Simple models inherently avoid over-complication; they can isolate the important parameters and, if accepted as preliminary tools or first approximations, are more likely to reasonably fit over a wide range of behaviours. They are also often the only choice due to limited data and/ or can serve to test the suitability of available data (e.g. DEM; Chapter 3).

For LAHARZ, inundation areas were converted to hazard zones using the inference that smaller volume flows are likely to occur more frequently (as they require less ‘forcing’ to initiate) and larger volumes will overlap inundation areas made by smaller flows. The areas inundated by the smaller flows thus represent the greatest (cumulative) hazard. For single-direction flow routing, the likelihood of a cell being classified as part of the main flow route was given by a probability map produced by stochastic simulation of elevation error. Thus, although different elements of lahar inundation were predicted, both models considered hazard in terms of probabilities or likelihoods. However, LAHARZ produced zones bounded by discrete lines, whereas the simple flow routing produced a gradational change in hazard or flow probability.

Inundation probability maps here are useful for showing dominant flow routes, but the single-direction flow routing methodology requires some refinement to be consistent with field observations in the lower-reach. Probability maps have shown distinct advantages over unique line boundaries or binary ‘safe/ unsafe’ maps for hazard assessment with respect to flooding, (e.g. Zerger, 2002; Smemoe *et al.*, 2007); and although the methodology may appear complex, probability maps generally translate well to decision makers and therefore a full understanding of the

concepts isn't a prerequisite (Zerger, 2002). However, given morphological change as a response to lahar perturbation, and the established influence of terrain on flow movement, dominant flow routes are liable to change. Thus, the single-direction flow routing approach has shown potential for short-term lahar route predictions.

LAHARZ (capable of mapping lahar dispersion) is more suitable for long-term hazard assessment synonymous with local land-use planning objectives. LAHARZ output also differs from the existing hazard mapping scheme as Figure 4.15a applies regardless of the activity at the volcano. This does not imply that the results presented here are an improvement on the existing Hazard Level System for public information; there are issues surrounding the over-complication of zones (hazard management issues will be discussed in Chapter 6). However, Figure 4.15 may be useful for micro-management and long-term planning.

Both methods used here operated within a GIS and the procedures can be largely automated. This gives two options for potential outputs: models (in a GIS) that can be transferred to users (with GIS) or hazard maps that can be tailored to user requirements (e.g. paper or electronic maps). Transfer of a working GIS has the advantage that updated data can easily be integrated (e.g. temporal and/or accuracy updates to the DEM). Both techniques require only surface characteristics and a set of scenarios to be tested (e.g. Figure 4.9); detailed knowledge of flow behaviour is not a prerequisite. Therefore, this researcher could be confident in the potential uses of the software if the model were transferred (Renschler, 2005).

Practically, LAHARZ and single-direction flow routing are easy to implement and can be used by hazard management personnel to quickly provide preliminary estimates of likely inundation areas. The single-direction flow routing approach was entirely automated in ArcGIS ModelBuilder. LAHARZ, written in Arc Macro Language, is already available from the USGS (Schilling, 1998). On Montserrat, MVO and the DMCA (in coordination with the Physical Planning Unit) have set up ArcGIS which will enable them to operate the programs discussed if required (subject to software licence agreements). However, it should be noted that these techniques are most valuable for preliminary assessments and for use as portable 'lahar hazard tools'. This is especially relevant for transfer to other volcanic systems where more detailed data may be available to inform more complex models.

4.8 CONCLUSIONS

Single-direction flow routing results generally replicated observed dominant flow routes and channel braiding in the lower-reach. However, these inundation probability maps had limited value for hazard zonation as only the centroid of the lahar mass was simulated, thereby not permitting dispersion. In contrast, LAHARZ mapped total planimetric inundation area using a sequential range of input volumes to create hazard zones. In a confined channel (upper- and mid-reach) LAHARZ was able to map inundation of the entire valley floor, as observed in the field; yet in the lower reaches the valley widened, resulting in jagged hazard zone predictions. Consequently, while LAHARZ may not be successful for predicting the main routes of an individual flow event (over the current topographic surface), it can indicate the areas likely to be affected by cumulative flows over a long time. Results suggest that despite its original calibration for sediment-rich debris flows, LAHARZ can also be applied to dilute lahars on Montserrat.

Ultimately, these inundation simulations provide improved knowledge of the likelihood of inundation, thereby also decreasing uncertainty in long-term hazard zonation. These two GIS approaches are complementary for hazard management of the Belham Valley, Montserrat. To get the 'full picture' for short- to long-term lahar inundation forecasting they should be viewed synchronously. Both methods are implemented in a GIS and therefore outputs can be manipulated to user-demands, models have potential to be refined and data can be updated.

The following chapter considers whether modifications can be made to improve model performance for flow predictions in the lower-reach.

CHAPTER 5: DEVELOPING A SIMPLIFIED GIS APPROACH TO DILUTE LAHAR MODELLING

Single-direction flow routing over an elevation-only cost surface predicted lahar paths largely consistent with field observations of recent lahars in the Belham River Valley, Montserrat (Chapter 4). The semi-empirical lahar model, LAHARZ, also predicted viable inundation areas from a variety of lahar volumes, useful to inform long-term local hazard management. Viewed together the results from each model were more meaningful for hazard assessment. However, both of these established GIS techniques were unable to adequately replicate observations in the unconfined lower-reach of the Belham Valley. An approach is proposed here that couples a form of single-direction flow routing with LAHARZ. The modified single-direction flow routing technique includes consideration of surface roughness and conservation of momentum using Manning's formula for normal stream-flow. LAHARZ was used as a mass conserver to examine the spread of lahar volume.

Application to Montserrat yielded support for this approach as an innovative dilute lahar hazard assessment tool. Observed dominant flow paths were reproduced and improved results were found in the lower valley. For the first time in this study area, velocities (magnitudes and spatial distribution) and average travel times were estimated for large volume lahars. Flow depth approximations were also made using (modified) LAHARZ and these helped refine inputs for the flow routing model. Flow depths were verified by order of magnitude to field observations and velocity predictions were supported by proxy measurements and published data. Forecasts from this coupled method operated on short to mid-term timescales; an update of the surface representation would be required for a new forecast.

5.1 INTRODUCTION

Currently, no one model can explain all observed features for a particular lahar (Fagents and Baloga, 2006). Lahars are highly complex mixtures of volcanic debris and water, demonstrating a wide range of sediment concentrations. They can be classified as debris flows (greater than about 60% sediment by volume) and hyperconcentrated flows (greater than about 30% sediment by volume), with water-rich hyperconcentrated flows having a volumetric sediment concentration as low as 20% (Vallance, 2000). Sediment concentration can also increase progressively downstream due to the highly erosive nature of the flow, which can transform flood flows and hyperconcentrated flows to more sediment rich phases (Vallance, 2000).

The dynamics of both stream-flow and hyperconcentrated-flow are controlled by the liquid phase and so can be successfully described using standard stream-flow approaches (Macedonio and Pareschi, 1992). Flow velocities, flow depths and discharges are controlled by channel characteristics such as cross-section shape, slope, sinuosity and roughness. In contrast, the dynamics of debris flows are controlled by the sediment phase, so their behaviour additionally depend on solid-fluid variables such as density, viscosity and yield strength (Pierson, 1995). However, there are similarities between debris flows and normal stream-flow. Similar behaviours have been observed for turbulent water and turbulent debris flows as the ratio of flow depth to particle size increases (Caruso and Pareschi, 1993). Further, the mean velocity of debris flows and clear water flows has been adequately described to a first approximation using the same mathematical formulation for steady stream-flow (Rickenmann, 1999).

Numerical modelling of lahars is advantageous as it allows the derivation of parameters such as flow velocity, flow width, depth and discharge (Aguilera *et al.*, 2004). Previous mathematical modelling of lahars has employed both steady and unsteady descriptions of the equations of motion, and empirical approximations of these. In addition, more recent work has incorporated digital spatial information. Early approaches focused on describing one-dimensional steady flow using equations for mass and momentum conservation, with an empirical law for resisting

forces such as the Chezy or Manning formulae (Macedonio and Pareschi, 1992; Caruso and Pareschi, 1993). Other approaches have attempted to solve the full Saint-Venant equations (for mass and momentum conservation) to model unsteady, non-uniform flows (see Hungr, 2000). However, models become more computationally intensive with each step closer to the reality of flow physics, e.g. Delft3D (Carrivick *et al.*, 2009). Alternatively, statistical and empirically-based models have been used to capture the gross underlying physics using coefficients e.g. LAHARZ (Iverson *et al.*, 1998; Schilling, 1998).

Within this chapter the objective is to investigate an approach appropriate for rapid hazard assessment of dilute lahars (sediment-rich stream-flow and hyperconcentrated-flow; Chapter 2). Dilute lahars can be approximated as floods and, consistent with that, the use of Manning's equation as a simplified momentum equation is justified. For inundation predictions, a simplified statement of mass conservation is also needed, and the use of LAHARZ to provide this description will be explored. This synergistic approach will be developed in a geographical information system (GIS).

5.2 METHODS

5.2.1 Model Formulation

In this section, a simplified model for dilute lahar movement in a GIS environment is formulated. Generating and manipulating topographic data is straightforward in a GIS. The spatial distribution of elevation data is commonly represented by a regular grid or matrix, known as a digital elevation model (DEM). The use of a DEM for flow modelling permits two-dimensional calculations and can rapidly generate inundation maps.

The model consists of an empirical standard channel flow equation (Manning's equation) as an equation of motion, and the semi-empirical lahar inundation model LAHARZ (Schilling, 1998) is used as a highly simplified expression of conservation of

mass. The implementation of these formulations in a GIS framework is described, and a consideration of error propagation is provided.

5.2.1.1 Equation of Motion - Manning's Equation

Manning's empirical formula for the mean velocity of turbulent flows in rough open channels is widely used by hydrologists for normal stream-flow, but it has also been successfully applied to hyperconcentrated flows and potentially may be extended to approximate debris-flow behaviour. The Manning formula is typically written in the form,

$$u = \frac{1}{n} S^{1/2} R^{2/3}, \quad \text{[Equation 5.1]}$$

where u is the cross-sectionally averaged velocity, n is the Manning coefficient, whose numerical value describes the channel roughness, S is the energy slope (inclination of the channel base, Figure 5.1a), and R is the hydraulic radius of the channel (the ratio of the channel cross-sectional area to wetted perimeter, Figure 5.1b). The form of the Manning formula is dimensionally inconsistent. To balance the dimensions of Equation 5.1, the $1/n$ term must have units of $\text{m}^{1/3}\text{s}^{-1}$, but the convention is to leave n dimensionless and attach the remaining units to an implicit coefficient, with a value $1 \text{ m}^{1/3}\text{s}^{-1}$ (Smith *et al.*, 2007). Although the formula was originally derived as an empirical description of flow observations, more recent work identifies a theoretical basis in terms of turbulent dissipation at a rough boundary (Gioia and Bombardelli, 2002).

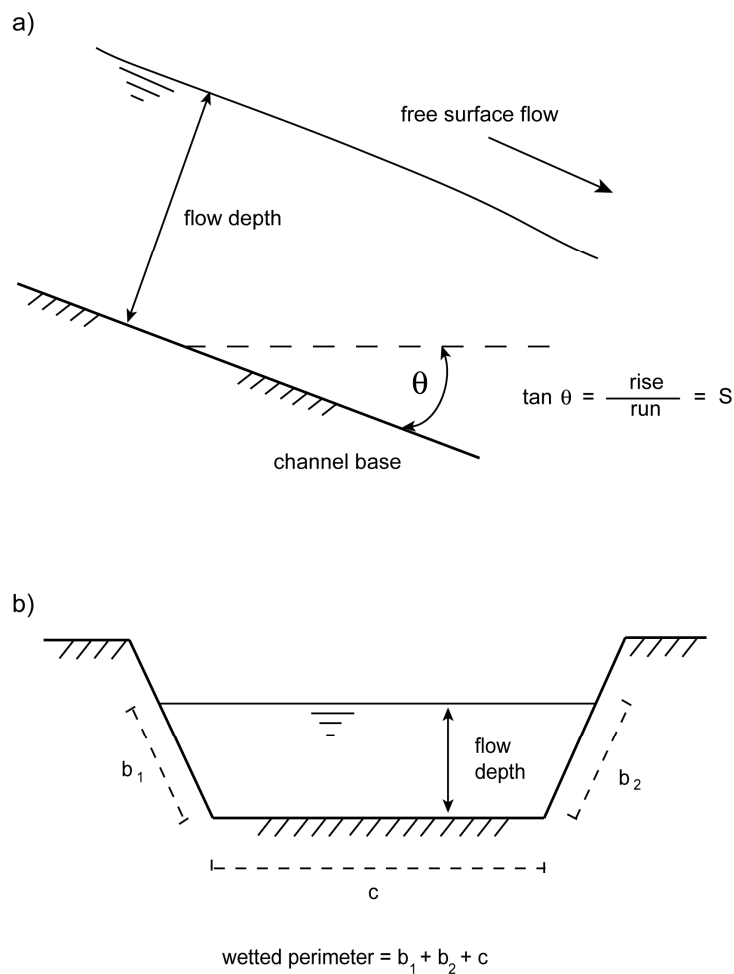


Figure 5.1 a) definition sketch for two-dimensional free surface flow; b) an example channel cross-section showing wetted perimeter (both after Brutsaert, 2005).

Acrement and Schneider (1990) have summarised Manning n values for an extensive variety of surfaces. These values correspond to natural low particle concentration streams and floods, performing best through a straight stream of fairly constant cross-section where mean velocity and bed roughness can be considered uniform (Gordon *et al.*, 2004). Recently, and as an alternative to defining uniform sections (reaches) of the channel with only one roughness value, a cell-by-cell specification of Manning's n has been adopted for use in a GIS (e.g. Liu *et al.*, 2003; Candela *et al.*, 2005; Wang *et al.*, 2008; Wu *et al.*, 2007). Every channel will

have different sensitivities to surface friction, therefore the important task becomes summarising the variation with available information. Effective values are functions of both model resolution and dimensionality (Horritt, 2005). For example, the correction for bends in the channel should not be necessary in many 2D models as they will be considered in the DEM. This approach allows sub-reach scale roughness variation to be considered.

For lahars, there is a complex relationship between sediment content and velocity which may be oversimplified by this formula. For example, debris flows are able to smooth their own bed by a combination of erosion and deposition, decreasing n values and increasing velocity (Pierson, 1995; Laenen and Hansen, 1988). Sediment loss will also decrease momentum. The net effect depends on whether the bed is rough or smooth and whether the flow is laminar or turbulent (Hessel, 2006). Notwithstanding the complexities introduced when considering lahars, the Manning formula has been shown to give acceptable results for modelling historic lahars with a range of flow properties (Caruso and Pareschi, 1993). Laenen and Hansen (1988) also found debris flows can be predicted with reasonable accuracy, if roughness is adequately portrayed.

Manning's roughness coefficient, n

For a gravitational flow down a channel, viscous and pressure drag over the wetted perimeter may be conceptually divided into three components: soil grain roughness, form roughness and vegetative roughness (Wu *et al.*, 1999). The value of n may be computed by a base value of n for a straight, uniform, smooth channel in natural materials, a correction factor for the effect of surface irregularities, a value for variations in shape and size of the channel cross section, a value for obstructions and a value for vegetation and flow conditions (Acrement and Schneider, 1990).

The use of Manning's formula has been criticised for requiring calibration of publicised values and the problem of equifinality with multiple roughnesses (e.g. Pappenberger *et al.*, 2005). Although standards exist, (Acrement and Schneider, 1990), some researchers have opted to adjust Manning's n values for specific channels (e.g. Cenderelli and Wohl, 2001); others have found channel geometry errors would be dominant over n -value errors and therefore have chosen not to

calibrate (Yochum *et al.*, 2008). The sensitivity of the Manning roughness coefficient has further been analysed by Hall *et al.* (2005) and Wu *et al.* (2007).

Whilst for clear water flows n is primarily a function of the basal friction, the flow-resistance parameters of debris flows might depend in addition on the mechanical properties of the mixture (Rickenmann, 1999). For a debris-flow the most important factors influencing flow resistance are the addition and removal of debris and presence of bends (Bulmer *et al.*, 2002). Laenen and Hansen (1988) were able to vary Manning's n to incorporate transitory behaviour of lahars from Mt St Helens, Washington (USA). The slowing effects of bridges and other natural barriers can be introduced by increasing the Manning coefficient (e.g. Macedonio and Pareschi, 1992).

Here, the spatial distribution of Manning's n was digitised in a GIS and converted to a regular grid with each cell assigned a roughness value. Therefore, roughness in a cell was the sum of sediment contribution and vegetation contribution (Brookes *et al.*, 2000). Spatial variations in suspended sediment concentration were not considered (i.e. normal stream-flow was assumed).

Slope, S

Slope of the energy grade line (metres per metre) is in practice assumed to be parallel to the water surface slope and the bed slope (Figure 5.1). Thus for the Manning formula, S , can be given by the gradient of the bed. Slope, the first derivative of an elevation surface, is defined by a plane tangent to the surface as modelled by a DEM at any given point. Although the mathematical definition of slope is quite clear, its implementation based on grid-based DEM may vary, since some assumptions must be made on how the continuous surface is approximated by discrete sample points (Zhou and Liu, 2004).

The derivative is calculated locally for each cell in the grid by computations made within a 3×3 neighbourhood. The SLOPE function of ArcGIS used here implements the third order finite difference method (Horn, 1981). This algorithm has performed well in mathematical tests (Skidmore, 1989; Jones, 1998). Furthermore, the influence of elevation error is much larger than the influence of algorithm error (Zhou and Liu, 2004).

Hydraulic radius, R

Geometry of the channel cross-section is characterised by a single parameter, R . This hydraulic radius is defined as the area of the cross-section of the channel divided by the length of the wetted perimeter. In the case of a wide channel, where the width is much larger than flow depth, the hydraulic radius can be approximated by the average flow depth (Caruso and Pareschi, 1993; Gioia and Bombardelli, 2002). Savat (1977) specified that a channel can be assumed infinitely wide if the bottom width is at least five times greater than the depth of the flow. However, while it may be reasonable to assume the hydraulic radius equal to flow depth in the lower reaches of a valley, flow depth will be greater in the confined upstream channel (owing to conservation of volume).

In order to determine the hydraulic radius, or the average flow depth, the distribution of the lahar volume over the channel topography has to be constrained. This was done in a GIS framework using the semi-empirical approach of Iverson *et al.* (1998) to provide a simplified mass conservation relation. Two fixed flow depths were also used for comparison purposes (1.5 m and 2 m; $R = 1.5$ or 2).

5.2.1.2 Conservation of mass: LAHARZ

LAHARZ (Schilling, 1998) uses proportionality rules that relate planimetric and cross-sectional areas to lahar volume (Iverson *et al.*, 1998). Semi-empirical equations predict the valley cross-sectional area, A (Equation 5.2) and planimetric area, B (Equation 5.3), inundated by lahars with various volumes (V). Further details are given in Chapter 4. A fundamental simplification of this program is the assumption that for a given event, lahar volume is assumed constant from source, through transport in the proximal hazard zone to deposition in the distal zone. Transitory behaviour is difficult to simulate and thus most predictive models assume lahars have the same character during transit (e.g. Canuti *et al.*, 2002; Pitman *et al.*, 2003; Aguilera *et al.*, 2004). This mass conservation principle was exploited here to ascertain lahar volume distribution and flow depths.

$$A = 0.05V^{2/3}$$

[Equation 5.2]

$$B = 200V^{2/3} \quad \text{[Equation 5.3]}$$

5.2.2 Implementation in a GIS

5.2.2.1 Generating a velocity-cost surface

Steady flow velocity from cell-to-cell was calculated over a regular grid using Manning's equation combined with regular grids of hydraulic radius, R , Manning's roughness coefficient, n , and surface slope, S (Figure 5.1). Using the PathDistance function in ArcGIS, flow movement was assigned to the direction of maximum downslope velocity flow. Following similar methodology to the established technique for an elevation-only cost surface (Chapter 4), flow was connected from an end point to a start point upstream using a flow direction (cost back-link) raster. End points, A and B, were consistent with observations used in earlier research in the Belham Valley (Chapter 4). The PathDistance function was used in order to ensure that upslope flow was impeded and that flow was prohibited up slope with angles $> 5.74^\circ$ (1 m rise over 10 m run); a linear function was used to define this. Huggel *et al.* (2003) also used this function in their modified single-flow direction (MSF) model for assessment of hazards from glacial lake outbursts. However, they permitted flow to divert from steepest flow direction up to 45° on both sides; thus although they used an elevation-only cost surface, they also considered dispersion. A smaller angle of diversion was considered here to permit only the representation of the dominant flow route. Preliminary testing demonstrated that without such an allowance flows could become 'stuck' in local sinks in the cost surface.

The flow path produced was time- and discharge-invariant (i.e. the velocity field was fixed per run of the model). Residence time (or time taken for flow to pass through a cell) was then calculated using a surface-distance grid (SurfaceLength function in ArcGIS) and velocity grid. For each simulated flow path, the residence time was calculated on a cell-by-cell basis and summed to give total travel time from start point to end point.

5.2.2.2 Quantification and propagation of error

The quality of the input DEM is paramount for flow routing (Chapter 3). DEM resolution is also important. Flow inundation areas have been underestimated due to the resolution of input topographic data (Davila *et al.*, 2007); finer DEM resolution is especially important for smaller flows (Hubbard *et al.*, 2007; Oramas Dorta *et al.*, 2007). These vulnerabilities, and their potential influence on model predictions, have been acknowledged from the outset.

Whilst the sensitivity of LAHARZ to elevation errors on shallow slopes and complex drainages has been acknowledged (e.g. Stevens *et al.*, 2002), only minor differences in inundation areas have been observed from direct comparison of different input DEMs (Hubbard *et al.*, 2007; Huggel *et al.*, 2008). Elevation error propagation to lahar simulations was not considered for LAHARZ for the above and following reasons: (a) the DEM was previously assessed for fitness for lahar simulation (Chapter 4); (b) thalweg position (and deviation due to error) has been previously considered (Chapter 4); (c) without knowledge of actual distribution of errors random perturbation could cause unrealistic inundation results (flow could stop due to relatively minor peaks in cross-section shape); and (d) the time taken to run the program, and current necessary manual user inputs, would render multiple iterations impractical without a significant rewrite of the LAHARZ source code.

Error in elevation was considered for simple flow routing, consistent with the established methodology in Chapter 4 (Section 4.5.2). As before, Monte Carlo sampling of elevation error was conducted after DEM construction (see Figure 5.2). The range of perturbation values was defined by the standard deviation of error (*stdv*); *stdv* values were either 0.1 m or 0.5 m.

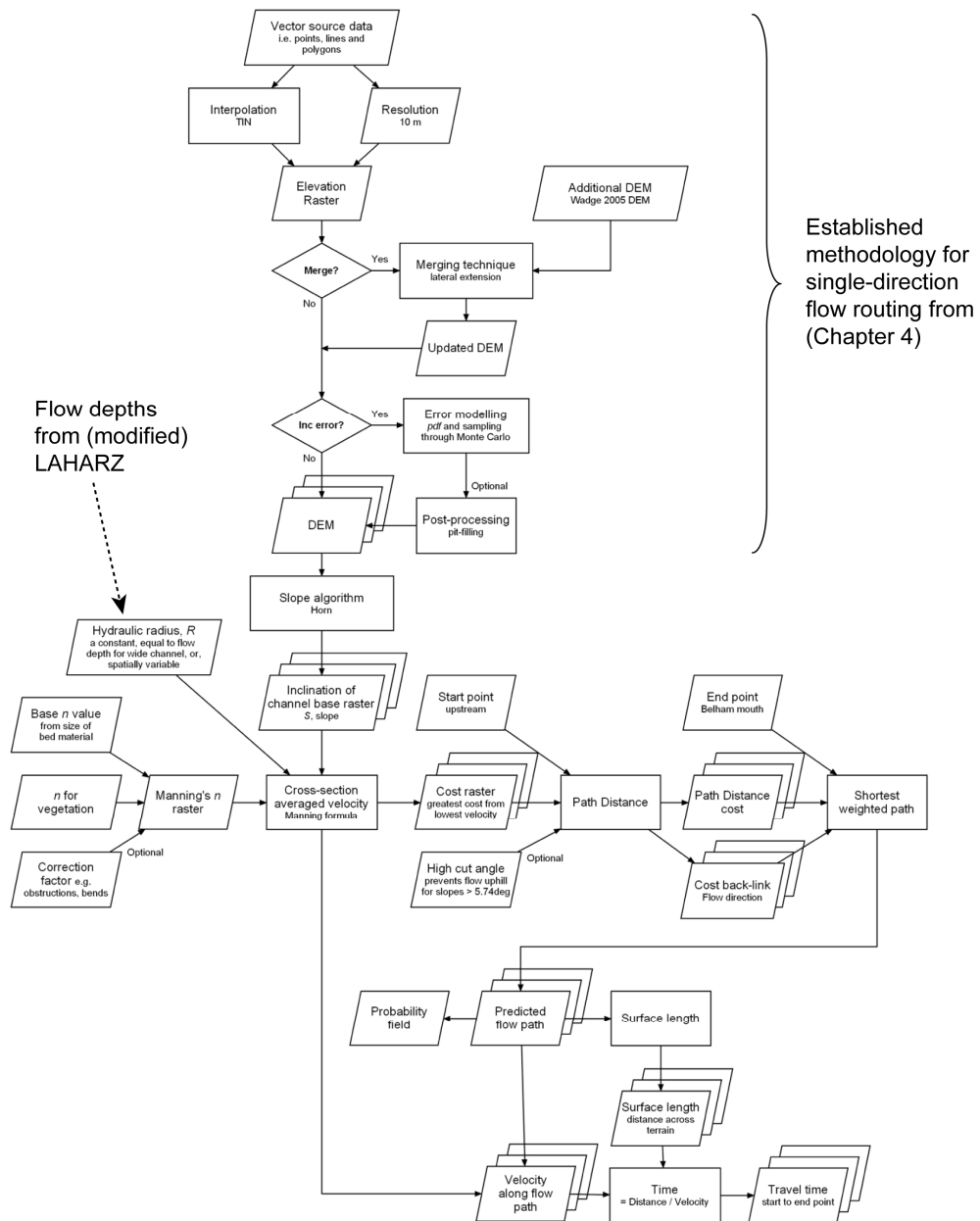


Figure 5.2 Methodological overview for deriving velocity cost surface(s) and likely flow paths

5.2.2.3 Movement of mass

In addition to the inundation area predictions from LAHARZ, the source code was modified to allow more information to be exported from the model and written to an output text file; this included coordinates for the stream cell being processed,

and an identification number, a cross-section identifier (as each stream cell simulated a minimum of three cross-sections) and fill levels at each processing step (Figure 5.3a). A maximum fill level was then calculated per cross-section, per stream and then converted to a peak flow depth. For a given input volume, the maximum flow depth on a cell-by-cell basis was then incorporated into a GIS.

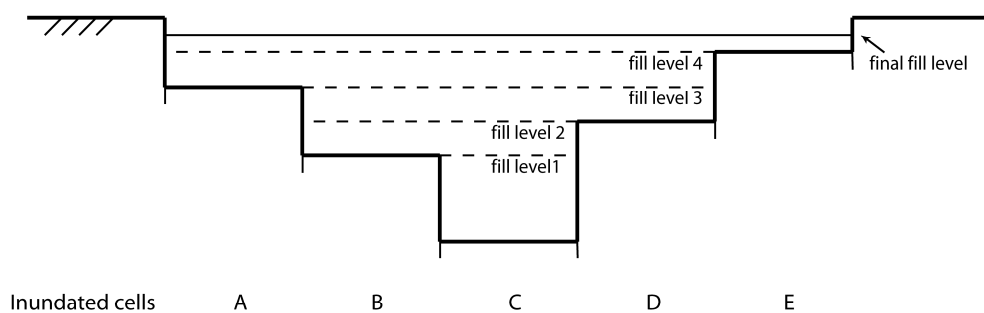
Due to micro-topographic changes (with their associated errors) and the 'stepped' nature of a DEM viewed in cross-section (Figure 5.3a), flow depths were not used directly to calculate the hydraulic radius as these produced overestimates of the wetted perimeter. Rather, the minimum (rectangular) wetted perimeter was estimated at each of the three (or more) processing cross-sections. Assuming a rectangular channel, the minimum wetted perimeter was established per cross-section; an approximate depth across the cross-section was given by dividing calculated cross-sectional area, A , by the number and resolution of cells inundated (Figure 5.3b). Therefore, the maximum hydraulic radius per cross-section was calculated. This was considered the 'worst-case' scenario as it would give the greatest velocities according to Equation 5.1.

In reality the schematic representation in Figure 5.3a was an over-exaggeration of the topographic difference between adjacent cells, thus depth approximation by averaging (Figure 5.3b) was a feasible approach. Furthermore, because (a minimum of) three cross sections were taken per stream cell, there were a large number of cells for which maximum depth was calculated multiple times (due to overlapping cross-sections), effectively 'evening out' any anomalous heights. For each cell coordinates and approximate depth(s) were extracted. These data were added as points into ArcGIS and converted to a raster (regular grid) using a nearest-neighbour approximation (the neighbourhood was less than the cell resolution to retain depths). A local (3×3) low pass filter was finally applied to smooth the maximum depth results.

Furthermore, to get these inundation depths it must be assumed that maximum flow height was not taken from the flow front; lahar depth is variable near the front (Vignaux and Weir, 1990). Predicted flow depths had their magnitude verified with stage indicators in the field (e.g. high-water markers on buildings and static trees) (e.g. Figure 5.4). These markers were not taken immediately after a lahar; therefore,

they represent a minimum estimate of the peak flow height for an unknown event (erosion and deposition could have occurred after the indicator was established yet prior to field observations).

a)



b)

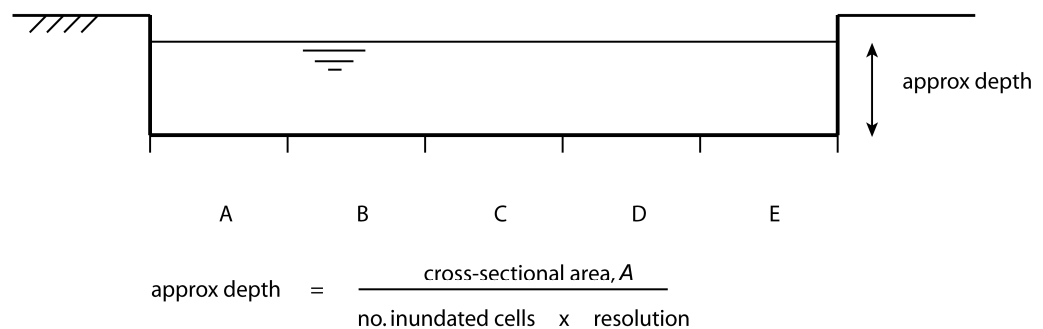


Figure 5.3 a) A channel cross-section showing intermediate fill-levels that can be extracted from LAHARZ, the final fill level can also be calculated and used to ascertain flow depths at each of the inundated cell locations (after Schilling, 1998); b) the minimum (rectangular) wetted perimeter can be established by calculating an approximate depth from the number of inundated cells (given by LAHARZ) and their resolution. The cross-sectional area, A , is the same for both diagrams and can be given by the semi-empirical equation in LAHARZ (Equation 5.2).

5.2.3 Application to dilute lahars on Montserrat, West Indies

5.2.3.1 Setting and model suitability

Soufrière Hills Volcano, Montserrat has been active for over 14 years, intermittently ejecting ash and other volcanic debris; these deposits accumulate on the flanks for the volcano and are frequently remobilised by rain into lahars (Barclay *et al.*, 2007). Among numerous drainages from the volcano (locally known as ‘ghauts’), the Belham River Valley, initiating from Tyers Ghaut, is the only major drainage that could channel lahars into inhabited areas (Chapter 2).

Lahars on Montserrat are characteristically dilute. Newtonian flow behaviour is dominant and lahars are principally hyperconcentrated-, concentrated- or ‘normal’ stream-flow (Barclay *et al.*, 2004). Despite typically low sediment content, flows can be competent enough to carry large boulders (up to 2 m diameter) and deposition *en masse* has also occurred (Susnik, 2009). Although rare, non-Newtonian flow behaviour has been observed and can be explained by greater sediment availability (Barclay *et al.*, 2007).

Initial testing of existing GIS-based models demonstrated the potential of single-phase, two-dimensional models for modelling dilute Montserratian lahars (Chapter 4). While a single-direction flow routing model over an elevation-only cost surface predicted flow results in broad agreement with observations, it was concluded that there were probably additional factors influencing flow directions (Chapter 4, Section 4.7.1). In the absence of internal lahar measurements (e.g. rheology), and assuming these dilute lahars are controlled by their water-phase, a suitable way forward was to investigate the controlling effect of other channel characteristics (e.g. channel roughness and shape).



Figure 5.4 Stage (flow height) indicators included damaged vegetation, stranded boulders and high-water marks. These photographs progress in sequence from the lower-reach (i and ii) to mid-reach (iii) to upper-reach (iv, v and vi); arrows represent flow directions. A measuring stick with 0.1 m divisions was used for scale.

5.2.3.2 Selection of roughness coefficients

For the study period, the valley floor in the lower reaches was considered gently sloping, with pockets of dense vegetation, associated with rapid changes in elevation (raised terraces). Channels carved out by the lahars, and the ephemeral river, were features of this landscape and there were also areas of high surface roughness where coarse clasts carried by the lahars had been deposited *en masse*. Terrain undulated on a local scale with micro-topographic changes including sediment banks (0.5 to 2 m for this section of the study area) and dense blocks of persistent vegetation on raised terraces (0.75 to 2.5 m). In the upper-reach, a single thread channel, greater than 2 m deep, was incised into older lahar deposits and the sandy-gravel valley floor was scattered with larger pebbles, cobbles and boulders (Susnik, 2009). Coarse clasts (up to 2 m) occur in discrete locations, described here as 'boulder-beds', were distributed throughout the valley, often splitting the dominant channel.

Montserrat has approximately 800 native plant species, three of which are endemic (Jones, 2008). Cactus and dry scrub woodland, littoral vegetation, semi-evergreen forest and small areas of mangrove are climax vegetation for low altitudes (Procter and Fleming, 1999). The principal vegetation in the Belham Valley consists of thorn woodland, moist broadleaf forest, bamboos and grassland in surrounding area (Gibbs, 1986). Aerial photography and field experience were used to estimate vegetation distribution and density. Vegetative resistance can be a complex parameter to incorporate as it varies with the flow depth or the degree of submergence (Wu *et al.*, 1999), is rarely rigid, and is dependent on the hydraulic forces, which subsequently feed back into the hydraulics at a series of different scales (Hardy, 2006).

Five classes were adequate to distinguish major changes in land-cover and surface roughness, with an additional category for areas permanently submerged by seawater. Examples are shown in Figure 5.5. Digitised boundaries for the land-cover types are shown in Figure 5.6 and associated *n*-values are given in Table 5.1. Acrement and Schneider (1990) and Chow (1959) provided the basic reference texts for selecting suitable roughness values. Other sources consulted include calibrations for glacial outburst floods (Alho *et al.*, 2007; Alho and Aaltonen, 2008), dam failures

(Yochum, 2003; Yochum *et al.*, 2008), river flooding (Bates and De Roo, 2000; Wang *et al.*, 2008) and floods from ephemeral streams (Brookes *et al.*, 2000).

Thus, a Manning's n raster was developed for the Belham Valley and the methodology outlined in Figure 5.2 was implemented.



Figure 5.5 Photographic examples of roughness, arrows represent flow direction. Geographical locations of the photos (A–F) can be seen in Figure 5.6.

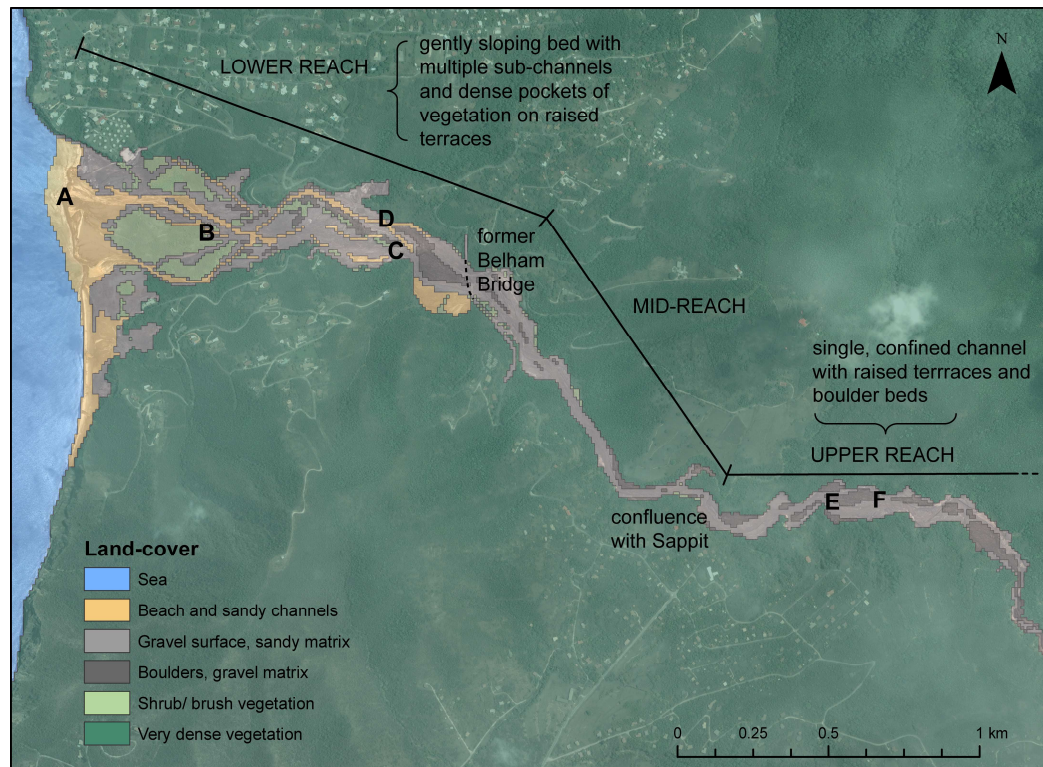


Figure 5.6 Digitised boundaries for six different land-cover classes (laid over aerial image taken 24 June 2006, DigitalGlobe Incorporated); letters A—F represent the approximate locations of the roughness indicators in Figure 5.5.

Land-cover	Roughness, n
Sea	0.01
Beach and (coarse) sandy channels	0.03
Gravel surface with sand matrix (medium sediment)	0.04
Boulders with gravel matrix (rough sediment)	0.06
Shrub/ brush vegetation over high roughness (rough sediment with 0.04 vegetation correction)	0.10
Very dense over-bank vegetation (rough sediment with 0.09 vegetation correction)	0.15

Table 5.1 Manning's coefficient values for different land-cover types

5.3 RESULTS

5.3.1 Dominant routes and flow depths

Visual inspection of predicted pathways revealed the dominant routes were very similar for different end points and *stdv* (Figure 5.7). Greater error perturbation induced greater flow path variability. For example, for end point A, 260% more cells were inundated at *stdv* 0.5 m. This corresponds to a 0.13 km² difference in area; however, this area reflects a lateral spread from the dominant route rather than a drastic change in flow direction(s). Similar observations can be made from examining end point B results; the difference in model outcomes induced by a change in end point was negligible.

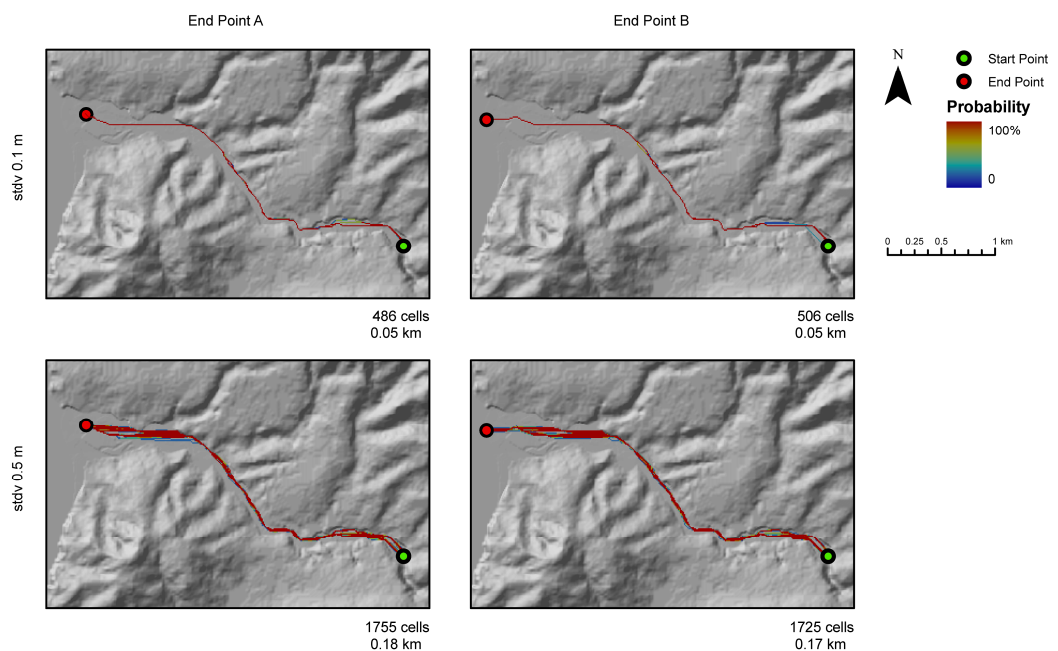


Figure 5.7 Inundation probability maps for velocity cost surface with spatially distributed *R* (using LAHARZ for flow depths). Inundated cell count and total area also shown.

Predicted flows tended to split in the upper-reach, near initiation, 'hug' the northern side of valley floor in the mid-reach and proceed centrally through the lower-reach (see Figure 5.6 for a description of the reaches, or sections, of the Belham). These results are supported by field observations (see evidence from sandy channels digitised in Figure 5.6).

Use of a fixed (1.5 or 2) or variable R did not have a discernable impact on inundated areas beyond that expected from any stochastic simulation. Therefore, coupling with LAHARZ for flow depths did not influence the delineation of major flow routes.

For LAHARZ, greater input volumes travelled further downstream (Chapter 4); therefore, it was necessary to define the lahar volume required to meet each end point. Initial testing (Chapter 4) specified the volumes needed to reach end points A and B were $1.25 \times 10^5 \text{ m}^3$ and $1.5 \times 10^5 \text{ m}^3$ respectively. These corresponded to 'large' individual events, occurring two or three times during the rainy season (Chapter 4, Section 4.4.4).

Given Equation 5.2, the inundated cross-sectional area was 125 m^2 for point A and 141 m^2 for point B; using this information, LAHARZ (modified) was able to estimate the maximum flow depth at every inundated cell (Section 5.2.2.3). Once converted into a regular grid and filtered, sample points were taken corresponding to the approximate locations of stage indicators in the field (Figure 5.4). The variation of maximum estimated flow depth with distance downstream is presented in Figure 5.8 and Table 5.2. These sample points suggest for a given lahar, the maximum calculated flow depth decreases downstream, broadly agreeing with field observations (stage indicators i—vi Figure 5.4). However, from these few sample points, and large variation shown by the range and standard deviation in Table 5.2, it is not possible to infer a direct relationship.

Flow depths at each of the sample locations were approximately the same for both input volumes; this was expected from their similar inundated cross-sectional areas. Furthermore, these results also serve to support the methodology for obtaining the depth estimates; if the averaging and filtering techniques had distorted the data the depths calculated from the separate model runs would probably show more of a disparity at sample locations.

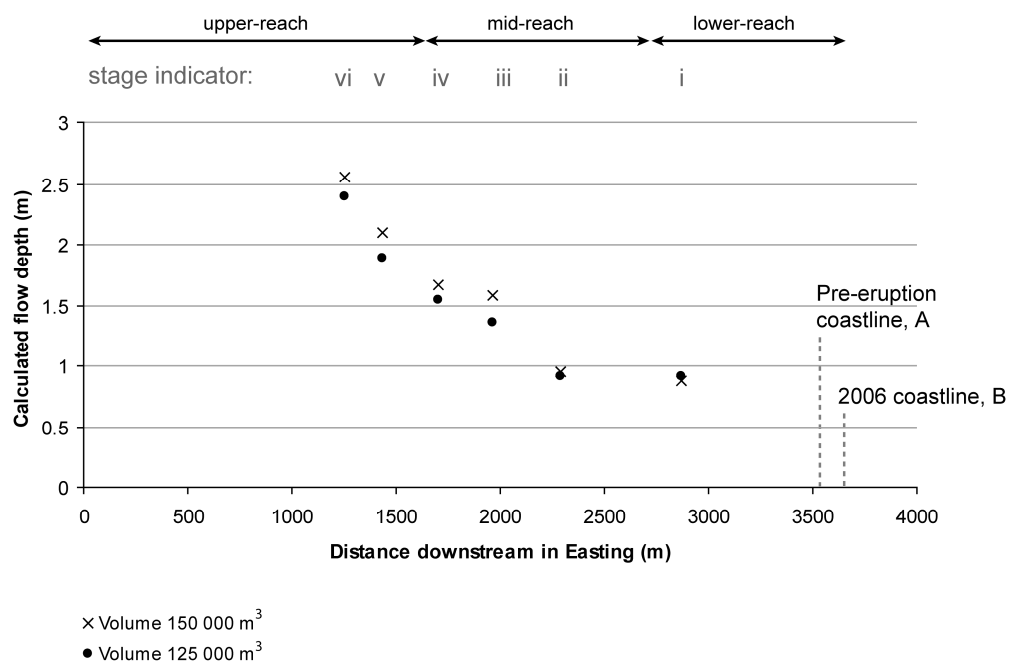


Figure 5.8 Calculated maximum flow depths from LAHARZ at stage indicator locations i—vi for two input volumes.

End point A	Range (m)	Mean, μ (m)	Standard deviation, σ (m)
125 000 m³			
Lower-reach	0—14.10	0.83	0.54
Mid-reach	0.01—3.00	1.42	0.53
Upper-reach	0.02—5.31	1.63	0.70
End point B			
150 000 m³			
Lower-reach	0—12.50	0.83	0.58
Mid-reach	0.01—2.83	1.31	0.49
Upper-reach	0—5.96	1.48	0.66

Table 5.2 Zonal statistics of the regular grid of maximum flow depths shows the variation of flow depths within each reach of the channel

5.3.2 Flow velocities and travel times

Figure 5.7 shows the cells encountered after 100 flow path simulations. The spatial distribution of fast and slow flowing areas can also be examined across these inundated cells. For one complete model run (100 iterations), averaged velocity per cell was calculated from the number of times a cell experienced some flow (inundated on one or more of the model iterations) and the sum of all (100) velocities experienced by that cell. For end point A, averaged velocity ranged from near zero to over 26 ms^{-1} , a similar range was recorded for end point B. Figure 5.9 suggests lahars have the greatest velocity, and by inference greatest energy, on leaving the boulder beds in the upper-reach and downstream surrounding the Sappit confluence. The lowest velocities occur downstream. However, while a simple statistical analysis indicates a general decrease in velocity downstream, there is also great variability of velocity in each of the channel reaches (as shown by the standard deviation of values) (Figure 5.9). Averaged velocity per cell was then examined across inundated cells to give the global summaries provided in Table 5.3. For the different scenarios, global mean velocities ranged from $6.5\text{--}9 \text{ ms}^{-1}$ across the total inundated area, with high variability (Table 5.3). Global mean velocities were lower when the spatially variable R was used.

Averaged velocities per individual flow path (Table 5.4) were greater and less variable than averages taken from global inundation maps. For the different scenarios, individual flow paths had a mean velocity along their length of $8\text{--}10 \text{ ms}^{-1}$, with standard deviation ranging from 0.03 ms^{-1} to 0.25 ms^{-1} . Again, the spatially variable R gave the most conservative values. Travel time was calculated from the start point to an end point for all simulated flow paths. Some summary statistics are provided in Table 5.4 and represent the averaged results from these individual flow path queries. Simulated travel times were generally greater when a spatially variable R was used, as may be anticipated from the global mean velocities (Table 5.3). A variable R gave the maximum travel time of approximately 600 seconds, or ten minutes; the minimum travel time, 450 seconds was given by a fixed R of 2 (for a wide channel, with a constant flow depth of 2 m). Thus, a variable R reduced the estimated travel time by approximately two and a half minutes.

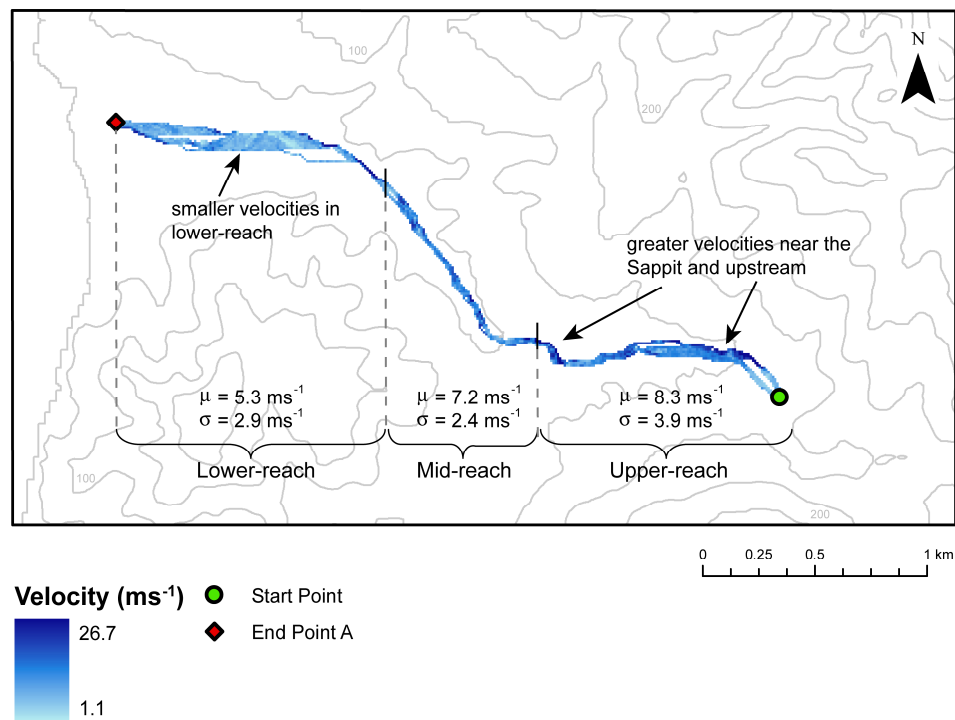


Figure 5.9 Example averaged velocity distribution over simulated probability field, for $stdv = 0.5$ m and spatially variable R (identifier: pb05h574vrf2); mean, μ , and standard deviation, σ , of velocity in each reach of the Belham are also shown.

Input parameters			Global probability map output statistics (velocity averaged for inundated count per cell)		
Model run identifier	$stdv$ (m)	R (fixed or variable)	Total inundated area (km ²)	Mean velocity (ms ⁻¹)	Standard deviation of velocity (ms ⁻¹)
Pb05h574vrf2	0.5	Variable	0.176	6.52	3.50
Pb01h574vrf	0.1	Variable	0.049	8.23	4.66
Pb05h574r15n	0.5	Fixed, 1.5	0.191	7.08	2.84
Pb01h574r15	0.1	Fixed, 1.5	0.042	7.71	4.06
Pb05h574r2	0.5	Fixed, 2	0.191	8.43	3.36
Pb01h574r2	0.1	Fixed, 2	0.048	8.98	4.82

Table 5.3 Probability map statistics for different input parameters, end point A

Input parameters			Output individual flow path statistics (averaged for 100 flow paths)			
Model run identifier	<i>stdv</i> (m)	<i>R</i> (fixed or variable)	Mean velocity (ms^{-1})	Standard deviation of velocity (ms^{-1})	Mean travel time (s)	Standard deviation of travel time (s)
Pb05h574vrf2	0.5	Variable	8.24	0.33	601	22.5
Pb01h574vrf	0.1	Variable	8.28	0.09	619	11.7
Pb05h574r15n	0.5	Fixed, 1.5	8.25	0.20	501	21.7
Pb01h574r15	0.1	Fixed, 1.5	8.01	0.03	584	24.0
Pb05h574r2	0.5	Fixed, 2	10.01	0.25	450	12.5
Pb01h574r2	0.1	Fixed, 2	9.72	0.04	491	7.3

Table 5.4 Individual flow path statistics for different input parameters, end point A

5.4 DISCUSSION

5.4.1 Potential utility of the approach

Previous work (Chapter 4) has achieved some success for mapping long-term lahar hazard. While an elevation-only cost surface was unable to adequately represent the lahar hazard in a section of the lower-reach (Chapter 4), the method presented here (velocity cost surface) has been able to replicate the dominant lahar route observed in the field. Therefore, additional terrain characteristics (e.g. channel shape and roughness) are likely to influence future lahars.

Change in lahar velocity downslope was examined. The spatial distribution of fast and slow flowing cells gave extra information on the response of lahars to variable terrain properties. These changes in velocity may also be indicative of areas of erosive and depositional behaviour, for example faster moving flows have greater energy and thus greater propensity to incise and entrain material. However, a

general decrease in velocity with distance travelled downstream was not predicted with any confidence; there were many local fluctuations in calculated velocities.

Travel time for flows to reach end point A in the lower Belham was approximately seven to 10 minutes and the minimum input volume required to reach this point downstream was $1.25 \times 10^5 \text{ m}^3$. Inundated cross-sections predicted by LAHARZ enabled calculations of (maximum) velocity for varying cross-section geometry downstream. However, using a fixed value of 2 for R (equivalent to a constant flow depth of 2 m for a wide channel) gave the quickest travel times; this approach may be more useful to hazard managers as it is more cautious and requires fewer assumptions (i.e. it didn't use LAHARZ and associated assumptions to calculate a variable R). End point B showed similar results for a slightly greater volume ($1.5 \times 10^5 \text{ m}^3$).

It has been stated that the simplicity of the principles behind LAHARZ renders the model unable to trace the evolution of other key parameters of interest in mitigating lahar hazards, e.g. flow thickness, discharge, velocity and transit time to points downstream (Fagents and Baloga, 2006). While for most parameters this was certainly true (to any accuracy), it was possible here to get estimates for the maximum flow depth by modifying the default LAHARZ output. Actual flow depths have not been documented for a lahar event on Montserrat, but stage indicators have been recorded in the field. This enabled flow depths from LAHARZ to be verified by order of magnitude for several discrete locations (due to erosion and deposition between successive flow events exact figures cannot be known).

Debris-flow depth and velocity are typically used in conjunction with probability estimates to convey intensity for hazard assessment (Hurlimann *et al.*, 2008). Although both flow depth and velocity here showed an apparent decrease downstream, velocity was very locally variable. Therefore, quantifying lahar hazard in relation to intensity and probability was not justified.

Nevertheless, this is the first time this kind of analysis (velocity and travel times) has been applied to this study area; thus, for the first time, the gross behaviour of a lahar has been captured and estimates of likely travel times and velocities can be given to agencies making decisions on movements in and around the valley. The probability-of-flow maps can be useful in their current form to show the dominant

lahar routes. These can be used in combination with velocities, travel times and flow depths to inform short- to mid-term management decisions, thereby demonstrating the utility of relatively simple GIS-based models for *preliminary* hazard assessment.

Moreover, although similar parameters have been estimated for lahars on other systems, it has typically been done in a more complex and data intensive manner. A cost-surface implementation of Manning's formula coupled with LAHARZ, is a novel approach that can have potential benefits for application to dilute lahars on other volcanic systems, particularly where a rapid approach is needed and data are restricted.

5.4.2 Verification and uncertainties

Elevation error in the DEM has been shown to propagate to global average velocities (Table 5.3). However, through an informal and qualitative local sensitivity analysis (one-variable-at-a-time testing), hydraulic radius had the greatest impact on velocities and travel times. Nevertheless, the approach to discern the spatial distribution of probable flow routes (through a velocity cost surface) has been shown to be relatively robust to elevation error (Figure 5.7). Therefore, a high level of confidence can be placed in the methodology for determining the dominant flow routes and these have been verified by field observations.

Absolute values for the hydraulic radius, and channel roughness could not be verified by (current) field data and thus had high associated uncertainties. In order to verify the velocity predictions only proxies can currently be used. Calculated velocities in the lower-reach were supported by proxy measurements of $1\text{--}2.5\text{ ms}^{-1}$ taken from standing waves (Barclay *et al.*, 2007). Mean flow path velocities were more generally verified with lahars generated by intense rainfall $2\text{--}8\text{ ms}^{-1}$ (Pierson, 1995). Further, the full range of predicted velocities fit within the bounds given by Rickenmann (1999) from direct and indirect measurements from a range of small- and large-scale debris flows ($0.8\text{--}28\text{ ms}^{-1}$).

MVO were shown the predicted travel times (Table 5.4) and the 'spatial distribution of velocity' map (Figure 5.9) and both sets of results agreed with their

informal field observations (personal comm., November visit, 2009; see Chapter 6). With current activity at Soufrière Hills (Alert Level 3, April 2010) it is possible that scientific measurements will be made for an individual flow event in the near future. Current research could also be advanced by testing the approach with another field area possessing lahar of similar characteristics. Velocities for other volcanic systems may be obtained from published data; however, this work has shown an accurate DEM and good knowledge of surface roughness are also fundamental. Chapter 7 will discuss suitable test areas and extensions to this study.

5.5 CONCLUSIONS

A GIS-based single-direction flow routing approach has previously been adopted for debris flows (e.g. Huggel *et al.*, 2003), but the use of cost-surfaces with application of Manning's equation to dilute lahars is entirely novel. Likely mean velocities and travel times for large flows were calculated using least-cost flow paths over a velocity cost surface. Whilst average magnitudes were not greatly affected by elevation error, they were sensitive to changes in the hydraulic radius (a parameter summarising channel geometry). Due to channel confinement in the upper-reach of the Belham Valley and the semi-confined nature in the mid- and lower-reach, the hydraulic radius varied greatly with distance downstream. LAHARZ was used to calculate likely maximum flow depths and inundated cross-sectional areas, thereby providing feedback to improve the performance of the velocity cost surface method. This decreased the estimated minimum travel time for large flows by approximately two and a half minutes. Dominant flow routes were adequately predicted by the flow routing approach but LAHARZ was loosely coupled to refine velocity magnitudes. LAHARZ has not been used for this type of function before.

Absolute values for the hydraulic radius, and channel roughness, used for the velocity cost surface could not be verified by field data and thus had high associated uncertainties. Despite this admission, all estimated velocities, travel times, flow depths and volumes were of an order of magnitude consistent with field

observations/ proxies. Ultimately, confidence can be placed in the spatial variation of velocity, and in *relative* velocities and travel times.

It can be concluded, that with current data limitations, the best strategy for lahar hazard assessment on Montserrat is this synergistic Manning's and LAHARZ GIS-based approach. The simplicity of the methods gives this approach practical use as a rapid hazard tool and it has shown great potential to capture the gross behaviour of a lahar. However, due to the rapidly changing nature of the terrain, on which these models are reliant, results will only be applicable for short- to mid-term forecasts. Thus, it will be necessary to update the inputs regularly if such an approach is adopted by hazard managers.

In Chapter 6 the overarching concerns for hazard management will be discussed. Furthermore, alternative future scenarios for the Belham Valley consider how predictions developed within Chapter 5 are liable to change with surface (roughness and form) alteration.

CHAPTER 6: PRACTISING EFFECTIVE RESEARCH OF SECONDARY VOLCANIC HAZARDS DURING A PROLONGED ERUPTION: LAHARS ON MONTSERRAT, WEST INDIES

A novel methodology for predicting dominant lahar paths was developed using GIS-based techniques in Chapter 5; as part of this process, spatially variable velocity along these routes was also calculated and used to estimate travel times for large flows. This methodology was most useful for short- to mid-term lahar forecasts and ultimately for use as a rapid, preliminary hazard assessment tool. Earlier results, with an established GIS-based model, also achieved some success in delineating (cumulative) hazard zones that had utility for longer term planning (Chapter 4). In this current chapter, effective transfer of such research findings for hazard management is discussed, in retrospect of the approach to the entire project.

To maximise the potential for application of new knowledge, consultations were conducted with local scientists and decision-makers in the research design phase, and at project completion. This exceeds a traditional 'end-of-pipe' delivery of products of science, which has been highlighted as an ineffective communication method.

In the study area (Montserrat, West Indies), lahars are regularly generated by rainfall on ejecta from the (active) Soufrière Hills Volcano. However, primary volcanic hazards (e.g. pyroclastic flows) take precedence for management and lahars, as secondary hazards, are not formally monitored. Potential end-users of new research on lahars had differing requirements and it was not easy to match these against modelling options constrained by data acquisition and the difficulties of working on an active volcanic system. The research conducted in Chapters 4 and 5 was designed to provide a new dimension (lahars) to the existing hazard

management agenda, to inform short-, mid- and long-term forecasts for lahar routes, dispersion, velocities and travel times. The GIS-based models were not data intensive, but outputs were tailored to be consistent with end-user requirements. These new findings were evaluated by both the researcher and end-users.

One of the key obstacles to the effective uptake of lahar research is identified as a lack of opportunity for decision-makers and local scientists to monitor secondary volcanic hazards, especially during periods of increased activity. However, there is potential for the research to be filtered into the official warning process and planning activities.

6.1 INTRODUCTION

6.1.1 Volcanic hazard preparedness

A volcanic eruption is an uncontrollable natural phenomenon that produces a plethora of direct and indirect hazards (Chapter 2, Section 2.1.1). The various hazards operate over a variety of timescales and distances from the volcano, although historically, the majority of fatalities associated with volcanic eruptions have resulted from post-eruption famine and disease (Tanguy *et al.*, 1998). However, with current international relief and assistance such indirect consequences have been dramatically reduced (Tilling, 1989). In contrast, comparatively little improvement has been observed for the total number of deaths associated with primary volcanic hazards such as pyroclastic flows (Tilling, 1989). In the 20th Century, pyroclastic flows and surges accounted for the largest proportion of deaths, and lahars caused the majority of non-fatal injuries (Witham, 2005). Within the total 20th Century death toll of 91,724, two disasters dominate; at Mt Pelée (Martinique) pyroclastic flows (and, to a lesser extent, lahars) killed 29 000 in 1902, and at Nevado del Ruiz (Columbia) lahars killed approximately 23 000 in 1985 (Witham, 2005).

Nonetheless, volcanic hazards occur infrequently relative to the human life-span (Tilling, 1989). It is unfeasible to abandon or prevent all settlement in the areas where volcanic hazards exist; local populations must learn to live with them as safely as possible (UNDRO, 1985). Crucially, a volcanic eruption does not occur spontaneously; it is the final manifestation of a process within the earth's crust and thus precursors typically can be observed (UNDRO, 1985). These signs of instability or unrest, including an eruptive phase should it develop, are collectively termed a volcanic crisis and require continuous scientific monitoring (IAVCEI Subcommittee for Crisis Protocols, 2000).

The primary challenge to both the scientific community and the decision-makers is to prevent volcanic crises from turning into disasters (Tilling, 1989). Volcanic disasters can occur due to rapid changes in the nature of the event without warning

(e.g. lateral blast at Mount St Helens, 1980, see Fisher, 1990); due to inadequate management (e.g. communication failure at Nevado del Ruiz, 1985, see Voight, 1990); and can even be socio-economic when a predicted event fails to materialise (e.g. Guadeloupe, 1976, see Fiske, 1984).

For volcanic crises, protocol stipulates that warnings of serious events that are known to be possible are issued before such events are forecast as probable (IAVCEI Subcommittee for Crisis Protocols, 1999). Forecasts function on different timescales: long-term, mid-term and short-term (Newhall and Hoblitt, 2002); and consequently require different preparedness and mitigation strategies. Short-term forecasts typically operate on the timescale of minutes to hours, and can be termed predictions when based on interpretations and measurements of ongoing processes (Tilling, 1989). Long-term forecasts can inform planning decisions many years prior to an event.

Academic research performs an important role in increasing knowledge of volcanic processes but, in terms of practical hazard management, any improvements in understanding are rarely well-translated to local interested parties. Generally detection of the hazard and assessment of the risk it presents are well considered, yet onward communication of hazard and risk information to those responsible for crisis management is typically inadequate (McGuire *et al.*, 2009).

6.1.2 Communication issues and an emerging knowledge transfer gap

Independent of timescales, a warning process for geological hazards will operate on three levels, involving different interested parties: technical (scientists), organisational (administrators) and social (public); and the linkages between the three components tend to be fragile (Alexander, 2007). Effective communication between and amongst these parties is essential to disaster management in a volcanic crisis.

6.1.2.1 Communication between scientists

Often there will be a number of scientists working in a volcanic crisis: permanent staff monitor activity changes, temporary scientists provide additional assistance, and 'independent' scientists conduct academic research. These scientists may come from disparate disciplines with different nomenclature, perspectives and understandings; they may also be working independently on smaller aspects of the problem. For these scientists working on volcanic systems, the greatest obstacle is often data availability and uncertainty in data, models and results; the former is in turn controlled by logistical issues, such as access and funding. External scientists can be an asset as they can be independently financed and arguably have disposable time to test and develop ideas. However, if external scientists are too isolated from the local team this can lead to divergence of research including pre-emptive publication by visitors while the host scientists are preoccupied with the crisis (IAVCEI Subcommittee for Crisis Protocols, 1999). Furthermore, the volume of academic volcanic research, mainly generated by these external scientists, is escalating, building a repository of existing knowledge in the sciences. However, there is a concern that such findings are not being effectively applied to inform crisis situations (e.g. Gomez-Fernandez, 2000; Alexander, 2007), perhaps due to a lack of involvement with local scientists.

6.1.2.2 Communication between administrators and scientists

Scientists and decision-makers have different roles and responsibilities in a volcanic crisis and these should be respected. Whilst scientists can provide predictions, models and maps; response and mitigation options ought to be determined by local decision-makers. The latter are local authorities responsible for public safety and hazard management, government bodies and stakeholders all with their own goals and agenda (Barclay *et al.*, 2008). For these responsible agencies there are two main options for reducing hazards: (i) modify the natural system and/or (ii) modify human behaviour. Decision-makers are in the unique position to weigh-up the socio-economic advantages and disadvantages of mitigation options; for example, there may be pressures between continual improvement in mitigation, including refining preparedness and response plans, and moving on to other priorities (e.g. Keys,

2007). In the face of scientific uncertainty and socio-economic political pressure, decision-makers may not follow scientific advice (IAVCEI Subcommittee for Crisis Protocols, 1999). Debate and uncertainty is inherent in scientific research, and to some extent can be tolerated by decision-makers. However, in relatively new relationships, uncertainty in forecasts may be misinterpreted as scientific incompetence (e.g. Haynes *et al.*, 2008b). Furthermore, new relationships are often formed under times of great stress with the onset of a volcanic crisis. Thus, a single scientific voice providing information is needed to avoid confusion (IAVCEI Subcommittee for Crisis Protocols, 1999).

6.1.2.3 Communication methods

With all these interested parties, communication and information transfer can breakdown as a consequence of the lack of a 'common language' (e.g. Wisner *et al.*, 2004) or the 'informing-only remit' of traditional science (Solana, 2001; Barclay *et al.*, 2008). Ultimately, mutual interaction between interested parties can only be improved through better understanding and appreciation of respective agenda, expectations and limits (IAVCEI Subcommittee for Crisis Protocols, 1999; Solana, 2001). For enduring crises, sustainable disaster preparedness necessitates continual input from the earth science community of a kind sensitive to the needs, objectives and cultures of the other participants in the process (Alexander, 2007).

The traditional top-down strategy for disaster management can limit technology transfer by neglecting user requirements (Zerger and Smith, 2003; Chapter 2, Section 2.2.1). In the natural hazard sciences, more researchers are now explicitly calling for the involvement of stakeholders in user-oriented research (Merz *et al.*, 2006), framing research based on user-receptivity (McIntosh *et al.*, 2007) and finding common objectives for management and models (Wilcock *et al.*, 2003). To maximise uptake and effectiveness of research, any deliverables must be translated into pre-existing knowledge and working practices (McIntosh *et al.*, 2007) and ultimately integrated into regional management and development plans (Thierry *et al.*, 2008).

While the issues raised above are not novel revelations, for the visiting scientist in particular, conducting independent academic research with transitory funding, it can be harder to find a niche and transfer their research into applied science.

6.1.3 Mitigation of lahar hazards

During an eruption, loose material (the products of primary hazards such as pyroclastic flows and ashfall) accumulate on the slopes of a volcano. This material can be remobilised through sudden injection of water (Chapter 2, Section 2.1.2) and generate rapidly moving lahars (secondary volcanic hazards). Their high density combined with their fluidity means that they are capable of travelling large distances, destroying everything in their path; furthermore, after coming to rest, their deposits can be too deep, too soft or too hot to cross (UNDRO, 1985).

By definition, mitigation activities (natural system or human behaviour modifications) eliminate or reduce the probability of disaster occurrence, or reduce the effects of unavoidable hazards. Some volcanic hazards can be tempered by engineering measures or structures to lessen impact or extent (Tilling, 1989). For lahars, natural system modifications can include hillside treatments to reduce runoff and channel treatments to reduce the volume of available material (e.g. De Wolfe *et al.*, 2008). Structural engineering measures include sediment-retention dams, diversion dams and dikes and, where appropriate, draining of dangerous crater lakes/ dammed lakes (Vallance, 2005), but these are expensive to install and maintain. The volume and force of lahars has traditionally been beyond human ability to control (UNDRO, 1985).

Human behaviour modifications focus on potential damage and mitigate the hazard by reducing population exposure, e.g. land-use planning and, in times of crisis, evacuation (Huebl and Fiebiger, 2005). Ideally, to mitigate the effect of lahars, settlement should be avoided on previous deposits and, in the event of an eruption, all permanent homesteads in the valleys around the volcano should be evacuated; daytime access may be permitted but an effective warning system must be in place (UNDRO, 1985). Mitigation options are dependent on the timescale for forecasts and are often inextricably linked with preparedness efforts, especially with the issue of warnings. For example, in a reaction to long-term forecasts, human behaviour can be mitigated through a) education for self-warning and evacuation, and/ or b) instrument-based event-warning systems (e.g. an acoustic signal from a moving debris-flow) that enable short-term preparedness (Scott *et al.*, 2001).

These are ideal recommendations, but mitigation in practice has high demands not least of which is an appreciation of the contrasting responsibilities and needs of different organisations involved. New research using geospatial information and technology may be able to assist lahar hazard management. Geographical information systems (GISs) can provide tools throughout the hazard management cycle (Johnson, 2000; NRC, 2007), but the potential role in preparedness and mitigation is particularly great (Chapter 2, Section 2.4). For example, before a crisis, maps can aid land-use planning, depicting those areas previously inundated by lahars; during a crisis, maps can establish boundaries defining access restrictions and evacuation zones (Chapter 2, Section 2.2.2.1). GIS can also be tightly coupled with modelling to predict future inundation areas (Chapters 4 and 5) and investigate the plausibility of management scenarios. This chapter tests how well GIS-based lahar hazard research can be applied on an active system, building on earlier work in the Belham Valley (Montserrat) study area.

6.1.4 Aims

The broad aim of the wider research project was an assessment of the usefulness of GIS-based technologies for making ‘on the ground’ planning decisions on an active volcanic system prone to lahars. Given an actual crisis situation, with real data limitations, there is a challenge to develop methodologies that have a practical utility for hazard managers and local decision-makers. In this chapter the aim is to assess how well the cutting-edge research (Chapters 4 and 5) serves the needs of end-users; this aim is distilled into three main research questions:

- Having identified the key players in hazard management, what kinds of information (pertaining to lahars) are they interested in? And, are there similar or conflicting demands from these potential end-users?
- Given current lahar knowledge, and data restrictions, how can these requirements be approached?

- How can new research findings be effectively transferred to local scientists and decision-makers on an active volcanic system?

These research questions were informed by established guidelines for scientists in volcanic crises (IAVCEI Subcommittee for Crisis Protocols, 1999), and involved three methodological phases of the wider research project. Phase I consisted of an information gathering exercise, conducted through a reconnaissance mission to Montserrat and elicitation of the needs of end-users through a combination of meetings and semi-structured interviews with local scientists and decision-makers. Input data for modelling were also acquired and assessed in this initial phase. Phase II of the project predicted lahar routes and cumulative inundation areas (Chapters 4 and 5); extension was made here by considering a range of alternative scenarios, e.g. to consider valley perturbation as a response to successive lahars, and mitigation options. A range of hazard zone visualisations were generated. Finally, Phase III revisited end-users to evaluate the potential of the research as whole for effective application on Montserrat. This chapter reflects on all phases.

6.2 REGIONAL SETTING

6.2.1 The people and the place: Belham Valley, Montserrat

Soufrière Hills Volcano has been active on the island of Montserrat (West Indies) since 1995, requiring continuous hazard monitoring and management. Montserrat has effectively lost two-thirds of its land area to the volcano, with over 60% of the island permanently designated as unsafe for human habitation or activity. With a pre-eruption population of around 11 000, the country of Montserrat is now home to only 4 500 people (Chapter 2.5) who live in the north and along the north-west and west coast of the island (Figure 6.1).

Disaster status has been internationally declared twice following mandatory evacuations of parts of Montserrat in 1997 and 2007 (Glide number: VO-1997-

000050-MSR; VO-2007-000007-MSR – see <http://www.glidenumber.net>).

Approximately 20 fatalities have been attributed to the prolonged eruption, resulting from pyroclastic flows on 25th June 1997 and 3rd August 1997 (Loughlin *et al.*, 2002); the relatively small number is a reflection of generally good management practices (Voight, 1998; Wisner *et al.*, 2004). However, these deaths have been attributed, in part, to failures of communication in the early stages of the eruption (Clay *et al.*, 1999; Chapter 2.5). To date there have been no reported deaths from lahars.

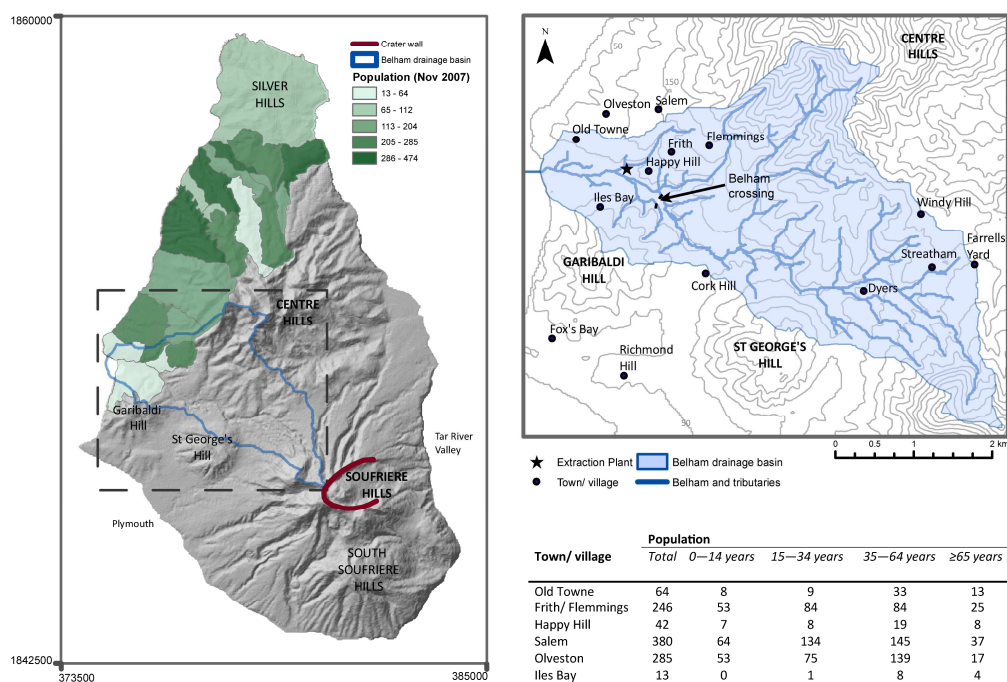


Figure 6.1 Permanent population on Montserrat by official enumeration district; all other areas are uninhabited. The Belham River drainage basin has been highlighted and towns and villages in close proximity to the catchment have been labelled; those retaining inhabitants have their demographic breakdown shown in tabular form. (Population information from the Physical Planning Unit; statistics correct as of November 2007).

Whilst local people are now located away from most primary hazards (e.g. ballistics, pyroclastic flows), and relatively sheltered from tephra fall, lahars are far-reaching secondary hazards. Lahars, more commonly referred to locally as 'mudflows', represent a persistent problem because they can occur without an associated escalation in volcanic activity. The Belham River Valley, draining from the Soufrière Hills towards the west coast of Montserrat is the only conduit for (predominantly rainfall-triggered) lahars into inhabited and public access areas (Figure 6.1). The Belham catchment covers an area of 12.5 km², is home to 300 permanent families (Haynes *et al.*, 2007) and is used for limited daytime activities (volcanic activity permitting).

The majority of low-lying properties flanking the ephemeral Belham River have already been destroyed by lahars. However, people continue to live in Iles Bay, the most southerly inhabitable village, and access the rest of the island by crossing the Belham Valley floor. In daylight hours the valley is occupied for small-scale industrial extraction of sand and gravel. Permanent evacuation of the towns and villages surrounding the Belham Valley is not currently considered an option. Temporary evacuation notices are issued for Iles Bay at heightened levels of volcanic activity, and sometimes as far north as Nantes River if the probability of pyroclastic flows towards the north-west is substantial e.g. in January 2007 (De Angelis *et al.*, 2007).

The size of the island of Montserrat has had costs and benefits for hazard managers throughout the (ongoing) eruption. The small size precluded the duplication of facilities (Clay *et al.*, 1997) and constrained population development mainly to the gentler flanks of the volcano (Kokelaar, 2002; Haynes *et al.*, 2007). The close proximity to volcanic hazards has meant that scientists can interact directly with the public and preparedness can spread by word of mouth (Davis *et al.*, 1998). However, in times of lower volcanic activity public perceptions can be lowered by what is (or is not) observable at the volcano (Haynes *et al.*, 2008b). It has been recognised that the communication issue (and relations between decision-makers and scientists) is particularly pertinent to volcanic crises on small islands (McGuire *et al.*, 2009). Montserrat is a good test case for trying to make scientific findings, of otherwise secondary importance, relevant and effective in times of (volcanic) crisis. The methodology may be applicable to other volcanic systems prone to lahars.

6.2.2 Existing hazard management

The initial volcanic crisis on Montserrat has officially passed, and the volcano has entered a prolonged eruption. However, the volcanic situation presents challenges for hazard managers, requiring a spectrum of management decisions, from short-term forecasts of individual events, to long-term planning decisions for multiple hazards. There also remains the possibility of activity escalation or unexpected individual events (e.g. major dome collapse, as observed in 2003 (Herd *et al.*, 2005)). Therefore, in terms of the hazard management cycle (Chapter 2, Figure 2.1), there are small-scale responses to individual hazard events, general recovery is largely unattainable (due to ongoing hazards), mitigation concentrates on refining hazard assessments, education and training, and forecasts operate for preparedness on all timescales. Currently lahars (as secondary hazards) are not formally managed.

Scientific monitoring of the Soufrière Hills Volcano is carried out by Montserrat Volcano Observatory (MVO); volcanologists conduct dome growth surveys, ground deformation surveys and perform seismic, gas and environmental monitoring. Scientists at MVO also have a recorded interest in scientific publication and research with external collaborators. However, responsibility for determining the Hazard Level and response falls to the National Disaster Preparedness and Response Advisory Committee (NDPRAC). The committee is comprised of a panel including the Governor, representatives of the Government of Montserrat, Disaster Management Coordination Agency (DMCA) and MVO. The DMCA implement decisions, act on scientific advice and have the primary responsibility for liaising and communicating with the public. As a British Overseas Territory, other interested parties include the Governor's Office, which is responsible for day-to-day safety and security, and Her Majesty's Government in London. At the ground level, the local police sound the siren and help mobilise the public. Further details can be found on the MVO website (<http://www.mvo.ms/>) and in Chapter 2 (Section 2.5).

The Hazard Level System (instigated in August 2008) divides the island into seven zones. These zones are defined on the basis of geographic markers; for example, Nantes River divides zone A from the 'safe' northern part of the island, the confluence of the Sappit tributary with the Belham River marks the boundary

between zones B and V, and zone T allows daytime workers for sand and gravel extraction (Figure 6.2a). All primary hazards within those zones are identified and, considering hazard probability, community and individual risk, access restrictions are made appropriate for that zone, for that time. A prescribed combination of access restrictions across these zones represents the Hazard Level. There are five tiers to the Hazard Level System, e.g. Level 1 requires more than one year with no measured activity and Level 5 is indicative of probable pyroclastic flows to the north/ north-west or threat of a lateral blast. The current Hazard Level is communicated through an island-wide map given four colours representative of different access permissions (e.g. Figure 6.2b). However, people only live in zones A, B, and C (see Figure 6.1) and the Level at zone A changes only in the most extreme circumstances (i.e. Level 5). The northern sector of the island is thought to be sheltered by the Centre Hills and therefore access is permanently unrestricted.

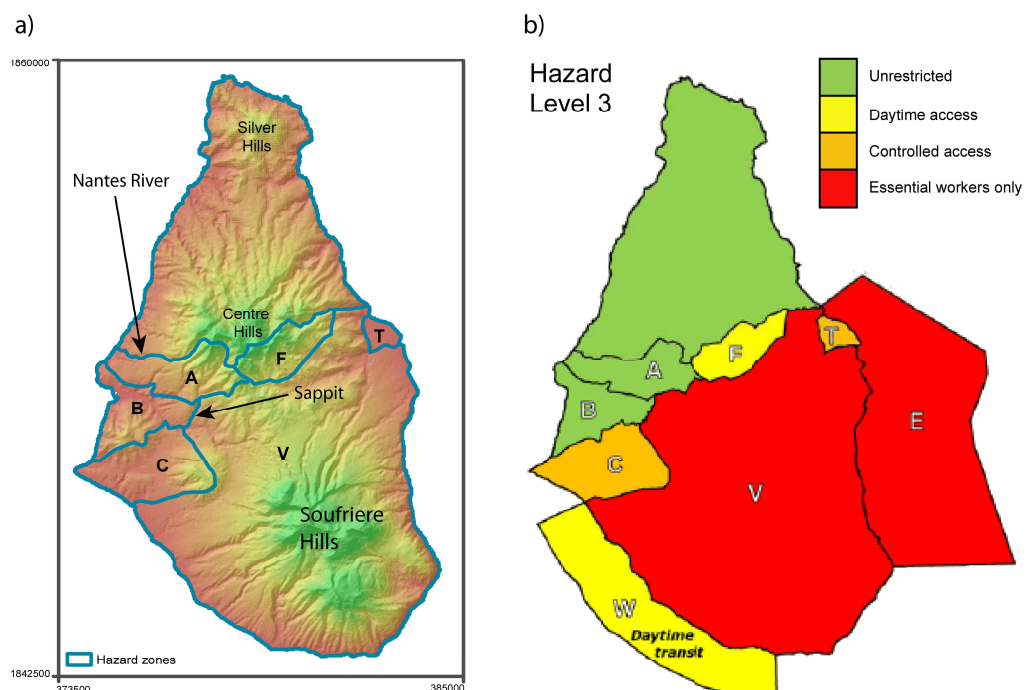


Figure 6.2 a) zones of the Hazard Level System with some defining features highlighted; b) current Hazard Level 3 (March 2010, courtesy of MVO).

When necessary, access is restricted to other hazard zones through a series of check-points (physical barriers, often policed) across roads. In addition, warning signs are permanently in place at the main Belham crossing point (former Belham Bridge) to alert people of the 'hidden' dangers of lahars (Chapter 2). Using these signs the general public are informed not to cross the valley floor during, or following, periods of heavy rainfall. Development of the Belham Valley area in the near-future has been restricted and there are no plans for government investment (DMCA, pers. comm.). Serious considerations for rebuilding the Belham Bridge or moving the Belham crossing are also currently unfeasible. Engineers have revealed load-bearing capacity varies considerably across the valley (Donnelly, 2007), a characteristic of lahar deposits (UNDRO, 1985). However, there are continuous pressures for use of the valley floor for private industrial extraction and also for limited daytime access and transit to Iles Bay (Figure 6.1). This frequent use of the valley (in periods of low volcanic activity) produces a dual management problem; in addition to dangers to the public and workers from lahars, modification to the physical character of the valley (topography, surface roughness and vegetation) may have a (currently unknown) influence on lahar flow routes and behaviour.

6.3 PHASE I: EVALUATION OF MANAGEMENT OPTIONS

6.3.1 Methodological overview of Phase I

A total of three trips were made to speak to officials on Montserrat; the first two were a year apart and were for the purpose of information gathering (both Phase I), the third was two years later (Phase III, November 2009) to ascertain opinions on the project outputs (produced through Phase II modelling and informed by Phase I consultations).

Phase I of the project was carried out on Montserrat in November 2006, against a management backdrop of a large lava dome and accelerating dome growth (Chapter 2, Section 2.5.3). Initial meetings (informal interviews) were held with senior

scientists at MVO and also with representatives from agencies that have to make decisions involving movements in and around the Belham Valley (decision-makers). All respondents were treated as foreign elites because of the positions of power they held. Considerations for interviewing foreign elites are discussed comprehensively in Herod (1999). Meetings were organised in advance of arrival using the researcher's university affiliation (University of East Anglia, UEA) to gain access. Due to the imbalance of status, the researcher was introduced by a mutual contact, a former director of MVO. These informal interviews established the role of the researcher as an external visiting scientist (consistent with established protocols (IAVCEI Subcommittee for Crisis Protocols, 1999)), and enabled official procedures to be ascertained (e.g. a research and data policy contract was signed with MVO). A key finding from these initial meetings was that the Belham Valley was an area of concern for management officials.

Semi-structured interviews were conducted during a second visit to Montserrat in November 2007 using open-ended questions, augmented with closed questions to clarify. The merits of using open-ended questions with elites are discussed by Aberbach and Rockman (2002). On this second trip the primary researcher was accompanied by a senior colleague (UEA) with experience of both research and interviewing on Montserrat. A dialogue with respondents was precipitated by both researchers. Furthermore, as a partial incentive to grant interview, the primary researcher presented findings from some exploratory work. Volcanic activity at this time was minimal as lava dome growth had ceased and the eruption was in a reposed state (Chapter 2, Section 2.5.3). However, the dome was large and a collapse was forecast in the mid-term (weeks—months).

Specific interview objectives were to complete a needs-assessment, discuss preferences for (optimal) communication of hazard information on Montserrat, and also consider the future management of the Belham Valley. As part of the dialogue, respondents were shown a variety of example visualisation products including (and combinations of) traditional plan-view maps, oblique-view maps of 3D renderings, 3D demonstrations and aerial photographs. Potentially relevant spatial data were also taken from respondents as it was recognised that elites often have greater access to resources and documents (Herod, 1999).

The detailed responses were recorded, with permission, and analysed according to timescales for management. Short- and mid-term issues mainly related to mitigation and warnings, and longer term concerns pertained to planning issues.

6.3.2 End-user requirements for short- and mid-term mitigation

Short-term mitigation strategies operate over minutes to hours, requiring near-immediate preparedness and response. At the time of interview the DMCA had a goal of implementing the 'Belham Valley Flood Warning Project'; a primary aim of this project was to acquire an automatic lahar warning system for the Belham, to produce warning of the order of minutes to hours before a hazardous event. Ideally, they wanted a real-time traffic light system, providing continuous information to the public on the safety of entering the Belham Valley. It was perceived that a project such as this would allow continued occupation of areas immediately south of the valley and potentially permit economic activity in this area. DMCA recognised that cooperation with scientists and researchers would be necessary to achieve this goal. The Governor's Office was also interested in the potential for designing a warning system to provide local alerts for lahars. A manual warning procedure was also discussed (by both sets of decision-makers) where warnings could be issued on the basis of a threshold rainfall; the correlation of lahars with rainfall is well-recognised by both local scientists and administrators.

Mid-term mitigation and preparedness is defined by changes and warnings that occur over weeks and months, and includes localised evacuations. DMCA's perceived need in this matter was to enhance communication and understanding of the hazards behind the evacuations and warnings. The use of aerial photographs augmented with model outputs showing lahar hazard-affected areas was seen as valuable to educate the public on the lahar hazard. Such a specific request followed positive feedback from a similar strategy adopted after the January 2007 disaster declaration; aerial photographs were used to position check-points for access restrictions and to educate the public on the heightened probability of pyroclastic flow hazard towards the north-west. DMCA stated that aerial photographs are

understood better by locals as they can identify houses and local landmarks, as found by Haynes *et al.* (2007). Furthermore, the Governor's Office strongly wanted to 'move away from the perception that the whole island is affected (by the Hazard Level)'. The northern part of the island to date has only ever been affected by tephra fall and elevated concentrations of volcanic gases (relatively non-severe), yet in the current system the Hazard Level applies to the whole island.

MVO did not express any specific needs for short- to mid-term mitigation of lahars. Mid-term warnings (evacuations) are governed by primary, not secondary, hazards and the possibility of being able to provide short-term warnings was currently scientifically unfeasible. However, MVO were interested in the behaviour (e.g. flow routes, velocities etc.) of individual lahars for improving scientific understanding.

6.3.3 End-user requirements for mid- and long-term planning

During the initial interviews, DMCA raised some specific mid- to long-term (weeks—years) management questions for the Belham Valley: can people continue to extract sand and gravel in the Belham? What effect does extraction have on flows? Can a new bridge be constructed (physically)? If so, is the original Belham crossing site the most suitable? To answer these questions required a forecast of how long lahars were going to be destructive for, how much cumulative deposit would be expected and what the main flow channels would be. These issues are also related to more oblique questions regarding volcanic activity and the supply of sediment. At the time of the interview, excavation was temporarily suspended (due to the potential for dome collapse in November 2007) but was due to resume when 'scientifically safe to do so'. The pressures on hazard management officials resulting from the suspension of economic activities such as this were strongly expressed throughout the interview.

For strategic planning purposes, DMCA specifically requested 'scientific' maps (clarified as lahar inundation areas drawn over plan-view topographic maps). After being shown examples of different visualisations, MVO were 'happy with regular

maps' (hazard information drawn over plan-view topographic maps) but stressed 'angled views' (showing topography) were better for the public and local officials. The Governor's Office felt aerial photographs were a useful presentation aid, but more traditional maps were better for looking at larger areas, for a longer-term view. However, whilst they were interested in seeing hazard maps, they would ultimately receive official feedback through the DMCA; thus, consultation with the Governor's Office ended at Phase I.

6.4 REFLECTION ON USER-REQUIREMENTS VS. ATTAINABLE OUTPUTS

OWING TO DATA RESTRICTIONS AND MODELLING OPTIONS

6.4.1 Evaluation of requirements

All agencies interviewed were interested in the research and provided their requirements as end-users; they also offered additional assistance in various forms (e.g. MVO gave permissions and equipment for fieldwork, DMCA provided political GIS data through the Government of Montserrat's Physical Planning Unit). End-users focused their requirements on different timescales for hazard management and these are summarised in Table 6.1; this is a subjective summary based on a reflection of the interviews.

	Short-term mitigation (minutes/ hours)	Mid-term planning (weeks/ months)	Long-term planning (years/ decades)
<i>MVO</i>		✓	✓
<i>DMCA</i>	✓	✓	
<i>Governor's Office</i>	✓		✓

Table 6.1 Potential users for lahar hazard information and their timescale(s) of interest

DMCA and the Governor's Office were primarily interested in short-term warning systems. At Ruapehu, six lahar warning systems have been successfully installed, each with active response plans, and some infrastructure isolated from, or hardened against, lahars (Keys, 2007). However, Ruapehu is a much larger volcanic complex with a greater distance between initiation and settlements. Furthermore, an alarm system automatically connected with a traffic light was suggested for vulnerability reduction in the Italian Dolomites; however, this device was ruled ineffective for mitigation as warning time would be insufficient for evacuation (Pasuto and Soldati, 2004). Lahar warning systems do not protect property and only work when there is sufficient distance and time between source areas and population centres (Vallance, 2005). On Montserrat the travel distance is roughly 3 km from lahar source areas to the (frequently used) lower-reach of the Belham Valley. Evacuation time would depend on the velocity of individual flows; however, Montserratian lahars are currently poorly understood. The surest way to avoid risk is through lahar hazard maps and strict land-use regulation (Vallance, 2005), although this was not recognised by decision-makers at the time of interview. Therefore, a functioning automatic lahar warning system was immediately identified by the researcher as unfeasible; this was also consistent with MVO's expert knowledge.

Across all end-users, the dominant request was for a form of hazard map specific to the Belham Valley. The existing strategy for island-wide hazard zonation did not consider lahars observed in the Belham Valley. Focusing a hazard map on a smaller area would be beneficial as it would (a) allow finer detail of hazard variation in affected areas and (b) enable the wider inhabited area to be considered unaffected by hazard. Likely lahar routes would be necessary for short-term management and general scientific understanding. Depositional patterns over years would be needed for mid- to long-term planning. Therefore, both individual lahar behaviour, and cumulative behaviour (say, over one rainy season) were required by end-users.

Velocities, travel times and particulars of lahar behaviour would be necessary to inform the feasibility of any short-term manually-operated warning system. Such characteristics would also be of general benefit to users of the valley, and improve general understanding of lahar hazards, consistent with desires from MVO.

6.4.2 Defining research objectives and researcher role

6.4.2.1 Fieldwork and data constraints

Raw elevation data were gathered in the field in November 2006, and again in November 2007. MVO equipment was used on the first visit (details are provided in Chapter 4) and UEA equipment was taken for the second visit. These data enabled production of (two) up-to-date surface(s) for modelling lahars, and as the return period covered the duration of one rainy season, cumulative valley response to lahars over that period could be measured. Detailed field observations were also made on terrain characteristics (e.g. surface roughness). Other data acquired were one-minute resolution rainfall data from UEA pre-installed rainfall gauges, aerial imagery purchased from an external remote sensing provider (DigitalGlobe), and GIS data (political boundaries, road networks etc) and census data were obtained from the Government of Montserrat's Physical Planning Unit (courtesy of the DMCA). Crucially, physical data on recent and historic individual lahars were absent, and no lahars coincided with the field seasons; this further reduced the possibility of implementing threshold- or measurement-based warning systems. However, triggering mechanisms have been explored (rainfall data) and qualitative descriptions of flow types and rheologies have been made (e.g. Barclay *et al.*, 2007).

Modelling options were dependent on observed flow types (i.e. non-Newtonian, hyperconcentrated flow) and restricted by available data; these factors were discussed in Chapter 4 (Section 4.3.1).

6.4.2.2 Research objectives and model outputs

A review of attainable end-user requirements is summarised in Table 6.2. Given the findings from initial interviews, it was decided the primary output would be a map synthesising the relative hazard specific to the Belham catchment to aid and orientate the authorities' hazard management decisions (output *iii*, Table 6.2). It was believed that hazard could be communicated effectively both to local public and decision-makers using the same types of methods (i.e. overlays with aerial photographs). Thus, to meet the expectations of end-users, the hazard map was designed with a dual focus: (1) for mid- to long-term land-use planning and (2) for

setting access restrictions for mid-term mitigation. Furthermore, the hazard map was specific to lahars, and thus did not conform to the existing holistic multi-hazard assessment strategy; it would act as a potential complement to the Hazard Level System.

	Short- to mid-term hazard outputs		Mid- to long-term hazard outputs	
	(i) Velocities, travel times and flow depths to inform regular users of the Belham Valley and for scientific study	(ii) Routing map for short-term planning and improving knowledge of lahars	(iii) Dual focus hazard map	(iv) Scenarios (possible futures and/ or to aid mitigation)
<i>Information required</i>	Individual lahar velocities (average), distance travelled and stage indicators	Individual flow runout routes and inundation areas over forthcoming weeks Local landmarks for orientation	Inundation areas from lahars over forthcoming weeks and months Morphological change over one or more rainy seasons	Scenarios only
<i>Data restrictions</i>	----- No internal (physical) properties of individual lahars known -----			
<i>Key relevant available data</i>	Limited point velocities only and proxies Channel characteristics (including topography and roughness) Stage indicators	Observed flow routes and area of previous deposits Aerial imagery	Elevation data a year apart (one rainy season) Incidence of recorded lahars Rainfall data	As listed for other outputs
<i>Way forward</i>	Simulate flows through GIS-based models	Reproduce observed routes using GIS-based models	Simulate cumulative inundation over one rainy season and predicted future inundation areas	Consider alternative 'what-if' scenarios using GIS-based models

Table 6.2 Attainable outputs relevant to end-user requirements

Outputs relevant to short-term lahar management included simulating individual flow routes (output *ii*), velocities and travel times (output *i*), for improving general knowledge on lahar behaviour and also informing users on the ground, for example with likely escape times etc. While mapping is often the priority for hazard management, other information is also invaluable in the short-term, i.e. velocity and flow depth are good indicators of event intensity (Hurlimann *et al.*, 2008; Fell *et al.*, 2008). Determination of a rainfall threshold required to trigger lahars was beyond the scope of the project (see discussion in Chapter 4).

Additionally, it was recognised that morphological change, due to continued excavation and channel response to lahars, should be considered as part of a comprehensive hazard assessment. DMCA raised concerns regarding the uncertainty of the effect of continued excavation in the Belham Valley. This was extended by considering a range of scenarios for potential future characteristics of the valley; some of these could be possible mitigation aids (output *iv*). With the GIS approach taken, this is something that was recognised as possible, without explicit requests from consultations with end-users.

A GIS approach to lahar hazard assessment was taken because lahars are inherently spatial phenomena reliant on terrain (Chapter 3), their movement can be simplified and modelled in a GIS (Chapters 4 and 5), data can be easily updated and output manipulated to end-user demands (see Chapter 4, Section 4.7.3). Recently there has been increased recognition of the potential of GIS on small islands in the Caribbean. Montserrat is now starting to rely on ESRI's ArcGIS for spatial data infrastructure (Richardson, 2009) and has a dedicated GIS team in its Physical Planning Unit to respond to the needs of several government departments (including DMCA). Both DMCA and MVO have ArcGIS capabilities.

6.4.2.3 Researcher role

Finally, as an end to Phase I, a scientist contributing to hazard management must decide where their responsibility ends, i.e. with the conclusion of each element of the research project or application of the knowledge it produces (Alexander, 2007). An informing role was taken whereby the scientific research was used to communicate a greater understanding of the lahar hazard, and did not provide a

recommended course of action. To achieve scientific consensus before consultation with decision-makers (DMCA), it was decided that the findings from Phase II should first be presented to MVO. However, in the interests of anticipating the wider uses of the research (Renschler, 2005), eventual communication to the public was not excluded as a possibility.

The research objectives deliberately did not include a full risk assessment. The definition of 'hazard' used here denotes the probability of an event. Risk is the probability of suffering harm or loss and is derived from both hazard and vulnerability (Tilling, 1989). Thus, the transition from hazard to risk extends beyond geophysical processes to incorporate the social implications of natural hazard events (Merz *et al.*, 2006; Chapter 2, Section 2.2.1). Risk mapping typically involves listing and delineating exposed elements, analysing their respective values and assessing vulnerability (e.g. Throuret *et al.*, 2000; Merz *et al.*, 2006; Thierry *et al.*, 2008; Leone and Lesales, 2009). A risk map was not requested by the local agencies, it would remain their responsibility to factor in any socio-economic concerns.

6.5 PHASE II: LAHAR MODELLING AND HAZARD ASSESSMENT

6.5.1 Phase II overview

A methodology for modelling (Phase II) was adopted that was focused on end-user requirements (outputs *i–iv*, Table 6.2), but was also consistent with four steps proposed as standards for the approach to landslide hazard management (Hurlimann *et al.*, 2006): (1) geomorphic and geologic analysis: a susceptibility map (initiation zones); (2) runout analysis; (3) hazard zone delineation and hazard map production, and (4) hazard mitigation and reduction. Technical aspects of the first three steps have been detailed in Chapters 4 and 5; runout analysis (output *ii*) was taken from Chapter 5 (short- to mid-term hazard) and delineated cumulative hazard zones were produced using methodology from Chapter 4 (long-term hazard) (Figure 6.3).

depth was calculated for individual lahars using LAHARZ to predict the inundated cross-sectional area and thus used to refine the (wetted) channel shape. The model stopped at the pre-eruption shoreline, representing a large volume lahar. However, the model itself operated independently of lahar volume. Uncertainty was considered through multiple equally probable realisations of the input elevation surface (a Digital Elevation Model, DEM). This was achieved through Monte Carlo sampling of a probability density function, defined by a normal distribution (with no bias) and a standard deviation (*stdv*) representing spread of error values (see Chapter 4, Section 4.5.1.2).

Outputs were probability-of-flow maps and averaged velocities. Travel times were calculated (per model run) for individual paths by splitting the path into sections of uniform velocity, calculating the time taken to pass through those sections and summing for the entire path. These forecasts were only valid on short- to mid-term timescales as the valley changes shape as a response to successive lahars. An update of the DEM would be required for a new forecast.

6.5.3 Achieving mid- to long-term management outputs (*iii* and *iv*)

6.5.3.1 Modelling for long-term hazard assessment (output *iii*)

Mid- to long-term cumulative inundation from lahars was considered using LAHARZ which predicted planimetric inundation areas (see Chapter 4 for details). Six lahar volumes were selected for numerical simulations: 1 000, 5 000, 10 000, 50 000, 100 000 and 500 000 m³. Input volumes have been refined from Chapter 4 to exclude the most extreme (unlikely) event and allow two ‘small’ lahars, two ‘intermediate’ and two ‘large’ (Chapter 4). The first two volumes here represented relatively high probability events (daily—weekly), the middle two indicate medium probability of occurrence and the latter two indicated large events with annual return period. In the absence of recorded volumes, this semi-geometric progression of magnitudes was chosen.

Model outputs from LAHARZ were converted into hazard zones (see Chapter 4). Smoothing of jagged edges produced by cross-sections simulated at 45° angles is

sometimes necessary for communication purposes (Iverson *et al.*, 1998; Widiwijayanti *et al.*, 2009). However, this process is highly subjective, and jagged edges may represent important micro flow routes (Chapter 4). Here hazard zones were cropped to the extent of the 2006 coastline but additional smoothing was minimised.

6.5.3.2 Visualisation for a dual focus hazard map (output iii)

A catchment-scale, long-term planning and education map was therefore generated. There were different ways to display the hazard zones - for direct query in a GIS or as tangible (paper) interpretations. A range of visualisations were developed in both two and three dimensions using ArcMap and ArcScene (ESRI software).

Hazard zones were viewed semi-transparent and overlain over a high-resolution aerial photograph. Hazard magnitude was communicated through a red-to-blue colour scheme. Red represented the greatest hazard, consistent with the existing Hazard Level System. Furthermore, Montserratians associate red with increased danger (Haynes *et al.*, 2007). In comparison to the four discrete colours of the current Hazard Level System, more subtle colour changes (and more hazard classes) were used to infer a more gradually changing lahar-specific hazard.

Key locations were given as text on the map for orientation. Three dimensions were conveyed using a HILLSHADE function in ArcMap. This enabled topography to be easily interpreted on a printed map, i.e. in two dimensions. General map design was informed by the British Cartography Society's introductory text (BCS, 2008), Brewer (2005) and Muller *et al.* (2006). This map was viewed in ArcMap and also printed as paper copy.

Consistent with findings from Haynes *et al.* (2007) and discussion with end-users (Section 6.3), the hazard map was superimposed over 3D oblique views of terrain in ArcScene. Such interactive visualisations have long been recognised as an effective visual tool for volcanic hazard zoning and evacuation planning (Pareschi and Bernstein, 1989). In addition to formats compatible with those requested, a number of different example visualisations were prepared; for example, a fly-by animation of a lahar in motion (ESRI ArcScene) and 3D renderings of buildings (Google Sketchup).

6.5.3.3 Management options and mitigation scenarios (iv)

In a mitigation context, modifications to the human system include access restrictions and long-term land-use planning. These could be considered directly from the hazard map and related visualisations (output *iii*). Alternatively (or indeed additionally), physical modification to the natural system was a possible future for the Belham Valley. This may be a deliberate management act to adjust lahar behaviour, or a natural system response to lahars moving over the valley surface.

Possible futures were considered through alteration of the inputs to the coupled GIS approach (Chapter 5), and thus can also be thought of as testing the robustness of output *i*. Example channel modification could include changes to the roughness of the surface and/ or widening of the channel. By slowing flows, increased roughness would likely increase travel time (see Manning's formula, Chapter 5, Equation 5.1). Widening of the channel would increase cross-sectional area, thereby decreasing the hydraulic radius and ultimately velocity. The original roughness surface is described in Chapter 5 (Figure 5.6 and Table 5.1).

Four scenarios were considered for the future of the Belham Valley:

Scenario 1. The upper-reach was given a new roughness surface (elsewhere roughness was unaltered from Figure 5.6, Chapter 5). Manning's n was made uniform across the valley floor and considered to consist entirely of boulders with a gravel matrix ($n = 0.06$). This scenario could arise as the cumulative effect of many small volume flows, not travelling far downstream and rapidly depositing their load. There was evidence of existing boulder beds upstream; this scenario merely extended them. However, the DEM remained unchanged, equating to no new material. The reason for this is two-fold: (1) there was no deposit depth information at a finer temporal resolution than one rainy season; and (2) only one variable was changed to allow a direct comparison of the effects on the results.

Scenario 2. The mid-reach was uniform and the surface was considered to consist of boulders with gravel matrix ($n = 0.06$). Elsewhere the roughness surface was not altered. This was similar to Scenario 1, but now the majority of boulders remained in the mid-reach; enabling the effect of increased roughness in a different reach to be

compared. This would be representative of increasing roughness via a manual intervention.

Scenario 3. The mid-reach was widened to increase the cross-sectional area of the channel by three cells or 30 m at each bank. New areas were given a roughness value of $n = 0.04$ (equivalent to the average valley bottom of gravel with a sand matrix). This required a new DEM in addition to the revised roughness surface. This scenario is an extreme interpretation of what could happen if intensive extraction were to continue, or if large scale natural system modification was a viable mitigation option.

Scenario 4. All vegetation from the valley floor (and associated raised terraces) was removed. This required a new DEM and roughness surface. Newly exposed areas were given a roughness value of $n = 0.04$. This scenario was possible from multiple large lahars occur in rapid succession, destroying established vegetation and preventing the establishment of new pioneers.

6.6 PHASE II: RESULTS AND ANALYSIS

6.6.1 Results relevant to short- to mid-term planning objectives (*i* and *ii*)

Individual flow routes were predicted from the coupled GIS approach developed in Chapter 5. Thus, for final presentation to end-users, end point A, a variable hydraulic radius and *stdv* of 0.5 m were used (see Figure 5.7, Chapter 5). These results were used for mapping the location of the main channel (or moving centre of lahar mass). There was little variation in dominant routes despite incorporation of elevation data uncertainty. Model outputs thus showed lahar paths with high precision; and these agreed with field observations (Chapter 5, Section 5.3.1), implying high accuracy. Dominant flow routes relative to past deposits are shown in Figure 6.4a. Spatial variation of velocity for inundated cells is shown in Figure 6.4b. Red and blue end-

members to the colour scheme highlighted the areas of fast flowing lahar, and slow flowing lahar respectively. To show the topography contours and a HILLSHADE have been applied.

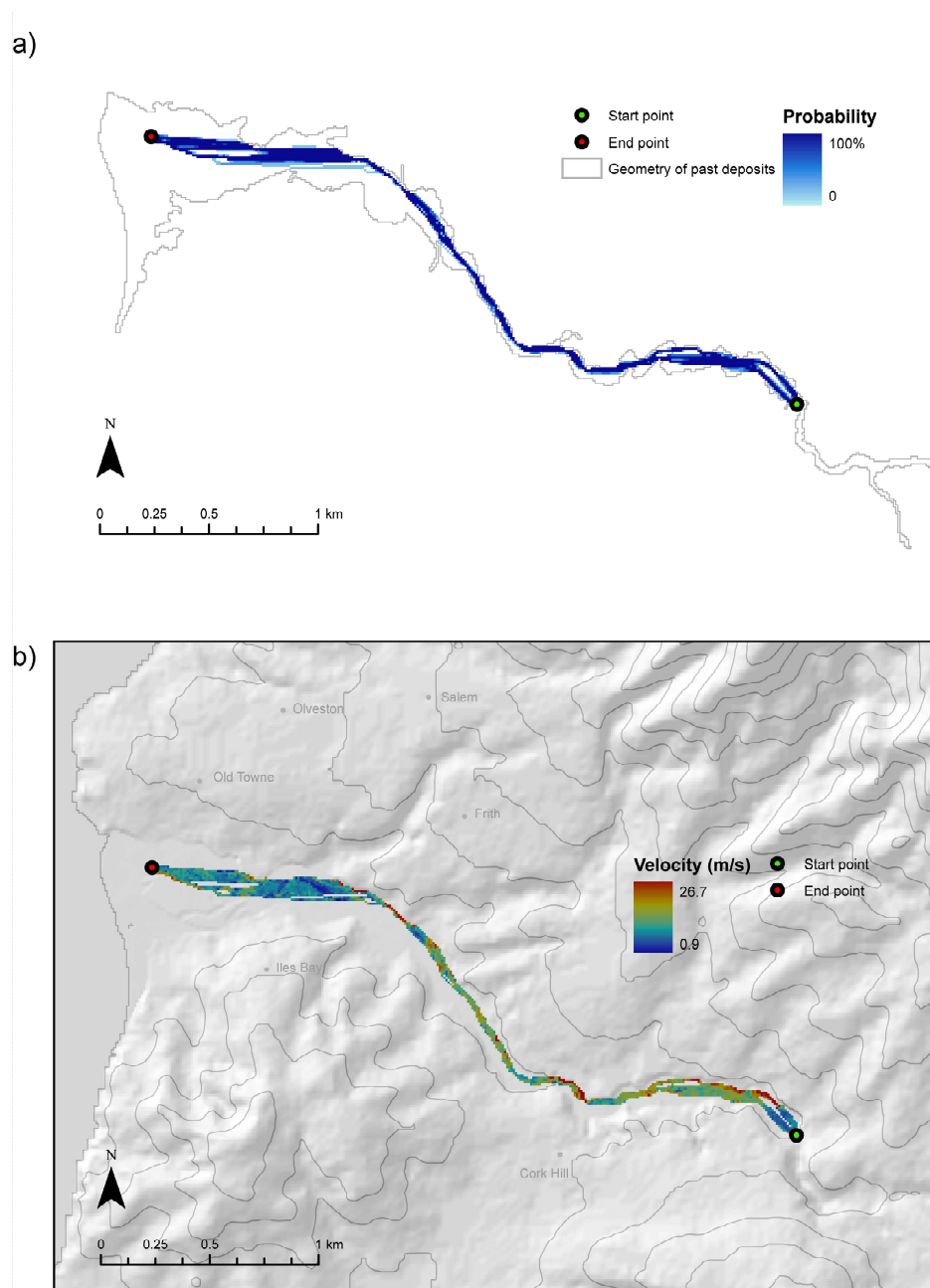


Figure 6.4 Alternate ways of conveying the short- to mid-term hazard: a) probable dominant flow routes and b) corresponding spatial distribution of velocity (after Figure 5.7 and Figure 5.9, Chapter 5)

Average velocity along the length of a flow path was $8.2\text{--}8.3\text{ ms}^{-1}$, these with the dominant routes gave average transit times of 601—619 seconds, or approximately ten minutes from initiation to the end point (full results are in Chapter 5, Section 5.3.2).

Results agreed by order of magnitude to proxy point velocities in the field (Barclay *et al.*, 2007), and to average velocities for similar flow types on other systems (e.g. Pierson, 1995; Rickenmann, 1999). However, further field measurements (i.e. instantaneous velocities) would be needed to increase confidence in absolute velocities and their spatial distribution. Consultation with MVO (Phase III) would be valuable to determine how reasonable it would be to communicate these (largely unverified) data to local decision-makers.

6.6.2 Results relevant to mid- to long-term planning strategies (*iii* and *iv*)

6.6.2.1 Inundation mapping (output *iii*)

Lahar inundation areas for different volume flows were predicted using LAHARZ (Figure 6.5). Inundation likelihoods were greatest upstream, near lahar source areas, and along the valley thalweg. Inundation likelihood diminished with distance from the volcano and lateral distance from the thalweg. Despite a small alteration in input volumes, these findings were consistent with those from Chapter 4 (Section 4.6.2). Although there are some shortcomings for application of LAHARZ to Montserrat, particularly in the calibration of the semi-empirical equations for more sediment-rich debris flows, the value of the results for a preliminary hazard assessment has been shown in Chapter 4.

A hazard map was generated using inundation results from LAHARZ (Figure 6.5) and visualisation requests from end-users (Section 6.3.3) (Figure 6.6). This represented the mid- to long-term lahar inundation hazard and had dual utility for setting access restrictions and longer term land-use planning. The hazard map was also produced in 3D and was explored interactively in ArcScene (Figure 6.7).

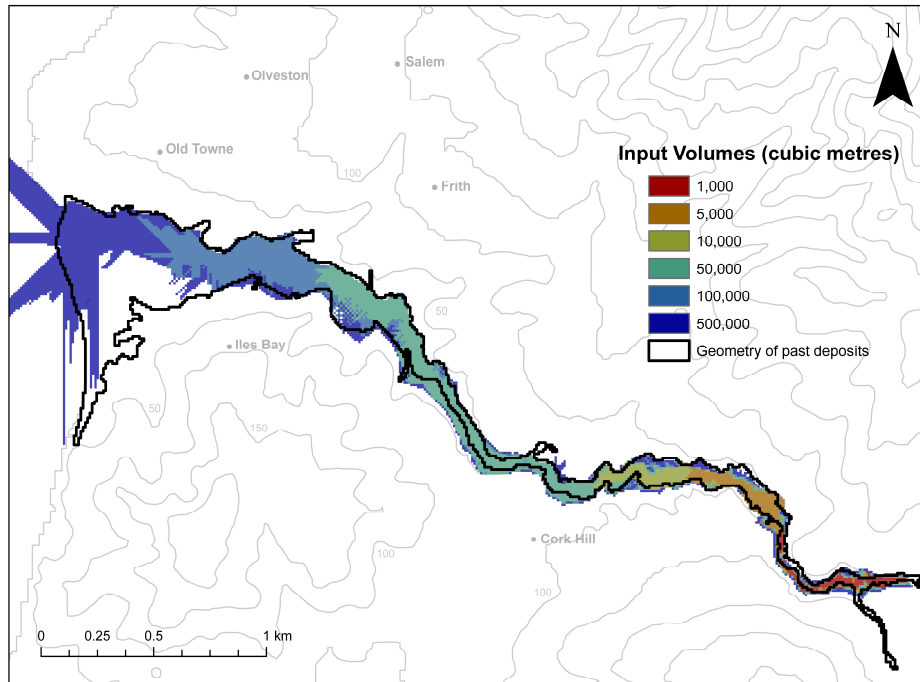


Figure 6.5 Planimetric inundation area from LAHARZ compared to the geometry of past deposits (as of November 2006).

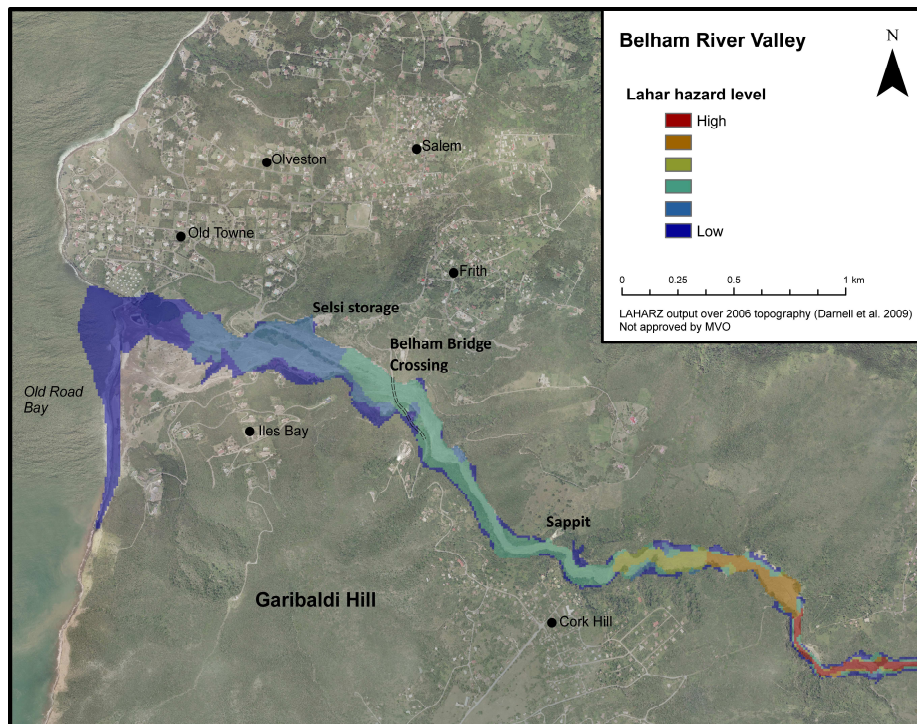


Figure 6.6 Belham Valley hazard map produced in ESRI's ArcMap (aerial photograph courtesy of the Physical Planning Unit Montserrat, permission by DMCA)

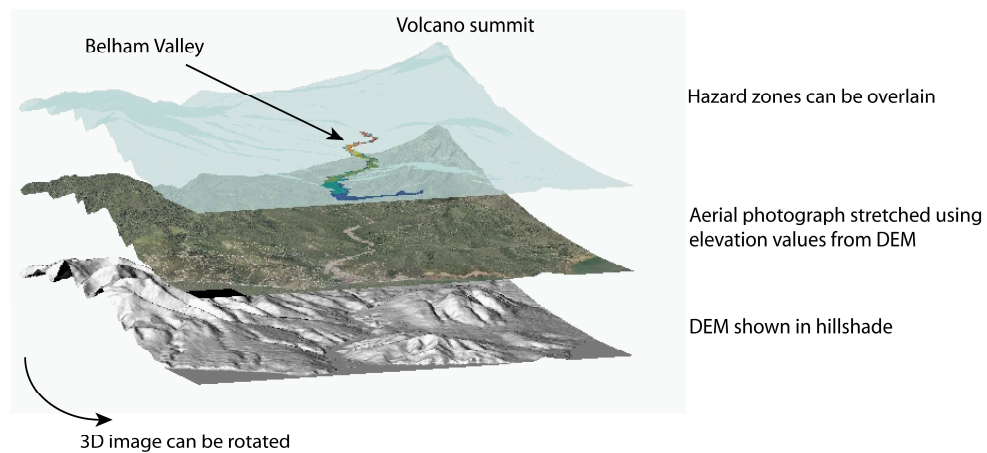


Figure 6.7 ‘Exploded’ 3D visualisation of the lahar hazard zones displayed in a GIS (ESRI’s ArcScene).

Given results shown in Figure 6.6, it is unlikely that flows will be diverted into current populated areas, even considering uncertainty in elevation values in the DEM. The greatest cumulative hazard is from multiple small volume flows that have a high likelihood of occurrence, but do not travel further downstream than the Sappit River confluence. However, the greatest potential threat to an individual (referring to current daytime activities) is from large flows that can reach the crossing area (former Belham Bridge) and where active sand and gravel extraction is undertaken.

6.6.2.2 Structural mitigation and possible futures (output iv)

Potential modifications to the natural system were considered through alternative scenarios, results are shown in Table 6.3. Results from Chapter 5 (variable hydraulic radius, end point A) were used as control data (Section 5.3.2). Scenarios of increased roughness (all-boulders) decreased mean velocity and increased travel time in the upper- and mid-reaches. For example, for low *stdv*, travel time was increased by 4.9% (29 seconds) in the upper-reach (Scenario 1) and by 9.7% (60 seconds) in the mid-reach (Scenario 2) relative to the control data. Widening the channel in the mid-reach (Scenario 3) did not slow lahars significantly (0.6–3% decrease in average velocity) and actually a small decrease in average travel time

was calculated (6–14 seconds). Removal of all vegetation and associated terraces (Scenario 4) induced a reduction in travel time, despite having little effect on the overall mean velocity.

Robustness of the method for defining main flow routes is reflected by comparison of the total area inundated. Greater elevation error (*stdv*) induced greater variability in the definition of flow routes, inundating a larger area for all scenarios. However, individual path length did not directly correlate with magnitude of *stdv* (although the standard deviation was always greater). Average travel times did not directly correlate with mean velocities, nor mean path lengths. The algorithm used actively seeks out the greatest changes in velocity between neighbouring cells, thus although a given path may be longer, the lahar may travel through sections faster than for a more direct, shorter route. Thus, a mean may be an inadequate description for path length and velocity.

Inputs		Outputs						
Scenario	<i>stdv</i> (m)	Total area inundated (km ²)	μ path length (m)	σ of path length (m)	μ path velocity (ms ⁻¹)	σ of velocity (ms ⁻¹)	μ path travel time (s)	σ of travel time (s)
Control_1	0.5	0.1755	3608.4	22.3	8.24	0.33	601.4	22.5
Control_1	0.1	0.0486	3442.9	16.4	8.28	0.09	618.6	11.7
1	0.5	0.1584	3345.3	105.8	7.38	0.13	606.9	29.2
1	0.1	0.0416	3267.7	40.3	7.27	0.03	645.7	17.3
2	0.5	0.1720	3372.3	72.4	7.50	0.30	630.6	24.1
2	0.1	0.0483	3379.4	15.4	7.64	0.07	678.9	10.9
3	0.5	0.2091	3489.5	105.9	8.02	0.33	587.9	27.9
3	0.1	0.0436	3506.4	68.9	8.23	0.08	612.3	16.2
4	0.5	0.1411	3366.0	72.13	8.13	0.29	551.3	19.8
4	0.1	0.0637	3327.2	32.0	8.16	0.12	583.1	9.85

Table 6.3 Area inundated (for one model run) and output statistics for individual flow paths, averaged from 100 simulations (control_1 data were taken from Chapter 5, Section 5.3.2); where μ = mean value and σ = standard deviation of values.

6.7 PHASE III: MAINTAINING COOPERATIVE RELATIONSHIPS AND MUTUAL FEEDBACK

6.7.1 Methodological overview

As specified by the researcher role in Section 6.6.3, Phase II results were first presented to the local or host scientific team (MVO). The Director of MVO changes periodically, and thus a mutual colleague established initial contact with the (new) Director of MVO in 2009. Email contact followed where the primary researcher sent a project briefing to the Director, and established a mutually convenient date (November 2009), consistent with the recommendations of the IAVCEI protocols (IAVCEI Subcommittee for Crisis Protocols, 1999). An invitation to endorse a paper, to be published from the research, was also extended to (and accepted by) the new Director.

Modelling results were presented at MVO to permanent staff (both scientists and non-scientists) and volunteer scientists in November 2009; in total there were less than 10 voluntary attendees or participants. Also, a real-time GIS demonstration explored 3D data layers in ArcScene. Both aspects were intended to facilitate discussion around different visualisation styles and the general issue of lahars on Montserrat. This was an informal focus group discussion; participants were encouraged to ask questions through the (10–15 minute) presentation and (5–10 minute) demonstration. Direct questions were also put to the group before presentation and demonstration, and repeated afterwards. Example questions included: do you understand the presentation of the hazard information? Do you have a preferred format?

Following the focus group session, an individual open-ended semi-structured interview (approximately 1 hr duration) was conducted with the Director of MVO. This interview focused on assessing the relative priority of the lahar hazard at MVO, identifying potential uses of this (external) research and the desired format. A secondary aim of the interview was to use the Director of MVO as an intermediary for acquiring further interviews with representatives from relevant agencies, i.e. a

'snowball' sampling strategy. The interview with the Director of MVO was not transcribed or coded as value patterns and perceptions were not being assessed.

6.7.2 Results from mutual feedback

6.7.2.1 Post-modelling consultations with scientists and non-scientists at MVO

The focus group highlighted frustrations felt by the host scientific team (MVO) when accommodating visiting external scientists. One staff member expressed the view that external researchers were frequently making data demands on MVO, but without providing feedback. This is sort of situation which the IAVCEI Protocols were designed to alleviate (IAVCEI Subcommittee for Crisis Protocols, 1999). However, the focus group did feel that this researcher's university (UEA) had acted honourably with a tradition of two-way information flow. The focus group meeting was seen as a positive action. Arguably, the desire to express this frustration at this opportunity overshadowed the primary practical objectives for this phase of the research, i.e. receiving feedback on the research.

As a group representative of MVO, focus group participants were generally interested in the research and acknowledged the existence of the lahar hazard. They also wanted to know the researcher's recommendations for a monitoring approach. A first step would be a formal procedure for recording the occurrence of individual lahars. However, in the absence of autonomous sensors in the field, it was unclear how a continuous dataset would be practically achieved. The researcher highlighted the need for point velocity measurements and stage indicators for individual flow events, to help validate model results (Chapter 5). Some amateur video footage of recent lahars had been obtained by MVO scientists, but there were no markers in the field for measurements to be taken. Nonetheless, upon examining the spatial distribution of velocities and magnitude range in the model results during the focus group section (Figure 6.4b), scientists confirmed that the fast and slow flowing areas were consistent with their observations.

Despite good local knowledge and an assumed spatial awareness that (arguably) comes with being in a scientific profession, naming of local villages was preferred by

members of MVO to aid orientation with mapping products. For example, when shown Figure 6.4a, spatial understanding was improved with place names.

During the one-on-one interview, the Director of MVO was interested in the modelling results (all outputs) as a potential tool to illustrate their opinion on the relative hazard when advising decision-makers. Furthermore, in the spirit of openness of scientific information, the Director of MVO (and hence the Observatory) would be willing to take output 2D visualisations and place them on the website for public access. The fly-by animation and Sketchup products were not viewed as useful educational tools in their current form, without high resolution landscape markers (i.e. more 3D houses). Interestingly, with the increasing popularity of computer technology and Internet on Montserrat, the Director would like to explore the possibility of using freely available 3D rendering software, Google Earth, as a repository for new output hazard maps.

Despite generally positive feedback, uptake of information on secondary hazards was not a priority at MVO. At the time of the interview pyroclastic flows entering the Belham were a more immediate concern and the Hazard Level was at 4. This unease manifested into reality on Friday 8th January 2010 when a pyroclastic flow travelled into the Belham Valley and reached as far as 300 m upstream of the Belham crossing; this was the longest flow down the Belham in the history of the eruption (<http://www.montserratvolcanoobservatory.info/> MVO activity report Friday 08 January 2010 17:02). Thankfully the Hazard Level during this time had limited permissions to essential workers only (i.e. monitoring scientists at MVO). The Hazard Level returned to tier 3 in March 2010.

Ultimately, it was concluded (by the researcher and Director of MVO) that the usefulness of such external research depends on the stage in the cycle of eruption. For example, if the volcano was at a lower activity level it would be far more likely that resources could be allocated to monitoring lahars.

6.7.2.2 Post-modelling consultations with decision makers

Preceding the final visit to Montserrat the researcher was informed by the Director of MVO that interviews with other agencies would be unlikely. Heightened activity, associated with new dome growth, in the months prior to the interview meant local

authorities would be occupied with planning meetings (a request for attendance at these meetings was politely denied). Furthermore, DMCA were in the process of changing their management hierarchy with the current director due to leave. Nevertheless, the Director of MVO endeavoured to schedule a meeting with DMCA, but this was not possible within the time period the researcher was on-island. Therefore, the 'snowball sampling method stalled at MVO. The Director of MVO was willing to transfer findings to DMCA when a suitable time could be arranged. However, pyroclastic flows occurred down the Belham Valley in January 2010 (see above, Section 6.9.2.1), and, to the author's knowledge, this transfer has not yet happened.

6.8 DISCUSSION

6.8.1 Reflecting on model outputs and end-user demands

Establishing end-user demands at project conception was seen as a way to maximise the potential transfer of new research. MVO, the Governor's Office and DMCA were established as key players in hazard monitoring and management on Montserrat. All were initially keen to be involved with the research. Balancing modelling options with end-user demands was discussed in Section 6.4.2.2. Reflection is now made on how well these end-user requirements were met.

6.8.1.1 Short- to mid-term outputs (i and ii)

DMCA were eager to maintain a mutual flow of information between themselves and UEA, making information stores such as the Physical Planning Unit available to the researcher. The Governor's Office was happy to receive feedback through official channels (i.e. via DMCA). Both of these governmental bodies expressed a request for a local automatic or manual threshold-based warning system for the lahar hazard.

Lahars are strongly correlated with periods of intense rainfall but there are outliers (Barclay *et al.*, 2007) and thus a rainfall threshold alone cannot provide an

infallible warning indicator. Furthermore, it is better to provide no short-term forecasts, rather than inaccurate ones. Further research is needed if a warning system can ever be implemented.

As a compromise, and consistent with the wishes of local scientists (MVO) for promoting understanding of lahars, the researcher produced predictions for individual flow routes, depths, velocities and travel times (Chapter 5). However, there remain some limitations to the models (discussed in Chapters 4 and 5) and a comprehensive lahar hazard assessment has only almost been achieved. Furthermore, it is unclear how desires have changed and whether the DMCA (and ultimately Governor's Office) would review the research as entirely successful (i.e. considering not all of their needs have been met).

6.8.1.2 Mid- to long-term outputs (iii and iv)

The Belham Valley lahar hazard map (Figure 6.6) can be used to inform mid- to long-term land-use planning decisions. Furthermore, due to visualisation using aerial photographs and 3D demonstrations, the map has the potential to inform mid-term access restrictions and education, i.e. fulfilling a dual purpose.

The existing Hazard Level System is a holistic approach, applying access restrictions and ensuring public safety, but has an insufficient consideration for lahars during periods of low activity, where there is unrestricted access to the lower Belham (Hazard Levels 1–3). A proviso to the Hazard Level System does state that (for all Hazard Levels): “(a)shfall and lahars can be significant hazards in all areas, and require appropriate precautions” (<http://www.mvo.ms/>). However, this ‘catch-all’ situation does not convey spatial variation of the hazard for land-use and activities. Furthermore, lahars are not necessarily linked with volcanic activity levels and therefore cannot be reflected by changing between Hazard Levels. The new hazard map would be a semi-permanent (long-term) reflection of the lahar hazard in the Belham Valley; a Belham-specific map was explicitly requested by the Governor's Office.

Interpretations from Section 6.6.2 and results from Table 6.3 demonstrate that altering the roughness of the valley floor and changing the morphology of the banks would not have a great impact on flow path variability, velocities or travel times. For

example, the range of mean travel times at a low *stdv* is only one minute 36 seconds (across all Scenarios). Thus, these results do not justify investment in channel modifications for lahar hazard mitigation, nor is continued industrial extraction likely to have a significant impact on lahars. Removal of all vegetation (and terraces) in the lower-reach would have the greatest impact (decrease) on flow travel times. Therefore, maintenance of these areas of vegetation may be an important management strategy. These findings are potentially very useful to DMCA.

6.8.2 Reflections on the interface between research and usage

MVO were keen to obtain findings from this research for more detailed consideration. However, time to do this was dependent on the other monitoring priorities and volcanic activity. MVO were content to receive final outputs (maps in electronic format) for distribution via their website without the associated raw data and analyses. This may mean liability for the map(s) rests with the primary (external) researcher, or, more probably, detailed discussion of information dissemination would take place when the volcano reached lower activity levels. Although transfer of science from the host scientific team (MVO) to the decision-makers (DMCA) was considered the best conduit for the research findings, in this case study the mechanism was unsuccessful. Volcanic activity levels at Soufrière Hills, and other administrative issues, at the time of the final visit inhibited feedback of final results to DMCA. Furthermore, perhaps such agencies are not familiar with receiving external science, and thus an absence of formal procedures for feedback.

Transfer of science to the grass-roots level (general public) remains the duty of the responsible agencies. Currently the public are informed by daily activity updates on local radio, ground personnel (police) and access gates that can be locked when the Hazard Level changes. However, increasingly technology is playing a more significant role with many Montserratian's using Internet resources such as MVO's website and social networking sites. Google Earth was suggested by the Director of MVO as a means for displaying (lahar) hazard information. Google Earth has been

highlighted for its power, accessibility and potential for use in humanitarian emergencies (NRC, 2007; MapAction, 2008).

6.8.3 Wider implications and further work

Velocities at various points along the valley would help validate model results (see Chapter 5). Gathering other parameters, such as sediment concentration and rheology information, could enable application of more sophisticated modelling approaches. However, visiting scientists are typically only on-island for a short time (one to three weeks) and may be unable to make observations of a lahar; furthermore, MVO have maximised their efficiency to meet their existing responsibilities and thus may not have the capacity or time for additional monitoring. MVO do have a regular influx of graduate and postgraduate level volunteer scientists who could potentially focus on secondary hazards. Furthermore, the public are also a possible untapped repository of information on lahars. Photographs, amateur videos and eye witness accounts could be useful when more formal monitoring is not possible (e.g. Aguilera *et al.*, 2004). Frequencies of events and inundation limits downstream have been proven valuable data for modelling. It is possible that this research has provided new momentum to put some of these monitoring instruments in place.

Translations of hazard into risk, and evaluation of public perceptions of the dangers, have not been considered within the scope of this project. These issues should also feed into successful management strategies. Haynes *et al.* (2007; 2008a; 2008b) have done initial work on risk communication, trust and public perception on Montserrat. However, a social-science focused assessment of the lahar hazard and associated risk has not been carried out to date. This would be interesting due to the unique socio-political setting and small, relatively static population.

The general formula for the approach (i.e. establish end-user demands, balance these with modelling options and acquire feedback), can be used to inform other study areas, particularly in similar active volcanic systems with multiple local

interested parties and visiting scientists. Furthermore, the GIS approach has contributed to lahar hazard mitigation and preparedness on Montserrat through:

- (Providing all) simulation and modelling of lahar routes and inundation areas
- Scenario testing for different volume events and for the impact of channel modifications
- Forecasting lahar routes and magnitudes
- Identifying data requirements (or absence of data)
- Visualisation of hazard distribution

These contributions are consistent with the roles outlined by Johnson (2000) and NRC (2007), and envelop a large proportion of the hazard management cycle (Chapter 2, Figure 2.1). Furthermore, there are opportunities for findings from this research to be used for education and to inform land-use planning. The use of GIS to aid hazard assessment can also be applied to other study areas.

6.9 CONCLUSION

Following guidelines for correct working practices in volcanic crises (IAVCEI Subcommittee for Crisis Protocols, 1999), a methodology was developed that was sensitive to the requirements of the user, while operating within reasonable data restrictions. The techniques used made optimum use of the available (and easily acquirable) data. Despite the absence of information on individual lahars, gathered terrain data were of high quality. Given what was wanted and what was provided, some findings of practical value (for Montserratians) can be taken from the work.

Consideration of 'what if' scenarios showed that channel modifications would not have a great impact on lahars; therefore, the most appropriate lahar hazard mitigation options would focus on human behaviour modifications. Crucially to inform the agenda of decision-makers, scenario testing suggested that continued extraction work in the lower- or mid-reach would not have a great impact on lahar behaviour (29–60 seconds). Early warning systems for lahars are currently

unfeasible due to a) the small travel distance, b) the lack detailed individual lahar observations and c) the lack of money (and financial incentive). Thus, it is recommended that, lahar hazard management should focus on land-use planning and hazard assessment should refine long-term inundation maps (i.e. Figure 6.6 is a good starting point). Short-term velocities and travel times can have value to people on the ground.

One of the overwhelming messages coming from this experience is the enthusiasm of local authorities and the host scientific team to support and assist external research. UEA affiliation with MVO will continue beyond this project and it is crucial to maintain such links, for both (new) external researchers and the host scientific team. However, despite planning and best intentions, sometimes feedback must yield to higher priorities, e.g. immediate management issues related to ongoing or elevated volcanic activity. Secondary hazards in a prolonged eruption will inevitably take a supplementary place and effective knowledge transfer becomes more challenging to obtain. Therefore, the usefulness of external research will depend on the stage of crisis. For example, it is likely that these findings will be more useful when the volcano quietens (enters another period of repose) and attention can be focused on long-term options.

Extensions to the research will be discussed in Chapter 7.

CHAPTER 7: CONCLUSIONS AND FUTURE RESEARCH

Reflections on the key findings from within Chapters 3, 4, 5 and 6 are provided in this final chapter. In Chapter 3 the importance of an informed approach to data uncertainty and data handling were highlighted, with respect to constructing a valid representation of the terrain surface. Within Chapters 4 and 5 models for lahar simulation were tested, developed and discussed. In Chapter 6 the practical utility and transfer of results were considered. The main themes of the thesis (data acquisition and handling, modelling and transfer) have been woven through these distinct chapters and this concluding chapter brings the findings together, ultimately leading to an evaluation and conclusion on the efficacy of GIS for lahar hazard assessment on an active volcanic system.

Furthermore, thesis contributions to new knowledge are explicitly identified under the disparate disciplines of volcanology (specifically lahar hazard assessment) and GI Science, and furthermore, specific benefits for hazard management on Montserrat are highlighted. Finally, given findings from this research, recommendations are provided for extending the work.

7.1 EVALUATION OF AIMS AND OBJECTIVES

It has been the aim of this research to examine the efficacy of Geographical Information Systems (GISs) for lahar hazard assessment on an active volcanic system. This was investigated with reference to a case study: lahars generated from Soufrière Hills Volcano, Montserrat. Project objectives were given in Chapter 1; an overview of the attainment of these objectives is provided in Table 7.1.

Objectives	Evidence
To understand the influence of lahars on the local environment using GIS.	<i>The main observed channels were interpreted from aerial photographs and in-field observations (Chapter 3). Valley perturbation by lahars over one rainy season was quantified in Chapter 4.</i>
To improve understanding of lahar movement using GIS-based modelling approaches.	<i>A GIS-based model was evaluated in Chapter 4 for its ability to reflect accurately the main flow routes. Informed by Chapter 4 results, a novel technique was developed in Chapter 5.</i>
To develop a digital elevation model (DEM) suitable for the objectives above.	<i>A DEM was constructed in Chapter 3 and improved (merged with another dataset to cover a greater area) in Chapter 4.</i>
To appreciate uncertainties in model predictions.	<i>Uncertainties were introduced with respect to elevation error in Chapter 3 and considered throughout.</i>
To delineate potential future inundation areas and quantify factors relating to lahar intensity; and, to translate this information into a formal hazard assessment.	<i>An established GIS-based model delineated hazard zones for the study area in Chapter 4; and Chapter 5 results provided lahar routes, velocities and travel times. Together these results informed a hazard assessment in Chapter 6.</i>
To assess effective application of research findings using consultations with local scientists and authorities.	<i>Local scientists and decision-makers provided vital input for the research from inception to completion (Chapter 6). Results have great potential for application.</i>

Table 7.1 Overview of evidence for attainment of project objectives

Furthermore, three intellectual themes emerged from the literature:

- (4) monitoring lahars, acquisition and handling of data;
- (5) improving knowledge of lahars through modelling; and
- (6) transfer of academic research on lahars to agencies of hazard management.

Reflection on the role of GIS tools across and within these themes will further evaluate fulfilment of the aims and objectives of the research.

7.2 EVALUATION OF EFFICACY OF GIS FOR LAHAR HAZARD ASSESSMENT

7.2.1 Monitoring lahars, data acquisition and handling

7.2.1.1 Review of lahar monitoring and data availability for lahar modelling

Despite a lack of preparedness for the onset of the 1995 volcanic crisis, and a shaky start to hazard management (Chapter 2, Section 2.5.5), primary hazards from Soufrière Hills Volcano are now continuously monitored (<http://www.mvo.ms>). Furthermore, the major population centres and facilities have been relocated away from the volcano and are offered some protection by the topographic high of the Centre Hills. However, lahars are a secondary hazard, frequent in occurrence, yet currently not formally monitored (Chapter 6). Eye-witness accounts and supplementary comments in MVO reports are the primary sources of information on lahars; few field measurements have been made of an event in progress.

The lack of formal lahar monitoring limited available data for this research. Fieldwork and data gathering experiences have also shown data acquisition from an active volcanic system can be extremely challenging for both the local scientific team and the visiting scientist (Chapter 6). Global Positioning System (GPS) equipment and field observations were used to map terrain changes when volcanic activity levels were low enough (Chapters 3 and 4). Other satellite data available for this time period were too expensive or suffered from cloud cover. Post-lahar field

investigations also examined the deposits and compared reported lahars to rainfall data (Chapter 4, Section 4.4.3). While estimations of lahar rheologies (flow behaviour) have been made (Chapter 2, Section 2.5), the magnitude of individual events cannot be determined from these data alone (Chapter 4). Basic administrative GIS data were also gathered from the GoM's Physical Planning Unit (PPU) and MVO provided georeferenced base maps. Nonetheless, the main source of primary data pertained to characteristics of terrain. All data were managed in a GIS database.

This research was conducted on a 'real-world', poorly-understood system, with real data restrictions. However, data limitations do not necessarily inhibit all predictive capabilities. For hazard assessment, runout and inundation areas from lahars are crucially important, and preliminary forecasts of these can be provided through relatively simple, undemanding GIS-based models and methods (e.g. Chapter 4). Some of the more complex predictive tools and models can be excellent research tools, i.e. improving knowledge of the intricacies of physical behaviour, but their practical utility can be low as they often require a vast amount of data and calibration. Furthermore, simple models can amply provide first-order solutions and identify important parameters and essential data requirements (i.e. the need for channel roughness to be considered was shown in Chapter 4).

These findings are also encouraging for other areas prone to lahar hazards where field data may be difficult to obtain.

7.2.1.2 Data handling: DEM construction

The influence of terrain on lahars is well-noted (Chapter 2, Section 2.3.5.1). It is evident that topography is of primary importance for determining lahar routing directions (Chapter 3) and lahar inundation areas are also obviously spatial (Chapter 4). Lahars will also perturb the surface inducing geomorphological change (Chapter 4). A GIS is ideally suited to generating (and updating) representations of terrain that are so crucial for lahar hazard management.

Here, as a result of perturbation by lahars, existing topographic maps and digital elevation models (DEMs) were outdated. GPS data were gathered to gain an up-to-date representation of the ground surface. However, such data needed to be

handled sympathetically to be useful. DEM accuracy and resolution issues have been known to affect results from lahar models (Chapter 2).

An application-driven approach to constructing DEMs was proposed in Chapter 3. This entailed incorporating auxiliary information from field notes with topographic changes digitised from (oblique) aerial photographs and with elevation data acquired with a GPS. Fusing of the different datasets was performed in a GIS. Synergistic use of these data sources greatly improved flow routing predictions, when compared to a DEM constructed with GPS data alone. These findings can be used to inform a standard approach to DEM construction and tailored to other systems/ applications.

Furthermore, to consider lateral spread of inundation areas the DEM needed to encapsulate a greater area than was accessible on-foot (i.e. beyond roving GPS coverage). Therefore, an older, regional DEM was used as a base and augmented with the new GPS-derived DEM (Chapter 4). However, again this had to be carried out sympathetic to the intended application, avoiding the creation of any artificial pits or peaks that could re-route flow, whilst prioritising conformity to the updated GPS-derived surface. A GIS was used to consider alternative approaches to fusing different datasets. Again, these techniques are applicable elsewhere.

As DEM data were acquired on two separate occasions, a year apart, morphological change as the effect of cumulative lahars could be evaluated by calculating a differential surface in a GIS. It was found that the valley was aggrading over the period of one rainy season, i.e. experiencing net deposition of sediment (Chapter 4).

7.2.1.3 Data handling: uncertainties and elevation error

Likely magnitudes of inaccuracy, or error, across a DEM could be estimated from knowledge of equipment accuracy, GPS sampling method, interpolation and construction technique (data handling) (Chapter 3).

Through a GIS, random error surfaces could be generated and used to disturb the DEM, creating multiple equally probable realisations of the 'true' surface (Chapter 3). Propagation of error to predicted flow routes was thereby considered by varying the different terrain surfaces as inputs to the GIS-based flow routing model and

observing the differences in output. Flow routing results were fairly robust to elevation error when the DEM construction method was application-driven, but not unresponsive (Chapter 3; 4). More complex methods of artificially perturbing the surfaces (e.g. estimation of spatial autocorrelation) were unnecessary as spatially independent error produced the 'worse case' scenario (Chapter 3). If higher accuracy surface data were available, disparity between this representation of the 'true surface' and the constructed DEM could be calculated for a more accurate understanding of error, but this would negate the need to use lower resolution/accuracy data.

DEM uncertainty can also impact the quantification of geomorphological change. For example, the quantified net deposition (Chapter 4) could, in theory, reflect error in the DEM rather than actual temporal elevation differences. However, with a mean elevation error of zero (no bias) the overall impact on the differential surface would be relatively low.

7.2.2 Improving knowledge of lahars through modelling

7.2.2.1 Utility and limitations of existing GIS models

GIS tightly coupled with modelling is an area where the potential of GIS is under-utilised (Chapter 2). The dependency of gravitational flows, such as lahars, on terrain, and the natural ability of GIS to represent the spatial variation of topography, strongly advocates lahar modelling through a GIS. Two established GIS-based modelling approaches were tested with lahars on Montserrat (Chapter 4).

Both the limitations and benefits of the models tested lies in their simplicity. Single-direction flow routing identified the main lahar routes, whilst incorporating uncertainty in their prediction. However, this model was unable to show inundation areas (i.e. spread). LAHARZ was able to map inundation areas, but performed poorly in an unconfined channel. Neither model required any input of the physical properties of the lahars and performed admirably when compared to deposits. Thus, GIS-based models have demonstrated their ability to provide preliminary predictions for hazard management; these can be useful when time is unavailable, yet also for

long-term trends as they are more likely to be adequate across a greater range of flow types.

7.2.2.2 Model improvements

The new model uses the principles of single-direction flow routing (Chapter 2; Chapter 4), combined with a simple equation for estimating the velocity of a Newtonian fluid over a rough surface which may be inclined (Manning's formula; Chapter 5). LAHARZ was used to refine calculations of the wetted channel shape. Flow was directed according to maximum velocity using a cost surface approach. This was also implemented in a GIS and considered uncertainties in predictions. Furthermore, this new approach enabled velocities and travel times to be predicted and observed flow routes were replicated with greater accuracy.

Therefore, the velocity cost surface approach could be used for short- to mid-term (days-months) prediction of lahar routes, average velocities and travel times. However, absolute velocities would benefit from more rigorous testing.

7.2.2.3 Treatment of unknowns and data uncertainties

Lahar magnitude was unknown, but a range of 'reasonable' volumes were inputs for LAHARZ to simulate the inundation areas of different likelihood events (Chapter 4). Undeniable uncertainties exist with the application of LAHARZ to the dilute flows on Montserrat. Uncertainty in the DEM was not considered for modelling with LAHARZ as (with the current source code) the different error surfaces would have had to be entered manually, greatly increasing model run time.

Observed dominant flow routes have been simulated, most successfully with the velocity cost-surface approach (Chapter 5). Uncertainties in these predictions with respect to terrain have been considered through elevation error propagation. The mechanism used was a Monte Carlo sampling strategy from a probability density function (i.e. normal distribution with no bias). Other sources of uncertainty could have been considered in a similar way. For example, Manning's roughness for a given cell could have been given a mean value from consultation with literature sources, but then allowed to deviate within a range specified by a standard deviation. Considering uncertainties in all parameters would develop a branching

structure similar to some previous work on Event Trees (Chapter 2). Sensitivity analysis could also show the relative importance of these factors/ parameters.

An exploration of different scenarios considering possible futures (natural and anthropogenic-induced) for the surface of the valley has enabled the robustness of simple flow routing to be examined. These scenarios, and their impact on lahar travel times, could inform local planning decisions and access provisions. The ability to demonstrate easily the consequences of ‘what if’ scenarios is a recognised benefit of GIS (Chapter 2).

7.2.3 Transfer of academic research on lahars

Communication and dissemination of scientific findings are relevant issues for hazard management that are gaining increasing attention (Chapter 2). One aspect of this is making sure that academic research is effectively applied.

Research was carried out with support and permissions from local authorities and local scientists. It was found that tensions are often sparked in a volcanic crisis when visiting scientists do not provide adequate feedback to the host scientific team (Chapter 6). In light of the current research and IAVCEI guidelines, some ‘best practices’ can be established for visiting scientists in crisis scenarios (Chapter 6). These are applicable to research conducted on any active volcano.

- Obtain permissions prior to commencing research;
- Assess end-user requirements to maximise potential uptake of findings;
- Establish the role of the visiting scientist as one which provides additional information on hazards, delivered to the local scientists;
- Offer feedback and receive feedback;
- Offer joint scientific publications.

GIS is a useful tool for pooling information, querying spatial data and producing outputs tailored to the requirements of end-users. Furthermore, GIS can be tightly coupled with the modelling process, enabling transfer of a simulation tool in addition to visualisations.

7.2.4 Summary of the utility of GIS for lahar hazard assessment on Montserrat

Geospatial methods for lahar hazard assessment that have been demonstrated through this research are presented in Figure 7.1.

Satellite technology has shown its use for gathering elevation data (GPS) and aerial photography can be used as auxiliary information for generating DEMs, and also for visualisation of results. DEMs can be generated in a GIS, uncertainty in elevations can be modelled through stochastic simulation in a GIS, and GIS-based models can be used to predict lahar routes and hazard zones. Mitigation scenarios can also be explored through a GIS and there is great potential to update model input data to develop further hazard predictions over time. Maps and model results can be tailored to end-user requirements (short-, mid- and long-term) through a GIS.

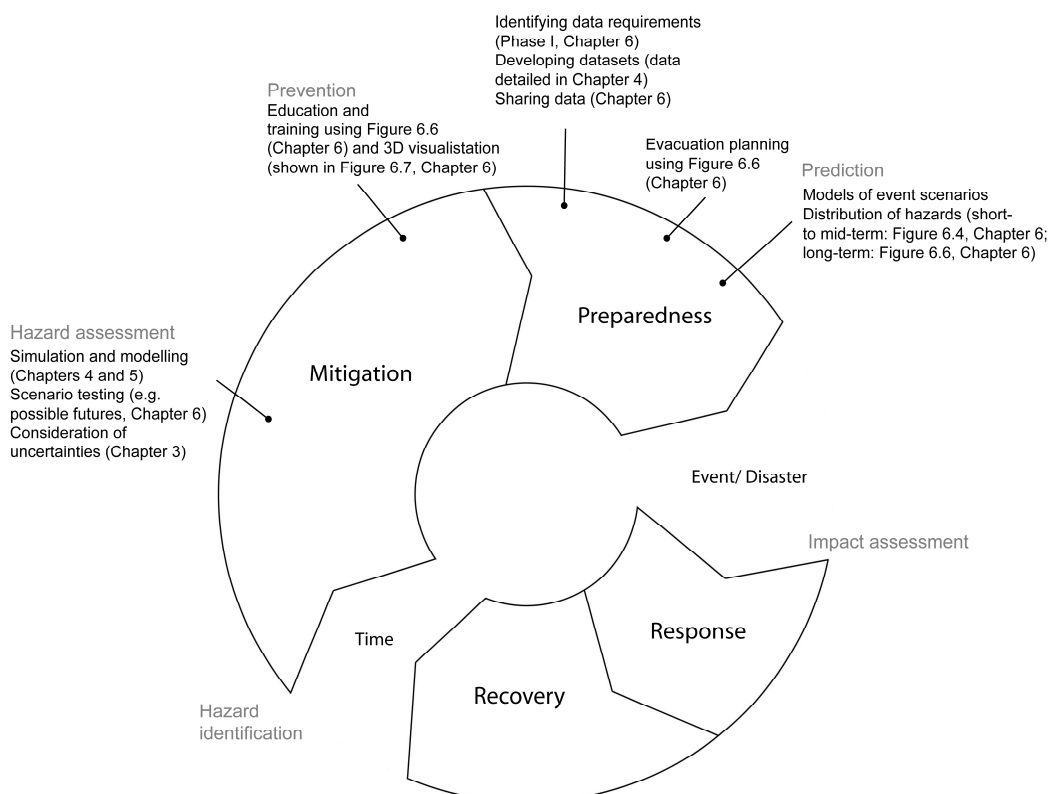


Figure 7.1 Geospatial methods that have contributed/ shown potential for contribution to lahar hazard management on Montserrat (amended from Chapter 2, Figure 2.12).

Currently, very short-term automated or manual warning systems are not feasible (Chapter 6), although a GIS could potentially be used to manage such a program.

Notable is the absence of potential GIS contributions to response and recovery on Montserrat (Figure 7.1). The Belham Valley area is in a perpetual state of response and unable to enter recovery due to the prolonged nature of the eruption of the Soufrière Hills Volcano. In terms of response to lahar events, these occur too frequently to require individual response and recovery.

7.3 SUMMARY OF CONTRIBUTIONS TO NEW KNOWLEDGE

Innovation and originality in scientific research are essential for advancing understanding of natural phenomena. Multidisciplinary research has been conducted that makes contributions to new knowledge across the fields of geology and GI Science; the work also has implications for the direct benefit of a specific regional setting, Montserrat, West Indies. Examples of these contributions are highlighted under different headings but there will be overlap between categories.

Furthering research on lahars and their hazard management

- LAHARZ, a standard preliminary tool for lahar hazard assessment, was used to map inundation areas of more water-rich flows. Although LAHARZ was originally calibrated for more sediment-rich debris-flow type lahars, and has been exclusively used for mapping these types of flows, the model was successfully applied to the more dilute flows of the Belham Valley, Montserrat.
- Hydrological modelling (single-direction flow routing) was used to simulate the dominant flow paths of more sediment-rich flows beyond its intended design. Principles of simple flow routing for water flows have been adopted to explain the underlying physics behind lahar movement. To the author's knowledge, implementation of a lahar model using a cost-surface in a GIS has not been done before.

- A novel GIS-based method for flow routing of more dilute lahars was developed to improve the performance of simple flow routing algorithms. Use of Manning's formula for water flow velocity had previously shown promising results for application to lahars, but in this research the formula was used to route flow according to greatest velocity.
- For the first time, LAHARZ was modified to output an estimated maximum flow depth. This parameter is a recognised indicator of lahar intensity. Further, this new output was used, with inundated planimetric area, to confine estimates for channel geometry necessary for the Manning's formula. In this way, two disparate GIS-based methods were coupled in a novel manner and used synergistically for lahar hazard assessment.
- The capability of GIS for considering 'what-if' scenarios was exploited and, in a novel approach for lahar hazard assessment, alternative futures were considered to assess the longevity of model results.
- Advancing previous research showing the importance of DEM accuracy, an application-driven approach to terrain construction for lahar simulation was used to improve hazard predictions.
- An original evaluation of producing effective science in an active volcanic environment was presented.

Advancements to GI Science

- An approach to terrain model construction was provided that prioritises fitness for its intended application, i.e. flow routing. This also provided an example of how to maximise accuracy using auxiliary information when elevation data were not optimal. This contributes to the GI Science research agenda for uncertainty in geographic information and geographic representation (see Chapter 2, Section 2.4.4.3).
- A new procedure for merging elevation datasets was developed. DEMs frequently require updating and often exist only in localised areas. The mechanisms for DEM merging can produce very different results but there are few established guidelines for achieving the best results. This also

contributes to GI Science research agenda for uncertainty in geographic information and geographic representation (see Chapter 2, Section 2.4.4.3).

- Possibilities for using ArcGIS's ModelBuilder for the creation of simple flow routing models with an integrated capacity for examining error propagation were highlighted. This simple tool allows the creation of models without the need for programming.

Tangible benefits for Montserrat

- Observed preferential lahar routes were simulated for the first time in this region. This is a step towards formal lahar hazard assessment for the Belham Valley.
- Lahar travel-times were also calculated in order to estimate the minimum evacuation time for daytime-access workers and visitors to the Belham Valley.
- Influences of continued anthropogenic activity in the valley and/ or intentional mitigation measures were considered for long-term hazard management.
- The first local scale hazard maps for Belham Valley lahar hazard management were created and distributed to local scientists.

7.4 AVENUES FOR FURTHER INVESTIGATION

7.4.1 Overview

Recommendations can be made for extensions to the current research. Detailed propositions follow justification for further research under three topics.

1. Given that:

- the new velocity-cost approach using Manning's formula produced plausible results for lahar routing, velocities and travel times (Chapter 5);

- there are currently no test data for individual events on Montserrat;
- recent elevated activity has decreased the likelihood of formal investment in lahar monitoring on Montserrat, and thus, reduced opportunity for formal monitoring initiatives;
- the model can be transferred to other areas providing there is a good knowledge of the local terrain (elevation, roughness etc.).

It is recommended that:

the newly developed velocity-cost surface approach be applied to another study area with similar flow types. Model testing in similar volcanic environments with greater data availability can help make inferences about the validity of the Montserrat results; if the method works well in other areas for predicting velocities, their spatial distribution, and flow routes, then the results for Montserrat are given support through analogy.

2. Given that:

- the relative importance of input parameters on results is a 'hot topic' in modelling;
- in the current research the relative importance of flow model parameters has only been qualitatively assessed for single-direction flow routing (Chapter 3);
- sensitivity testing has not been applied to the new velocity cost-surface model;
- the full range of uncertainties have not been considered for all model parameters;
- sensitivity analysis is an interesting area with potential to inform research in GI Science;

It is recommended that:

formal sensitivity testing be applied globally to consider uncertainties in all inputs and parameters for the velocity-cost surface model and how they interact with each other. This would concentrate efforts for model refinement by quantifiably identifying the most influential factors.

3. Given that:

- lahars can exhibit a wide range of flow behaviours;
- hydrological (water flow) modelling has been established as suitable for the more dilute flows on Montserrat (Chapter 5);
- GIS-based methods are good for manipulating elevation datasets, can run simple models, are ideal for hazard mapping and visualisations;
- lahars are a continual threat on Montserrat, likely to outlive the duration of the current eruption;
- there are other literature sources that could be explored in further detail (e.g. flash floods, dam-breaks).

It is recommended that:

other established GIS-based hydrological models are tested for the suitability for modelling dilute Belham Valley lahars. Such models need to be minimal in their data requirements. Forward modelling should predict long-term changes to the Belham Valley.

7.4.2 Useful analogues for lahar model testing

7.4.2.1 Merapi Volcano, Central Java, Indonesia

Merapi volcano, Central Java, is an andesitic stratovolcano, characterised by viscous magma generating dome-collapse pyroclastic flows (Thouret *et al.*, 2000); thus the volcano is very similar to Montserrat (Chapter 2, Section 2.5). Merapi has been historically active (2007), but is not currently erupting (Siebert and Simkin, 2010).

About 440 000 people live in areas with some risk of pyroclastic flows and surges, lahars and floods (Thouret *et al.*, 2000); 120 000 people live along the 13 rivers prone to lahars (Lavigne *et al.*, 2000). Lahars from Merapi travel as far as 30 km (Thouret *et al.*, 2000; Lavigne *et al.*, 2000) and can reach volumes of 10^6 m^3 (Lavigne *et al.*, 2000). Thus, the scale of the system (volcanic and hydrological catchment) is greater than Montserrat.

At Merapi, lahars are commonly triggered by rainfall and most occur in the rainy season after a threshold of 40 mm in 2 h (Lavigne *et al.*, 2000). Debris-flow behaviour is typically restricted to the lahar front and lahars tend to transform downstream to longer hyperconcentrated-flow phases as sediment load fluctuates during the flow (Lavigne and Thouret, 2002). However, hyperconcentrated flows often also precede the flow front, and sometimes debris-flow phases are absent (Lavigne and Thouret, 2002). Average velocities are typically from $5\text{--}7 \text{ ms}^{-1}$ (Lavigne *et al.*, 2000) and peak flow of 15 ms^{-1} has been observed in one of the river valleys (Lavigne *et al.*, 2000). Therefore, the lahar-triggering mechanism, flow types and velocities are analogous to Montserrat.

Crucially, there is also an abundance of data on Merapi lahars. There has been deployment of acoustic flow monitors, real-time seismic amplitude measurement, and seismic spectral amplitude monitoring for lahar detection (Thouret *et al.*, 2000). Thouret *et al.* (2000) also used a 10 m resolution DEM for modelling block-and-ash falls, so topographic data are available. However, to this author's knowledge, there has been little modelling of lahars undertaken.

7.4.2.2 Mt Ruapehu, New Zealand

Mt Ruapehu, New Zealand, is also an andesitic stratovolcano that has been historically active (2007, Siebert and Simkin, 2010). There are four types of lahar triggering mechanisms at Ruapehu: (1) partial collapse of the crater-lake rim; (2) eruptive episodes displacing crater-lake waters; (3) eruptions onto snow and ice covered slopes; and (4) heavy rains on slopes (Lecointre *et al.*, 2004). Failure of a lake dam has been found to be the most efficient mechanism for generating a fast lahar with a high peak discharge (Cronin *et al.*, 1997). In addition to small lahars

(<10⁵ m³), lahar volumes in excess of 10⁷ m³ have been observed (Lecointre *et al.*, 2004).

Cronin *et al.* (1997; 1999) describe lahars in 1995 generated from water ejected explosively from the crater-lake (lake-outburst). There were four distinct phases for these lahars, from initial streamflow 'pushed' ahead of the lahar, to debris-flow, hyperconcentrated-flow then normal streamflow (Cronin *et al.*, 1999). Average velocities were 4–4.5 ms⁻¹, and flows travelled over 90 km, thus velocities at the source were probably higher. Peak discharge was at the head of the lahar (Cronin *et al.*, 1999). Average velocities were obtained through eruptions and travel times, instantaneous velocities were recorded by timing floating objects over a set distance, or using a 'superelevation' method where the height difference across a lahar channel is measured as it flows round a bend (Cronin *et al.*, 1999).

A general model for Ruapehu lahars using Manning-type laws of friction, for lahars generated by a single explosive mechanism, has successfully been compared to 1968 lahars (Vignaux and Weir, 1990). A more complex fluid dynamics approach using the Delft3D program has been applied to the well-monitored March 2007 lahar (Carrivick *et al.*, 2009). An interesting study may be comparing performance of these earlier models with the novel methodology developed here.

Therefore, although Ruapehu is a larger system, there is justification for the application of the velocity-cost model (Chapter 5).

7.4.2.3 Others

The two comparable study areas above have been suggested due to the relative abundance of data. Other volcanoes with similar lahars include Volcan de Colima, Mexico and possibly Mt Pinatubo, Philippines, but these suggestions are not exhaustive.

Colima lahars are also rainfall-triggered and they are initiated as sediment laden stream flows which transform with entrainment to hyperconcentrated- and debris flows (Capra *et al.*, 2009). These lahars reach distances up to 15 km, flow depths 1.5–2 m for recent events and instantaneous velocities of 6 ms⁻¹ (Capra *et al.*, 2009). Colima is also currently active (Siebert and Simkin, 2010). LAHARZ has been used to model Colima lahars (Davila *et al.*, 2007).

Pinatubo is a stratovolcano that had its first historic eruption in 1991 and last known eruption in 1993 (Siebert and Simkin, 2010). Widespread rain-triggered lahars following the 1991 eruption have been extensively discussed by Newhall and Punongbayan (1996).

7.4.3 Formal sensitivity testing

Sensitivity analysis is the study of how uncertainty in model predictions is determined by uncertainty in model inputs and parameter values (Lilburne and Tarantola, 2008). This enables identification of aspects of the model that contribute to uncertainty and those that make no significant contribution (Hall *et al.*, 2005). Therefore, specific inputs can be targeted for further refinement. For example, sensitivity analyses can be used to construct logic trees focusing attention on the parameters that have greater impact on the hazard (Barani *et al.*, 2007). Modellers can also specify the quality of data inputs needed for outputs to have fitness-for-use (or utility in solving the problems to which they are applied) (e.g. Li *et al.*, 2000). Further, sensitivity analysis can provide objective criteria of judgement for different phases of the model-building process: model identification and discrimination, model calibration and model corroboration, treating the choice of the model as one of the sources of uncertainty (Saltelli *et al.*, 2000a).

Review articles of sensitivity analysis methods are provided by Frey and Patil (2002) and Lilburne and Tarantola (2008), and moreover the comprehensive discussion by Saltelli *et al.* (2000b). One-at-a-time (OAT) sensitivity analysis is currently the most commonly used type of sensitivity analysis (Saltelli *et al.*, 2000a; Lilburne and Tarantola, 2008). This involves independent variation of model inputs (or parameters etc.) to see the effect on model output. Local sensitivity analysis is a particular case of the OAT approach in which the input variables are only allowed to vary within a small interval around a nominal value (Saltelli, 2000). However, OAT approaches have as a major limitation the neglect of parameter interaction which can induce bias in the results (Campiongo *et al.*, 2000).

Global sensitivity analysis considers the potential effects from the simultaneous variation of model inputs across their finite range of uncertainty (Lilburne and Tarantola, 2008). Global sensitivity analysis, coupled with uncertainty analysis, is the best tool to assess the robustness of decisions and to understand whether the current state of knowledge is sufficient to enable a decision to be made (Tarantola *et al.*, 2002). For implementation see Saltelli *et al.* (2000b).

Sensitivity analysis has been used for a range of environmental applications including the modelling of hydrological processes (Cloke *et al.*, 2008), flood wave propagation (Elhanafy *et al.*, 2008), flood inundation model calibration (Hall *et al.*, 2005), sustainable planning of a hazardous waste disposal site (Gomez-Delgado and Tarantola, 2006), and seismic hazard (Barani *et al.*, 2007) etc.

Inputs for the current model (Chapter 5) could be tested, including DEM and slope, hydraulic radius and Manning's n . This would be a challenging endeavour, but would provide rewarding insight for lahar modelling and volcanology in general, disciplines where there is little evidence of formal sensitivity testing.

7.4.4 Alternative modelling approaches

Accepting that a hydrological approach has produced some positive results for the Belham Valley lahars (simple flow routing in Chapter 4; a velocity cost surface approach using Manning's formula in Chapter 5), it is reasonable to look beyond the lahar literature for modelling techniques. FLO-2D is perhaps the obvious choice, and has been applied to rainfall-triggered debris flows (e.g. Calvo and Savi, 2009). However, the software is demanding in terms of its input data requirements and is relatively expensive to purchase individually for small-scale research. Alternatively, HEC-RAS (Hydrologic Engineering Center-River Analysis System), developed by the US Army Corps of Engineers (Hydrologic Engineering Center, 2008), is a popular one-dimensional hydraulic model designed for simulating the flow of water through natural rivers and other channels.

HEC-RAS allows description of the river channel and floodplain as a series of discrete cross-sections perpendicular to the flow direction. Calculations proceed

along a previously selected topographic profile and water surface elevation is output at each cross-section; this can be directly overlain on a DEM to simulate flood inundation extent (e.g. Tayefi *et al.*, 2007). Two modelling approaches are possible with HEC-RAS: (1) steady flow simulations and (2) unsteady flow simulations. The steady flow version of the model solves one-dimensional step-backwater equations where a user specified discharge is routed through a channel with known geometry and roughness. Resultant water-surface profiles (from a calculation of energy balance between cross-sections) are then matched to surveyed water surface profiles in an iterative procedure until the discharge producing the best match is identified (Chow, 1959; Hydrologic Engineering Center, 2008). Although commonly applied commercially for floodplain management, this approach has been used for simulation of floods in ephemeral rivers (e.g. Merritt and Wohl, 2003) and glacial-lake outburst-floods (Cenderilli and Wohl, 2001; Alho *et al.*, 2005; Alho *et al.*, 2007). When applying the steady flow model to natural channels a number of assumptions must be made: (1) flow is comparatively steady along the whole reach; (2) flow varies gradually between cross-sections; (3) flow is one-dimensional; (4) the bed slope of the channel is less than 10%; and (5) the energy slope is constant over the cross-section (Hydrologic Engineering Center, 2008). Discharge is distributed according to the conveyance, which is given by channel geometry and roughness, represented by Manning's n (see explanation in Alho and Aaltonen, 2008).

Newer releases of the HEC-RAS model can also solve the full 1D St Venant equations (mass and momentum conservation) for unsteady open channel flow. This incarnation of the model has shown good performance, against more sophisticated 2D counterparts, for predicting river flood inundation (Horritt and Bates, 2002), complex upland floodplains (Tayefi *et al.*, 2007); and has been used for simulating dam-break floods (Yochum *et al.*, 2008) and jökulhlaups (Icelandic glacial-lake outburst-floods) (e.g. Alho *et al.*, 2007; Alho and Aaltonen, 2008). Sources of uncertainties and sensitivity analyses of input parameters have been extensively discussed (e.g. Hall *et al.*, 2005; Pappenberger *et al.*, 2005; Pappenberger *et al.*, 2008).

HEC-RAS has potential for dilute lahar simulation if the flow is assumed to be single-phase, where Newtonian flow behaviour is dominant (using similar reasoning

as presented in Chapter 5; Section 5.1.1). To implement for Belham Valley lahars, in addition to the roughness values estimated in Chapter 5, a set of cross-sections separated by 'uniform' sections of channel would be needed (easily obtained from the DEM) and evidence of stage and discharge changes downstream. High water levels can be measured from recent events (e.g. Yochum *et al.*, 2008) or from palaeostage indicators (e.g. Cenderelli and Wohl, 2001). Hypothetical hydrographs (discharge over time) can be estimated where such data are unknown as an upstream boundary condition (Alho *et al.*, 2007; Tayefi *et al.*, 2007; Alho and Aaltonen, 2008; Yochum *et al.*, 2008). Therefore, HEC-RAS is still relatively undemanding in terms of data input. It is also available for public use at no cost (<http://www.hec.usace.army.mil/software/hec-ras/>, accessed March 2010).

HEC-RAS hydraulic modelling can be linked with ArcGIS for import and export of files using a program called HEC-GeoRAS (see Ackerman *et al.*, 2000; Hydrologic Engineering Center, 2008; Yochum *et al.*, 2008). Moreover, the capabilities of HEC-RAS are not only limited to inundation modelling, the program has also been used by geomorphologists for its potential to relate variations in velocity, shear stress or unit stream power to specific erosive or depositional features (e.g. see Alho *et al.*, 2005). If such areas could be located for the Belham Valley, Montserrat, long-term system response could be predicted.

7.5 CLOSING REMARKS

"The need for geospatial data and tools may be everywhere, but in a sense it is also nowhere in minds that are overwhelmed by the circumstances of disaster."
(NRC, 2007, p. 146).

Application of geographical information and technology for disaster management is reaching a critical phase; in particular, there is a rising trend in the use of GISs beyond geography in other scientific disciplines including volcanology. More generally, there is a new era of information dissemination and rapid emergence of

user-generated content facilitated by the Internet and ubiquitous use of computers; GIS tools are becoming familiar to non-scientists, i.e. decision-makers and general public. While this is not necessarily true worldwide (i.e. in poorer countries), GIS tools are not being used to their full potential, even where the facilities exist (e.g. Montserrat).

The benefits of using a GIS for lahar hazard assessment have been demonstrated by this thesis; the challenge is to ensure such research is effectively taken from academia to benefit on-the-ground planning and decision-making. This is especially difficult on an active volcanic system, where data acquisition is difficult, scientists are already working to full capacity and relationships with decision-makers and visiting researchers may be strained.

“[missing from volcano hazard simulation,] is a way to structure model development, selection, and application in a way that maintains the ability to account for fundamental environmental processes at the scale of interest, while accommodating realistic data availability and explicit accounting for uncertainty introduced at each step.” (Renschler, 2005, p. 74).

While the author believes that data-driven lahar modelling should be avoided, if a model is to be selected for application to a real-world problem, model development should be mindful of the limitation of readily available data. It is also fundamental that end-users of models are appreciative of the importance of data quality and how error and uncertainty can propagate from model inputs to outputs, and subsequent decisions.

Ultimately, a lahar hazard assessment, generated in academia, can only be effectively applied to an active volcanic system through consultation and collaboration with end-users.

REFERENCES

-
- ABDALLA, R., TAO, C. V., AND LI, J., 2007, Challenges for the application of GIS interoperability in emergency management. In LI, J., ZLATANOVA, S., AND FABRI, A. G., (Eds.) *Geomatics solutions for disaster management*. Lecture notes in Geoinformation and Cartography, Springer-Verlag, Berlin, p. 389-405.
- ABERBACH, J. D., AND ROCKMAN, B. A., 2002, Conducting and coding elite interviews. *Political Science and Politics*, **35**, 673-676.
- ACKERMAN, C. T., EVANS, T. A., AND BRUNNER, G. W., 2000, HEC-GeoRAS: linking GIS to hydraulic analysis using Arc/Info and HEC-RAS. In MAIDMENT, D., AND DJOKIC, D., (Eds.) *Hydrologic and hydraulic modeling support with geographic information systems*, ESRI Press, Redlands, California, p. 155-176.
- ACREMENT, G. J. AND SCHNEIDER, V. R., 1990, *Guide for selecting Manning's roughness coefficients for natural channels and floodplains*. United States Geological Survey Water Supply Paper 2339, pp. 67.
- AERTS, J. C. J. H., GOODCHILD, M. F., AND HEUVELINK, G. B. M., 2003, Accounting for uncertainty in optimization with spatial decision support systems. *Transactions in GIS*, **7**, 211-230.
- AGUILERA, E., PARESCHI, M. T., ROSI, M., AND ZANCHETTA, G., 2004, Risk from lahars in the Northern Valleys of Cotopaxi Volcano (Ecuador). *Natural Hazards*, **33**, 161-189.
- AGUMYA, A., AND HUNTER, G. J., 1999, A risk-based approach to assessing the 'fitness for use' of spatial data. *Journal of the Urban and Regional Information Systems Association*, **11**, 33-44.
- ALHO, P., RUSSELL, A. J., CARRIVICK, J. L., AND KAYHKO, J., 2005, Reconstruction of the largest Holocene jokulhlaup within Jokulsa a Fjolllum, NE Iceland. *Quaternary Science Reviews*, **24**, 2319-2334.
- ALHO, P., ROBERTS, M. J., AND KAYHKO, J., 2007, Estimating the inundation area of a massive, hypothetical jokulhlaup from northwest Vatnajokull, Iceland. *Natural Hazards*, **41**, 21-42.
- ALHO, P., AND AALTONEN, J., 2008, Comparing a 1D hydraulic model with a 2D hydraulic model for the simulation of extreme glacial outburst floods. *Hydrological Processes*, **22**, 1537-1547.
- ALEXANDER, D., 2007, Making research on geological hazards relevant to stakeholders' needs. *Quaternary International*, **171-172**, 186-192.
- ALEXANDER, D. E., 2008, A brief survey of GIS in mass-movement studies, with reflections on theory and methods. *Geomorphology*, **94**, 261-267.

-
- ALEXANDER, J., BARCLAY, J., SUSNIK, J., LOUGHLIN, S. C., HERD, R. A., DARNELL, A., AND CROSWELLER, S., in press, Sediment-charged flash floods on Montserrat: the influence of previous eruption-related vegetation damage and synchronous tephra-fall. *Journal of Volcanology and Geothermal Research*, DOI: 10.1016/j.jvolgeores.2010.05.002.
- ANDRIENKO, N., AND ANDRIENKO, G., 2006, Intelligent visualisation and information presentation for civil crisis management. *Transactions in GIS*, **11**, 889-909.
- ARNSTEIN, S. R., 1969, A ladder of citizen participation. *American Institute of Planners Journal*, **35**, 216-224.
- ASPINALL, W., AND COOKE, R. M., 1998, Expert judgement and the Montserrat volcano eruption. In MOSLEH, A., AND BARI, R. A., (Eds.) *Proceedings of the 4th International Conference on Probabilistic Safety Assessment and Management*, 13-18th September, New York City, USA, 2113-2118.
- ASPINALL, W. P., LOUGHLIN, S. C., MICHAEL, F. V., MILLER, A. D., NORTON, G. E., ROWLEY, K.C., SPARKS, R. S. J., AND YOUNG, S. R., 2002, The Montserrat Volcano Observatory: its evolution, organization, role and activities. In DRUITT, T. H., AND KOKELAAR, B. P., (Eds.), *The eruption of Soufrière Hills Volcano, Montserrat from 1995 to 1999*. Geological Society of London, Memoir **21**, 71-91.
- BARANI, S., SPALLAROSSA, D., BAZZURRO, P., AND EVA, C., 2007, Sensitivity analysis of seismic hazard for Western Liguria (North Western Italy): a first attempt towards the understanding and quantification of hazard uncertainty. *Tectonophysics*, **435**, 13-35.
- BARCLAY, J., ALEXANDER, J., MATTHEWS, A., JOHNSTONE, J., CHIVERS, C., JOLLY, A., AND NORTON, G., 2004, *Rainfall-induced lahar activity in the Belham Valley*. Report for the Scientific Advisory Committee to the Government of Montserrat, pp. 36.
- BARCLAY, J., JOHNSTONE, J. E., AND MATTHEWS, A. J., 2006, Meteorological monitoring of an active volcano: implications for eruption prediction. *Journal of Volcanology and Geothermal Research*, **150**, 339-358.
- BARCLAY, J., ALEXANDER, J., AND SUSNIK, J., 2007, Rainfall-induced lahars in the Belham Valley, Montserrat, West Indies. *Journal of the Geological Society of London*, **164**, 815-827.
- BARCLAY, J., HAYNES, K., MITCHELL, T., SOLANA, C., TEEUW, R., DARNELL, A., CROSWELLER, H. S., COLE, P., PYLE, D., LOWE, C., FEARNLEY, C., AND KELMAN, I., 2008, Framing volcanic risk communication with disaster risk reduction: finding ways for the social and physical sciences to work together. In LIVERMAN, D. G. E., PEREIRA, C. P. G., AND MARKER, B., (Eds.), *Communicating environmental geoscience*, Geological Society of London, Special Publications, **305**, 163-177.

-
- BASHER, R., 2006, Global early warning systems for natural hazards: systematic and people-centred. *Philosophical Transactions of the Royal Society A: Mathematical, Physical & Engineering Sciences*, **364**, 2167-2182.
- BATES, P. D., AND DE ROO, A. P. J., 2000, A simple raster-based model for flood inundation simulation. *Journal of Hydrology*, **236**, 54-77.
- BCS, 2008, *Cartography: an introduction*. British Cartographic Society, London, pp. 64.
- BERNKNOFF, R. L., RABINOVICI, S. J. M., WOOD, N. J., AND DINITZ, L. B., 2006, The influence of hazard models on GIS-based regional risk assessments and mitigation policies. *International Journal of Risk Assessment and Management*, **6**, 369-387.
- BERTI, M., AND SIMONI, A., 2007, Prediction of debris flow inundation areas using empirical mobility relationships. *Geomorphology*, **90**, 144-161.
- BESSIS, J.-L., BEQUIGNON, J., AND MAHMOOD, A., 2004, Three typical examples of activation of the International Charter 'space and major disasters'. *Advances in Space Research*, **33**, 244-248.
- BEVEN, K., 2000, On model uncertainty, risk and decision making. *Hydrological Processes*, **14**, 2605-2606.
- BOVIS, M. J., AND JAKOB, M., 1999, The role of debris supply conditions in predicting debris flow activity. *Earth Surface Processes and Landforms*, **24**, 1039-1054.
- BOWEN, W., 1997, *Montserrat: First Report of the International Development Committee, Session 1997-98*. HC 267, Stationery Office, House of Commons, London, pp. 206. Available online: <http://www.publications.parliament.uk/pa/cm199798/cmselect/cmintdev/267i/id0102.htm>, accessed March 2010.
- BREWER, C. A., 2005, *Designing better maps: a guide for GIS users*. ESRI Press, Redlands California, pp. 203.
- BROOKES, C. J., HOOKE, J. M., AND MANT, J., 2000, Modelling vegetation interactions with channel flow in river valleys of the Mediterranean region. *Catena*, **40**, 93-118.
- BROWN, J. D., SPENCER, T., AND MOELLER, I., 2007, Modeling storm surge flooding of an urban area with particular reference to modeling uncertainties: a case study of Canvey Island, United Kingdom. *Water Resources Research*, **43**, W06402.
- BRUTSAERT, W., 2005, *Hydrology: an introduction*. Cambridge University Press, Cambridge, UK, pp. 605.

-
- BULMER, M. H., BARNOUIN-JHA, O. S., PEITERSEN, M. N., AND BOURKE, M., 2002, An empirical approach to studying debris flows: implications for planetary modeling studies. *Journal of Geophysical Research*, **107**, 5033.
- BURROUGH, P. A., 1998, Dynamic Modelling and Geocomputation. In LONGLEY, P., BROOKS, S., McDONNELL, R., AND MACMILLAN, B., (Eds.), *Geocomputation: A Primer*. John Wiley & Sons, Chichester, p. 165-191.
- BUTLER, D., 2006A, Mashups mix data into global service. *Nature*, **439**, 6-7.
- BUTLER, D., 2006B, The web-wide world. *Nature*, **439**, 776-778.
- CALLOW, J. N., VAN NIEL, K. P., AND BOGGS, G. S., 2007, How does modifying a DEM to reflect known hydrology affect subsequent terrain analysis? *Journal of Hydrology*, **332**, 30-39.
- CALVO, B., AND SAVI, F., 2009, A real-world application of Monte Carlo procedure for debris flow risk assessment. *Computers & Geosciences*, **35**, 967-977.
- CAMPOLONGO, F., KLEIJEN, J., AND ANDRES, T., 2000, Screening methods. In SALTELLI, A., CHAN, K., AND SCOTT, E. M., (Eds.), *Sensitivity analysis*. John Wiley & Sons, Chichester, p. 65-80.
- CANDELA, A., NOTO, L. V., AND ARONICA, G., 2005, Influence of surface roughness in hydrological response of semiarid catchments. *Journal of Hydrology*, **313**, 119-131.
- CANUTI, P., CASAGLI, N., CATANI, F., AND FALORNI, G., 2002, Modeling the Guagua Pichincha volcano (Ecuador) lahars. *Physics and Chemistry of the Earth*, **27**, 1587-1599.
- CAPRA, L., NORINI, G., GROPELLI, G., MACIAS, J. L., AND ARCE, J. L., 2008, Volcanic hazard zonation of the Nevado de Toluca volcano, Mexico. *Journal of Volcanology and Geothermal Research*, **176**, 469-484.
- CARLISLE, B. H., 2005, Modelling the spatial distribution of DEM error. *Transactions in GIS*, **9**, 521-540.
- CARRANZA, E. J. M., AND CASTRO, O. T., 2006, Predicting lahar-inundation zones: case study in West Mount Pinatubo, Philippines. *Natural Hazards*, **37**, 331-372.
- CARRIVICK, J. L., AND RUSHMER, E. L., 2006, Understanding high-magnitude outburst floods. *Geology Today*, **22**, 60-65.
- CARRIVICK, J. L., MANVILLE, V., AND CRONIN, S. J., 2009, A fluid dynamics approach to modelling the 18th March 2007 lahar at Mt. Ruapehu, New Zealand. *Bulletin of Volcanology*, **71**, 153-169.

-
- CARUSO, P., AND PARESCHI, M. T., 1993, Estimation of lahar and lahar-runout flow hydrograph on natural beds. *Environmental Geology*, **22**, 141–152.
- CARVER, S., 2003, The future of participatory approaches using geographic information: developing a research agenda for the 21st Century. *URISA Journal*, **15**, 61-71.
- CENDERILLI, D. A., AND WOHL, E. E., 2001, Peak discharge estimates of glacial-lake outburst floods and ‘normal’ climatic floods in the Mount Everest region, Nepal. *Geomorphology*, **40**, 57-90.
- CHESTER, D. K., DIBBEN, C. J. L., AND DUNCAN, A. M., 2002, Volcanic hazard assessment in western Europe. *Journal of Volcanology and Geothermal Research*, **115**, 411-435.
- CLOKE, H. L., PAPPENBERGER, F., AND RENAUD, J.-P., 2008, Multi-method global sensitivity analysis (MMGSA) for modelling floodplain hydrological processes. *Hydrological Processes*, **22**, 1660-1674.
- CHOW, V. T., 1959, *Open channel hydraulics*. McGraw-Hill, New York, pp. 677.
- CLAY, E., BARROW, C., BENSON, C., DEMPSTER, J., KOKELAAR, P., PILLAI, N., AND SEAMAN, J., 1999, *An evaluation of HMG’s response to the Montserrat volcanic emergency*. Department for International Development, Evaluation Report EV635, pp. 87.
- CODILEAN, A. T., BISHOP, P., AND HOEY, T. B., 2006, Surface process models and the links between tectonics and topography. *Progress in Physical Geography*, **30**, 307-333.
- COHEN, J., 1960, A coefficient of agreement for nominal scales. *Educational and Psychological Measurement*, **20**, 37-46.
- COPPOCK, J. T., 1995, GIS and natural hazards: an overview from a GIS perspective. In CARRARA, A., AND GUZZETTI, F., (Eds.), *Geographical information systems in assessing natural hazards*, Kluwer Academic, Netherlands, p. 21–34.
- COUCLELIS, H., 2003, The certainty of uncertainty: GIS and the limits of geographic knowledge. *Transactions in GIS*, **7**, 165-175.
- COVA, T. J., AND CHURCH, R. L., 1997, Modelling community evacuation vulnerability using GIS. *International Journal of Geographical Information Science*, **11**, 763-784.
- COVA, T. J., 1999, GIS in emergency management. In Longley, P.A., Goodchild, M.F., Maguire, D.J., Rhind, D.W. (Eds.), *Geographical Information Systems: Principles, Techniques, Applications, and Management*, John Wiley & Sons, New York, p. 845-858.

-
- CRANDELL, D. R., BOOTH, B., KUSUMADINATA, K., SHIMOZURU, D., WALKER, G. P. L., AND WESTERCAMP, D., 1984, Source-book for volcanic-hazards zonation. United Nations Educational, Scientific and Cultural Organization, France, pp. 97.
- CRED, 2010, *EM-DAT: the international disaster database*. Centre for Research on the Epidemiology of Disasters. Available online: <http://www.emdat.be/disaster-list>, accessed May, 2010.
- CRONIN, S. J., HODGSON, K. A., NEALL, V. E., PALMER, A. S., AND LECOINTRE, J. A., 1997, 1995 Ruapehu lahars in relation to the late Holocene lahars of Whangaehu River, New Zealand. *New Zealand Journal of Geology and Geophysics*, **40**, 507-520.
- CRONIN, S. J., NEALL, V. E., LECOINTRE, J. A., AND PALMER, A. S., 1999, Dynamic interactions between lahars and stream flow: a case study from Ruapehu volcano, New Zealand. *GSA BULLETIN*, **111**, 28-38.
- CRONIN, S. J., GAYLORD, D. R., CHARLEY, D., ALLOWAY, B. V., WALLEZ, S., AND ESAU, J. W., 2004A, Participatory methods of incorporating scientific with traditional knowledge for volcanic hazard management on Ambre Island, Vanuatu. *Bulletin of Volcanology*, **66**, 652-668.
- CRONIN, S. J., PETTERSON, M. G., TAYLOR, P. W., AND BILIKI, R., 2004b, Maximising multi-stakeholder participation in government and community volcanic hazard management programs; a case study from Savo, Solomon Islands. *Natural Hazards*, **33**, 105-136.
- CROSETTO, M., AND TARANTOLA, S., 2001, Uncertainty and sensitivity analysis: tools for GIS-based model implementation. *International Journal of Geographical Information Science*, **15**, 415-437.
- CROZIER, M., MCCLURE, J., VERCOE, J., AND WILSON, M., 2006, The effects of hazard zone information on judgements about earthquake damage. *Area*, **38.2**, 143-152.
- CUTTER, S. L., 2003, GI Science, disasters, and emergency management. *Transactions in GIS*, **7**, 439-445.
- CUTTER, S. L., RICHARDSON, D. B., AND WILBANKS, T. J., 2003, *The geographical dimensions of terrorism*. Taylor and Francis, London, pp. 274.
- DARNELL, A. R., TATE, N. J., AND BRUNSDON, C., 2008, Improving user assessment of error implications in digital elevation models. *Computers, Environment and Urban Systems*, **32**, 268-277.
- DARNELL, A., LOVETT, A., BARCLAY, J., AND HERD, R., 2009, DEM fitness for delineation of lahar inundation hazard zones. *Proceedings of the GIS Research UK 17th Annual Conference, 1st-3rd April 2009*, University of Durham, p. 197-201.

-
- DARNELL, A. R., LOVETT, A. L., BARCLAY, J., AND HERD, R. A., 2010, An application-driven approach to terrain model construction. *International Journal of Geographical Information Science*, **24**, 1171-1191.
- DAVILA, N., CAPRA, L., GAVILANES-RUIZ, J. C., VARLEY, N., NORINI, G., GOMEZ VAZQUEZ, A., 2007, Recent lahars at Volcan de Colima (Mexico): drainage variation and spectral classification. *Journal of Volcanology and Geothermal Research*, **165**, 127-141.
- DAVIS, I., SANDERSON, D., PARKER, D., AND STACK, J., 1998, The dissemination of warnings. In LEE, B. E., AND DAVIS, I., (Eds.), *Forecasts and warnings, UK International Decade for Natural Disaster Reduction Flagship Programme*, UK National Coordination Committee, Department for International Development, Thomas Telford, London, pp. 300. Available online: <http://desastres.usac.edu.gt/documentos/pdf/eng/doc12098/doc12098.htm>, accessed March 2010.
- DE ANGELIS, S., BASS, V., HARDS, V., AND RYAN, G., 2007, Seismic characterisation of pyroclastic flow activity at Soufrière Hills Volcano, Montserrat, 8 January 2007. *Natural Hazards and Earth Systems Sciences*, **7**, 467-472.
- DE BRUIN, S., BREGT, A., AND VAN DE VAN, M., 2001, Assessing fitness for use: the expected value of spatial data sets. *International Journal of Geographical Information Science*, **15**, 457-471.
- DENLINGER, R. P., AND IVERSON, R. M., 2001, Flow of variably fluidized granular masses across three-dimensional terrain 2. numerical predictions and experimental tests. *Journal of Geophysical Research*, **106**, 553-566.
- DE WOLFE, V. G., SANTI, P. M., EY, J., AND GARTNER, J. E., 2008, Effective mitigation of debris flows at Lemon Dam, La Plata County, Colorado. *Geomorphology*, **96**, 366-377.
- DFID, 2005, *Montserrat Country Policy Plan*. Department for International Development, pp. 18. Available online: <http://www.dfid.gov.uk/Documents/publications/montserrat-cpp05.pdf>, accessed March 2010.
- DITTMER, J., 2004, The Soufrière Hills Volcano and the postmodern landscapes of Montserrat. *Focus on Geography*, **47**, 1-7.
- DONNELLY, L. J., 2007, Engineering geology of landslides on the volcanic island of Montserrat, West Indies. *Quarterly Journal of Engineering Geology and Hydrogeology*, **40**, 267-292.
- DORLING, D., AND FAIRBAIRN, D., 1997, *Mapping: ways of representing the world*. Longman, London, pp. 192.

-
- DRABEK, T. E., AND HOETMER, G. J., 1991, *Emergency management: principles and practice for local government*. International City Management Association, Washington DC, pp. 368.
- DRUITT, T. H., AND KOKELAAR, B. P., 2002, *The eruption of Soufrière Hills Volcano, Montserrat from 1995 to 1999*. Geological Society of London, Memoir **21**.
- DUNN, C. E., 2007, Participatory GIS – a people’s GIS? *Progress in Physical Geography*, **31**, 616-637.
- ECONOMIST, 2003, Disaster area: How to make a living from a volcano. *Economist*, **368**, 36.
- EDMONDS, M., HERD, R. A., AND STRUTT, M. H., 2006, Tephra deposits associated with a large lava dome collapse, Soufrière Hills Volcano, Montserrat, 12-15 July 2003. *Journal of Volcanology and Geothermal Research*, **153**, 313-330.
- ELHANAFY, H., COPELAND, G. J. M., AND GEJADZE, I. Y., 2008, Estimation of predictive uncertainties in flood wave propagation in a river channel using adjoint sensitivity analysis. *International Journal for Numerical Methods in Fluids*, **56**, 1201-1207.
- ELWOOD, S., 2006, Critical issues in participatory GIS: deconstructions, reconstructions, and new research directions. *Transactions in GIS*, **10**, 693-708.
- ELWOOD, S., 2008, Volunteered geographic information: key questions, concepts and methods to guide emerging research and practice. *GeoJournal*, **72**, 133-135.
- EMMI, P. C., AND HORTON, C. A., 1995, A Monte Carlo simulation of error propagation in a GIS-based assessment of seismic risk. *International Journal of Geographical Information Science*, **9**, 447-461.
- ESRI, 2002, *Lessons from 9/11: good metadata is key*. ESRI Press, California, pp. 2. Available online: <http://www.esri.com/library/fliers/pdfs/lessons-learned.pdf>, accessed May 2010.
- FAGENTS, S. A., AND BALOGA, S. M., 2005, Calculation of lahar transit times using digital elevation data. *Journal of Volcanology and Geothermal Research*, **139**, 135-146.
- FAGENTS, S. A., AND BALOGA, S. M., 2006, Toward a model for bulking and debulking of lahars. *Journal of Geophysical Research*, **111**, B10201.
- FEDRA, K., 1993, Models, GIS and expert systems: Integrated water resources models, *Proceedings of HydroGIS'93: Application of Geographic Information System in Hydrology and Water Resources, 19th-22nd April*, Vienna, Austria, **211**.

-
- FELL, R., COROMINAS, J., BONNARD, C., CASCINI, L., LEROI, E., AND SAVAGE, W. Z., 2008. Guidelines for landslide susceptibility, hazard and risk zoning for land use planning. *Engineering Geology*, **102**, 85-98.
- FELPETO, A., ARANA, V., ORTIZ, R., ASTIZ, M., AND GARCIA, A., 2001, Assessment and modelling of lava flow hazard on Lanzarote (Canary Islands). *Natural Hazards*, **23**, 247-257.
- FELPETO, A., MARTI, J., AND ORTIZ, R., 2007, Automatic GIS-based system for volcanic hazard assessment. *Journal of Volcanology and Geothermal Research*, **166**, 106-116.
- FERRIER, N., AND HAQUE, C. E., 2003, Hazard risk assessment methodology for emergency managers: a standardized framework for application. *Natural Hazards*, **28**, 271-290.
- FISCHOFF, B., 1995, Risk perception and communication unplugged: twenty years of process. *Risk Analysis*, **15**, 137-145.
- FISHER, R. V. AND HEIKEN, G., 1982, Mt Pelee, Martinique: May 8 and 20, 1902, pyroclastic flows and surges. *Journal of Volcanology and Geothermal Research*, **13**, 339-371.
- FISHER, R. V., 1990, Transport and deposition of a pyroclastic surge across an area of high relief: the 18 May 1980 eruption of Mount St Helens, Washington. *Geological Society of America Bulletin*, **102**, 1038-1054.
- FISHER, P., 1998, Improved modelling of elevation error with geostatistics. *Geoinformatica*, **2**, 215-233.
- FISHER, P. F., 1999, MODELS OF UNCERTAINTY IN SPATIAL DATA. In LONGLEY, P., GOODCHILD, M., MAGUIRE, D., AND RHIND, D., (Eds.), *Geographical Information Systems: Principles, Techniques, Management and Applications*. John Wiley & Sons, New York, p. 191-205.
- FISHER, P., 2000, Sorites paradox and vague geographies. *Fuzzy Sets and Systems*, **113**, 7-18.
- FISHER, P. F., 2010, Remote sensing of land cover classes as type 2 fuzzy sets. *Remote Sensing of Environment*, **114**, 309-321.
- FISHER, P, AND TATE, N. J., 2006, Causes and consequences of error in digital elevation models. *Progress in Physical Geography*, **30**, 467-489.

-
- FISKE, R. S., 1984, Volcanologists, journalists, and the concerned local public: A tale of two crises in the eastern Caribbean. In National Research Council, *Explosive Volcanism: Inception, Evolution, and Hazards*. Studies in Geophysics, National Academy Press, Washington, DC, p. 170-176.
- FOX, A., 2002, Montserrat – a case study in the application of multiple methods to meet a post-disaster housing shortage. *Proceedings of the 1st international conference on Improving post-disaster reconstruction in developing countries*, 23rd-25th May, University of Montreal, Canada. Available online: <http://www.grif.umontreal.ca/pages/i-rec%20papers/andrew.PDF>, accessed March 2010.
- FREY, H. C., AND PATIL, S. R., 2002, Identification and review of sensitivity analysis methods. *Risk Analysis*, **22**, 553-578.
- GAHEGAN, M., 1999, Four barriers to the development of effective exploratory visualisation tools for the geosciences. *International Journal of Geographical Information Science*, **13**, 289-309.
- GAMPER, C. D., THONI, M., AND WECK-HANNEMANN, H., 2006, A conceptual approach to the use of Cost Benefit and Multi Criteria analysis in natural hazard management. *Natural Hazards and Earth Systems Sciences*, **6**, 293-302.
- GATRELL, A. C., VINCENT, P., 1991, Managing natural and technological hazards. In MASSER, I., BLAKEMORE, M., (Eds.), *Handling geographical information: methodology and potential applications*. Longman, Harlow, UK, p. 148–180.
- GIBBS, D., 1986, Montserrat. In SCOTT, D. A., AND CARBONNELL, M., (Eds.) *A directory of neotropical wetlands*. Page Bros., Norwich, p. 547-549.
- GILLESPIE, T. W., CHU, J., FRANKENBERG, E., AND THOMAS, D., 2007, Assessment and prediction of natural hazards from satellite imagery. *Progress in Physical Geography*, **31**, 459-470.
- GIOIA, G., AND BOMBARDELLI, F. A., 2002, Scaling and similarity in rough channel flows. *Physical Review Letters*, **88**, 014501.
- GOGU, R. C., DIETRICH, V. J., JENNY, B., SCHWANDNER, F. M., AND HURNI, L., 2006, A geo-spatial data management system for potentially active volcanoes—GEOWARN project. *Computers & Geosciences*, **32**, 29-41.
- GoM, 2005, *Montserrat national report and information on disaster reduction*. Report submitted to World Conference on Disaster Reduction, Kobe-Hyogo, Japan, 18-22 January 2005, Government of Montserrat, pp. 10. Available online: <http://www.unisdr.org/eng/mdgs-drr/national-reports/Montserrat-report.pdf>, accessed May 2010.

-
- GOMEZ-DELGADO, M., AND TARANTOLA, S., 2006, GLOBAL sensitivity analysis, GIS and multi-criteria evaluation for a sustainable planning of a hazardous waste disposal site in Spain. *International Journal of Geographical Information Science*, **5**, 449-466.
- GOMEZ-FERNANDEZ, F., 2000, Contribution of geographic information systems to the management of volcanic crises. *Natural Hazards*, **21**, 347-360.
- GOODCHILD, M. F., 1992, Geographical Information Science. *International Journal of Geographical Information Systems*, **6**, 31-45.
- GOODCHILD, M. F., 2003a, Geospatial data in emergencies. In CUTTER, S. L., RICHARDSON, D. B., AND WILBANKS, T. J., (Eds.), *The Geographical Dimensions of Terrorism*. Routledge, New York, p. 99-104.
- GOODCHILD, M. F., 2003b, Data modeling for emergencies. In CUTTER, S. L., RICHARDSON, D. B., AND WILBANKS, T. J., (Eds.), *The Geographical Dimensions of Terrorism*. Routledge, New York, p. 105–110.
- GOODCHILD, M. F., 2006, GIS and disasters: planning for catastrophe. *Computers, Environment and Urban Systems*, **30**, 227-229.
- GOODCHILD, M. F., 2008, Geographic information science: the grand challenges. In WILSON, J.P., AND FOTHERINGHAM, A.S., (Eds.), *The Handbook of Geographic Information Science*. Blackwell, Malden, USA, p. 596–608.
- GOODCHILD, M. F., 2009, Geographic information systems and science: today and tomorrow. *Annals of GIS*, **15**, 3-9.
- GORDON, N. D., McMAHON, T. A., FINLAYSON, B. L., GIPPEL, C. J., AND NATHAN, R. J., 2004, *Stream hydrology: an introduction for ecologists*. John Wiley & Sons, Chichester, pp. 444.
- Goss, J., 1995, Marketing the new marketing: The strategic discourse of geodemographic information systems. In PICKLES, J., (Ed.) *Ground Truth: The Social Implications of Geographic Information Systems*. Guilford Press, London. p. 130–170.
- GRISWOLD, J.P., AND IVERSON, R.M., 2008. Mobility statistics and automated hazard mapping for debris flows and rock avalanches. *Scientific Investigations Report 2007-5276*, United States Geological Survey, Reston, VA.
- GROHMAN, G., KROENUNG, G., AND STREBECK, J., 2006, Filling SRTM voids: the Delta surface fill method. *Photogrammetric Engineering and Remote Sensing*, **72**, 213-216.

-
- HALL, J. W., TARATOLA, S., BATES, P. D., AND HORRITT, M. S., 2005, Distributed sensitivity analysis of flood inundation model calibration. *Journal of Hydraulic Engineering*, **131**, 117-126.
- HALLISEY, E. J., 2005, Cartographic visualization: an assessment and epistemological review. *The Professional Geographer*, **57**, 350-364.
- HARDY, R. J., 2006, Fluvial geomorphology. *Progress in Physical Geography*, **30**, 553-567.
- HARFORD, C. L., PRINGLE, M. S., SPARKS, R. S. J., AND YOUNG, S. R., 2002, The volcanic evolution of Montserrat using Ar/ Ar geochronology. In DRUITT, T. H. AND KOKELAAR, B. P. (Eds.) *The eruption of Soufriere Hills Volcano, Montserrat from 1995 to 1999*. Geological Society of London, Memoir **21**, p. 93-114.
- HASSAN, M. M., 2005, Arsenic poisoning in Bangladesh: spatial mitigation planning with GIS and public participation. *Health Policy*, **74**, 247-260.
- HAYASHI, J. N., AND SELF, S., 1992, A comparison of pyroclastic flow and debris avalanche mobility. *Journal of Geophysical Research*, **97**, 9063–9071.
- HAYES, S. K., MONTGOMERY, D. R., AND NEWHALL, C. G., 2002, Fluvial sediment transport and deposition following the 1991 eruption of Mount Pinatubo, *Geomorphology*, **45**, 211-224.
- HAYNES, K., BARCLAY, J., AND PIDGEON, N., 2007, Volcanic hazard communication using maps: an evaluation of their effectiveness. *Bulletin of Volcanology*, **70**, 123-138.
- HAYNES, K., BARCLAY, J., AND PIDGEON, N., 2008A, The issue of trust and its influence on risk communication during a volcanic crisis. *Bulletin of Volcanology*, **70**, 605-621.
- HAYNES, K., BARCLAY, J., AND PIDGEON, N., 2008B, Whose reality counts? Factors affecting the perception of volcanic risk. *Journal of Volcanology and Geothermal Research*, **172**, 259-272.
- HEO, J., 2003, Steepest descent method for representing spatially correlated uncertainty in GIS. *Journal of Surveying Engineering*, **129**, 151 – 157.
- HERD, R. A., EDMONDS, M., AND BASS, V. M., 2005, Catastrophic lava dome failure at Soufriere Hills Volcano, Montserrat, 12-13 July 2003. *Journal of Volcanology and Geothermal Research*, **148**, 234-252.
- HEROD, A., 1999, Reflections on interviewing foreign elites: praxis, positionality, validity, and the cult of the insider. *Geoforum*, **30**, 313-327.

-
- HESSEL, R., 2006, Consequences of hyperconcentrated flow for process-based soil erosion modelling on the Chinese Loess Plateau. *Earth Surface Processes and Landforms*, **31**, 1100-1114.
- HEUVELINK, G. B. M., 1998, *Error Propagation in Environmental Modelling with GIS*. Research monographs in GIS series. Taylor and Francis, London, pp. 127.
- HEUVELINK, G. B. M., BROWN, J. D., AND VAN LOON, E. E., 2007, A probabilistic framework for representing and simulating uncertain environmental variables. *International Journal of Geographical Information Science*, **21**, 497-513.
- HINCKS, T. K., SPARKS, R. S. J., DUNKLEY, P., COLE, P., 2005, Montserrat. In LINDSAY, J. M., ROBERTSON, R. E. A., SHEPHERD, J. B. AND ALI, S., (Eds.), *Volcanic Hazard Atlas of the Lesser Antilles*. Seismic Research Unit, The University of the West Indies, Trinidad and Tobago, W.I., p. 148-167.
- HINCKS, T. K., ASPINALL, W. P., BAXTER, P. J., SEARL, A., SPARKS, R. S. J., AND WOO, G., 2006, Long term exposure to respirable volcanic ash on Montserrat: a time series simulation. *Bulletin of Volcanology*, **68**, 266-284.
- HOLMES, K. W., CHADWICK, O. A., AND KYRIAKIDIS, P. C., 2000, Error in a USGS 30-meter digital elevation model and its impact on terrain modeling. *Journal of Hydrology*, **233**, 154-173.
- HOOPER, D. M., AND MATTIOLI, G. S., 2001, Kinematic modelling of pyroclastic flows produced by gravitational dome collapse at Soufrière Hills Volcano, Montserrat. *Natural Hazards*, **23**, 65-86.
- HORN, B. K. P., 1981, Hill shading and the reflectance map, *Proceedings of IEEE*, **69**, 14-47.
- HORRITT, M. S., 2005, Parameterisation, validation and uncertainty analysis of CFD models of fluvial and flood hydraulics in the natural environment. In BATES, P. D., LANE, S. N., AND FERGUSON, R. I., (Eds.), *Computational Fluid Dynamics Applications in Environmental Hydraulics*. John Wiley & Sons, Chichester, p. 193-213.
- HORWELL, C. J., SPARKS, R. S. J., BREWER, T. S., LLEWELLIN, E. W., AND WILLIAMSON, B. J., 2003, Characteristics of respirable volcanic ash from the Soufriere Hills volcano, Montserrat, with implications for human health hazards. *Bulletin of Volcanology*, **65**, 346-362.
- HUBBARD, B. E., SHERIDAN, M. F., CARRASCO-NUNEZ, G., DIAZ-CASTELLON, R., RODRIGUEZ, S. R., 2007, Comparative lahar hazard mapping at Volcan Citlaltepétl, Mexico using SRTM, ASTER and DTED-1 digital topographic data. *Journal of Volcanology and Geothermal Research*, **160**, 99-124.

-
- HUEBL, J., AND FIEBIGER, G., 2005, Debris-flow mitigation measures. In JAKOB, M., AND HUNGR, O., (Eds.) *Debris-flow hazards and related phenomena*. Springer-Verlag, Berlin, p. 445-488.
- HUGENTOBLER, M AND SCHNIEDER, B, 2005, Breaklines in Coons surfaces over triangles for the use in terrain modelling. *Computers & Geosciences*, **31**, 45-54.
- HUGGEL, C., KAAB, A., HAEBERLI, W., AND KRUMMENACHER, B., 2003, Regional-scale GIS-models for assessment of hazards from glacier lake outburst: evaluation and application in the Swiss Alps. *Natural Hazards and Earth System Sciences*, **3**, 647-662.
- HUGGEL, C., SCHNEIDER, D., JULIO MIRANDA, P., DELGADO GRANADOS, H., AND KAAB, A., 2008, Evaluation of ASTER and SRTM DEM data for lahar modelling: a case study on lahars from Popocatepetl Volcano, Mexico. *Journal of Volcanology and Geothermal Research*, **170**, 99-110.
- HUGHES, M. L., MCDOWELL, P. F., AND MARCUS, W. A., 2006, Accuracy assessment of georectified aerial photographs: implications for measuring lateral channel movement in a GIS. *Geomorphology*, **74**, 1-16.
- HUNGR, O., 2000, Analysis of debris flow surges using the theory of uniformly progressive flow. *Earth Surface Processes and Landforms*, **25**, 483-495.
- HUNTER, G. J., CAETANO, M, AND GOODCHILD, M. F., 1995, A methodology for reporting uncertainty in spatial database products. *Journal of the Urban and Regional Information Systems Association*, **7**, 11-21.
- HUNTER, G. J., AND DE BRUIN, S., 2006, A case study in the use of risk management to assess decision quality. In DEVILLERS, R., AND JEANSOULIN, R., (Eds.), *Fundamentals of Spatial Data Quality*. Geographical Information Systems Series, ITSE, London, p. 271- 282.
- HUNTER, G. J., AND GOODCHILD, M. F., 1995, Dealing with error in spatial databases: a simple case study. *Photogrammetric Engineering & Remote Sensing*, **61**, 529-537.
- HUNTER, G. J., AND GOODCHILD, M. F., 1997, Modelling the uncertainty of slope and aspect estimates derived from spatial databases. *Geographical Analysis*, **29**, 35-49.
- HURLIMANN, M., RICKENMANN, D., MEDINA, V., AND BATEMAN, A., 2008, Evaluation of approaches to calculate debris-flow parameters for hazard assessment. *Engineering Geology*, **102**, 152-163.
- HYDROLOGIC ENGINEERING CENTER, 2008, *HEC-RAS River Analysis System user's manual, version 4.0*. US Army Corps of Engineers, Institute for Water Resources, Hydrologic Engineering Center, pp. 747.

-
- IAVCEI SUBCOMMITTEE FOR CRISIS PROTOCOLS, 1999, Professional conduct of scientists during volcanic crises. *Bulletin of Volcanology*, **60**, 323-334.
- IAVCEI SUBCOMMITTEE FOR CRISIS PROTOCOLS, 2000, Reply. *Bulletin of Volcanology*, **62**, 62-64.
- IVERSON, R. M., 1997, The physics of debris flows. *Reviews of Geophysics*, **35**, 245-296.
- IVERSON, R. M., AND DENLINGER, R. P., 2001, Flow of variably fluidized granular masses across three-dimensional terrain 1. Coulomb mixture theory. *Journal of Geophysical Research*, **106**, 537-552.
- IVERSON, R. M., SCHILLING, S. P., VALLANCE, J. W., 1998, Objective delineation of lahar-inundation hazard zones. *Geological Society of America Bulletin*, **110**, 972-984.
- JAKOB, M., 2005, Debris-flow hazard analysis. In JAKOB, M., AND HUNGR, O., (Eds.), *Debris-flow hazards and related phenomena*. Springer-Verlag, Berlin, p. 411-443.
- JAKOB, M., AND WEATHERLY, H., 2008, Integrating uncertainty: Canyon Creek hyperconcentrated flows of November 1989 and 1990. *Landslides*, **5**, 83-95.
- JANKOWSKI, P., ANDRIENKO, N., AND ANDRIENKO, G., 2001, Map-centred exploratory approach to multiple criteria spatial decision making. *International Journal of Geographical Information Science*, **15**, 101-127.
- JARVIS, C. H., STUART, N., BAKER, R. H. A., AND MORGAN, D., 1999, To interpolate and thence to model, or vice versa? In GITTINGS, B., (Ed.) *Integrating Information Infrastructures with GI Technology*. Innovations in GIS 6, Taylor and Francis, London, p. 229-242.
- JASONOFF, S., 1999, The songlines of risk. *Environmental Values*, **8**, 135-152.
- JENSEN, J., SAALFELD, A., BROOME, F., COWEN, D., PRICE, K., RAMSEY, D., LAPINE, L., AND USERY, E. L., 2005, Spatial data acquisition and integration. In MCMMASTER, R. B., AND USERY, E. L., (Eds.), *A research agenda for geographical information science*. CRC Press, Florida, USA, p. 17-60.
- JENSON, S. K., AND DOMINGUE, J. O., 1988, Extracting topographic structures from digital elevation data for geographic information system analysis. *Photogrammetric Engineering & Remote Sensing*, **54**, 1593-1600.
- JOHNSON, R., 2000, *GIS technology for disasters and emergency management*. ESRI White Paper, Redlands, California, pp. 12. Available online: <http://www.esri.com/library/whitepapers/pdfs/disastermgmt.pdf>, accessed May 2010.
- JONES, K. H., 1998, A comparison of algorithms used to compute hill slope as a property of the DEM. *Computer and Geosciences*, **24**, 315-323.

-
- JONES, M., 2008, *Distribution and conservation of Montserrat's endemic flora*. A thesis submitted in partial fulfilment of the requirements for the degree of Master of Science and the Diploma of Imperial College London, pp. 75.
- JOYCE, K. E., SAMSONOV, S., MANVILLE, V., JONGENS, R., GRAETTINGER, A., AND CRONIN, S. J., 2009, Remote sensing data types and techniques for lahar path detection: a case study at Mt Ruapehu, New Zealand. *Remote Sensing of Environment*, **113**, 1778-1786.
- KENNY, F., AND MATTHEWS, B., 2005, A methodology for aligning raster flow direction data with photogrammetrically mapped hydrology. *Computers & Geosciences*, **31**, 768-779.
- KERLE, N., AND OPPENHEIMER, C., 2002, Satellite remote sensing as a tool in lahar disaster management. *Disasters*, **26**, 140-160.
- KERLE, N., FROGER, J.-L., OPPENHEIMER, C., AND VAN WYK DE VRIES, B., 2003, Remote sensing of the 1998 mudflow at Casita volcano, Nicaragua. *International Journal of Remote Sensing*, **24**, 4791-4816.
- KERVYN, M., KERVYN, F., GOOSSENS, R., ROWLAND, S. K., AND ERNST, G. G. J., 2007, Mapping volcanic terrain using high-resolution and 3D satellite remote sensing. In TEEUW, R. M., (Ed.) *Mapping hazardous terrain using remote sensing*. Geological Society of London, Special Publications, **283**, 5-30.
- KEYS, H. J. R., 2007, Lahars of Ruapehu Volcano, New Zealand: risk mitigation. *Annals of Glaciology*, **45**, 155-162.
- KLING, G. W., CLARK, M. A., COMPTON, H. R., DEVINE, J. D., EVANS, W. C., HUMPHREY, A. M., KOENIGSBERG, E. J., LOCKWOOD, J. P., TUTTLE, M. L., AND WAGNER, G. N., 1987, The 1986 Lake Nyos gas disaster in Cameroon, West Africa. *Science*, **236**, 169-175.
- KOKELAAR, B. P., 2002, Setting, chronology and consequences of the eruption of Soufriere Hills Volcano, Montserrat (1995-1999). In DRUITT, T. H. AND KOKELAAR, B. P. (Eds.) *The eruption of Soufrière Hills Volcano, Montserrat from 1995 to 1999*. Geological Society of London, Memoir **21**, p. 1-43.
- KUUSKIVI, T., LOCK, J., LI, X., DOWDING, S., AND MERCER, B., 2005, Void fill of SRTM elevation data: performance evaluations. *Proceedings of the ASPRS 2005 Annual Conference, 7th-11th March*, Baltimore, MD, USA. Available online: <ftp://ftp.ecn.purdue.edu/jshan/proceedings/asprs2005/Files/0087.pdf>, accessed May 2010.
- KWAN, M.-P., AND LEE, J., 2005, Emergency response after 9/11: the potential of real-time 3D GIS for quick emergency response in micro-spatial environments. *Computers, Environment and Urban Systems*, **29**, 93-113.

-
- KYRIAKIDIS, P. C., SHORTRIDGE, A. M., AND GOODCHILD, M. F., 1999, Geostatistics for conflation and accuracy assessment of digital elevation models. *International Journal of Geographical Information Science*, **13**, 677-707.
- LAENEN, A., AND HANSEN, R. P., 1988, *Simulation of three lahars in the Mount St. Helens area, Washington, using a one-dimensional, unsteady stream flow model*. United States Geological Survey Water-Resources Investment Report, 88-4004, pp. 20.
- LANDIS, J. R., AND KOCH, G. G., 1977, The measurement of observer agreement for categorical data. *Biometrics*, **33**, 159-174.
- LAURINI, R., AND THOMPSON, D., 1992, *Fundamentals of Spatial Information Systems*. The APIC Series Number 37, Academic Press, London, pp. 680.
- LAVIGNE, F., THOURET, J. C., VOIGHT, B., SUWA, H., AND SUMARYONO, A., 2000, Lahars at Merapi volcano, Central Java: on overview. *Journal of Volcanology and Geothermal Research*, **100**, 423-456.
- LAVIGNE, F., AND THOURET, J.-C., 2002, Sediment transportation and deposition by rain-triggered lahars at Merapi Volcano, Central Java, Indonesia. *Geomorphology*, **49**, 45-69.
- LECOINTRE, J., HODGSON, K., NEALL, V., AND CRONIN, S., 2004, Lahar-triggering mechanism and hazard at Ruapehu Volcano, New Zealand. *Natural Hazards*, **31**, 85-109.
- LEONE, F., AND LESALES, T., 2009, The interest of cartography for a better perception and management of volcanic risk: from scientific to social representations the case of Mt Pelee volcano, Martinique (Lesser Antilles). *Journal of Volcanology and Geothermal Research*, **186**, 186-194.
- LI, Y., BRIMICOMBE, A. J., AND RALPHS, M. P., 2000, Spatial data quality and sensitivity analysis in GIS and environmental modelling: the case of coastal oil spills. *Computers, Environment and Urban Systems*, **24**, 95-108.
- LILBURNE, L., AND TARANTOLA, S., 2008, Sensitivity analysis of spatial models. *International Journal of Geographical Information Science*, **23**, 151-168.
- LIRER, L., AND VITELLI, L., 1998, Volcanic risk assessment and mapping in the Vesuvian area using GIS. *Natural Hazards*, **17**, 1-15.
- LIU, Y. B., GEBREMESKEL, S., DE SMEDT, F., HOFFMANN, L., AND PFISTER, L., 2003, A diffusive transport approach for flow routing in GIS-based flood modeling. *Journal of Hydrology*, **283**, 91-106.
- LONGLEY, P. A., GOODCHILD, M. F., MAGUIRE, D. J., AND RHIND, D. W., 2001, *Geographical information systems and science*. John Wiley & Sons, Chichester, pp. 472.

-
- LONGLEY, P. A., GOODCHILD, M. F., MAGUIRE, D. J., AND RHIND, D. W., 2005, *Geographical information systems and science, second edition*. John Wiley & Sons, Chichester, pp. 517.
- LOUGHLIN, S. C., BAXTER, P. J., ASPINALL, W. P., DARROUX, B., HARFORD, C. L., AND MILLER, A. D., 2002, Eyewitness accounts of the 25 June 1997 pyroclastic flows and surges at Soufrière Hills Volcano, Montserrat, and implications for disaster mitigation. In DRUITT, T. H. AND KOKELAAR, B. P., (Eds.), *The eruption of Soufrière Hills Volcano, Montserrat from 1995 to 1999*. Geological Society of London, Memoir **21**, 211-230.
- LUEDLING, E., SIEBERT, S., AND BUERKERT, A., 2007, Filling the voids in the SRTM elevation model – a TIN-based delta surface approach. *ISPRS Journal of Photogrammetry & Remote Sensing*, **62**, 283-294.
- MACEDONIO, G., AND PARESCHI, M. T., 1992, Numerical simulation of some lahars from Mount St. Helens. *Journal of Volcanology and Geothermal Research*, **54**, 65-80.
- MACIAS, J. L., CAPRA, L., ARCE, J. L., ESPINDOLA, J. M., GARCIA-PALOMO, AND SHERIDAN, M. F., 2008, Hazard map of El Chichon volcano, Chiapas, Mexico: constraints posed by eruptive history and computer simulations. *Journal of Volcanology and Geothermal Research*, **175**, 444-458.
- MAGRIL, C. S., GRIFFITHS, P. G., AND WEBB, R. H., 2010, Analyzing debris flows with the statistically calibrated empirical model LAHARZ in southeastern Arizona, USA. *Geomorphology*, **119**, 111-124.
- MAIDMENT, D. R., OLIVERA, F., CALVER, A., EATHERALL, A., AND FRACZEK, W., 1996, Unit hydrograph derived from a spatially distributed velocity field. *Hydrological Processes*, **10**, 831- 844.
- MALIN, M. C., AND SHERIDAN, M. F., 1982, Computer-assisted mapping of pyroclastic surges. *Science*, **217**, 637-640.
- MANVILLE, V., NEMETH, K., AND KANO, K., 2009, Source to sink: a review of three decades of progress in the understanding of volcanoclastic processes, deposits, and hazards. *Sedimentary Geology*, **220**, 136-161.
- MAPACTION, 2008, *Google Earth and its potential in the humanitarian sector: a briefing paper*. MapAction, pp. 10. Available online: http://www.mapaction.org/images/stories/google_earth_and_its_potential_in_the_humanitarian_sector.pdf, accessed May 2010.
- MARK, D. M., 2000, Geographic information science: critical issues in an emerging cross-disciplinary research domain. *URISA Special Report*, **12**, 45-54.

-
- MARK, D. M., 2003, Geographic information science: defining the field. In DUCKHAM, M., GOODCHILD, M. F., AND WORBOYS, M. F., (Eds.), *Foundations of Geographic Information Science*, Taylor and Francis, London, pp. 1-15.
- MARTI, J., ASPINALL, W.P., SOBRADELO, R., FELPETO, A., GEYER, A., ORTIZ, R., BAXTER, P., COLE, P., PACHECO, J., BLANCO, M. J., AND LOPEZ, C., 2008, A long-term volcanic hazard event tree for Teide-Pico Viejo stratovolcanoes (Tenerife, Canary Islands). *Journal of Volcanology and Geothermal Research*, **178**, 543-552.
- MARZOCCHI, W., SANDRI, L., GASPARINI, P., NEWHALL, C., AND BOSCHI, E., 2004, Quantifying probabilities of volcanic events: the example of volcanic hazard at Mt. Vesuvius. *Journal of Geophysical Research*, **109**, B11201.
- MARZOCCHI, W., SANDRI, L., AND SELVA, J., 2008, BET_EF: a probabilistic tool for long- and short-term eruption forecasting. *Bulletin of Volcanology*, **70**, 623-632.
- MASOOD, E., 1998, Montserrat residents 'lost faith' in volcanologists' warnings. *Nature*, **392**, 743-744.
- MATTHEWS, A.J., BARCLAY, J., CARN, S., THOMPSON, G., ALEXANDER, J., HERD, R., AND WILLIAMS, C., 2002, Rainfall-induced volcanic activity on Montserrat. *Geophysical Research Letters*, **29**, 1644-1647.
- MATTHEWS, A. J., BARCLAY, J., AND JOHNSTONE, J. E., 2009, The fast response of volcano-seismic activity to intense precipitation: triggering of primary volcanic activity by rainfall at Soufrière Hills Volcano, Montserrat. *Journal of Volcanology and Geothermal Research*, **184**, 405-415.
- MAUNE, D. F., 2007, *Digital elevation model technologies and applications: the DEM users manual, second edition*. American Society for Photogrammetry and Remote Sensing, Bethesda, USA, pp. 655.
- MCDOUGALL, S., AND HUNGR, O., 2004, A model for the analysis of rapid landslide motion across three-dimensional terrain. *Canadian Geotechnical Journal*, **41**, 1084-1097.
- MCGUIRE, W. J., SOLANA, M. C., KILBURN, C. R. J., AND SANDERSON, D., 2009, Improving communication during volcanic crises on small, vulnerable islands. *Journal of Volcanology and Geothermal Research*, **183**, 63-75.
- MCINTOSH, B. S., SEATON, R. A. F., AND JEFFREY, P., 2007, Tools to think with? Towards understanding the use of computer-based support tools in policy relevant research. *Environmental Modelling & Software*, **22**, 640-648.
- MCMASTER, R. B., AND USERY, E. L., (2005). *A research agenda for geographical information science*. CRC Press, Florida, USA, pp. 402).

-
- MEJIA-NAVARRO, M., WOHL, E. E., AND OAKS, S. D., 1994, Geological hazards, vulnerability, and risk assessment using GIS: model for Glenwood Springs, Colorado. *Geomorphology*, **10**, 331-354.
- MERRIT, D. M., AND WOHL, E. E., 2003, Downstream hydraulic geometry and channel adjustment during a flood along an ephemeral, arid-region drainage. *Geomorphology*, **52**, 165-180.
- MERRY, C., WRIGHT, D., WENTZ, E., ANDERSON, S., BUDGE, A., AND HEPNER, G., 2000, *Remotely acquired data and information in GIScience*. University Consortium for Geographic Information Science White Paper: long-term research challenges, pp. 6. Available online: http://www.ucgis.org/priorities/research/research_white/2000%20Papers/emerging/ASPRS.pdf, accessed May 2010.
- MERZ, B., FRIEDRICH, J., DISSE, M., SCHWARZ, J., GOLDAMMER, J. G., AND WACHTER, J., 2006, Possibilities and limitations of interdisciplinary, user-oriented research: experiences from the German Research Network Natural Disasters. *Natural Hazards*, **38**, 3-20.
- MITASOVA, H., AND MITAS, L., 1993, Interpolation by regularized spline with tension: I. Theory and implementation. *Mathematical Geology*, **25**, 641-655.
- MONMONIER, M., 1998, *Cartographies of danger: mapping hazards in America*. University of Chicago Press, Chicago, USA, pp. 396.
- MONTELLO, D. R., FREUNDSCHUH, S., GOPAL, S., HIRTLE, S. C., 1998, *Cognition of spatial information*. University Consortium for Geographic Information Science White Paper: long-term research challenges. Available online: http://www.ucgis.org/priorities/research/research_white/1998%20Papers/cog.html, accessed May 2010.
- MULLER, M., VOROGUSHYN, S., MAIER, P., THIEKEN, A. H., PETROW, T., KRON, A., BUCHELE, B., AND WACHTER, J., 2006, CEDIM Risk Explorer – a map server solution in the project 'Risk Map Germany'. *Natural Hazards and Earth Systems Sciences*, **6**, 711-720.
- MULTINATIONAL ANDEAN PROJECT, 2008, Guidelines for landslide hazard mapping in the Andes: speaking one language. In LIVERMAN, D. G. E., PEREIRA, C. P. G., AND MARKER, B., (Eds.), *Communicating environmental geoscience*, Geological Society of London, Special Publications, **305**, 53-61.
- MUNICH RE, 2010, *Great natural disasters since 1950*. NatCatSERVICE, Munich Reinsurance Company. Available online: http://www.munichre.com/en/reinsurance/business/non-life/georisks/natcatservice/long-term_statistics_since_1950/default.aspx, accessed May 2010.

-
- MUNOZ-SALINAS, E., CASTILLO-RODRIGUEZ, M., MANEA, V., MANEA, M., AND PALACIOS, D., 2009, Lahar flow simulations using LAHARZ program: application for the Popocatepetl volcano, Mexico. *Journal of Volcanology and Geothermal Research*, **182**, 13-22.
- MURILLO, M. L., AND HUNTER, G. J., 1997, Assessing uncertainty due to elevation error in a landslide susceptibility model. *Transactions in GIS*, **2**, 289-298.
- NATURE, 1997, Cooperation can help to get the message across. *Nature*, **388**, 1.
- NERI, A., ASPINALL, W. P., CIONI, R., BERTAGNINI, A., BAXTER, P. J., ZUCCARO, G., ANDRONICO, D., BARSOTTI, S., COLE, P. D., ESPOSTI ONGARO, T., HINCKS, T. K., MACEDONIO, G., PAPALE, P., ROSI, M., SANTACROCE, R., AND WOO, G., 2008, Developing an event tree for probabilistic hazard and risk assessment at Vesuvius. *Journal of Volcanology and Geothermal Research*, **178**, 397-415.
- NEWHALL, C. G., AND PUNONGBAYAN, R. S., 1996, *Fire and mud: eruptions and lahars of Mount Pinatubo, Philippines*. Philippine Institute of Volcanology and Seismology and the University of Washington Press, pp. 1126.
- NEWHALL, C., HENDLEY II, J. W., AND STAUFFER, P. H., 1997, The cataclysmic 1991 eruption of Mount Pinatubo, Philippines. *USGS Factsheet*, **113-97**, 1-2.
- NEWHALL, C. G., BRONTO, S., ALLOWAY, B., BANKS, N. G., BAHAR, I., DEL MARMOL, M. A., HADISANTONO, R. D., HOLCOMB, R. T., MCGEEHIN, J., MIKSIC, J. N., RUBIN, M., SAYUDI, S. D., SUKHYAR, R., ANDREASTUTI, S., TILLING, R. I., TORLEY, R., TRIMBLE, D., AND WIRAKUSUMAH, A. D., 2000, 10,000 years of explosive eruptions of Merapi Volcano, Central Java: archaeological and modern implications. *Journal of Volcanology and Geothermal Research*, **100**, 9-50.
- NEWHALL, C. G., AND HOBLITT, R. P., 2002, Constructing event trees for volcanic crises. *Bulletin of Volcanology*, **64**, 3-20.
- NIKOLAKOPOULOS, K., KAMARATAKIS, E. AND CHRYSOULAKIS, N., 2006, SRTM vs. ASTER Elevation Products: comparison for two regions in Crete, Greece. *International Journal of Remote Sensing*, **27**, 4819-4838.
- NRC, 2007, *Successful response starts with a map*. National Academic Press, Washington DC, USA, pp. 184.
- NOETZLI, J., HUGGEL, C., HOELZLE, M., AND HAEBERLI, W., 2006, GIS-based modelling of rock-ice avalanches from Alpine permafrost areas. *Computational Geosciences*, **10**, 161-178.
- NORTON, G., 2005, Living with an active volcano. *Earthwise*, **22**, 26-27.
- NOURBAKSH, I., 2006, Mapping disaster zones. *Nature*, **439**, 787-788.

-
- O'BRIEN, J. S., JULIEN, P. Y. AND FULLERTON, W. T., 1993, Two-dimensional water flood and mudflow simulation. *Journal of the Hydraulic Engineering*, **119**, 244-261.
- O'CALLAGHAN, J. F., AND MARK, D. M., 1984, The extraction of drainage networks from digital elevation data, *Computer Vision Graphics Image Processing*, **28**, 328-344.
- OERTL, H., 2004, *Prandtl's essentials of fluid mechanics*. Applied mathematical sciences 158, Springer-Verlag, New York, pp. 723.
- OPENSHAW, S., 1984, *The modifiable areal unit problem*. Concepts and Techniques in Modern Geography 38, GeoBooks, Norwich, pp. 40.
- ORAMAS DORTA, D., TOYOS, G., OPPENHEIMER, C., PARESCHI, M. T., SULPIZIO, R., AND ZANCHETTA, G., 2007, Empirical modelling of the May 1998 small debris flows in Sarno (Italy) using LAHARZ. *Natural Hazards*, **40**, 381-396.
- OWENS, R. G., AND PHILLIPS, T. N., 2002, *Computational rheology*. Imperial College Press, London, pp. 417.
- PAPPENBERGER, F., BEVEN, K., HORRITT, M., AND BLAZKOVA, S., 2005, Uncertainty in the calibration of effective roughness parameters in HEC-RAS using inundation and downstream level observations. *Journal of Hydrology*, **302**, 46-69.
- PAPPENBERGER, F., BEVEN, K. J., RATTO, M., AND MATGEN, P., 2008, Multi-method global sensitivity analysis of flood inundation models. *Advances in Water Resources*, **31**, 1-14.
- PARESCHI, M. T., AND BERNSTEIN, R., 1989, Modeling and image processing for visualization of volcanic mapping. *IBM Journal of Research and Development*, **33**, 406-416.
- PARESCHI, M. T., CAVARRA, L., FAVALLI, M., GIANNINI, F., AND MERIGGI, A., 2000A, GIS and volcanic risk management. *Natural Hazards*, **21**, 361-379.
- PARESCHI, M. T., FAVALLI, M., GIANNINI, F., SULPIZIO, R., ZANCHETTA, G., AND SANTRACROCE, R., 2000B, May 5, 1998 debris flows in circum-Vesuvian areas (southern Italy): insights for hazard assessment. *Geology*, **28**, 639-642.
- PASUTO, A., AND SOLDATI, M., 2004, An integrated approach for hazard assessment and mitigation of debris flows in the Italian Dolomites. *Geomorphology*, **61**, 59-70.
- PATTULLO, P., 2000, *Fire from the mountain: the tragedy of Montserrat and the betrayal of its people*. Constable, London, pp. 217.
- PEDUZZI, P., DAO, H., AND HEROLD, C., 2005, Mapping disastrous natural hazards using global datasets. *Natural Hazards*, **35**, 265-289.

-
- PIERSON, T. C., JANDA, T. J., THOURET, J-C., AND BORRERO, C. A., 1990, Perturbation and melting of snow and ice by the 13 November 1985 eruption of Nevado del Ruiz, Columbia, and consequent mobilization, flow and deposition of lahars. *Journal of Volcanology and Geothermal Research*, **41**, 17-66.
- PIERSON, T. C., JANDA, R. J., UMBAL, J. V., AND DAAG, A. S., 1992, *Immediate and long-term hazards from lahars and excess sedimentation in rivers draining Mt. Pinatubo, Philippines*. United States Geological Survey Water-Resources Investment Report, 92-4039, pp. 35.
- PIERSON, T. C., 1995, Flow characteristics of large eruption-triggered debris flows at snow-clad volcanoes: constraints for debris-flow models. *Journal of Volcanology and Geothermal Research*, **66**, 283-294.
- PIERSON, T. C., 2005, Hyperconcentrated flow – transitional process between water flow and debris flow. In JAKOB, M., AND HUNGR, O., (Eds.) *Debris-flow hazards and related phenomena*. Springer-Verlag, Berlin, p. 159-202.
- PITMAN, E. B., PATRA, A., BAUER, A., SHERIDAN, M., BURSIK, M., 2003, Computing debris flows and landslides. *Physics of Fluids*, **15**, 3638–3646.
- PITMAN, E. B., AND LE, L., 2005, A two-fluid model for avalanche and debris flows. *Philosophical Transactions of the Royal Society A: Mathematical, Physical and Engineering Sciences*, **363**, 1471-2962.
- PROCTOR, D., AND FLEMING, L., V., 1999, *Biodiversity: The UK Overseas Territories*, Joint Nature Conservation Committee, p. 82–87.
- PROCTER, J. N., CRONIN, S. J., FULLER, I. C., SHERIDAN, M., NEALL, V. E. AND KEYS, H., 2009, Lahar hazard assessment using Titan2D for an alluvial fan with rapidly changing geomorphology: Whangaehu River, Mt. Ruapehu. *Geomorphology*, **116**, 162-174.
- PUDASAINI, S. P., WANG, Y., AND HUTTER, K., 2005, Modelling debris flows down general channels. *Natural Hazards and Earth Systems Sciences*, **5**, 799-819.
- PULLAR, D., 2003, Simulation modelling applied to runoff modelling using MapScript. *Transactions in GIS*, **7**, 267-283.
- QUINN, P. F., BEVEN, K. J., CHEVALLIER, P., AND PLANCHON, O., 1991, The prediction of hillslope paths for distributed hydrological modeling using digital terrain models, *Hydrological Processes*, **5**, 59–79.
- RAAFLAUB, L. D., AND COLLINS, M. J., 2006, The effect of error in gridded digital elevation models on the estimation of topographic parameters. *Environmental Modelling and Software*, **21**, 710-732.

-
- RADKE, J., COVA, T., SHERIDAN, M. F., TROY, A., LAN, M., AND JOHNSON, R., 2000, Application challenges for Geographical Information Science: implications for research, education, and policy for emergency preparedness and response. *URISA Journal*, **12**, 15-30.
- RASHED, T., WEEKS, J., COUCLELIS, H., AND HEROLD, M., 2007, An integrative GIS and remote sensing model for place-based urban vulnerability analysis. In MESEV, V., (Ed.), *Integration of GIS and Remote Sensing*, John Wiley & Sons, Chichester, p. 199-231.
- RATTO, M., TARANTOLA, S., AND SALTELLI, A., 2001, Sensitivity analysis in model calibration: GSA-GLUE approach. *Computer Physics Communications*, **136**, 212-224.
- RENSCHLER, C. S., 2005, Scales and Uncertainties in volcano hazard prediction - optimizing the use of GIS and models. *Journal for Volcanology and Geothermal Research*, **139**, 73-87.
- REFICE, A., AND CAPOLONGO, D., 2002, Probabilistic modeling of uncertainties in earthquake-induced landslide hazard assessment. *Computers & Geosciences*, **28**, 735-749.
- REUTER, H. I., NELSON, A., AND JARVIS, A., 2007, An evaluation of void-filling interpolation methods for SRTM data. *International Journal of Geographical Information Science*, **21**, 983-1008.
- RICHARDSON, K., 2009, Small islands spatial data infrastructure. *GEOconnexion International Magazine*, June, 28-30.
- RICKENMANN, D., 1999, Empirical relationships for debris flows. *Natural Hazards*, **19**, 47-77.
- RICKENMANN, D., 2005, Runout prediction methods. In JAKOB, M., AND HUNGR, O., (Eds.) *Debris-flow hazards and related phenomena*. Springer-Verlag, Berlin, p. 305-324.
- ROOBOL, M. J., AND SMITH, A. L., 1975, A comparison of the recent eruptions of Mt. Pelee, Martinique and Soufriere, St. Vincent. *Bulletin of Volcanology*, **39**, 214-240.
- ROSE, W. I., 1972, Notes on the 1902 eruption of Santa Maria Volcano, Guatemala. *Bulletin of Volcanology*, **36**, 29-45.
- ROSE, W. I., 1973, Pattern and mechanism of volcanic activity at the Santiaguito Volcano dome, Guatemala. *Bulletin of Volcanology*, **37**, 73-94.
- ROSENBAUM, M., AND CULSHAW, M. G., 2003, Communicating the risks arising from geohazards. *Journal of the Statistical Society: Series A*, **166**, 261-270.

-
- SAC8, 2007, *Assessment of the hazards and risks associated with the Soufrière Hills Volcano, Montserrat: Eighth Report of the Scientific Advisory Committee on Montserrat Volcanic Activity*, 20th-22nd March, pp. 38. Available online: http://www.montserratvolcanoobservatory.info/index.php?option=com_rokdownloads&view=folder&Itemid=184&id=5:sac-reports&lang=en, accessed May 2010.
- SAC9, 2007, *Assessment of the hazards and risks associated with the Soufrière Hills Volcano, Montserrat: Ninth Report of the Scientific Advisory Committee on Montserrat Volcanic Activity*, 1st-3rd October, pp. 37. Available online: http://www.montserratvolcanoobservatory.info/index.php?option=com_rokdownloads&view=folder&Itemid=184&id=5:sac-reports&lang=en, accessed May 2010.
- SAHA, A. K., ARORA, M. K., GUPTA, R. P., VIRDI, M. L., AND CSAPLOVICS, E., 2005, GIS-based route planning in landslide-prone areas. *International Journal of Geographical Information Science*, **19**, 1149-1175.
- SALTELLI, A., TARANTOLA, S., AND CAMPOLONGO, F., 2000A, Sensitivity analysis as an ingredient of modeling. *Statistical Science*, **15**, 377-395.
- SALTELLI, A., 2000, What is sensitivity analysis? In SALTELLI, A., CHAN, K., AND SCOTT, E. M., (Eds.) *Sensitivity Analysis*. John Wiley & Sons, Chichester, p. 3-14.
- SALTELLI, A., CHAN, K., AND SCOTT, E. M., 2000B, *Sensitivity Analysis*. John Wiley & Sons, Chichester, pp. 475.
- SAVAGE, S. B., AND HUTTER, K., 1989, The motion of a finite mass of granular material down a rough incline. *Journal of Fluid Mechanics*, **199**, 177.
- SAVAT, J., 1977, Hydraulics of sheet flow on a smooth surface and the effect of simulated rain. *Earth Surface Processes and Landforms*, **2**, 125-140.
- SCHILLING, S.P., 1998. LAHARZ: GIS programs for automated mapping of lahar-inundation hazard zones U.S. *Geological Survey Open-File Report*, **93-638**, p. 79.
- SCHNEIDER, B., 2001, Phenomenon-based specification of the digital representation of terrain surfaces. *Transactions in GIS*, **5**, 39-52.
- SCHNEIDER, D., DELGADO GRANADOS, H., HUGGEL, C., AND KAAB, A., 2008, Assessing lahars from ice-capped volcanoes using ASTER satellite data, the SRTM DTM and two different flow models: case study on Iztacchuatl (Central Mexico). *Natural Hazards and Earth Systems Sciences*, **8**, 559-571.
- SCHUURMAN, N., 2000, Trouble in the heartland: GIS and its critics in the 1990s. *Progress in Human Geography*, **24**, 569-590.

-
- SCHUURMAN, N., 2002, Reconciling social constructivism and realism in GIS. *ACME: An International E-Journal for Critical Geographies*, **1**, 73-90.
- SCOTT, K. M., MACIAS, J. L., NARANJO, J. A., RODRIGUEZ, S., AND MCGEEHIN, J. P., 2001, *Catastrophic debris flows transformed from landslides in volcanic terrains: mobility, hazard assessment, and mitigation strategies*. United States Geological Survey Professional Paper 1630, p. 70.
- SCOTT, K. M., VALLANCE, J. W., KERLE, N., MACIAS, J. L., STRAUCH, W., AND DEVOLI, G., 2005, Catastrophic precipitation-triggered lahar at Casita volcano, Nicaragua: occurrence, bulking and transformation. *Earth Surface Processes and Landforms*, **30**, 59-79.
- SEIBERT, J., AND MCGLYNN, B. L., 2007, A new triangular multiple flow direction algorithm for computing upslope areas from gridded digital elevation models. *Water Resources Research*, **43**, 1-8.
- SHEPHERD, J. B., TOMBLIN, J. F., AND WOO, D. A., 1971, Volcano-seismic crisis in Montserrat, West Indies, 1966-67. *Proceedings of the IAVCEI Symposium on Volcanoes and their Roots*. Oxford, September 1969.
- SHERIDAN, M. F., 1979, A model of pyroclastic surge. *Geological Society of America Special Publication*, **180**, 125-136.
- SHERIDAN, M. F., 2004, Information technology and volcanic hazards. *Proceedings of the Geological Society of America, Penrose Conference, 12th-16th January*, Mexico. Available online: http://www.geofisica.unam.mx/vulcanologia/penrose/abstracts_prs/prs7_ms.pdf, accessed November, 2006.
- SIEBER, R. E., 2007, Spatial data access by the grassroots. *Cartography and Geographic Information Science*, **34**, 47-62.
- SIEBERT, L., AND SIMKIN, T., 2010, *Volcanoes of the World: an Illustrated Catalog of Holocene Volcanoes and their Eruptions*. Smithsonian Institution, Global Volcanism Program Digital Information Series, GVP-3. Available online: <http://www.volcano.si.edu/world/>, accessed May 2010.
- SIGURDSSON, H., 2007, Gas bursts from Cameroon crater lakes: a new natural hazard. *Disasters*, **12**, 131-146.
- SIMKIN, T., 1993, Terrestrial volcanism in space and time. *Annual Review of Earth and Planetary Sciences*, **21**, 427-452.
- SIMKIN, T., AND SIEBERT L., 1994, *Volcanoes of the World*, 2nd edition. Geoscience Press in association with the Smithsonian Institution Global Volcanism Program, Tucson, USA, pp. 368.

-
- SKIDMORE, A. K., 1989, A comparison of techniques for the calculation of gradient and aspect from a gridded digital elevation model. *International Journal of Geographical Information Systems*, **3**, 323–334.
- SMEMOE, C. M., NELSON, E. J., ZUNDEL, A. K., AND WOODRUFF MILLER, A., 2007, Demonstrating floodplain uncertainty using flood probability maps. *Journal of the American Water Resources Association*, **43**, 359–371.
- SMITH, M. W., COX, N. J., AND BRACKEN, L. J., 2007, Applying flow resistance equations to overland flows. *Progress of Physical Geography*, **31**, 363–387.
- SMITH, G., AND LOWE, A., 1991. Lahars: volcano– hydrologic events and deposition in the debris-flow– hyperconcentrated flow continuum. In FISHER, R. V., AND SMITH, G., (Eds.), *Sedimentation in Volcanic Settings*, SEPM Special Publication, **45**, pp. 59–70.
- SMOLKA, A., 2006, Natural disasters and the challenge of extreme events: risk management from an insurance perspective. *Philosophical Transactions of the Royal Society A: Mathematical, Physical and Engineering Sciences*, **364**, 2147–2165.
- SOLANA, M. C., 2001, *Communication during volcanic emergencies: an operations manual for the Caribbean*. DFID Project R7406, pp. 37.
- SOSIO, R., CROSTA, G. B., AND FRATTINI, P., 2007, Field observations, rheological testing and numerical modelling of a debris-flow event. *Earth Surface Processes and Landforms*, **32**, 290–306.
- SPARKS, R. S. J., YOUNG, S. R., AND BARCLAY, J., 1998, Magma production and growth of the lava dome of the Soufrière Hills Volcano, Montserrat, West Indies: November 1995 to December 1997. *Geophysical Research Letters*, **25**, 3421–3424.
- SPARKS, R. S. J., AND YOUNG, S. R., 2002, The eruption of Soufrière Hills Volcano, Montserrat (1995–1999): overview of scientific results. In DRUITT, T. H., AND KOKELAAR, B. P., (Eds.), *The eruption of Soufrière Hills Volcano, Montserrat from 1995–1999*. Geological Society of London, Memoir **21**, 45–69.
- SPARKS, R. S. J., 2003, Forecasting volcanic eruptions. *Earth and Planetary Science Letters*, **210**, 1–15.
- STAFFLER, H., POLLINGER, R., ZISCHG, A., AND MANI, P., 2008, Spatial variability and potential impacts of climate change on flood and debris flow hazard zone mapping and implications for risk management. *Natural Hazards and Earth Systems Sciences*, **8**, 539–558.
- STEFANOVIC, I. L., 2003, The contribution of philosophy to hazards assessment and decision making. *Natural Hazards*, **28**, 229–247.

-
- STEVENS, N. F., MANVILLE, V., AND HERON, D. W., 2002, The sensitivity of a volcanic flow model to digital elevation model accuracy: experiments with digitised map contours and interferometric SAR at Ruapehu and Taranaki volcanoes, New Zealand. *Journal of Volcanology and Geothermal Research*, **119**, 89-105.
- STONE, R., 2003, Bracing for the big one on Montserrat. *Science*, **299**, 2027-2031.
- SUI, D. Z., AND MAGGIO, R. C., 1999, Integrating GIS with hydrological modeling: practices, problems, and prospects. *Computers, Environment and Urban Systems*, **23**, 33-51.
- SUSNIK, J., 2009, *Lahars in the Belham River Valley, Montserrat, West Indies*. A thesis submitted to the School of Environmental Sciences at the University of East Anglia, pp. 314.
- TANGUY, J.-C., RIBIRIE, CH., SCARTH, A., AND TJETJEP, W. S., 1998, Victims from volcanic eruptions: a revised database. *Bulletin of Volcanology*, **60**, 137-144.
- TARANTOLA, S., GIGLIOLI, N., JESINGHAUS, J., AND SALTELLI, A., 2002, Can global sensitivity analysis steer the implementation of models for environmental assessments and decision-making? *Stochastic Environmental Research and Risk Assessment*, **16**, 63-76.
- TARBOTON, D. G., 1997, A new method for the determination of flow directions and upslope areas in grid digital elevation models. *Water Resources Research*, **33**, 309-319.
- TAYEFI, V., LANE, S. N., HARDY, R. J., AND YU, D., 2007, A comparison of one- and two-dimensional approaches to modelling flood inundation over complex upland floodplains. *Hydrological Processes*, **21**, 3190-3202.
- TAYLOR, G. A., 1954, Vulcanological observations Mount Lamington 29th May, 1952. *Bulletin Volcanologique*, **15**, 81-89.
- TEEUW, M. R., 2007, Introducing the remote sensing of hazardous terrain. *Geological Society of London, Special Publications*, **283**, 1-3.
- THIERRY, P., STIELTJES, L., KOUOKAM, E., NGUEYA, P., AND SALLEY, P. M., 2008, Multi-hazard risk mapping and assessment on an active volcano: the GRINP project at Mount Cameroon. *Natural Hazards*, **45**, 429-456.
- THOURET, J.-C., ABDURACHMAN, K. E., BOURDIER, J.-L., AND BRONTO, S., 1998, Origin, characteristics, and behaviour of lahars following the 1990 eruption of Kelud volcano, eastern Java (Indonesia). *Bulletin of Volcanology*, **59**, 460-480.

-
- THOURET, J.-C., LAVIGNE, F., KELFOUN, K., AND BRONTO, S., 2000, Toward a revised hazard assessment at Merapi volcano, Central Java. *Journal of Volcanology and Geothermal Research*, **100**, 479-502.
- TILLING, R. I., 1989, Volcanic hazards and their mitigation: progress and problems. *Reviews of Geophysics*, **27**, 237-269.
- TILLING, R. I., 2009, El Chichon's "surprise" eruption in 1982: lessons for reducing volcano risk. *Geofisica Internacional*, **48**, 3-19.
- TOMBLIN, J., 1977, Disaster prevention and control in the earth sciences. *Impact of Science in Society*, **27**, 131-139.
- TOYOS, G., ORAMAS DORTA, D., OPPENHEIMER, C., PARESCHI, M.T., SULPIZIO, R., AND ZANCHETTA, 2007, GIS-assisted modelling for debris flow hazard assessment based on the events of May 1998 in the area of Sarno, Southern Italy: Part 1 Maximum run-out. *Earth Surface Processes and Landforms*, **32**, 1491-1502.
- UCGIS, 1998, *Uncertainty in geographic data GIS-based analyses*. University Consortium for Geographic Information Science White Paper: long-term research challenges. Available online: http://www.ucgis.org/priorities/research/research_white/1998%20Papers/uncert.html, accessed May 2010.
- UN/ISDR, 2009, *2009 UNISDR terminology on disaster risk reduction*. United Nations International Strategy for Disaster Reduction, Geneva, Switzerland, pp. 30.
- UNDRO, 1979, *Natural disasters and vulnerability analysis*. UN Office of the Disaster Relief Co-ordinator, Report of the Expert Meeting, 9th-12th July, pp. 49.
- UNDRO, 1985, *Volcanic emergency management*. UN Office of the Disaster Relief Co-ordinator, 2802, New York, US, pp. 86.
- VALLANCE, J.W., 2000, Lahars. In: SIGURDSSON, H. (Ed.), *Encyclopedia of Volcanoes*. Academic Press, San Diego, p. 601-616.
- VALLANCE, J. W., 2005, Volcanic debris flows. In JAKOB, M., AND HUNGR, O., (Eds.) *Debris-flow hazards and related phenomena*. Springer-Verlag, Berlin, p. 247-274.
- VAREKAMP, J. C., LUHR, J. F., AND PRESTEGAARD, K. L., 1984, The 1982 eruptions of El Chichon volcano (Chiapas Mexico): character of the eruptions, ash-fall deposits, and Gasphase. *Journal of Volcanology and Geothermal Research*, **23**, 39-68.
- VEREGIN, H., 1997, The effects of vertical error in digital elevation models on the determination of flow-path direction. *Cartography and Geographical Information Systems*, **24**, 67-79.

-
- VIGNAUX, M., AND WEIR, G. J., 1990, A general model for Mt. Ruapehu lahars. *Bulletin of Volcanology*, **52**, 381-390.
- VOELLMY, A., 1955, Uber die Zerstorkraft von Lawinen. *Schweizerische Bauzeitung*, **73**, 159-165.
- VOIGHT, B., 1990, The 1985 Nevado del Ruiz volcano catastrophe: anatomy and retrospection. *Journal of Volcanology and Geothermal Research*, **44**, 349-386.
- VOIGHT, B., 1998, Volcanologists' efforts on Montserrat praiseworthy. *Bulletin of Volcanology*, **60**, 318-319.
- WADGE, G., ODBERT, H.M., MACFARLANE, D.G., AND JAMES, M.R., 2006, *The November 2005 DEM of the Soufriere Hills crater*. MVO Open File Report 03/06. pp. 6.
- WADGE, G., AND ISAACS, M. C., 1987, *Volcanic Hazards from Soufrière Hills Volcano Montserrat*. Report to the Government of Montserrat and the Pan Caribbean Disaster Preparedness and Prevention Project. University of Reading, Reading.
- WADGE, G., AND ISAACS, M. C., 1988, Mapping the volcanic hazards from Soufrière Hills Volcano, Montserrat, West Indies using an image processor. *Journal of the Geological Society of London*, **145**, 541-551.
- WADGE, G., ODBERT, H. M., MACFARLANE, D. G., AND JAMES, M. R., 2005, The November 2005 DEM of the Soufrière Hills Crater, MVO Open File Report 03/06. DEM available at: http://www.nerc-essc.ac.uk/~gw/www_data/Montydems.html, accessed May 2010.
- WADGE, G., MATTIOLI, G. S. AND HERD, R. A., 2006, Ground deformation at Soufriere Hills Volcano, Montserrat during 1998-2000 measured by radar interferometry and GPS. *Journal of Volcanology and Geothermal Research*, **152**, 157-173.
- WANG, H., LIU, G., XU, W., AND WANG, G., 2005, GIS-based landslide hazard assessment: an overview. *Progress in Physical Geography*, **29**, 548-567.
- WANG, X., GU, X., WU, Z., AND WANG, C., 2008, Simulation of flood inundation of Guiyang City using remote sensing, GIS and hydrologic model. *International Archives of the Photogrammetry, Remote Sensing, and Spatial Information Sciences, Proceedings of Commission VIII, ISPRS Congress, 3rd-11th July, Beijing, China*. Available online: <http://www.isprs.org/proceedings/XXXVII/congress/tc8.aspx>, accessed May 2010.
- WARREN, S. D., HOHMANN, M. G., AUERWALD, K., AND MITASOVA, H., 2004, An evaluation of methods to determine slope using digital elevation data. *Catena*, **58**, 215-233.

-
- WECHSLER, S. P., AND KROLL, C. N., 2006, Quantifying uncertainty and its effect on topographic parameters. *Photogrammetric Engineering & Remote Sensing*, **9**, 1081-1090.
- WECHSLER, S. P., 2007, Uncertainties associated with digital elevation models for hydrologic applications: a review. *Hydrology and Earth System Science*, **11**, 1481-1500.
- WIDIWIJAYANTI, C., VOIGHT, B., HIDAYAT, D., AND SCHILLING, S. P., 2009, Objective rapid delineation of areas of risk from block-and-ash pyroclastic flows and surges. *Bulletin of Volcanology*, **71**, 687-703.
- WILCOCK, P. R., SCHMIDT, J. C., WOLMAN, M. G., DIETRICH, W. E., DEWITT, D., DOYLE, M. W., GRANT, G. E., IVERSON, R. M., MONTGOMERY, D. R., PIERSON, T. C., SCHILLING, S. P., AND WILSON, R. C., 2003, When models meet managers: examples from geomorphology. In WILCOCK, P. R., AND IVERSON, R. M., (Eds.), *Prediction in Geomorphology*. American Geophysical Union, **135**, 27-40.
- WILLIAMS, C., AND DUNN, C. E., 2003, GIS in participatory research: assessing the impact of landmines on communities in north-west Cambodia. *Transactions in GIS*, **7**, 393-410.
- WILLIAMS, S. N., AND SELF, S., 1983, The October 1902 Plinian eruption of Santa Maria Volcano, Guatemala. *Journal of Volcanology and Geothermal Research*, **16**, 33-56.
- WILLIAMS, R., STINTON, A. J., AND SHERIDAN, M. F., 2008, Evaluation of the Titan2D two-phase flow model using an actual event: case study of the 2005 Vazcun Valley lahar, *Journal of Volcanology and Geothermal Research*, **177**, 760-766.
- WISNER, B., BLAIKIE, P., CANNON, T., AND DAVIS, I., 2004, *At risk: natural hazards, people's vulnerability and disasters*, second edition. Routledge, Oxon, pp. 472.
- WITHAM, C. S., 2005, Volcanic disasters and incidents: a new database. *Journal of Volcanology and Geothermal Research*, **148**, 191-233.
- WOLOCK, D. M., AND MCGABE JR., G. J., 1995, Comparison of single and multiple flow direction algorithms for computing topographic parameters in TOPMODEL. *Water Resources Research*, **31**, 1315-1324.
- WOO, G., 2008, Probabilistic criteria for volcano evacuation decisions. *Natural Hazards*, **45**, 87-97.
- WOOD, D., 1992, *The power of maps*. Guilford Press, New York, pp. 260.
- WOOD, D., AND FELS, J., 2008, *The natures of maps: cartographic constructions of the natural world*. University of Chicago Press, Chicago, USA, pp. 231.

-
- WU, F., SHEN, H. W., AND CHOU, Y., 1999, Variation of roughness coefficients for unsubmerged and submerged conditions. *Journal of Hydraulic Engineering*, **125**, 934-942.
- WU, R.-S., SHIH, D.-S., AND CHEN, S.-W., 2007, Rainfall-runoff model for typhoons making landfall in Taiwan. *Journal of the American Water Resources Association*, **43**, 969-980.
- YOCHUM, S., 2003, *Kearney Reservoir dam breach analysis, Johnson and Sheridan Counties, Wyoming*. United States Department of Agriculture Natural Resources Conservation Service, WY0200, pp. 26.
- YOCHUM, S. E., GOERTZ, L. A., AND JONES, P. H., 2008, Case study of the Big Bay Dam failure: accuracy and comparison of breach predictions. *Journal of Hydraulic Engineering*, **134**, 1285-1293.
- YOUNG, S. R., SPARKS, R. S. J., ASPINALL, W. P., LYNCH, L. L., MILLER, A. D., ROBERTSON, R. E. A., AND SHEPHERD, J. B., 1998, Overview of the eruption of Soufrière Hills Volcano, Montserrat, 18 July 1995 to December 1997. *Geophysical Research letters*, **25**, 3389-3392.
- ZERGER, A., 2002, Examining GIS decision utility for natural hazard risk modelling. *Environmental Modelling & Software*, **17**, 287-294.
- ZERGER, A., AND SMITH, D. I., 2003, Impediments to using GIS for real-time disaster decision support. *Computers, Environment and Urban Systems*, **27**, 123-141.
- ZERGER, A., AND WEALANDS, S., 2004, Beyond modelling: linking models with GIS for flood risk management. *Natural Hazards*, **33**, 191-208.
- ZERGER, A., SMITH, D. I., HUNTER, G. J., AND JONES, S. D., 2002, Riding the storm: a comparison of uncertainty modelling techniques for storm surge risk management. *Applied Geography*, **22**, 307-330.
- ZHANG, J., AND GOODCHILD, M., 2002, *Uncertainty in geographical information*. Taylor and Francis, London, pp. 266.
- ZHOU, Q., AND LIU, X., 2004, Error analysis on grid-based slope and aspect algorithms. *Photogrammetric Engineering & Remote Sensing*, **70**, 957-962.

APPENDICES

APPENDIX 1: FIELD DATA

Raw and interpreted field data on accompanying CD

APPENDIX 2: ANIMATION

Animation of lahar (Chapter 6) on accompanying CD